University of Nevada

Reno

FRACTAL CHARACTER OF LANDSLIDE BLOCK DISTRIBUTION

A thesis submitted in partial fulfillment

of the requirements for the degree of

Master of Science in Geological Engineering

by

Yoshihiro Yokoi

Dr. Robert J. Watters, Thesis Adviser

May 1995

The thesis of Yoshihiro Yokoi is approved:

Thesis Advisor

Department Chair

Dean, Graduate School

University of Nevada

Reno

May 1995

ACKNOWLEDGEMENTS

First of all, I would like to thank Dr. Bob Watters for his encouragement and guidance. His enthusiasm for research spurred on my interest in my studies and his open mindedness created good environment for my creative thinking. I learned a great deal about geological engineering and consulting through our conversations, despite the difficulties of communication we encountered due to my Japanese English and his Scottish accent.

I also would like to thank Dr. Carr for his patient advice about fractals, numerical analysis, and modeling. I could never accomplish my thesis without his help. In addition to that, his encouragement of my writing a paper for an academic journal gave me a lot of confidence. The advice of Dr. Gary Norris, one of the members of my committee, improved my thesis.

Dr. Nobuyuki Takahama of Niigata University and Dr. Yukinori Fujita, who were my undergraduate advisers, and Mr. Tomio Ohtsuka, a Niigata University graduate geologist, helped me conduct field work in Los Angeles last summer and advised me about landslide development process. They gave me important hints and inspirations for my work.

My employer, Kisojiban Consultants Co., Ltd., has given me generous support financially. My colleagues in Hiroshima and Matsuyama, Japan, sent me detailed landslide data and encouragement.

Special thanks are due to Dr. William Gate; the Ministry of Agriculture of Japan - Hokuriku Branch; Dr. Nobuyuki Takahama, Niigata University; Nittoc Construction Co., - Toyama Geotechnical Laboratory; and the Ministry of Construction of Japan - Public Works Research Institute, who sent me the unpublished data about landslides that form the basis of my thesis.

My friends Mr. Sangwon Cheong, Mr. Tomoaki Miura, and Mr. Rolf Swainston have always advised and encouraged me. I would have gone crazy without conversation and drinking parties with them.

Finally, I would like to thank my wife Leah and our cats, who came here with us. In first place, I wouldn't have come to a university in U.S. without my wife. Then, there is no way I would have undertaken or been able to complete my studies without Leah's support. In paticular, what I wrote couldn't have been understood without her turning my Japanese English into English. Our older cat, Lorenzo, kept me amused and irritated by walking on and messing up my papers. The biggest

sacrifice for my work was made by our little cat, Chibi, who died during last Thanks giving week.

At Paul Laxalt Mineral Research Center 165D, UNR

Reno, Nevada

March 22, 1995

Yoshihiro Yokoi

ABSTRACT

Landslide blocks can be classified into first, second, and third levels. Not only whole blocks but also second and third level blocks have unique fractal dimensions. The fractal dimension is reversely proportional to the logarithm of standard deviation of the blocks' size. Numerical analysis revealed that fractal dimension correlates to the geometry of the landslide, discontinuities of the base rock, and activity of the landslide. Fractal dimension is independent of the size of the landslide, angle of slide surface and slope, and geology of the base rock. The fractal character of landslide block distribution can be explained by self-similar geometry, the unique fractal dimension made by combining second and third level blocks, and fractal erosional process. Fractal character of landslide block distribution can be used to identify potential landslides and can be used as a numerical index to describe landslides including their level of activity.

TABLE OF CONTENTS

APPENDICES

FIGURES

TABLES

CHAPTER ONE: INTRODUCTION

"Fractal geometry is not just a chapter of mathematics, but one that helps Everyman to see the same old world differently." , Mandelbrot, B. B., from Foreword of "An Eye for Fractals", (Mcguire, 1991).

The distribution of landslide blocks seems random and chaotic. This apparent random and chaotic distribution was analyzed using fractals. Fractals provide a workable new middle ground between the excessive geometric order of Euclid and the geometric chaos of roughness and fragmentation (Mandelbrot, 1990). Furthermore, fractals provide both a description and mathematical model for many of the seemingly complex forms found in nature (Voss, 1988). A few researches suggested that the distribution of landslide blocks indicates fractal character (Ueno and others, 1993; Higaki and others, 1994; Yokoi and others, 1995).

The purpose of this thesis is to investigate the fractal character of landslide blocks, analyze the relationship between fractal and other attributes (properties) of landslides, and discuss landslide block development process.

Therefore, the objective of this investigation is to:

1) collect slide-block distribution data from huge landslides through interpretation of areal photography and topography maps, field investigation, and the available literature on the subject;

2) determine the fractal character, if any, of these landslide block distribution and calculate their fractal dimensions;

3) conduct statistical analyses to find the relationship between their fractal dimensions and other properties;

4) analyze the landslide block distribution using fractal models; and

5) analyze block development process of landslides

CHAPTER TWO: CLASSIFICATION OF MASS MOVEMENT

2.1 INTRODUCTION

Mass movement, like other natural phenomena, is difficult to classify. Many researchers have tried to classify mass movement and their efforts have contributed to our understanding of it.

Not all researchers agree on the definition of mass movement. Varnes (1978) believed that the term *mass movement* is not proper because it includes subsidence and he proposed the alternate term *slope movement*. On the other hand Hutchinson (1968) defined *mass movement* as not including the subsidence (Hansen, 1984). *Mass movement* is used to mean the movement of slope material except subsidence and tectonic movement. This means that *mass movement* includes falls, topples, slides, spreads, flows, and creep.

Many researchers, including Sharp (1938), Varnes (1978), and Zaruba and Mencl (1969), use the term *landslide* interchangeable with *mass movement*. Hutchinson (1988) divided *mass movement* into rebound, creep, sagging of mountain slopes, landslides, debris movements of flow-like form, topples, and falls. He limited the concept of *landslide* to rotational slips, transnational slides, and compounds of these. Japanese researchers divide *mass movement* into rockfall, debris flow,

and landslides. The Japanese term for landslide, *jisuberi*, has a similar connotation to Hutchinson's *landslide* plus *sagging* or Varnes' *slide*. In this paper, *landslide* is used with same definition as the slide and creep of Varnes (1978), because my study is focused on slides; and the broader meaning of landslide can be expressed by mass movement.

2.2 DISCRIMINATING FACTORS FOR THE CLASSIFICATION

Table 2.1 shows the discriminating factors used for classification of mass movement.

Most researchers agree in using the type of movement as the discriminating factor. Many American and European researchers have used the material moved as the discriminating factor, whereas their Japanese counterparts have used the base rock geology. In Japan, the distribution of landslides is concentrated in tertiary mudstone areas, metamorphic areas, and altered volcanic rock areas (Kotachibana, 1979). Therefore, it is convenient to classify landslides by base rock geology.

Table 2.1 Comparison of discriminating factors for mass movement classification

Auther	Climate	Material moved	Coherence of material	Size of material	Geology	Type of movement	Speed of movement	Water/ air/ice	Triggering mechanism	Morphological attribute	Process of development	Size of block
Heim (1882)		XX				XX						
Ladd (1935) *					XX				X			
Sharpe (1938) *				X		XX	X	XX				
Ward (1945) *	X	X				XX		X				
Zaruba and Menci (1969)		XX	XX		X	X						
Blong (1973) *				X		XX				XX		
Crozier (1973) *						XX				XX		
Coates (1973) *		XX	X	X		XX	X					
Varnes (1978)		XX				XX	X	X				
Huchinson (1988)				X		XX						
Wakimizu (1912) **		XX				XX						
Nakamura (1955) **					XX	XX	X					
Koide (1955) **					XX	X					XX	
Takano (1960) **						X	XX			XX		
Taniguchi (1963) **					XX	XX						
Akutagawa, Kaneko (1965) **					XX	XX	X					
Kuroda (1968) **					XX	XX						
Miyazaki, ** Takahashi (1970)		X				X					XX	
Watari (1977)		XX				XX					XX	
Takahama, Ito (1989)											XX	X

Reference
* Hansen (1984)
** Konuki (1971)

XX: Main factor
X: Secondary factor

The unique factor used by Japanese researchers is the process of development. There are two variations of this concepts. One is *the cycle of the landslide* which is landslide version of *the cycle of erosion* (Davis, 1923). The other is *the multiple level character of the landslide*, which is explained in the next section. Figure 2.1 shows a conceptional picture of *the cycle of the landslide* process. Watari (1977) indicated that landslides begin as a huge rock slide (young stage). After initial failure, the landslide body is weathered mainly by ground water permeating through cracks and becomes weathered rock (mature stage). In the weathered rock type slide, many small rotational slides occur and the landslide body becomes colluvial and then muddy soil (old and ultimate stage).

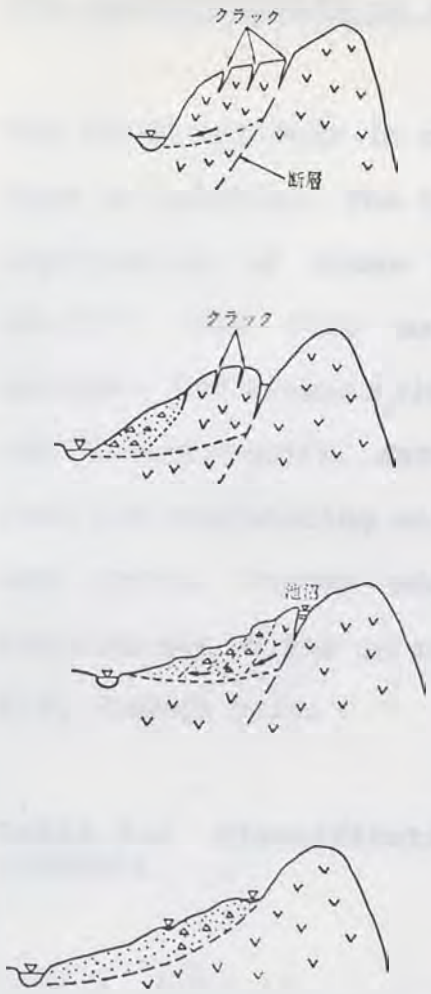

a) YOUNG STAGE
Landslide begin as a huge rock slide.

↓

b) MATURE STAGE
Weathered rock slide

↓

c) OLD STAGE
Debris slide

↓

d) ULTIMATE STAGE
Clayish soil slide

Figure 2.1 Conceptional picture of *the cycle of landslide process* (reprinted from Watari, 1977)

2.3 THE CLASSIFICATION USED IN THIS THESIS

Varnes' classification (1978) is used to describe the landslides because it is well organized and widely used. The classification based on the multiple level character of landslides is also used because it is useful in analyzing the fractal character of landslides.

THE CLASSIFICATION OF VARNES (1978)

The chief criteria in classification are type of movement and type of material. The type of mass movement is expressed as a combination of these two criteria. Types of movement are divided into five main groups: falls, topples, slides, spreads, and flows; slides are further divided into rotational and translational. Materials are divided into two classes: rock and engineering soil; soil is further divided into debris and earth. Varnes added the complex type which is the combination of two or more principal types of movement (Table 2.2, Figure 2.2).

Table 2.2 Classification of mass movement by Varnes (1978) (verbal)

TYPE OF MOVEMENT			TYPE OF MATERIAL		
			BEDROCK	ENGINEERING SOILS	
				PREDOM. COARSE	PREDOMINANTLY FINE
FALLS			ROCK FALL	DEBRIS FALL	EARTH FALL
TOPPLES			ROCK TOPPLE	DEBRIS TOPPLE	EARTH TOPPLE
SLIDES	ROTATIONAL	FEW UNITS	ROCK SLUMP	DEBRIS SLUMP	EARTH SLUMP
	TRANSLATIONAL	FEW UNITS	ROCK BLOCK SLIDE	DEBRIS BLOCK SLIDE	EARTH BLOCK SLIDE
		MANY UNITS	ROCK SLIDE	DEBRIS SLIDE	EARTH SLIDE
LATERAL SPREADS			ROCK SPREAD	DEBRIS SPREAD	EARTH SPREAD
FLOWS			ROCK FLOW (DEEP CREEP)	DEBRIS FLOW (SOIL CREEP)	EARTH FLOW
COMPLEX			COMBINATION OF TWO OR MORE PRINCIPAL TYPES OF MOVEMENT		

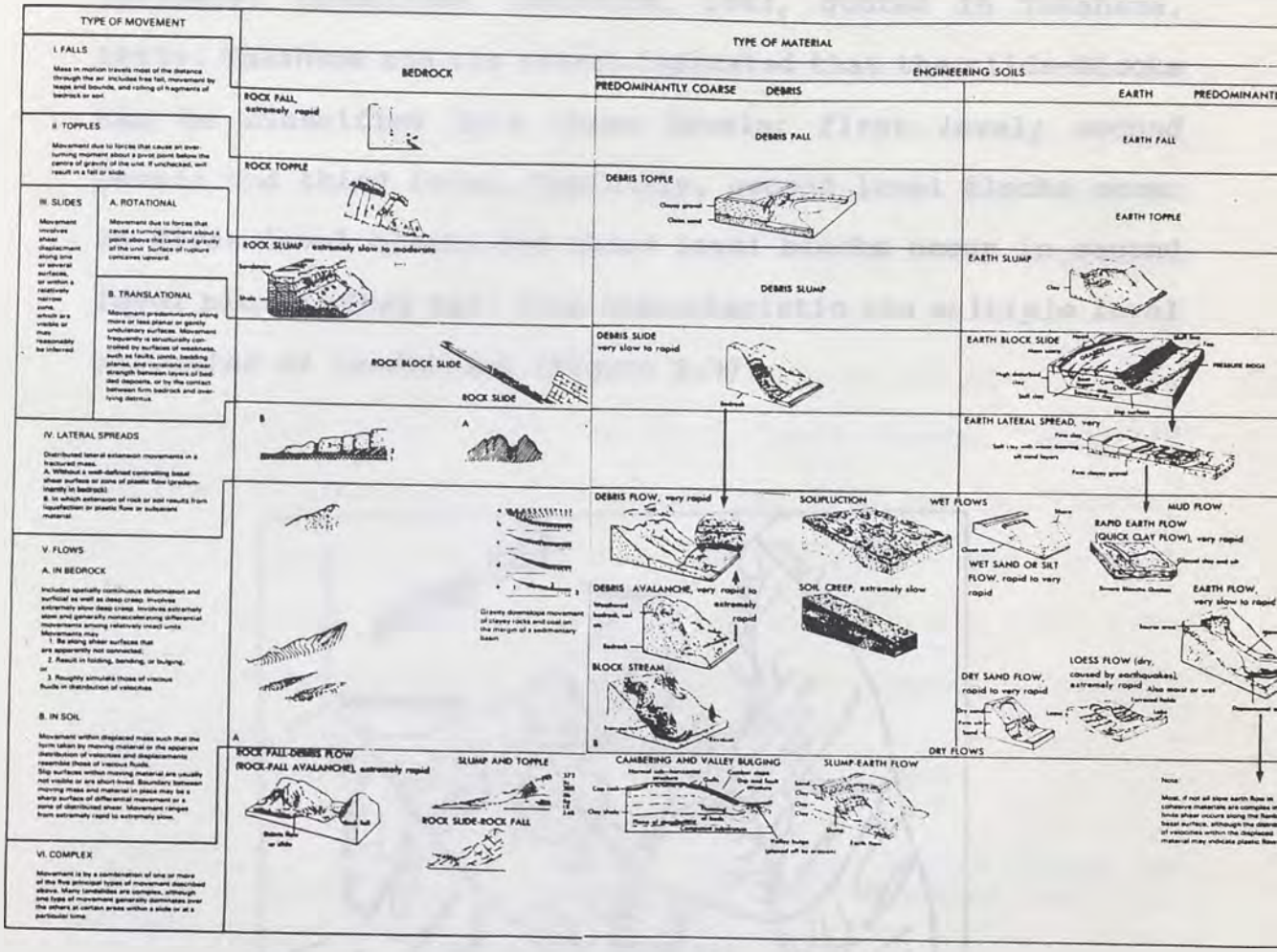

Figure 2.2 Classification of mass movement by Varnes (1978) (pictorial) (reprinted from Hansen, 1984)

THE MULTIPLE LEVEL CHARACTER OF LANDSLIDE

In Japan, almost all presently active landslides are considered reactivation of parts or entire ancient huge (primary) landslides (Nakamura, 1963, quoted in Takahama, 1993). Takahama and Ito (1988) indicated that the slide-blocks can be classified into three levels: *first level; second level;* and *third level*. Typically, second level blocks occur in first level blocks and third level blocks occur in second level blocks. They call this characteristic *the multiple level character of landslides* (Figure 2.3).

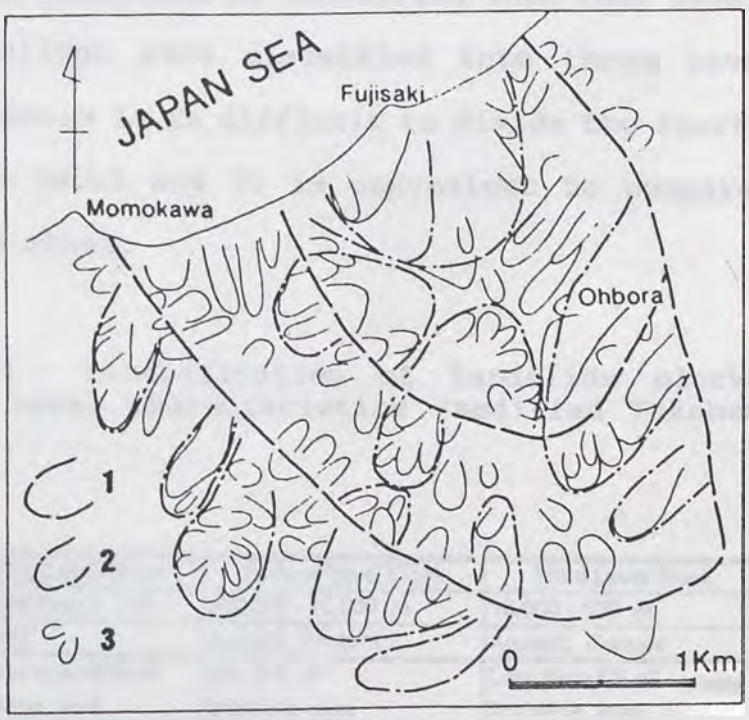

Figure 2.3 Distribution of slide-blocks of No. 34, Ohbora landslide (reprinted from Takahama and Ito, 1989)
1: First level block; 2: Second level block; 3: Third level block

Takahama and Ito classified first, second, and third level blocks mainly by absolute size and activity age of the blocks (Table 2.3). However, the relationship of the levels are relative. Therefore, I decided that it is more convenient and applicable to classify these blocks by relative size and relative activity age of the blocks. In this thesis, first level blocks are defined as blocks which cover more than 50% of the landslide area; second level blocks as blocks whose area is 50-3% of the first level block and in which third level blocks occur; and third level blocks as blocks whose area is less than 5% of the first level blocks. Landslide blocks can sometimes be classified into four levels. However, all landslides were classified into three levels in this thesis because it is difficult to divide the fourth level from the third level and it is convenient to compare landslides with each other.

Table 2.3 Classification of landslide blocks based on multiple level characteristics (modified Takahama and Ito, 1989)

	First Level Block	Second Level Block	Third Level Block	
Area	Greater than 1 km	100,000 - 10,000 m	10,000 - 100 m	Takahama and Ito (1989)
Age	Ancient	Ancient, Present	Ancient, Present	
Area	Greater than 50% of landslide area	50 - 3 % of landslide area	Less than 5% of landslide area	This thesis
Age	Initial (ancient) Block	Develp inside 1st level Include 3rd level blocks	Don't include blocks inside	

The concept of the multiple level characteristics of landslides combines both size and age criteria; consequently, the level of the blocks is not classified objectively and mechanically but rather subjectively and experimentally.

CHAPTER THREE: FRACTAL

3.1 DEFINITION

The term *fractal* was coined by Mandelbrot (1977). It is derived from the Latin word *frangere*, which means *to break* (Peitgen and others, 1992). Mandelbrot himself is reluctant to define *fractal*, saying, "I continue to believe that one (fractal) would do better without definition." (Mandelbrot, 1977). However, for the purposes of this thesis, it is necessary to define the term as clear and simple as possible.

Some of the definitions Mandelbrot offered were, "Something that exhibits invariance under contraction or dilation" (Mandelbrot, 1989, quoted in Carr, 1994) and "A fractal is shape made of parts similar to the whole in some way" (Mandelbrot, 1987, quoted in Feder, 1988). Other definitions have included, "A fractal looks the same whatever the scale" (Feder, 1988) and "A fractal is a geometrical figure in which an identical motif repeats itself on an ever diminishing scale" (Lauwerier, 1991). A neat and complete characterization of fractals is still lacking (Mandelbrot, 1987, quoted in Feder, 1988). In this thesis, The term *fractal* is used in accordance with the rather broad definitions mentioned above or more practically that geometry whose $\log(N(r))$ versus

log(r) plot (see Section 3.3) can be approximated to (a) line(s).

3.2 SELF-SIMILARITY AND SELF-AFFINITY

Fractals are characterized by so-called 'symmetries', which are invariance under dilation and/or contractions (Mandelbrot, 1990). These so-called 'symmetries' can be divided to two categories: *self-similarity* and *self-affinity*.

Self-similarity expresses the idea that each part is a linear geometric reduction of the whole, with the same reduction ratios in all directions (Mandelbrot, 1990). It can be expressed using mathematical symbols as follows. A similarity transformation transforms points $x = (x_1,.....,x_E)$ in E-dimensional space into new points $x' = (rx_1,.....,rx_E)$ with the same value of scaling ratio $r > 0$. (Mandelbrot, 1977; Feder, 1988).

Self-affinity expresses the idea that each part is still a linear geometric reduction of the whole but the reduction ratios in different directions are different (Mandelbrot, 1989). It can be expressed using mathematical symbols as follows. An affine transformation transforms points $x = (x_1,.....,x_E)$ into new points $x' = (r_1x_1,.....,r_Ex_E)$, where

the scaling ratios $r = (r_1,.....,r_E)$ are not all equal (Mandelbrot, 1977; Feder, 1988).

We can treat self-affine geometry as self-similar as long as the scale of the x axis and y axis of two topological dimensions is the same (Carr and Warriner, 1989). For simplicity the word *self-similar* is used for both self-similar and self-affine geometry. When a strict distinction between self-similar and self-affine is required, the distinction is made clear.

3.3 FRACTAL DIMENSION

The fractal dimension of a set is a number which tells how densely the set occupies the metric space in which it lies. It is invariant under various stretching and squeezing of the underlying space. This makes the fractal dimension meaningful as an experimental observable (Barnsley, 1988).

Three kinds of fractal dimensions are characterized by the calculation method. They are similarity dimension, D_s; divider dimension, D_d; and box-counting dimension, D_b (Peitgen and others, 1992).

1) SIMILARITY DIMENSION

Voss (1988) explained concept of similarity dimension, D_s, as follows:

An object normally considered as one-dimensional, a line segment, for example, also possesses a similar scale property. It can be divided into N identical parts each of which is scaled down by the ratio $s = 1/(N)$ from the whole. Similarly, a two-dimensional object, such as a square area in the plain, can be divided into N self-similar parts each of which is scaled down by a factor $s = 1/(\sqrt{N})$. A three dimensional object like a solid cube may be divided into N little cubes each of which is scaled down by a ratio $s = 1/(\sqrt[3]{N})$.

With self-similarity the generalization to fractal dimension is straight forward. A D-dimensional self-similar object can be divided into N smaller copies of itself each of which is scaled down by a factor s where $s = 1/(\sqrt[D]{N})$

$$N = 1/(s^D) \quad \text{.....Eq. 3.1}$$

Taking logarithm of both sides of Equation 3.1,

$$\log(N) = \log(1) - D * \log(s) \quad \text{.....Eq. 3.2}$$

Then, similarity dimension, D_s, is given by

$$D_s = \log(N)/\log(1/s) \quad \text{.....Eq. 3.3}$$

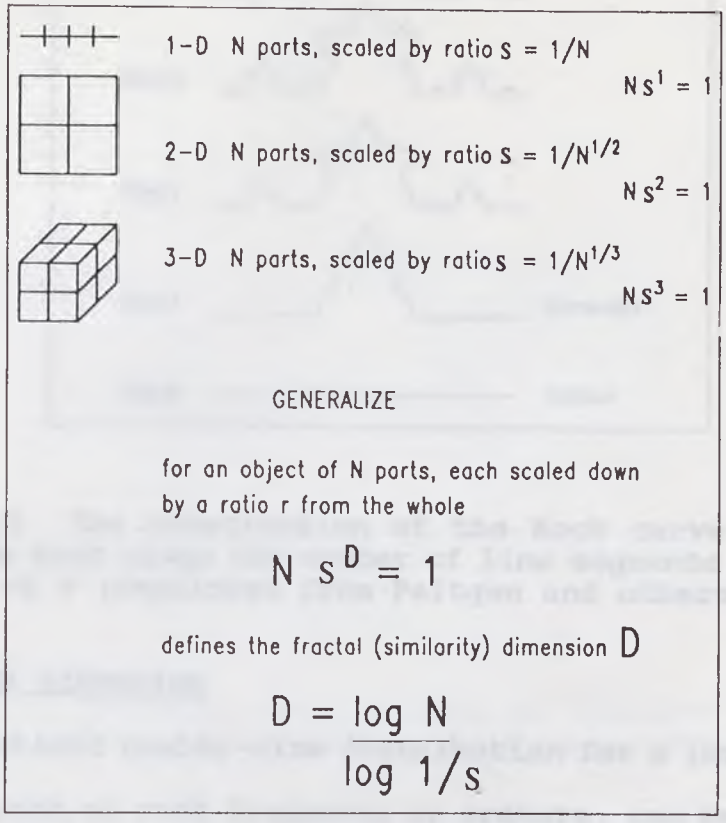

Figure 3.1 Interpretation of standard integer dimension figures in terms of exact self-similarity and extension to non-integer dimensioned fractal (reprinted from Peitgen and others, 1992).

For example, in a classic fractal figure, Koch coastline (Figure 3.2), a segment is replaced by 4 new segments (N = 4) and scaled down ratio, s, is 1/3, then similarity dimension is

$$D_s = \log(4)/\log(3) = 1.2618...$$

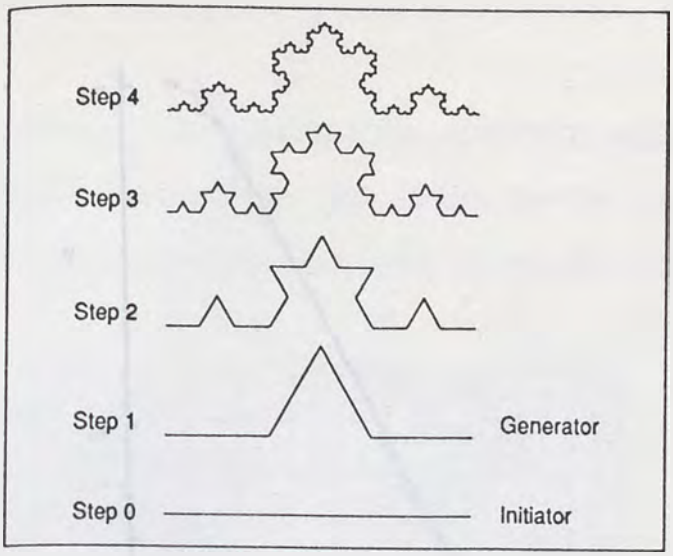

Figure 3.2 The construction of the Koch curve proceeds in stages. In each stage the number of line segments increases by a factor of 4 (reprinted from Peitgen and others, 1992).

2) DIVIDER DIMENSION

The statistical number-size distribution for a large number of objects, such as rock fragments or craters, can be fractal. It is expressed as

$$N(r) = C * r^{-Dd} \quad \text{.....Eq. 3.4}$$

where $N(r)$ is the number of objects whose size (diameter) is greater than r. C is a constant and D_d is divider dimension (Turcotte, 1992).

When we plot the statistical number-size distribution on $\log(N(r))$ versus $\log(r)$ diagram, the plot can be approximated by a straight line which has negative slope (Figure 3.3). Divider dimension, D_d, is obtained as absolute value of the slope.

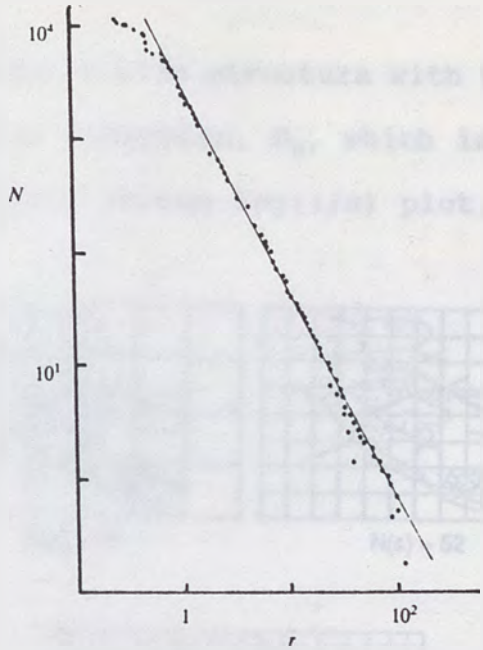

Figure 3.3 Diameter distribution of craters on the Moon (Mizunashi, 1980; reprinted from Takayasu, 1992)

3) BOX-COUNTING DIMENSION

The box-counting dimension, D_d, is the one most used in measurements in all of the sciences. I will explain the box-counting method by paraphrasing Peitgen and others (1992).

We put the structure onto a regular grid with mesh size r, and count the number of grid boxes which contain some of the structure. This gives a number $N(r)$, which depends on our choice of r. Change r to progressively smaller sizes and corresponding number $N(r)$. When we plot the measurement in a $\log(N(r))$ versus $\log(r)$ diagram, the slope of the best fitting

straight line of the plots is the box-counting dimension, D_b.

Figure 3.4. shows a wild structure with two underlying grids. The box-counting dimension, D_b, which is the negative of the slope of $\log(N(s))$ versus $\log(1/s)$ plot, is 1.55.

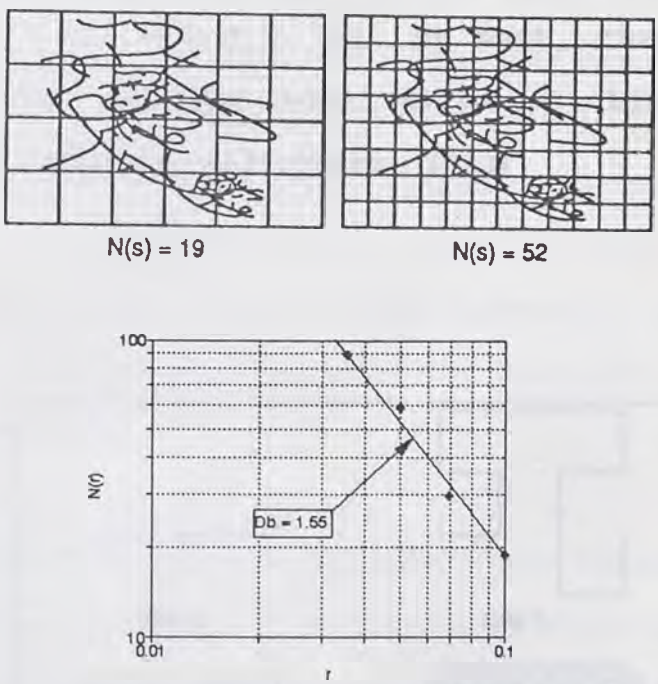

Figure 3.4 The wild structure with two underlying grids and its $\log(N(s))$ versus $\log(1/s)$ plot. D_b = 1.55. (reprinted from Peitgen and others, 1992)

4) RELATIONSHIP OF SIMILARITY, DIVIDER, AND BOX-COUNTING DIMENSIONS

The three kinds of fractal dimensions sometimes indicate the same number and sometimes not. The divider and box-counting

dimensions of the coastline of Great Britain are almost the same. On the other hand, the box-counting dimension will never exceed two, but similarity dimension and divider dimension can exceed two for a curve in the plane when the curve has an overlapping part. For example, the similarity dimension of the curve generated in Figure 3.5 is $D_s = \log(13)/\log(3) = 2.335$ (i.e., $s = 1/3$ and $N = 13$). We must, therefore, be very careful when dealing with different kinds of fractal dimensions (Peitgen and others, 1992).

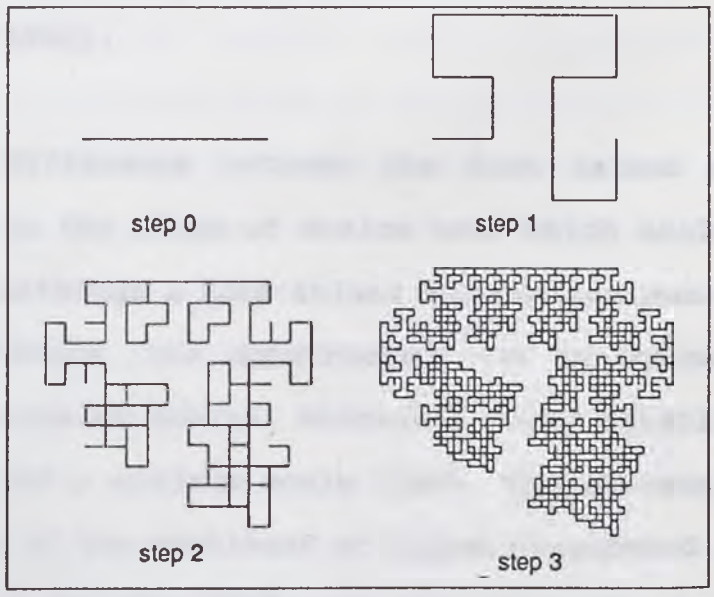

Figure 3.5 Fractal geometry with dimension, D_s = log(13)/log(3) = 2.335 (reprinted from Peitgen and others, 1992).

3.4 STATISTICAL SELF-SIMILARITY AND SCALE LIMITS

No ideal fractal geometry exists in nature. Ideal fractal geometry, such as the Koch island, is fundamentally different from fractal geometry in nature, such as a rocky coast line. The primary difference between the Koch island and a rocky coastline is that between the ideal and the statistical. The Koch island is identically scale invariant at all scales, so its shape is the same at any scale. The shapes of a rocky coastline at different scales look the same but are never exactly the same. Thus a rocky coastline and all fractal geometry in nature are statistically self-similar (Voss, 1988; Turcotte, 1992).

A second difference between the Koch island and a rocky coastline is the range of scales over which scale invariance extends. Although a Koch island has the maximum scale of the origin triangle, the construction can be extended over an infinite range of scales. Whereas a rocky coastline has both a maximum and a minimum scale limit. The maximum scale would be the size of the continent or island considered. The minimum scale would be the scale of the gain of the rocks. The existence of both upper and lower bounds is a characteristic of all naturally occurring fractal systems (Voss, 1988; Turcotte, 1992).

CHAPTER FOUR: HISTORY OF STUDY

"Self-similarity method are a potent tool in study of chance phenomena, including geostatistics, as well as economics and physics." In "How Long is the Coast of Britain?: Statistical Similarity and Fractional Dimension". Mandelbrot (1967)

4.1 FRACTALS IN GEOLOGY AND GEOLOGICAL ENGINEERING

Mandelbrot (1967) discussed Richardson's work, in which characteristics of coast lines are expressed by the negative slope of log(total length) versus log(length of ruler). Mandelbrot named this scale invariant characteristic *fractal*, and showed that very naturalistic landscapes of islands, planets, and canyons can be produced using fractals in "The Fractal Geometry of Nature" (Mandelbrot, 1982). These landscape pictures offer convincing evidence of fractal geometry's importance as a tool for the description of nature (Feder, 1988).

Feder (1988) showed the application of the fractal to fluid mechanics, drainage systems, and weather. Turcotte (1992) and Korvin (1992) showed the application of the fractal to geological and geophysical phenomena such as rock fragmentation, tectonics, fracture, earthquake, and ore grade.

In the geological engineering field, the fractal has been used for analysis of rock fragmentation (ex. Turcotte, 1986), fracture (ex. Merceron and Velde, 1991), fault system (ex. Aviles and Scholz, 1987). Carr and Warriner (1987) and Watters and others (1990) showed that the fractal dimension is effective in measuring the roughness of discontinuities surfaces subjectively and that it can be applied to rock mass classification.

4.2 FRACTALS IN SLOPE STABILITY

A few studies about fractal application to slope stability problems have been done. Some of the studies are in Japanese and are not familiar to the English-speaking scientific community so I will introduce them rather in detail.

SASAKI AND OTHERS (1991)

Sasaki and others (1991) showed that the slope failure size-number distribution had a fractal character. The sample location was rectangular area (265 km long (north-south) and 1 km wide (east-west)) of metamorphic rock area in north-west Japan. The slope failures occurred on the morning of the 23rd in July, 1983, caused by heavy rainfall (about 300 mm maximum). The summary is as follows:

1) The fractal dimension, D, in whole area investigated was 3.3. D was higher in the psammitic schist area (D = 3.5) than in the pelitic schist area (D = 3.2), and was higher in the area of needle-leaf tree woods (D = 3.7) than in that of broad-leaf tree woods (D = 3.1). D was not influenced by the amount of rainfall.

2) The fractal dimension of slope failures and counter lines has positive correlation.

3) The Y axis interception of the approximated line on log(r)-log(N(r)) graph, divided by the area is a parameter that indicates the slope instability and is influenced by rainfall, base rock geology, and vegetation. This parameter was named α_0.

4) Total slope failure volume is calculated as follows:

$$TotalVolume=\sum_{r=1}^{n} V(Lr)=k(1/\alpha_0)^{-(3/D)}\sum_{r=1}^{n} r^{-(3/D)} \quad \text{.....Eq.4.1}$$

where L is the width of greatest slope failure and k is constant. The relationship between α_0 and the amount of rainfall is shown in Figure 4.1. The total volume of slope failure at predicted levels of rainfall can be calculated using the above two relationships.

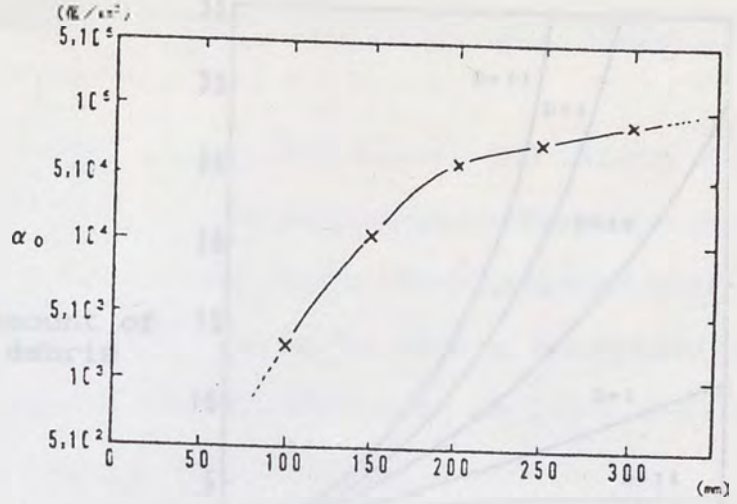

Figure 4.1 Relationship between α_0 and amount of rainfall per day (reprinted from Sasaki, 1991)

5) The relationship between the number of slope failures and the total volume of rock failure, when the greatest failure's volume is 1 is shown in Figure 4.2. When *D* is smaller, the large failure's volume is greater than small failure's erosion. The colluvial of the large failure (landslide) remains on the slope surface. On the other hand, when *D* is greater, small failures dominate and the large failure is eroded by the small failures, so the slope is covered with a thin layer of colluvial. This process explains, why a fractal dimension of a slope failure is high (D = 3.3) and that of a landslide is low (D = 1.2-1.4); and the fractal dimension's positive correlation between mass movement and contour lines.

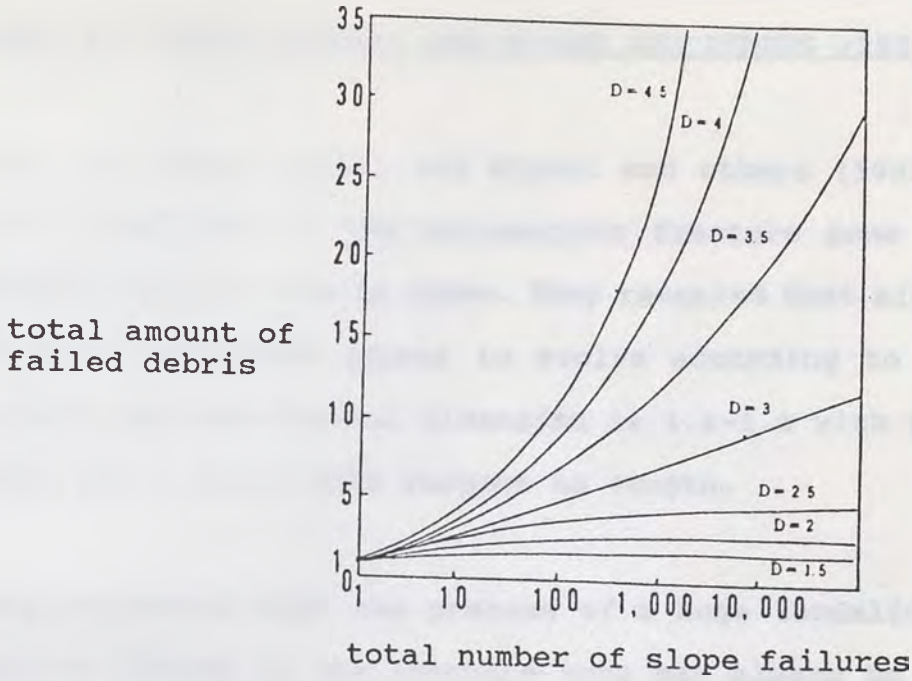

Figure 4.2 Relationship between total number of slope failures and total amount of debris of each fractal dimension. The amount of failed debris of maximum failure is assumed to be one (reprinted from Sasaki, 1991).

6) The fractal dimension of slope failure blocks varies with geology. The difference depended on weathering types. In rock weathered severely at the surface but not deep down, such as granite, small failures are dominant. In rock weathered gradually from the surface to the deep part, such as Tertiary mudstone, large failures are dominant. The fractal dimension is the parameter that indicates the ratio of the number of small to large blocks, so it is bigger in surface weathered geological areas than it is in gradually weathered geological areas.

UENO AND OTHERS (1993); AND HIGAKI AND OTHERS (1993)

Ueno and others (1993) and Higaki and others (1993) studied four landslides in the metamorphic fracture zone along the Median Tectonic Line in Japan. They revealed that slide-blocks in huge landslides appear to evolve according to a fractal pattern and the fractal dimension is 1.2-1.4 with respect to width and 1.4-1.5 with respect to length.

They suggested that the process of a huge landslide forming smaller blocks in the fracture zone may always be the same. They considered that this would indicate that there are similarities between the target area in terms of the extent and gradient of the slope; geology before the initial landslide; and formation of secondary slide planes by destruction and weakening of the ground after the initial landslide.

YOKOI AND OTHERS (1995)

Yokoi and others (1995) revealed that not only whole slide-blocks but also second and third level blocks have fractal character. The fractal character can be explained by self-similar geometry and unique fractal dimensions made by combining second and third level blocks. They also indicated

that fractal dimension of landslide blocks is independent from base rock geology.

A complete copy of Yokoi and others (1995) is shown in Appendix J.

CHAPTER FIVE: METHOD OF STUDY

5.1 INTRODUCTION

The purpose of this paper is to investigate the following points:

1) whether the distribution of landslide blocks has a fractal character and unique fractal dimension;

2) if 1) is positive, how the fractal dimension related to other attributes (properties), such as width, length, and base rock geology;

3) if 1) is positive, whether it is possible to design a model to reveal the landslide block development process; and

4) if 1) is positive, if it is possible to analyze the block development process of landslides.

To examine these hypotheses, data were gathered on 40 huge landslides. The divider method was used to reveal whether landslide block distribution has fractal character and to obtain fractal dimensions. The relationship between fractal dimensions and 15 other attributes of landslides were examined. Because there are so many attributes and samples, correspondence analysis was used to select possible attributes which may be related to the fractal dimensions. After the possible attributes were obtained, the metric attribute of each and the fractal dimensions were plotted on an X-Y graph

to see a more detailed relationship between them. Discriminant analysis was also used to analyze the relationship between categorical attributes and fractal dimensions. Two kinds of simple landslide block distribution models were made and calculated the theoretical fractal dimensions of the models to compare them to the actual fractal dimensions. Finally, block development process was discussed using these results. Data collection and method of measuring fractal dimension will be explained in this chapter. Method of numerical analysis and modeling will be mentioned in the later chapters.

5.2 DATA COLLECTION

COLLECTING THE DATA

Data of 40 landslides were obtained from field investigation, aerial photograph interpretation, topographical map interpretation, and examination of the available literature. Table 5.1 shows the landslide data obtained with designated numbers. Field investigations were performed at No. 1, Midway Bridge; No.2, Boca Ridge; No.3, Palos Verdes; and No.4, Big Rock Mesa, in the summer of 1994. Geotechnical investigations were performed at No.12, Kiritani; No.13, Katsurabara; and No.14,Hitohane, from 1985 to 1987 as projects of Nittoc Construction Company. Geotechnical investigations were performed at No.35, Urushinose; and No.36, Nishinotani, in

1988 as a project of Kisojiban Consultants Co., Ltd. Information on the other landslides were obtained from literature, aerial photography, and topographical maps. Due to the variety of investigative methods, the accuracy of the data for the landslides varies.

LOCATION OF LANDSLIDES

Available landslides are limited because detailed block configuration is necessary to analyze the fractal character of landslides. Figure 5.1 and Table 5.1 show the locations and outlines of landslides investigated.

Landslides Nos. 1 - 8 are located in United States. No. 1, Midway Bridge, and No. 2, Boca Ridge, are located in northern California near the Nevada border. No. 3, Palos Verdes, and No. 4, Big Rock Mesa, are in Los Angeles County in southern California. No. 5, Thistle, is 75 km south of salt Lake City, Utah. No. 6, Upper Gross, and No. 7, Lower Gross, are in north-western Wyoming. No. 8, Meadow Mountain, is in central Colorado. No. 9, Mayunmarca, is located in Peru in South America. No. 10, La Frasse, and No. 11, Arvey, are in Switzerland, Europe.

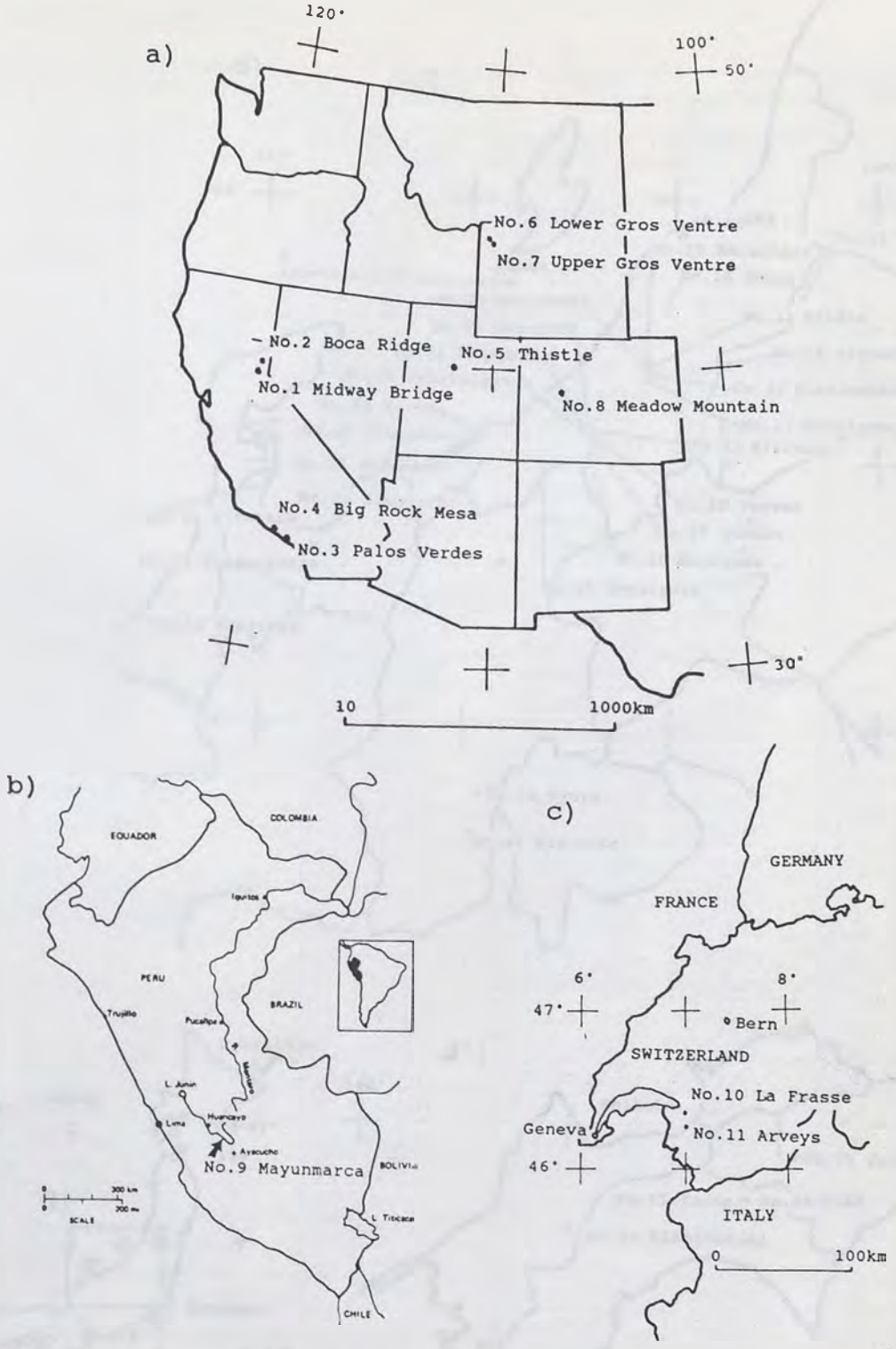

Figure 5.1 Location maps of landslides a) No. 1 to No. 8; b) No. 9; c) No. 10, No. 11; d) No. 12 to No. 34, No.39, No.40; d') No.35 to No. 38

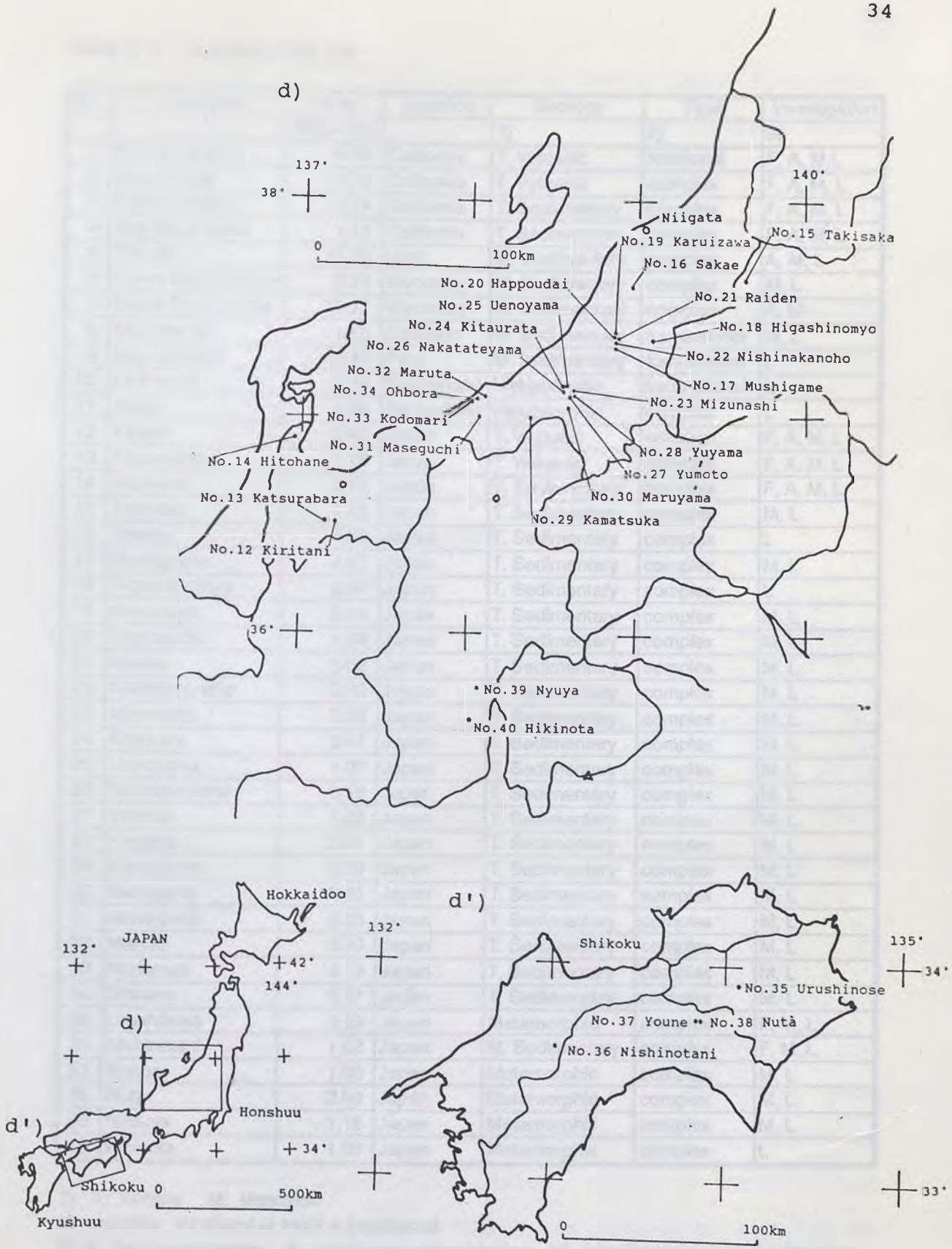
d)
137°
38°
0
100km
140°
Niigata
No.15 Takisaka
No.19 Karuizawa
No.16 Sakae
No.20 Happoudai
No.21 Raiden
No.25 Uenoyama
No.24 Kitaurata
No.18 Higashinomyo
No.26 Nakatateyama
No.22 Nishinakanoho
No.32 Maruta
No.17 Mushigame
No.34 Ohbora
No.23 Mizunashi
No.33 Kodomari
No.31 Maseguchi
No.28 Yuyama
No.14 Hitohane
No.27 Yumoto
No.13 Katsurabara
No.30 Maruyama
No.29 Kamatsuka
No.12 Kiritani
36°
No.39 Nyuya
No.40 Hikinota
Hokkaidoo
JAPAN
132°
42°
144°
d)
Honshuu
d')
34°
Shikoku
0
500km
Kyushuu
d')
132°
Shikoku
135°
34°
No.35 Urushinose
No.37 Youne
No.38 Nutà
No.36 Nishinotani
33°
0
100km

Table 5. 1 Landslide Data List

No.	Landslide	Area	Location	Geology	Type	Investigation
		(Squ. Km)		1)	2)	3)
1	Midway Bridge	4.84	California	T. Volcanic	rotational	F, A, M,L
2	Boca Ridge	13.72	California	T. Volcanic	complex	F, A, M, L
3	Palos Verdes	10.74	California	T. Sedimentary	complex	F, A, M, L
4	Bick Rock Mesa	1.17	California	T. Sedimentary	complex	F, A, M, L
5	Thristle	11.23	Utah	M. Sedimentary	complex	A, M, L
6	Lower Gros Ventre	8.77	Wyoming	M. Sedimentary	complex	M, L
7	Upper Gros Ventre	19.76	Wyoming	M. Sedimentary	complex	A, M
8	Meadow Mt.	1.50	Cololado	M. Sedimentary	translational	M, L
9	Mayunmarca	25.17	Peru	M. Sedimentary	translational	L
10	La Frasse	1.74	Switzerland	Metamorphic	translational	L
11	Arvey	1.25	Switzerland	Metamorphic	complex	L
12	Kiritani	3.40	Japan	T. Volcanic	complex	F, A, M, L
13	Katsurabara	1.46	Japan	T. Volcanic	complex	F, A, M, L
14	Hitohane	3.52	Japan	T. Sedimentary	complex	F, A, M, L
15	Takisaka	1.33	Japan	T. Sedimentary	complex	M, L
16	Sakae	3.30	Japan	T. Sedimentary	complex	L
17	Mushigame	4.47	Japan	T. Sedimentary	complex	M, L
18	Higashinomyo	2.54	Japan	T. Sedimentary	complex	L
19	Karuizawa	5.74	Japan	T. Sedimentary	complex	M, L
20	Happoudai	4.03	Japan	T. Sedimentary	complex	M, L
21	Raiden	5.02	Japan	T. Sedimentary	complex	M, L
22	Nishinakanoho	2.85	Japan	T. Sedimentary	complex	M, L
23	Mizunashi	3.29	Japan	T. Sedimentary	complex	M, L
24	Kitaurata	3.41	Japan	T. Sedimentary	complex	M, L
25	Uenoyama	1.07	Japan	T. Sedimentary	complex	M, L
26	Nakatateyama	3.16	Japan	T. Sedimentary	complex	M, L
27	Yumoto	1.32	Japan	T. Sedimentary	complex	M, L
28	Yuyama	2.81	Japan	T. Sedimentary	complex	M, L
29	Kamatsuka	2.72	Japan	T. Sedimentary	complex	M, L
30	Maruyama	18.08	Japan	T. Sedimentary	complex	M, L
31	Maseguchi	3.93	Japan	T. Sedimentary	complex	M, L
32	Maruta	6.90	Japan	T. Sedimentary	complex	M, L
33	Kodomari	4.19	Japan	T. Sedimentary	complex	M, L
34	Ohbora	6.07	Japan	T. Sedimentary	complex	M, L
35	Urushinose	0.25	Japan	Metamorphic	complex	F, M, L
36	Nishinotani	1.02	Japan	M. Sedimentary	complex	F, M, L
37	Youne	1.00	Japan	Metamorphic	complex	M, L
38	Nuta	2.90	Japan	Metamorphic	complex	M, L
39	Nyuuya	1.18	Japan	Metamorphic	complex	M, L
40	Hikinota	1.00	Japan	Metamorphic	complex	L

1) T: Tertiary M: Mesozoic
2) complex: rotational at head + traslational
3) F; field investigation; A: aerial photo interpretation; M: map interpretation; L: literature

Landslides Nos. 12 - 40 are located in Japan. Among them, Nos. 12 - 34 are in the Hokuriku region in central-northern Honshu (Main) Island. Nos. 35 - 38 are on Shikoku Island. Nos. 39 and 40 are in the Chubu Region in central Honshu.

The concentration of data sources is due to the availability of field and aerial photography, and literature. Outlines and block distribution maps are shown in Appendix A.

5.3 MEASURING FRACTAL DIMENSION

The divider method was used to calculate the fractal dimensions of landslides. As mentioned in Section 3.3, the fractal dimension, D, is obtained as the negative slope of the plot of $\log(N(r))$ versus $\log(r)$, where r is the ruler (divider) length and $N(r)$ is the number of slide-blocks whose width (or length) is greater than the ruler (Carr and Warriner, 1989).

To test the accuracy of the divider method for obtaining fractal dimensions of landslide block distribution, the fractal dimension of ideal self-similar landslides were calculated (Figure 5.2). An ideal self-similar landslide is equivalent to the Sierpinski Gasket, which is traditional fractal geometry by assuming the black triangles are blocks

(Figure 5.3). The reduction factor of the Sierpinski Gasket, s, is 1/2, and the number of pieces into which the structure is divided, b is 3. The number of nth stage total triangles (blocks), num, is calculated as:

$$num=\sum_{m=0}^{n} b^m=\frac{b^{n+1}-1}{b-1}$$

In this case b = 3, so num = $(3^{n+1} - 1)/2$. The smallest base of triangle (width), B_s, is calculated as:

$$B_s= B_0 * (1/2)^n$$

where B_0 is the base of the original triangle (assuming B_0 = 1, B_s = $1/2^n$). Figure 5.4 is the log(N(r)) versus log(r) plot of the Sierpinski Gasket. Divider dimension, D_d, is the negative of the slope of the plot. By changing values of s and b, we can get D_d of various (simple one to complex one) ideal self-similar landslides.

The similarity dimension, D_s, of the Sierpinski Gasket is D_s = log(b)/log(1/s) = log3/log2 = 1.58. Table 5.2.a shows D_d of each stage. As the number of blocks increases, D_d approaches D_s. However, when the number of blocks is 121 or 364, D_d is 9% to 6% higher than D_s.

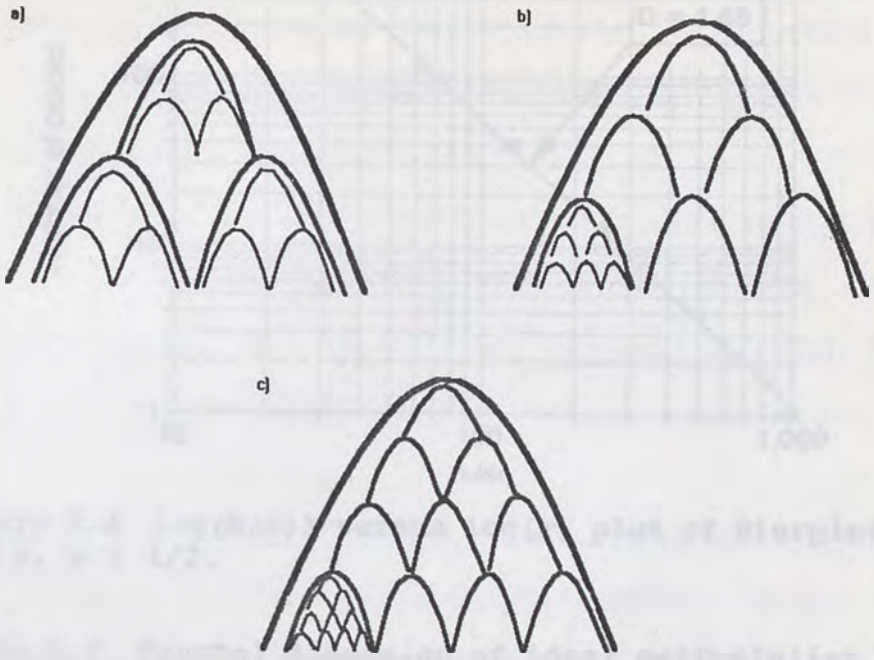

Figure 5.2 Conceptional picture of ideal self-similar landslide. a) $b = 3$, $s = 1/2$; b) $b = 6$, $s = 1/3$; c) $b = 10$, $s = 1/4$

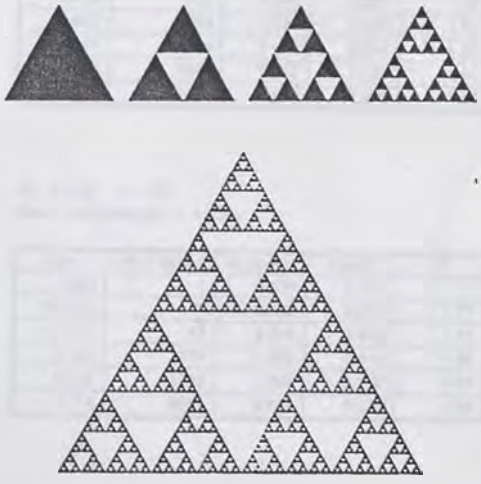

Figure 5.3 Construction and self-similar properties of Sierpinski gasket (Mandelbrot, 1990). By assuming the black triangles are blocks, the Sierpinski gasket is equivalent to ideal self-similar landslide with $b = 3$, $s = 1/2$.

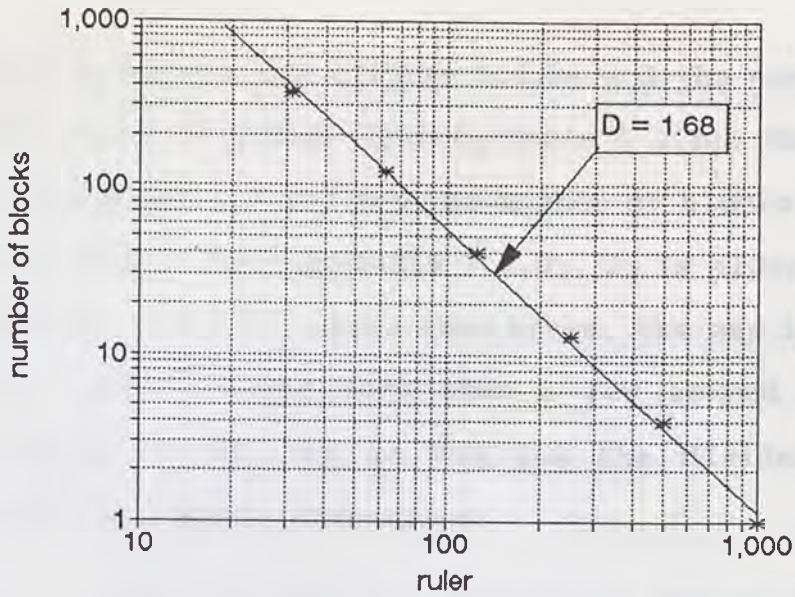

Figure 5.4 log($N(r)$) versus log(r) plot of Sierpinski gasket. $b = 3$, $s = 1/2$.

Table 5.2 Fractal dimension of ideal self-similar landslides

a) b = 3, s = 1/2 (Sierpinski Gasket)
Ds = log(3)/log(2) = 1.585

ruler	# of blocks	log(ruler)	log(#)	Di
1000	1	3.000	0.000	
500	4	2.699	0.602	2
250	13	2.398	1.114	1.85
125	40	2.097	1.602	1.77
62.5	121	1.796	2.083	1.72
31.25	364	1.495	2.561	1.68
15.625	1093	1.194	3.039	1.66
7.8125	3280	0.893	3.516	1.65
3.90625	9841	0.592	3.993	1.63
1.953125	29524	0.291	4.470	1.63

b) b = 6, s = 1/3
Ds = log(6)/log(3) = 1.631

ruler	# of blocks	log(ruler)	log(#)	Di
1000	1	3.000	0.000	
333.33	7	2.523	0.845	1.77
111.11	43	2.046	1.633	1.71
37.04	259	1.569	2.413	1.68
12.35	1555	1.092	3.192	1.67
4.12	9331	0.614	3.970	1.66

b) b = 10, s = 1/4
Ds = log(10)/log(4) = 1.661

ruler	# of blocks	log(ruler)	log(#)	Di
1000	1	3.000	0.000	
250.00	11	2.398	1.041	1.73
62.50	111	1.796	2.045	1.7
15.63	1111	1.194	3.046	1.68
3.91	11111	0.592	4.046	1.68
0.98	111111	-0.010	5.046	1.67

When b = 6 and s = 1/3 (Figure 5.2.b) and the number of blocks is 259, D_d is 3% higher than D_s(Table 5.2.b). When b = 10 and s = 1/4 (Figure 5.2.c); and the number of blocks is 111, D_d is about 2% higher than D_s(Table 5.2.c). D_d is always higher than D_s; however, when b is more than three, the gap is negligible. A huge landslide has more than a few second level blocks (equivalent to b), so we can use the divider method for calculating fractal dimensions.

Width is the maximum separation of the right and left flanks. When the tip of a landslide block is clear, length is measured as the distance between the crown and the tip. When the tip is not clear (as is usual), length is measured as distance between the crown and middle point of both edges of flanks (Figure 5.5).

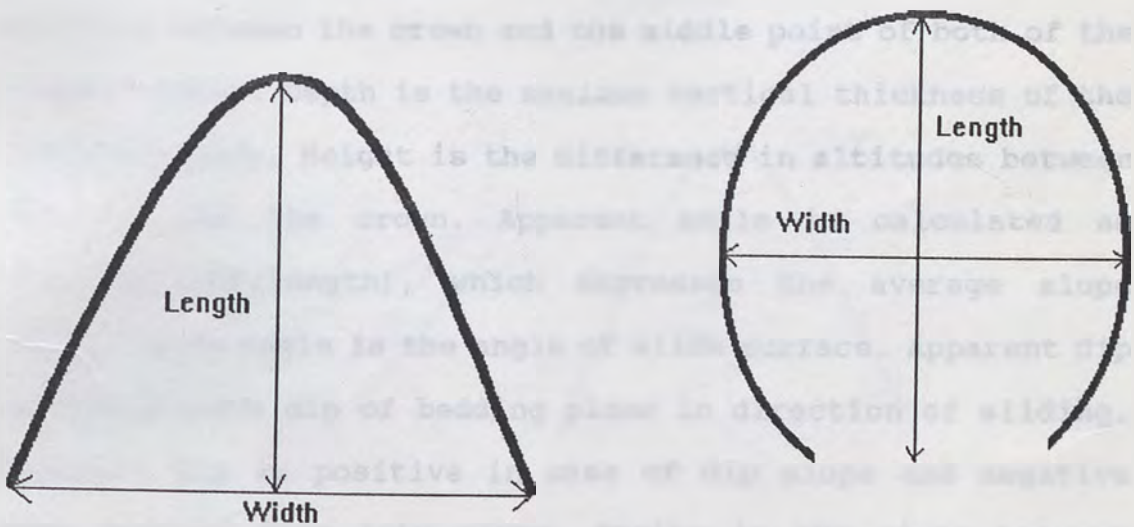

Figure 5.5 Measurement of block width and block length

CHAPTER SIX: LANDSLIDE DATA AND FRACTAL DIMENSION

6.1 LANDSLIDE DATA

The attributes (properties) of landslides gathered are width, length, area, depth, height, ratio of length to width (length/width), apparent angle (arctan(height/length)), slide surface angle (slide angle), topography, block shape, activity, base rock geology, geological period of base rock, strike of base rock, and apparent dip of base rock.

Figure 6.1 shows width, length, area, depth, height, apparent angle, slide angle, apparent dip, and strike. Width is the maximum separation of right and left flanks. Length is measured as the distance between the crown and the tip; however, when the tip is not clear, length is measured as the distance between the crown and the middle point of both of the flanks' edges. Depth is the maximum vertical thickness of the landslide body. Height is the difference in altitudes between the tip and the crown. Apparent angle is calculated as arctan(height/length), which expresses the average slope angle. Slide angle is the angle of slide surface. Apparent dip is approximate dip of bedding plane in direction of sliding. Apparent dip is positive in case of dip slope and negative when bedding dips into slope. Strike is the angle between strike of bedding plane and slide direction.

Figure 6.2 shows the classification of topography. Topography type 1 has concave traverse and longitudinal profiles. Topography type 2 has concave traverse and convex longitudinal profiles. Topography type 3 has convex traverse and longitudinal profiles. Topography type 4 has concave traverse and convex longitudinal profiles (Ministry of Agriculture of Japan, Hokuriku Branch, 1993). Figure 6.3 shows four classifications of block shape. They are triangle, horse shoe, rectangle, and bottle neck.

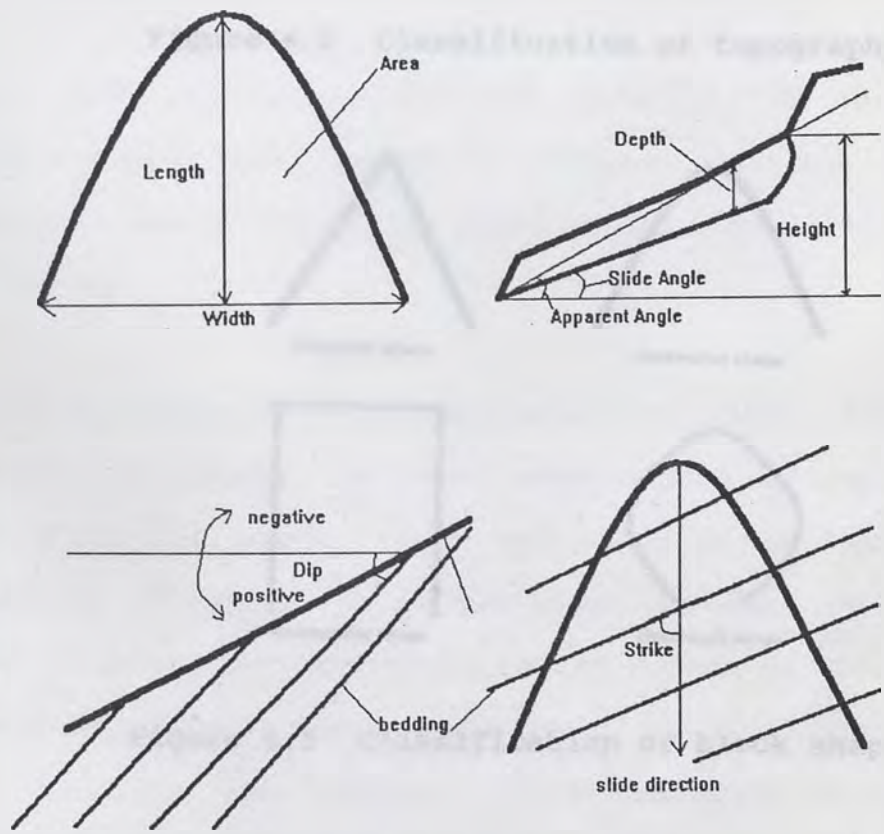

Figure 6.1 measurements of attributes of landslide

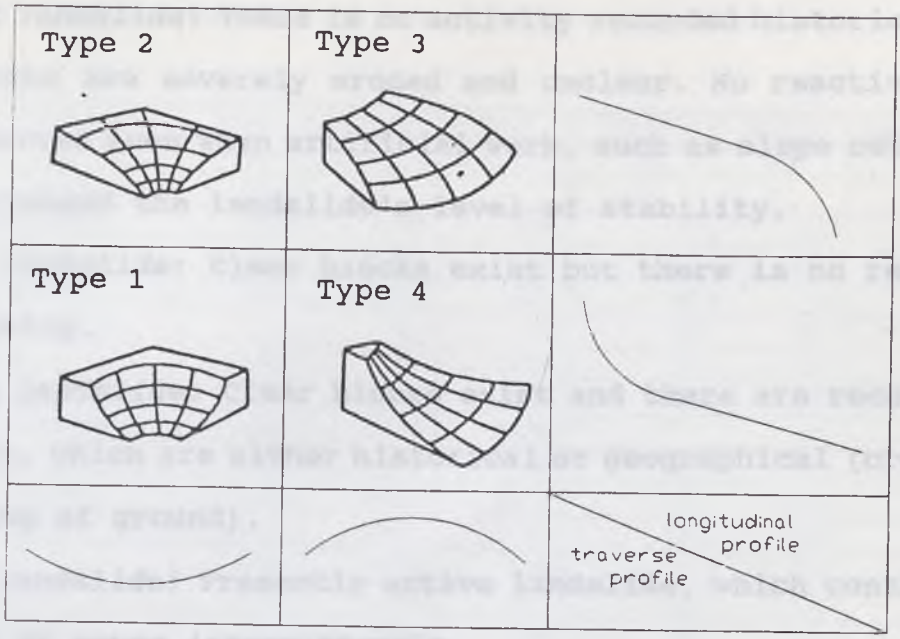

Figure 6.2 Classification of topography

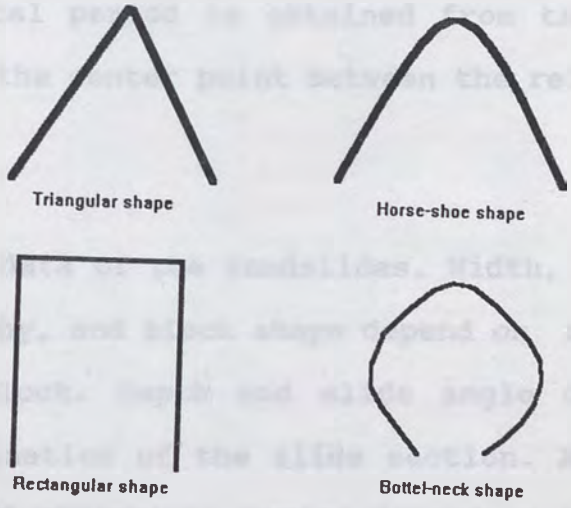

Figure 6.3 Classification of block shape

Activity has four ranks (Ministry of Agriculture of Japan, Hokuriku Branch, 1993). From stable to active, they are:

Ancient landslide: There is no activity recorded historically. The blocks are severely eroded and unclear. No reactivation has occurred even when artificial work, such as slope cutting, has decreased the landslide's level of stability.

Stable landslide: Clear blocks exist but there is no records of activity.

Dormant landslide: Clear blocks exist and there are record of activity, which are either historical or geographical (cracks, inclining of ground).

Active landslide: Presently active landslide, which continues to move or moves intermittently.

Base rock geology is the rock underlain by the landslide debris. Geological period is obtained from the literature. Absolute age is the center point between the relative periods or epochs.

Table 6.1 shows data of the landslides. Width, length, area, height, topography, and block shape depend on recognition of the landslide block. Depth and slide angle depend on the accuracy of estimation of the slide section. Activity, base rock geology, and geological period depend on the quality of field observation and information in the literature. Variance of quantity and quality of information is great and interpretation is subjective, so uncertainness in the data is unavoidable.

Table 6. 1 Landslide Data List

a)

No.	Landslide	Width	Length	Area	Depth	Height	Length/Width
		(m)	(m)	(Squ. Km)	(m)	(m)	
	Simbol	Wd	Ln	Ar	Dp	Ht	Lw
1	Midway Bridge	1,930	1,690	4.84	115	300	0.88
2	Boca Ridge	3,500	3,000	13.72	200	330	0.86
3	Palos Verdes	5,240	2,500	10.74	100	350	0.48
4	Bick Rock Mesa	2,140	960	1.17	120	200	0.45
5	Thristle	3,600	4,030	11.23	80	570	1.12
6	Lower Gros Ventre	3,410	3,600	8.77	130	600	1.06
7	Upper Gros Ventre	4,030	5,500	19.76		640	1.36
8	Meadow Mt.	1,350	2,560	1.50	55	400	1.90
9	Mayunmarca	5,400	6,500	25.17	150	1,500	1.20
10	La Frasse	1,060	2,300	1.74	100	300	2.17
11	Arvey	1,460	1,270	1.25		250	0.87
12	Kiritani	2,330	1,730	3.40	120	200	0.74
13	Katsurabara	1,120	1,760	1.46	80	220	1.57
14	Hitohane	2,360	2,640	3.52	100	180	1.12
15	Takisaka	1,100	1,470	1.33	130	230	1.34
16	Sakae	2,500	1,500	3.30	110	120	0.60
17	Mushigame	2,630	2,240	4.47	150	150	0.85
18	Higashinomyo	2,490	1,230	2.54	130	210	0.49
19	Karuizawa	2,300	3,500	5.74	85	260	1.52
20	Happoudai	2,380	1,750	4.03	85	200	0.74
21	Raiden	2,630	4,380	5.02	70	155	1.67
22	Nishinakanoho	1,280	2,700	2.85	75	220	2.11
23	Mizunashi	2,800	2,550	3.29	100	180	0.91
24	Kitaurata	2,040	1,950	3.41	110	220	0.96
25	Uenoyama	1,810	1,060	1.07	80	85	0.59
26	Nakatateyama	2,700	1,420	3.16	110	285	0.53
27	Yumoto	1,060	1,470	1.32	90	260	1.39
28	Yuyama	2,700	1,190	2.81	80	210	0.44
29	Kamatsuka	1,850	1,750	2.72	85	240	0.95
30	Maruyama	5,650	5,500	18.08	160	350	0.97
31	Maseguchi	2,480	2,130	3.93	80	320	0.86
32	Maruta	3,830	2,480	6.90	65	240	0.65
33	Kodomari	2,830	2,040	4.19	125	130	0.72
34	Ohbora	2,510	3,090	6.07	200	295	1.23
35	Urushinose	600	300	0.25	25	150	0.50
36	Nishinotani	1,200	1,300	1.02	20	350	1.08
37	Youne	1,360	950	1.00	35	250	0.70
38	Nuta	2,054	1,924	2.90		500	0.94
39	Nyuuya	1,210	1,370	1.18	40	550	1.13
40	Hikinota	1,200	1,300	1.00		400	1.08

Table 6. 1 Landslide Data List

b)

No.	Landslide	Aparent Angle	Slide Angle	Topography	Block Shape	Activity
		arctan(H/L)	(degree)			
	Simbol	Aa	Sa	To	Bs	Ac
1	Midway Bridge	10.1	15.0	Type 3	rectangle (3)	stable
2	Boca Ridge	6.3	3.0	Type 4	horse (2)	ancient
3	Palos Verdes	8.0	7.0	Type 1	rectangle (3)	active
4	Bick Rock Mesa	11.8	10.0	Type 3	horse (2)	dormant
5	Thristle	8.1	15.0	Type 3	horse (2)	dormant
6	Lower Gros Ventre	9.5	20.0	Type 3	horse (2)	dormant
7	Upper Gros Ventre	6.6		Type 4	rectangle (3)	ancient
8	Meadow Mt.	8.9	13.0	Type 1	horse (2)	dormant
9	Mayunmarca	13.0	23.0	Type 1	bottle (4)	dormant
10	La Frasse	7.4	15.0	Type 3	rectangle (3)	active
11	Arvey	11.1		Type 2	horse (2)	active
12	Kiritani	6.6	4.0	Type 3	horse (2)	stable
13	Katsurabara	7.1	8.5	Type 3	rectangle (3)	stable
14	Hitohane	3.9	2.5	Type 3	horse (2)	dormant
15	Takisaka	8.9	5.0	Type 4	rectangle (3)	active
16	Sakae	4.6	1.0	Type 1	horse (2)	ancient
17	Mushigame	3.8	4.2	Type 1	horse (2)	dormant
18	Higashinomyo	9.7	7.2	Type 3	rectangle (3)	active
19	Karuizawa	4.2	2.0	Type 3	triangle (1)	ancient
20	Happoudai	6.5	3.0	Type 3	rectangle (3)	stable
21	Raiden	2.0	2.0	Type 4	rectangle (3)	stable
22	Nishinakanoho	4.7	2.5	Type 4	rectangle (3)	stable
23	Mizunashi	4.0	5.0	Type 3	horse (2)	active
24	Kitaurata	6.4	8.5	Type 1	horse (2)	ancient
25	Uenoyama	4.6	3.0	Type 3	horse (2)	ancient
26	Nakatateyama	11.3	8.0	Type 3	rectangle (3)	dormant
27	Yumoto	10.0	9.5	Type 2	bottle (4)	dormant
28	Yuyama	10.0	5.0	Type 2	rectangle (3)	stable
29	Kamatsuka	7.8	3.0	Type 3	rectangle (3)	dormant
30	Maruyama	3.6	2.5	Type 3	triangle (1)	stable
31	Maseguchi	8.5	8.5	Type 3	rectangle (3)	active
32	Maruta	5.5	3.5	Type 3	horse (2)	stable
33	Kodomari	3.6	3.5	Type 2	horse (2)	stable
34	Ohbora	5.5	3.5	Type 1	horse (2)	dormant
35	Urushinose	26.6	25.0	Type 3	horse (2)	stable
36	Nishinotani	15.1	20.0	Type 1	horse (2)	active
37	Youne	14.7	17.0	Type 1	bottle (4)	active
38	Nuta	14.6		Type 3	triangle (1)	active
39	Nyuuya	21.9	25.0	Type 2	horse (2)	active
40	Hikinota	17.1		Type 3	horse (2)	dormant

Table 6. 1 Landslide Data List

c)

No.	Landslide	Geology	Geological Period	Strike	Dip
		(dummy code)	(absolute age: m.y.)	(degree)	(degree)
	Simbol	Ge 1)	Gp	Sk	Di
1	Midway Bridge	latite (7)	M. Miocene (15)	45	90
2	Boca Ridge	latite, diatomite (7)	M. Miocene (15)	60	10
3	Palos Verdes	ss, ms, basalt (4)	M. Miocene (15)	80	15
4	Bick Rock Mesa	ss, ms (4)	E. Miocene (20)	90	-40
5	Thristle	ss, shale, conglo (9)	Creta - Tertiary (65)	90	60
6	Lower Gros Ventre	shale,limestone,ss (9)	Mesozoic (150)	90	20
7	Upper Gros Ventre	shale,limestone,ss (9)	Mesozoic (150)	80	20
8	Meadow Mt.	limestone,ss, ms (9)	Pennsylvanian (300)	90	15
9	Mayunmarca	ss, slitstone (9)	Permian (250)	90	15
10	La Frasse	schist (8)	Jurassic (150)	90	15
11	Arvey	schist (8)	Mesozoic (150)		
12	Kiritani	tuff bressia, andesite (6)	E. Miocene (20)	0	0
13	Katsurabara	tuff bressia, andesite (6)	E. Miocene (20)	70	10
14	Hitohane	mudstone (3)	M. Miocene (15)	80	13
15	Takisaka	tuff, ms (2)	M. Miocene (15)	25	5
16	Sakae	mudstone (3)	L. Pliocene (3)	45	20
17	Mushigame	mudstone (3)	M. Miocene (15)	60	35
18	Higashinomyo	mudstone (3)	M. Miocene (15)	75	-30
19	Karuizawa	mudstone (3)	M. Miocene (15)	50	25
20	Happoudai	mudstone (3)	M. Miocene (15)	80	30
21	Raiden	mudstone (3)	E. Pliocene (5)	0	0
22	Nishinakanoho	mudstone (3)	E. Pliocene (5)	0	0
23	Mizunashi	ms, tuff (2)	M. Miocene (15)	75	30
24	Kitaurata	mudstone (3)	E. Pliocene (5)	80	-30
25	Uenoyama	ms,ss (4)	M. Miocene (15)	80	20
26	Nakatateyama	tuff (1)	M. Miocene (15)	50	20
27	Yumoto	ms, tuff (2)	M. Miocene (15)	90	30
28	Yuyama	ms, tuff (2)	M. Miocene (15)	45	30
29	Kamatsuka	sandstone (5)	M. Miocene (15)	80	-25
30	Maruyama	sandstone (5)	Pleistcene (1)	80	35
31	Maseguchi	mudstone (3)	L. Miocene (8)	90	30
32	Maruta	mudstone (3)	L. Pliocene (3)	70	15
33	Kodomari	ms,ss (4)	L. Miocene (8)	90	15
34	Ohbora	ms,ss (4)	L. Pliocene (3)	30	-15
35	Urushinose	schist (8)	Mesozoic (150)	80	-60
36	Nishinotani	ss, chart, limestone (9)	Mesozoic (150)	0	0
37	Youne	greenstone (8)	Mesozoic (150)	90	15
38	Nuta	greenstone (8)	Mesozoic (150)	90	45
39	Nyuuya	schist (8)	Mesozoic (150)	90	30
40	Hikinota	schist (8)	Mesozoic (150)		

1) ss: sandstone; ms: mudstone

6.2 FRACTAL CHARACTER OF LANDSLIDE BLOCK DISTRIBUTION

The fractal characters of whole blocks (all of first, and second, and third level blocks), second level blocks, and third level blocks from each landslide were examined. Appendix B shows $\log(N(r))$ versus $\log(r)$ plots. Most plots of not only whole blocks but also of second and third level blocks can be approximated to a straight line. This suggests that landslide blocks distribution of whole, second level, and third level blocks have a fractal character.

FRACTAL CHARACTER AND ITS SCALE LIMIT

Yokoi and others (1995) indicated that blocks less than 80 m wide (or long) don't show fractal character (slope of the plot become 0); possible explanations are that the scale of the aerial photography limits interpretation, or that blocks less than 80 m wide (or long) really don't have fractal character. Figure 6.4 shows the relationship between the scale of the aerial photography or topography maps which were used for fractal calculations and the minimum limit of fractal character. Although variance is high, they show a positive proportional relationship. So the limit of fractal character is due to the scale. All fractal geometry in nature should have a limitation, but it could not be found from my data.

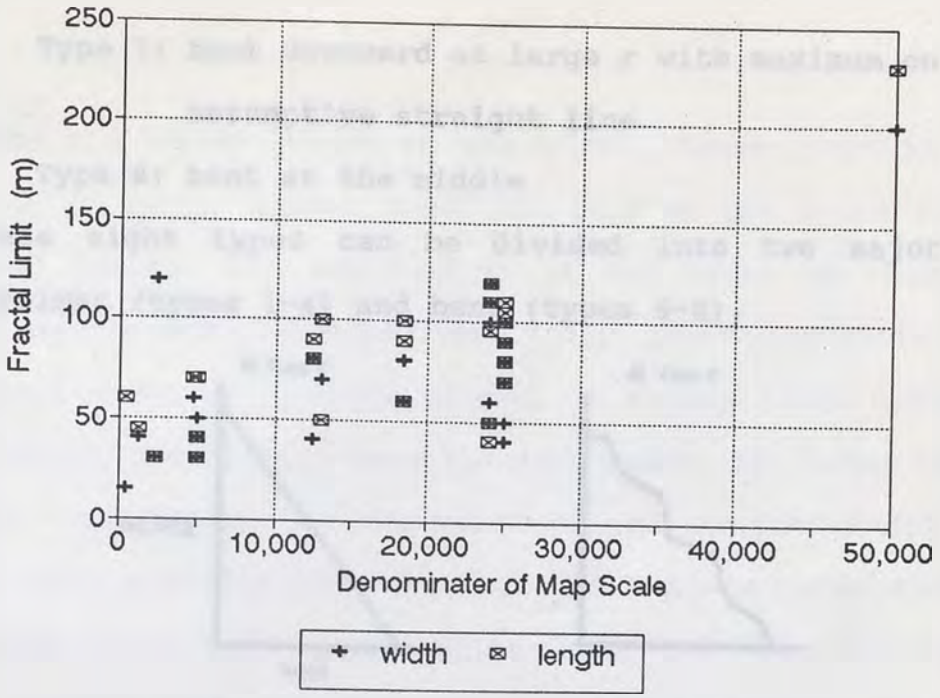

Figure 6.4 Relationship between scale of map or aerial photography and fractal character limit.

SHAPE OF LOG($N(r)$) - LOG(r) PLOTS

Shapes of log($N(r)$) versus log(r) plots were classified into eight types (Figure 6.5). They are as follows:

Type 1: straight

Type 2: zigzag

Type 3: straight with maximum on the left of the assumptive straight line

Type 4: straight with maximum on the right of the assumptive straight line

Type 5: bent downward at large r with maximum on the right of the assumptive straight line

Type 6: bent downward at large r with maximum on the left of assumptive straight line

Type 7: bent downward at large r with maximum on the assumptive straight line

Type 8: bent at the middle

These eight types can be divided into two major types: straight (types 1-4) and bent (types 5-8).

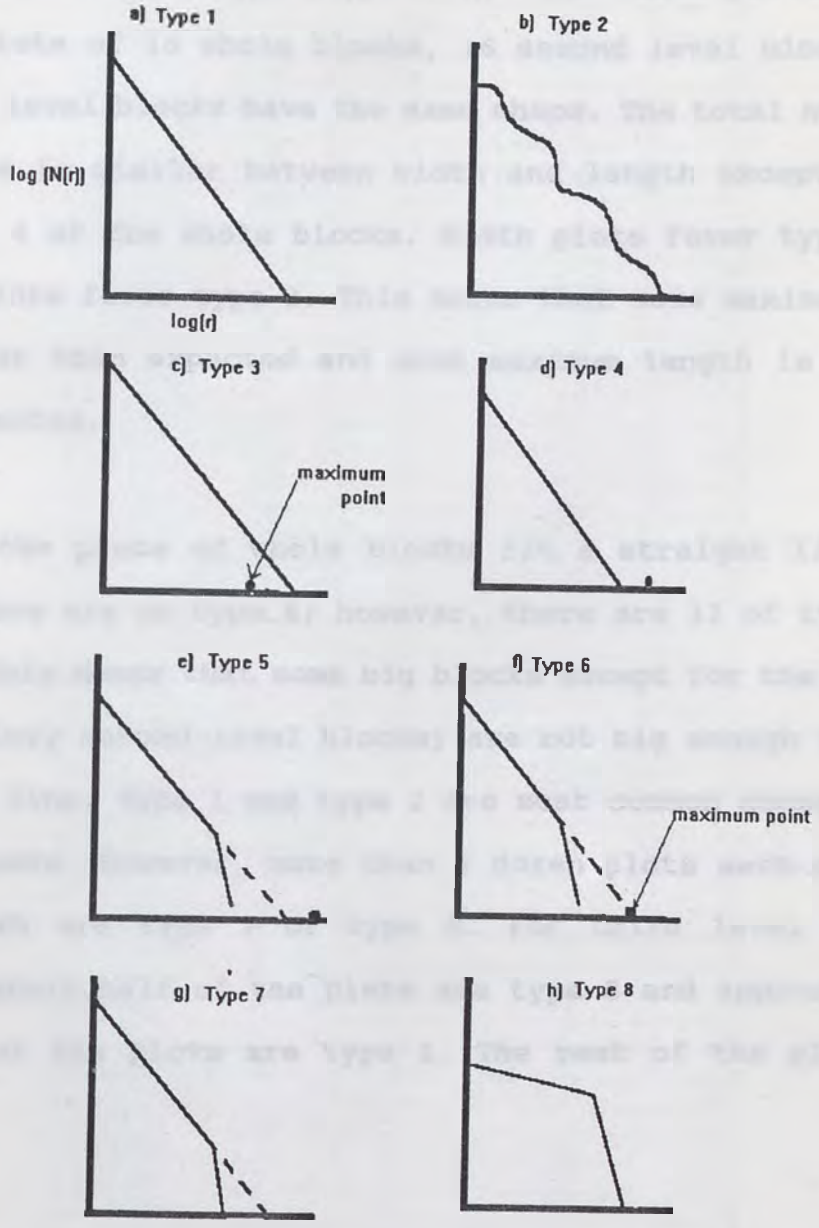

Figure 6.5 Classification of shape of $\log(N(r))$ versus $\log(r)$ plot

Table 6.2 shows shapes of the plots. Three quarters of the plots of whole blocks, more than half of the plots of second level blocks, and one quarter of the plots of third level blocks are straight type (type 1-4). The width plots and the length plots of 16 whole blocks, 16 second level blocks, and 27 third level blocks have the same shape. The total number of each type is similar between width and length except type 3 and type 4 of the whole blocks. Width plots favor type 4 and length plots favor type 3. This means that some maximum width is greater than expected and some maximum length is smaller than expected.

Most of the plots of whole blocks fit a straight line very well. There are no type 8; however, there are 11 of type 5 or type 6. This means that some big blocks except for the maximum ones (mainly second-level blocks) are not big enough to fit a straight line. Type 1 and type 2 are most common among second level blocks. However, more than a dozen plots each of width and length are type 7 or type 8. For third level blocks, approximately half of the plots are type 8 and approximately a dozen of the plots are type 1. The rest of the plots are type 7.

Table 6.2 List of shape of log($N(r)$) versus log(r) plot

No.		Whole Blocks		2nd Level Blocks		3rd Level Blocks	
		Width	length	Width	Length	Width	Length
1	Midway Bridge	5	5	1	2	1	1
2	Boca Ridge	1	1	2	1	8	8
3	Palos Verdes	5	7	2	8	8	8
4	Big Rock Mesa	5	3	8	8	1	1
5	Thristle	2	2	1	1	8	8
6	Lower Gross	2	2	8	1	8	8
7	Upper Gros	6	1	8	1	8	1
8	Meadow	2	6	1	8	8	8
9	Mayunmarca	1	1	1	1	8	8
10	La Frasse	2	2	1	1	8	8
11	Arvey	2	2	2	2	1	1
12	Kiritani	1	3	1	7	8	8
13	Katsurabara	2	2	1	1	7	8
14	Hitohane	5	5	8	7	8	8
15	Takisaka	1	1	7	1	7	7
16	Sakae	2	6	1	1	8	8
17	Mushigame	2	6	1	8	7	7
18	Higashinomyo	4	3	1	8	8	7
19	Karuizawa	4	5	1	8	7	1
20	Happoudai	1	1	1	8	8	7
21	Raiden	6	5	8	2	1	1
22	Nishinakanoho	1	5	8	8	8	8
23	Mizunashi	5	5	2	2	1	1
24	Kitaurata	2	2	7	8	1	1
25	Uenoyama	4	1	1	1	7	1
26	Nakatateyama	4	1	8	1	1	1
27	Yumoto	2	1	1	1	1	8
28	Yuyama	4	2	1	1	1	1
29	Kamatsuka	6	2	7	8	1	1
30	Maruyama	2	1	2	8	7	8
31	Maseguchi	5	4	7	8	8	7
32	Maruta	4	1	7	1	8	7
33	Kodomari	2	2	2	2	8	8
34	Ohbora	1	2	1	1	1	7
35	Urushinose	2	1	1	7	8	8
36	Nishinotani	5	6	8	7	7	7
37	Youne	2	2	1	1	8	1
38	Nuta	6	2	8	8	8	8
39	Nyuya	2	2	1	2	8	8
40	Hikinota						
	1 Total	7	11	19	16	11	13
	2 Total	15	13	6	6	0	0
	3 Total	0	3	0	0	0	0
	4 Total	6	1	0	0	0	0
	5 Total	7	6	0	0	0	0
	6 Total	4	4	0	0	0	0
	7 Total	0	1	5	4	7	8
	8 Total	0	0	9	13	21	18

If the plots are classified into the two types, straight and bent, there are eight possible combinations of whole blocks, second level blocks, and third level blocks (Table 6.3). 27% of the plots are the same type (all straight or all bent). 39% of the plots are of a straight-straight-bent pattern.

Table 6.3 Combination of shapes of log($N(r)$) versus log(r) of whole, 2nd, and third level blocks

No.		Shape		Total			
		Width	length		width	length	Total
1	Midway Bridge	BSS	BSS	SSS	4 (10.2%)	6 (15.4)	10 (12.8)
2	Boca Ridge	SSB	SSB	SSB	18 (46.2)	12 (30.8)	30 (38.5)
3	Palos Verdes	BSB	BBB	SBS	2 (5.1)	3 (7.7)	5 (6.4)
4	Big Rock Mesa	BBS	SBS	SBB	4 (10.3)	7 (17.9)	11 (14.1)
5	Thristle	SSB	SSB	BSS	2 (5.1)	3 (7.7)	5 (6.4)
6	Lower Gross	SBB	SSB	BSB	1 (2.6)	1 (2.6)	2 (2.6)
7	Upper Gros	BBB	SSS	BBS	3 (2.7)	1 (2.6)	4 (5.1)
8	Meadow	SSB	BBB	BBB	5 (12.8)	6 (15.4)	11 (14.1)
9	Mayunmarca	SSB	SSB				
10	La Frasse	SSB	SSB				
11	Arvey	SSS	SSS				
12	Kiritani	SSB	SBB				
13	Katsurabara	SSB	SSB	First Character: Shape of whole blocks			
14	Hitohane	BBB	BBB	2nd Character: Shape of 2nd level blocks			
15	Takisaka	SBB	SSB	3rd Character: Shape of 3rd level blocks			
16	Sakae	SSB	BSB				
17	Mushigame	SSB	BBB				
18	Higashinomyo	SSB	SBB				
19	Karuizawa	SSB	BBS				
20	Happoudai	SSB	SBB				
21	Raiden	BBS	BSS				
22	Nishinakanoho	SBB	BBB				
23	Mizunashi	BSS	BSS				
24	Kitaurata	SBS	SBS				
25	Uenoyama	SSB	SSS				
26	Nakatateyama	SBS	SSS				
27	Yumoto	SSS	SSB				
28	Yuyama	SSS	SSS				
29	Kamatsuka	BBS	SBS				
30	Maruyama	SSB	SBB				
31	Maseguchi	BBB	SBB				
32	Maruta	SBB	SSB				
33	Kodomari	SSB	SSB				
34	Ohbora	SSS	SSB				
35	Urushinose	SSB	SBB				
36	Nishinotani	BBB	BBB				
37	Youne	SSB	SSS				
38	Nuta	BBB	SBB				
39	Nyuya	SSB	SSB				
40	Hikinota						

6.3 FRACTAL DIMENSION OF LANDSLIDE BLOCK DISTRIBUTIONS

The fractal dimension, D, is obtained as the negative slope of the $\log(N(r))$ versus $\log(r)$ plot, where r is the ruler length and $N(r)$ is the number of slide-blocks whose width (or length) is greater than the ruler (Carr and Warriner, 1987, see Section 3.3 and Section 5.3).

Table 6.4 shows fractal dimensions of landslide distribution. Fractal dimension of width, D_W, are from 1.11 (No. 35, Urushinose) to 1.64 (No.14, Hitohane) and the mean is 1.37. Fractal dimensions of length, D_L, are from 1.17 (No.6, Lower Gross) to 1.64 (No. 23, Mizunashi) and the mean is 1.41. Rates of D_W to D_L are from 0.79 (No.16, Sakae) to 1.17 (No.10, La frasse) and the mean is 0.97. That means D_W is slightly smaller than D_L. Fractal dimension of landslide block distribution is about 10% higher than that of British coast.

With respect to the means, fractal dimension of second level blocks, D_{2nd}, is 23% (width) and 26% (length) higher than fractal dimension of whole blocks, D_{whole}. Fractal dimension of third level blocks, D_{3rd}, is 218% (width) and 206% (length) higher than D_{whole}.

Table 6.4 Fractal dimension of landslide block distribution

No.		Width			Length			Width/Length		
		Whole	2nd	3rd	Whole	2nd	3rd	Whole	2nd	3rd
1	Midway Bridge	1.53	2.77	3.27	1.42	1.79	2.90	1.08	1.55	1.13
2	Boca Ridge	1.33	1.49	3.62	1.29	1.35	3.01	1.03	1.10	1.20
3	Palos Verdes	1.48	1.84	2.21	1.57	2.59	2.08	0.94	0.71	1.06
4	Big Rock Mesa	1.48	1.86	3.39	1.53	1.63	3.37	0.97	1.14	1.01
5	Thristle	1.32	1.31	2.13	1.29	1.15	2.08	1.02	1.14	1.02
6	Lower Gross	1.28	1.30	2.17	1.17	1.62	2.89	1.09	0.80	0.75
7	Upper Gros	1.30	1.44	3.51	1.20	1.36	2.05	1.08	1.06	1.71
8	Meadow	1.43	2.15	3.41	1.24	1.48	2.41	1.15	1.45	1.41
9	Mayunmarca	1.52	1.64	2.31	1.40	2.10	2.02	1.09	0.78	1.14
10	La Frasse	1.59	2.13	3.57	1.36	2.11	3.49	1.17	1.01	1.02
11	Arvey	1.24	1.58	2.24	1.42	1.54	2.33	0.87	1.03	0.96
12	Kiritani	1.24	1.36	2.34	1.34	1.46	3.34	0.93	0.93	0.70
13	Katsurabara	1.38	1.37	1.90	1.44	1.82	2.26	0.96	0.75	0.84
14	Hitohane	1.64	1.84	3.80	1.66	1.83	3.96	0.99	1.01	0.96
15	Takisaka	1.36	1.57	2.86	1.30	1.44	3.02	1.05	1.09	0.95
16	Sakae	1.12	1.22	2.41	1.42	2.36	2.00	0.79	0.52	1.21
17	Mushigame	1.31	1.72	3.17	1.56	1.67	2.59	0.84	1.03	1.22
18	Higashinomyo	1.22	1.51	2.88	1.29	1.58	2.56	0.95	0.96	1.13
19	Karuizawa	1.61	2.30	3.29	1.43	1.82	3.08	1.13	1.26	1.07
20	Happoudai	1.35	1.78	2.63	1.46	1.73	3.25	0.92	1.03	0.81
21	Raiden	1.53	2.03	3.16	1.48	1.85	3.19	1.03	1.10	0.99
22	Nishinakanoho	1.51	2.09	3.53	1.35	2.00	3.32	1.12	1.05	1.06
23	Mizunashi	1.60	1.84	3.27	1.64	2.60	3.18	0.98	0.71	1.03
24	Kitaurata	1.19	1.13	3.95	1.43	1.41	4.17	0.83	0.80	0.95
25	Uenoyama	1.25	1.34	2.45	1.32	1.38	3.50	0.95	0.97	0.70
26	Nakatateyama	1.44	1.96	2.89	1.58	2.68	2.99	0.91	0.73	0.97
27	Yumoto	1.40	1.41	3.41	1.30	1.86	3.00	1.08	0.76	1.14
28	Yuyama	1.40	2.15	3.50	1.47	1.89	4.14	0.95	1.14	0.85
29	Kamatsuka	1.46	1.96	2.49	1.55	1.94	2.28	0.94	1.01	1.09
30	Maruyama	1.34	1.45	2.92	1.33	1.65	2.77	1.01	0.88	1.05
31	Maseguchi	1.49	1.39	3.56	1.54	1.53	3.15	0.97	0.91	1.13
32	Maruta	1.37	1.46	3.58	1.36	1.83	3.50	1.01	0.80	1.02
33	Kodomari	1.21	1.29	3.42	1.38	1.43	2.88	0.88	0.90	1.19
34	Ohbora	1.18	1.39	2.34	1.33	1.63	2.39	0.89	0.85	0.98
35	Urushinose	1.11	1.33	3.24	1.31	1.76	3.11	0.85	0.76	1.04
36	Nishinotani	1.54	2.09	2.82	1.52	2.00	2.65	1.01	1.05	1.06
37	Youne	1.35	1.77	2.71	1.62	2.11	2.29	0.83	0.84	1.18
38	Nuta	1.46	1.58	3.46	1.50	1.47	3.24	0.97	1.07	1.07
39	Nyuya	1.22	1.73	2.65	1.30	1.79	2.77	0.94	0.97	0.96
40	Hikinota	1.19								
	Average	1.37	1.68	2.99	1.41	1.78	2.90	0.97	0.95	1.03
	Standard deviation	0.141	0.353	0.542	0.122	0.351	0.565	0.094	0.199	0.180

D_{3rd} is about 10% lower than the fractal dimension of slope failure (D = 3.3, Sasaki and others, 1991). This may be because their common failure mechanics (rotational) and size, while first and second level blocks are bigger and their failure mechanics is complex of rotational at the head and translational.

Fractal dimension of the length of whole blocks, $D_{L\text{-}whole}$, is 3% higher than fractal dimension of the width of whole blocks, $D_{W\text{-}whole}$, and fractal dimension of the length of second level blocks, $D_{L\text{-}2nd}$, is 5% higher than fractal dimension of the width of second level blocks, $D_{W\text{-}2nd}$. However, fractal dimension of the length of third level blocks, $D_{L\text{-}3rd}$, is 3% lower than fractal dimension of the width of third level blocks, $D_{W\text{-}3rd}$. Neither of these relationships can be proved by a large sample statistical test (Dietrich and Kearns, 1989).

Figure 6.6 shows the relationship between D_W versus D_L; $D_{W\text{-}2nd}$ versus $D_{L\text{-}2nd}$; $D_{W\text{-}3rd}$ versus $D_{L\text{-}3rd}$. They have a positive relationship (coefficient of correlation, r, is from 0.39 ($D_{W\text{-}2nd}$ versus $D_{L\text{-}2nd}$) to 0.63 ($D_{W\text{-}3rd}$ versus $D_{L\text{-}3rd}$)). Figure 6.7 shows the relationship between D_{whole}, D_{2nd} and D_{3rd}. Although the number of third-level blocks is much greater than the number of second-level blocks, D_{whole} and D_{2nd} correlate better than D_{whole} and D_{3rd}.

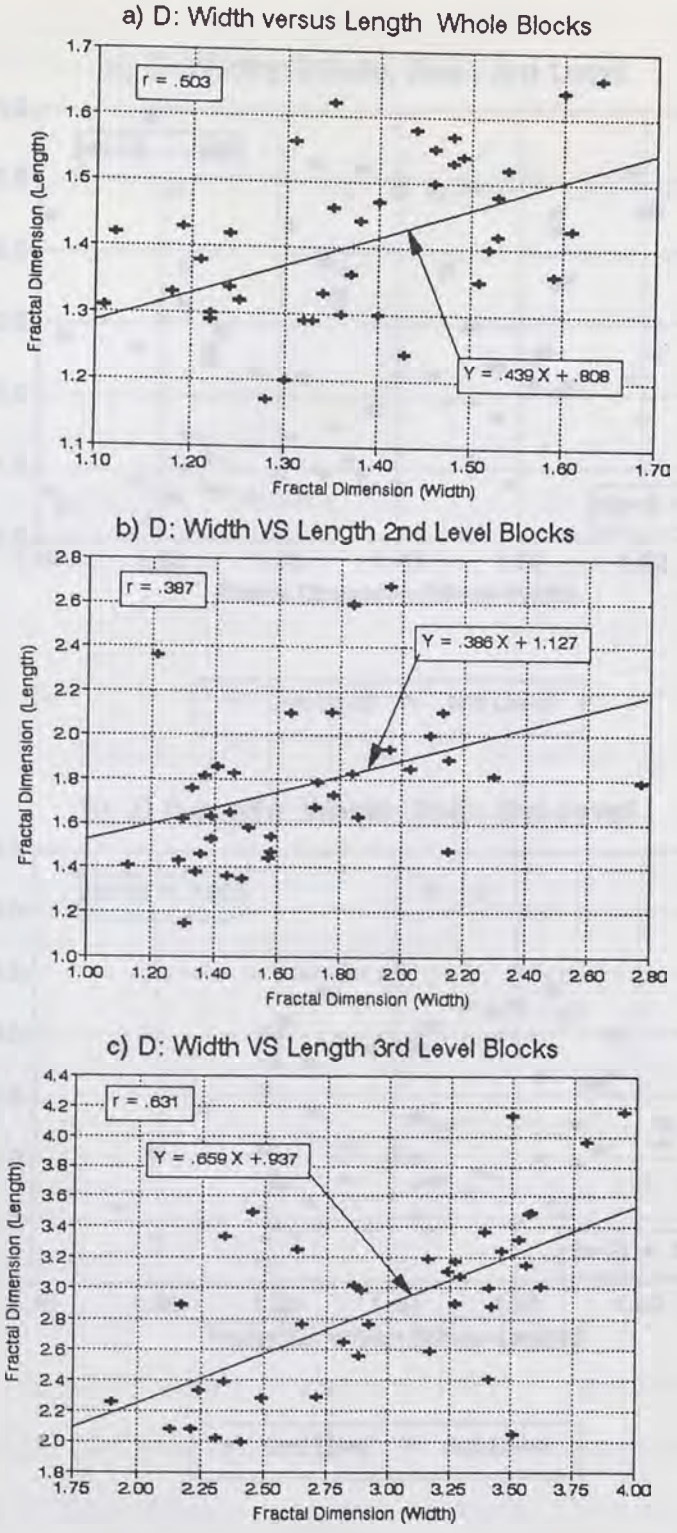

Figure 6.6 Relationship between fractal dimension of width and length. a) $D_{W\text{-}whole}$ versus $D_{L\text{-}whole}$ b) $D_{W\text{-}2nd}$ versus $D_{L\text{-}2nd}$ c) $D_{W\text{-}3rd}$ versus $D_{L\text{-}3rd}$

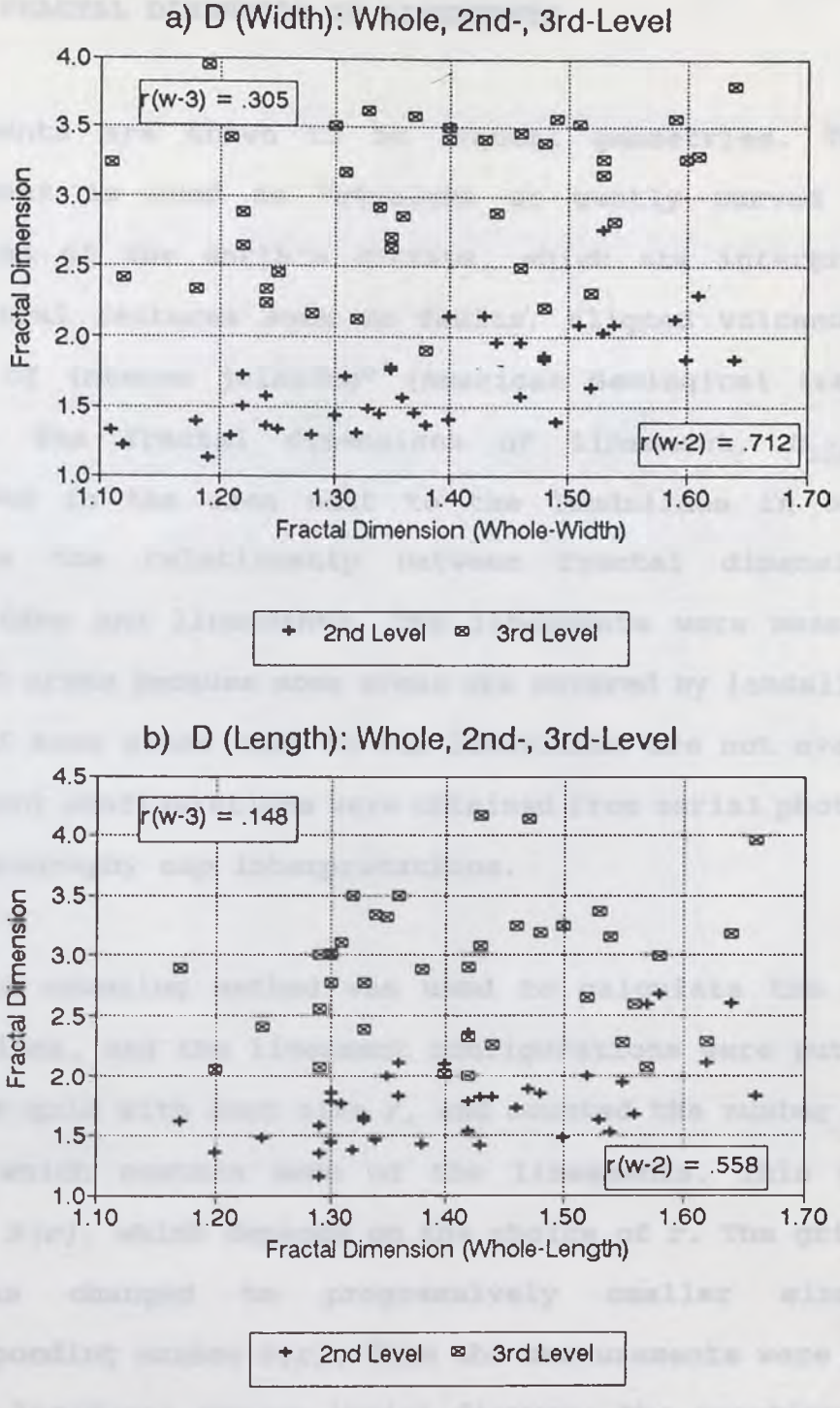

Figure 6.7 Relationship between fractal dimension of whole blocks; and second and third level blocks. a) $D_{W\text{-}whole}$ versus $D_{W\text{-}2nd}$ and $D_{W\text{-}3rd}$ b) $D_{L\text{-}whole}$ versus $D_{L\text{-}2nd}$ and $D_{L\text{-}3rd}$

6.4 FRACTAL DIMENSION OF LINEAMENTS

Lineaments are known to be fractal geometries. The term *lineament* is used as "straight or gently curved lengthy features of the earth's surface, which are interpreted as structural features such as faults, aligned volcanoes, and zones of intense jointing" (American Geological Institute, 1976). The fractal dimensions of lineament, D_{Lin}, were measured in the area next to the landslides in order to examine the relationship between fractal dimensions of landslides and lineaments. The lineaments were measured in only 19 areas because some areas are covered by landslides and maps of some areas next to the landslides are not available. Lineament configurations were obtained from aerial photography and topography map interpretations.

The box counting method was used to calculate the fractal dimensions, and the lineament configurations were put onto a regular grid with mesh size r, and counted the number of grid boxes which contain some of the lineaments. This gives a number $N(r)$, which depends on the choice of r. The grid size, r, was changed to progressively smaller sizes and corresponding number $N(r)$. Then the measurements were plotted on the $\log(N(r))$ versus $\log(r)$ diagram; the negative of the slope of the best fitting straight line of the plots is the fractal dimension of the lineaments, D_{Lin} (Peitgen and others,

1992, see section 3.3). The grid size, r, was changed from 2,000m to 62.5m. Appendix D shows $\log(N(r))$ versus $\log(r)$ plots and Table 6.5 shows fractal dimensions of lineaments.

Table 6.5 Fractal dimension of lineament and landslide block distribution

No.		Width			Length			Linearment
		Whole	2nd	3rd	Whole	2nd	3rd	
1	Midway Bridge	1.53	2.77	3.27	1.56	1.79	2.90	1.637
2	Boca Ridge	1.33	1.49	3.62	1.29	1.35	3.01	1.564
3	Palos Verdes	1.48	1.84	2.21	1.57	2.59	2.08	1.795
4	Big Rock Mesa	1.48	1.86	3.39	1.53	1.63	3.37	1.747
5	Thristle	1.32	1.31	2.13	1.29	1.15	2.08	1.690
7	Upper Gros	1.30	1.44	3.51	1.20	1.36	2.05	1.703
12	Kiritani	1.24	1.36	2.34	1.34	1.46	3.34	1.668
13	Katsurabara	1.38	1.37	1.90	1.44	1.82	2.26	1.759
15	Takisaka	1.36	1.57	2.86	1.30	1.44	3.02	1.717
17	Mushigame	1.31	1.72	3.17	1.56	1.67	2.59	1.711
19	Karuizawa	1.61	2.30	3.29	1.43	1.82	3.08	1.701
20	Happoudai	1.35	1.78	2.63	1.46	1.73	3.25	1.685
21	Raiden	1.53	2.03	3.16	1.48	1.85	3.19	1.736
22	Nishinakanoho	1.51	2.09	3.53	1.35	2.00	3.32	1.715
24	Kitaurata	1.19	1.13	3.95	1.43	1.41	4.17	1.710
31	Maseguchi	1.49	1.39	3.56	1.54	1.53	3.15	1.665
32	Maruta	1.37	1.46	3.58	1.36	1.83	3.50	1.643
37	Youne	1.35	1.77	2.71	1.62	2.11	2.29	1.745
39	Nyuya	1.22	1.73	2.65	1.30	1.79	2.77	1.647
	Average	1.39	1.71	3.02	1.42	1.70	2.92	1.697
	Standard deviation	0.114	0.384	0.572	0.117	0.318	0.555	0.051

Figure 6.8 shows the relationship between the fractal dimension of lineament, D_{Lin}, and the fractal dimension of landslide block distribution, D_{Land}. Although the variance is great, D_{whole} and D_{2nd} correlate to D_{Lin}. D_L correlates to D_{Lin} better than D_W. D_{2nd} has relatively good correlation to D_{Lin} and the mean of both fractal dimensions is very close, however D_{Land} was measured by the divider method and D_{Lin} was measured by the box counting method, so the agreement might be meaningless. On the other hand, D_{3rd} doesn't show any correlation to D_{Lin} (Figure 6.9).

This result suggests that lineaments (discontinuities) affect the propagation process of second level blocks but not of third level blocks. One reason may be that the size of lineaments is similar to that of second level blocks. D_{2nd} correlates to D_{whole} better than D_{3rd} despite the fact that the number of third level blocks is much greater than the number of second level blocks, so lineaments are considered an important factor influencing the fractal dimension of landslide block distribution.

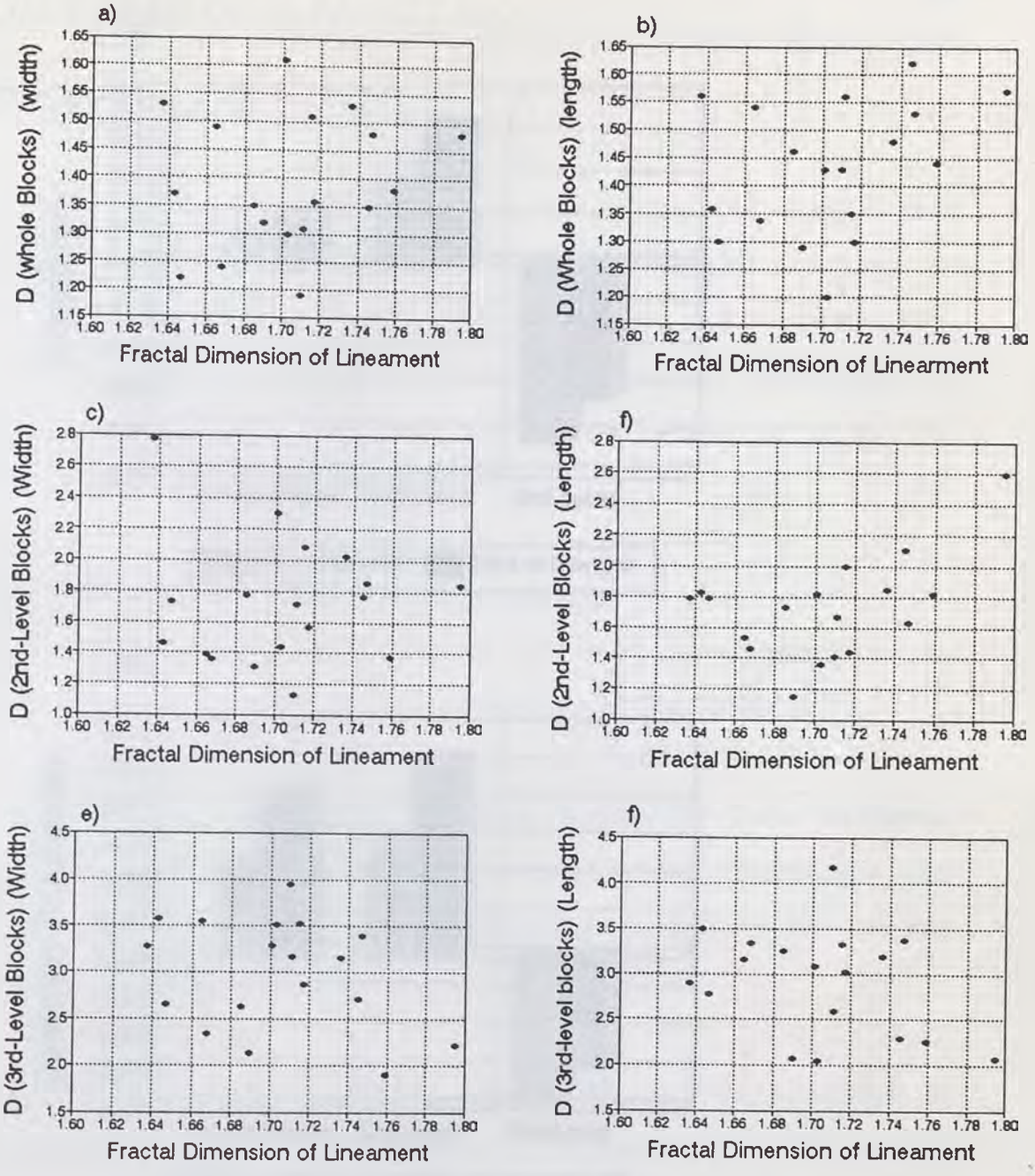

Figure 6.8 Relationship between fractal dimension of lineament, D_{Lin} and fractal dimension of landslide block. a) D_{Lin} versus $D_{W\text{-}whole}$ b) D_{Lin} versus $D_{L\text{-}whole}$ c) D_{Lin} and $D_{W\text{-}2nd}$ d) D_{Lin} versus $D_{L\text{-}2nd}$ e) D_{Lin} versus $D_{W\text{-}3rd}$ f) D_{Lin} and $D_{L\text{-}3rd}$

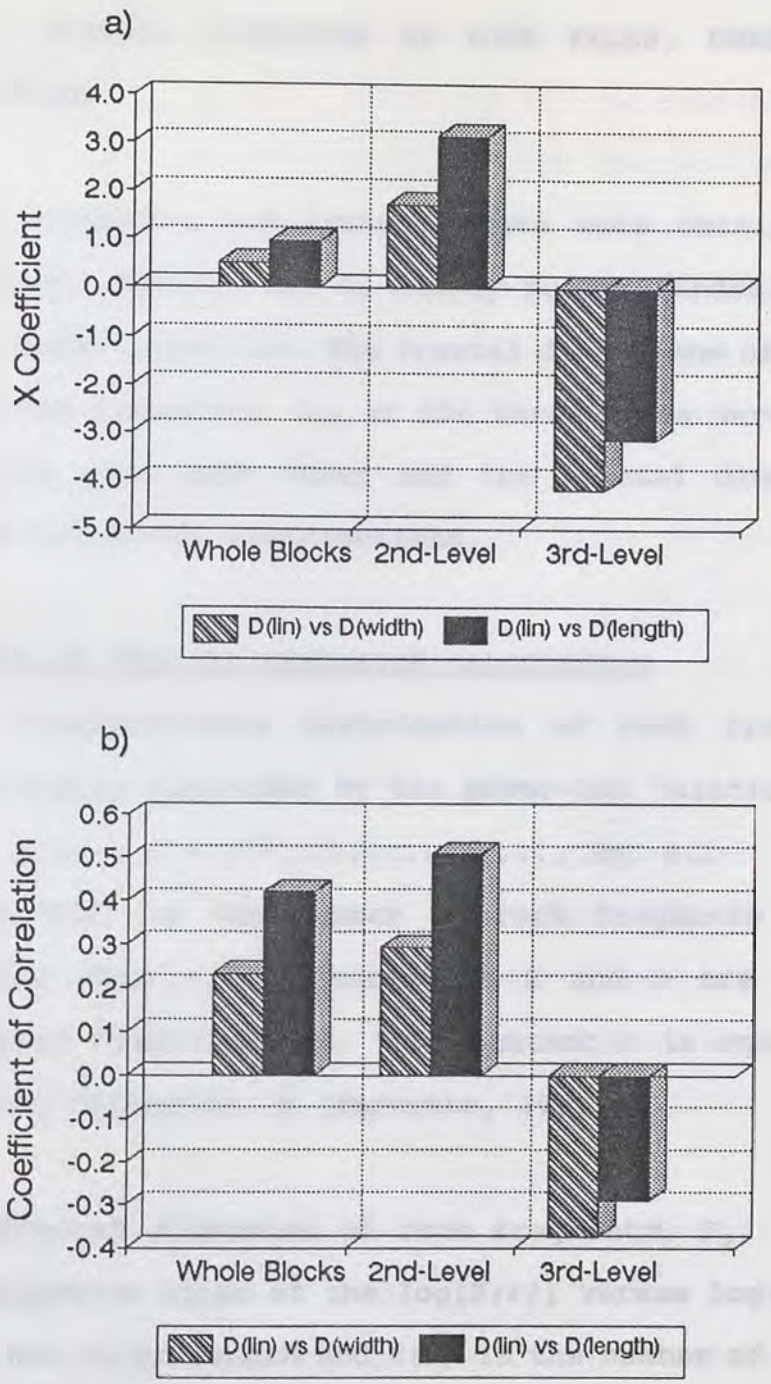

Figure 6.9 a) X coefficient and b) coefficient of correlation of fractal dimension of lineament and fractal dimension of landslide blocks

6.5 FRACTAL DIMENSION OF ROCK FALLS, DEBRIS FLOWS, AND FRACTURES

Rock fragments and fracture data were obtained from Slide Mountain, Nevada; No. 1, Midway Bridge Landslide; and No. 2, Boca Ridge Landslide. The fractal dimensions of fractures, D_F, and rock fragments, D_R, in the three areas were calculated to compare with each other and the fractal dimensions of the landslide block distributions.

METHOD OF FRACTAL DIMENSION CALCULATION

The frequency-size distribution of rock fragments can be empirically described by the power-law relationship:

$$N(r) = C * r^{-b} \quad \text{.....Eq. 6.1}$$

where $N(r)$ is the number of rock fragments with diameter greater than r. The constants C and b are chosen to fit observed distributions. The constant b is equivalent to the fractal dimension, D (Turcotte, 1992).

The fractal dimension of rock fragments, D_R, is obtained as the negative slope of the $\log(N(r))$ versus $\log(r)$ plot, where r is the ruler length and $N(r)$ is the number of rock fragments whose maximum diameter is greater than the ruler (Carr and Warriner, 1989, see Section 3.3).

Data collection locations are shown in Appendix A. Rock

fragment data were obtained by choosing a straight measure line arbitrarily and measuring the maximum diameters of all visible rock fragments bigger than one feet along the line. Fracture data were taken by making a measuring the line about three feet above the lower limit of the outcrop and measuring the space from one fracture to another along the line.

RESULTS

Log($N(r)$) versus log(r) plots are shown in Appendix D. Tables 6.6 and 6.7 show fractal dimensions of rock fragments and fractures respectively. Many of the plots can be approximated as a straight line, which means that the rock fragments and fractures are fractal. Some of them are rather convex. The means of fractal dimensions of rock fall fragments of granodiorite and volcanic rock (andesite in No. 1, Midway Bridge, and latite in No. 2, Boca Ridge) are 2.51 and 2.56 respectively. The mean of fractal dimension of fractures of both granodiorite and volcanic rock are 2.58.

Turcotte (1992) indicated that the fractal dimension of granite and basalt is about D = 2.5. The fractal dimensions yielded by my data agree with the above data. From limited data, a difference could not be found in fractal dimensions between granite and volcanic rocks. Figure 6.10 shows the relationship of fractal dimensions between rock fragments of rock falls and fractures of the origin of the fragments. It is

natural that they correlate very well because no sorting process occurs during rock fall.

Table 6.6 Fractal dimensions of rock fragments

Landslide	Line	Fractal D	Type of deposit	Age of Deposit	Rock
Slide Mt.	R-1	2.62	Rockfall	Present	granodiorite
Slide Mt.	R-2	2.39	Rockfall	Present	granodiorite
Slide Mt.	R-3	2.46	Rockfall	Present	granodiorite
Slide Mt.	R-4	2.49	Rockfall	Present	granodiorite
Slide Mt.	R-5	2.92	Rockfall	Present	granodiorite
Slide Mt.	R-6	2.33	Rockfall	Present	granodiorite
Slide Mt.	R-7	2.33	Rockfall	Present	granodiorite
Mean		2.506			
Std. Deviation		0.194			
Slide Mt.	D-1	2.52	Debris Flow	Anciant	granodiorite
Slide Mt.	D-2	2.48	Debris Flow	Anciant	granodiorite
Slide Mt.	D-3	2.59	Debris Flow	Present	granodiorite
Slide Mt.	D-4	2.38	Debris Flow	Present	granodiorite
Mean		2.493			
Std. Deviation		0.076			
Slide Mt.	C-1	3.64	Congromerate	Anciant	granodiorite
Boca Ridge	R-1	2.19	Rockfall	Present	Volcanic
Boca Ridge	R-2	2.74	Rockfall	Present	Volcanic
Boca Ridge	R-3	2.44	Rockfall	Present	Volcanic
Boca Ridge	R-4	3.19	Rockfall	Present	Volcanic
Boca Ridge	R-5	2.24	Rockfall	Present	Volcanic
Boca Ridge	R-6	2.78	Rockfall	Present	Volcanic
Midway	R-1	2.15	Rockfall	Present	Volcanic
Midway	R-2	2.74	Rockfall	Present	Volcanic
Mean		2.559			
Std. Deviation		0.341			

Table 6.7 Fractal dimensions of fractures

Landslide	Line	Fractal D	Rock
Slide Mt.	F-1	2.76	granodiorite
Slide Mt.	F-2	2.57	granodiorite
Slide Mt.	F-3	2.44	granodiorite
Slide Mt.	F-4	2.78	granodiorite
Slide Mt.	F-5	2.20	granodiorite
Slide Mt.	F-6	2.89	granodiorite
Slide Mt.	F-7	2.44	granodiorite
Mean		2.583	
Std. Deviation		0.224	
Boca Ridge	F-1	2.14	Volcanic
Boca Ridge	F-2	2.16	Volcanic
Boca Ridge	F-3	2.79	Volcanic
Boca Ridge	F-4	3.56	Volcanic
Boca Ridge	F-5	2.62	Volcanic
Boca Ridge	F-6	2.99	Volcanic
Boca Ridge	F-7	1.84	Volcanic
Boca Ridge	F-8	3.04	Volcanic
Midway	F-1	2.08	Volcanic
Midway	F-2	2.54	Volcanic
Mean		2.576	
Std. Deviation		0.505	

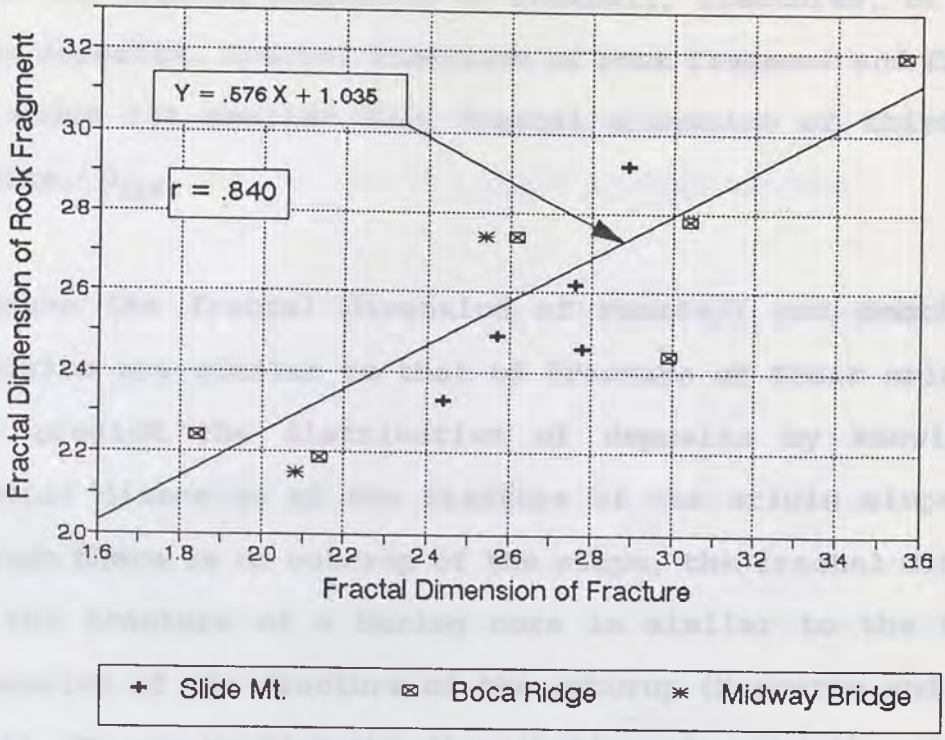

Figure 6.10 Relationship of fractal dimension between rock fragment of rock fall and fractures at the origin of the rock fragments.

The fractal dimensions of debris flow deposits were measured at four locations in Slide Mountain area. D-1 and D-2 are surface deposits, which are believed to be 1983 (present) debris flow deposits. D-3 and D-4 are at outcrops beside the canyon, so they are thought to be ancient debris flow deposits. The fractal dimensions of the debris flow deposits are from 2.38 to 2.59; the average is 2.49. A difference was not found between the fractal dimensions of present and ancient debris flow deposits. The fractal dimension of the

conglomerate (C-1) is 3.64, which is approximately 45% higher than the fractal dimension of rockfall, fractures, or debris flow deposits. Fractal dimension of rock fragment and fracture is about 13% smaller than fractal dimension of third level blocks, D_{3rd}.

Because the fractal dimension of rockfall and debris flow deposits are similar to that of fracture of their origin, we can predict the distribution of deposits by knowing the fractal dimension of the fracture of the origin slope. Even though there is no outcrop of the slope, the fractal dimension of the fracture of a boring core is similar to the fractal dimension of the fracture of the outcrop (Merceron and Velde, 1991). We can predict the distribution of rockfall and debris flow if we know the fractal dimension of the fracture of the outcrop or the boring core.

CHAPTER SEVEN: ANALYSIS OF LANDSLIDES USING FRACTAL DIMENSIONS

The characteristics of landslide block distributions using fractal dimensions and block development processes using their characteristics will be discussed in this chapter.

7.1 WHAT IS THE FRACTAL DIMENSION OF LANDSLIDE BLOCK DISTRIBUTION?

Generally, the fractal dimension of a set is a number which tells how densely the set occupies the metric space in which it lies (Barnsley, 1988). In other words, the more complex the figure, the higher the fractal dimension. In the case the landslide block distribution, fractal dimension can be expressed in terms of variance, which is a traditional and familiar concept in statistics.

Figure 7.1 shows the relationship between the logarithms of standard deviation (= square root of variance) and fractal dimension. They correlates well in reverse (coefficient of correlation, r = -0.840 for width data, r = -0.777 for length data). This means that the smaller variance block distribution has the higher fractal dimension and vice versa. The explanation for this is that smaller variance means the size of the blocks' width (or length) is concentrated in a small range so the slope of the $\log(N(r)$ versus $\log(r)$ plot is

steeper, which means the fractal dimension is higher (fractal dimension is the negative of the slope of the plot) (Figure 7.2).

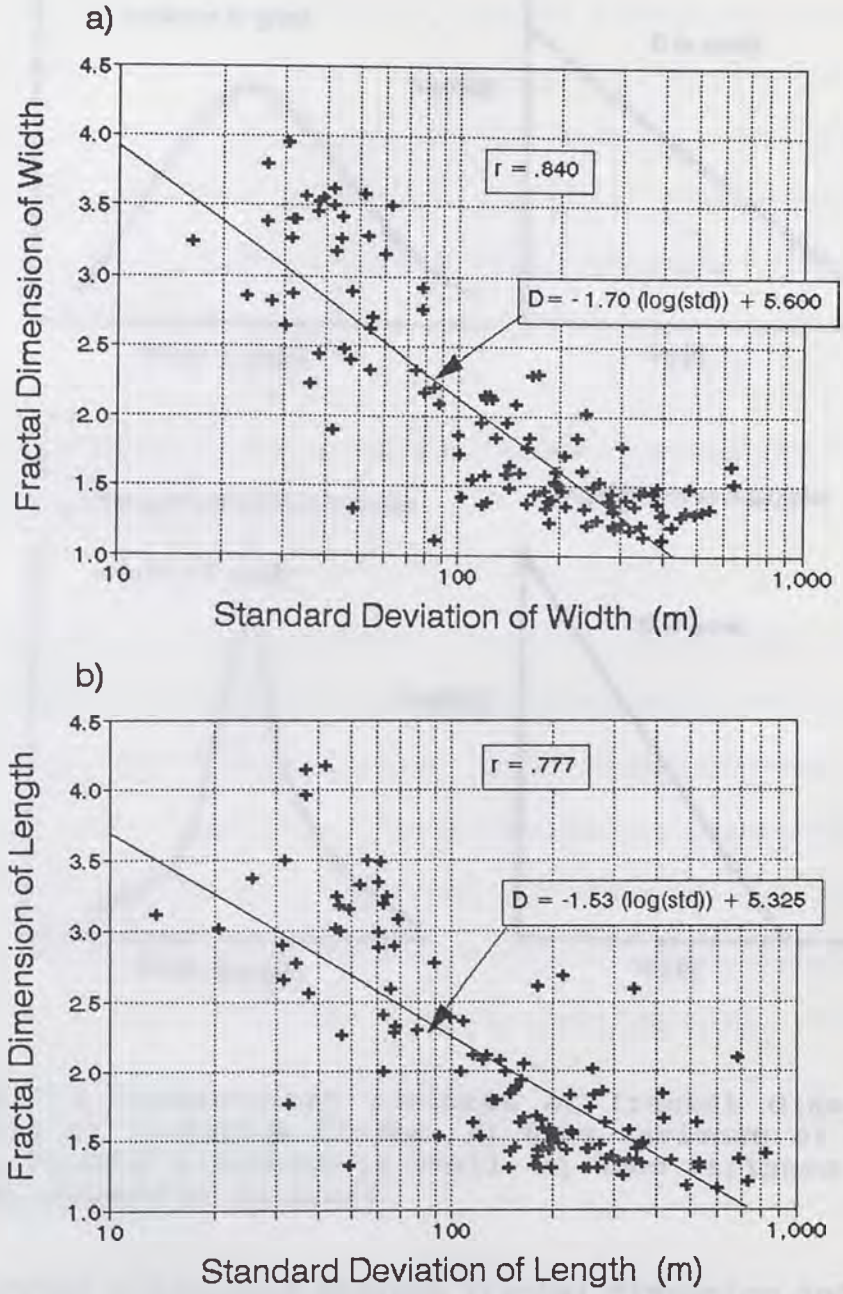

Figure 7.1 relationship between fractal dimension and logarithm of variance of landslide blocks. a) with respect to width, b) with respect to length of blocks.

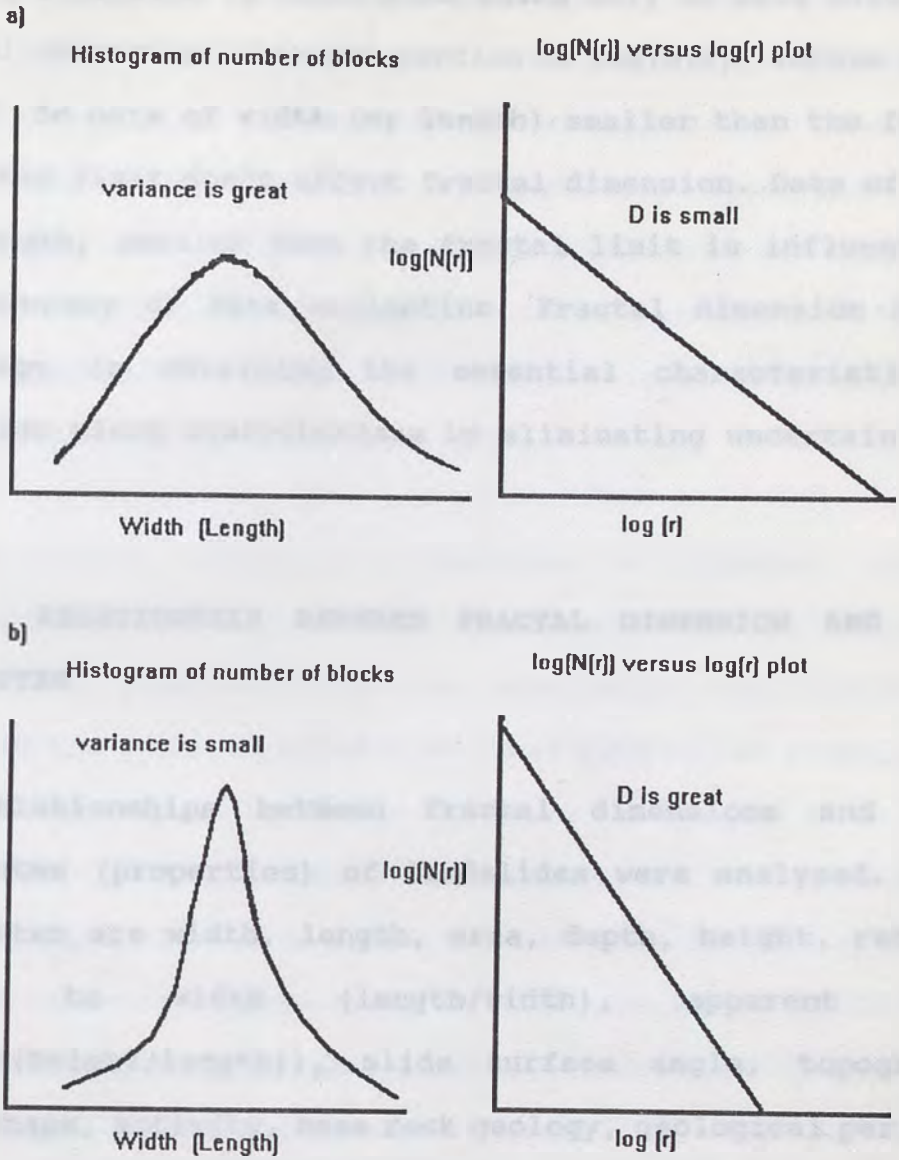

Figure 7.2 Conceptional pictures of fractal dimension and variance of landslide blocks. a) When variance of blocks is great, fractal dimension is small. b) When variance is small, fractal dimension is great.

The biggest difference between fractal dimension and variance is the range of data with which they are calculated. Variance is calculated based on all available data. On the other hand,

fractal dimension is calculated based only on data which show fractal character (straight portion of $\log(N(r))$ versus $\log(r)$ plots). So data of width (or length) smaller than the fractal character limit don't affect fractal dimension. Data of width (or length) smaller than the fractal limit is influenced by the accuracy of data collection. Fractal dimension has an advantage in obtaining the essential characteristics of landslide block distributions by eliminating uncertain data.

7.2 RELATIONSHIP BETWEEN FRACTAL DIMENSION AND OTHER ATTRIBUTES

The relationships between fractal dimensions and other attributes (properties) of landslides were analyzed. These attributes are width, length, area, depth, height, ratio of length to width (length/width), apparent angle (arctan(height/length)), slide surface angle, topography, block shape, activity, base rock geology, geological period of base rock, strike of base rock, and apparent dip of base rock (see Section 6.1).

CORRESPONDENCE ANALYSIS

METHOD

Correspondence analysis is a technique for displaying the rows and columns of a data matrix as points in low-dimensional

vector spaces. The geometry of the column entries (attributes) is related to the geometry of the rows (the individuals); hence, there is a "correspondence" to each other (Oleson and Carr, 1990). Application of correspondence analysis to the contingency table provides a graphical display to attributes and individuals where the distance between points is a measure of the similarity in their profiles; i.e., it describes their correlation (Oleson and Carr, 1989).

Correspondence analysis calculates a separate set of eigenvectors for both the attributes and the individuals. A combination plot of both the attributes and individuals involves the grouping of each of their respective eigenvectors to the corresponding other to form a merged axis i.g., eigenvector 1 of attributes and eigenvector 1 of individuals are combined into one axis. In addition to the graphical display, correspondence analysis also provides a printout of the calculated eigenvalues, percent of variation (non-trivial eigenvalues), and eigenvector coordinates. The percent of variation is important for determining the amount of variance represented by an eigenvector (Oleson, 1989).

Because correspondence analysis was developed in the social science field, it can handle quantitative data found in nominal variables e.g., activity and block shape (Hair and others, 1992). The final advantage of correspondence analysis

is that it can handle missing data values with their expected values, the product of the row and column sums on which the missing datum occurs. The computer software CORESPOND (Carr, 1990) was used to perform the analysis. For mathematical and quantitative description of correspondence analysis refer to Davis (1986) or Carr (1994).

RESULT

Data for the correspondence analysis comprise 39 individuals (No.40, Nuta, is excluded) with 17 attributes. The attributes are width, length, area, depth, height, length/width, apparent angle, slide surface angle, topography, block shape, activity, geology, geological period, strike, apparent dip, D_W, and D_L (Table 6.1).

The results are shown in Appendix F. Figure 7.3 shows the correspondence analysis plot of Factor 1 (X axis) versus Factor 2 (Y axis). Based on eigenvalue analysis, Factor 1 represents about 45% of the data and factor 2 represents about 22% of the data, so Figure 7. 3 represents about 67% of the data. Only this plot will be discussed. Because even though 67% is not a very high amount, my primary purpose in doing the correspondence analysis is to get some idea of the correlation between fractal dimensions and other attributes.

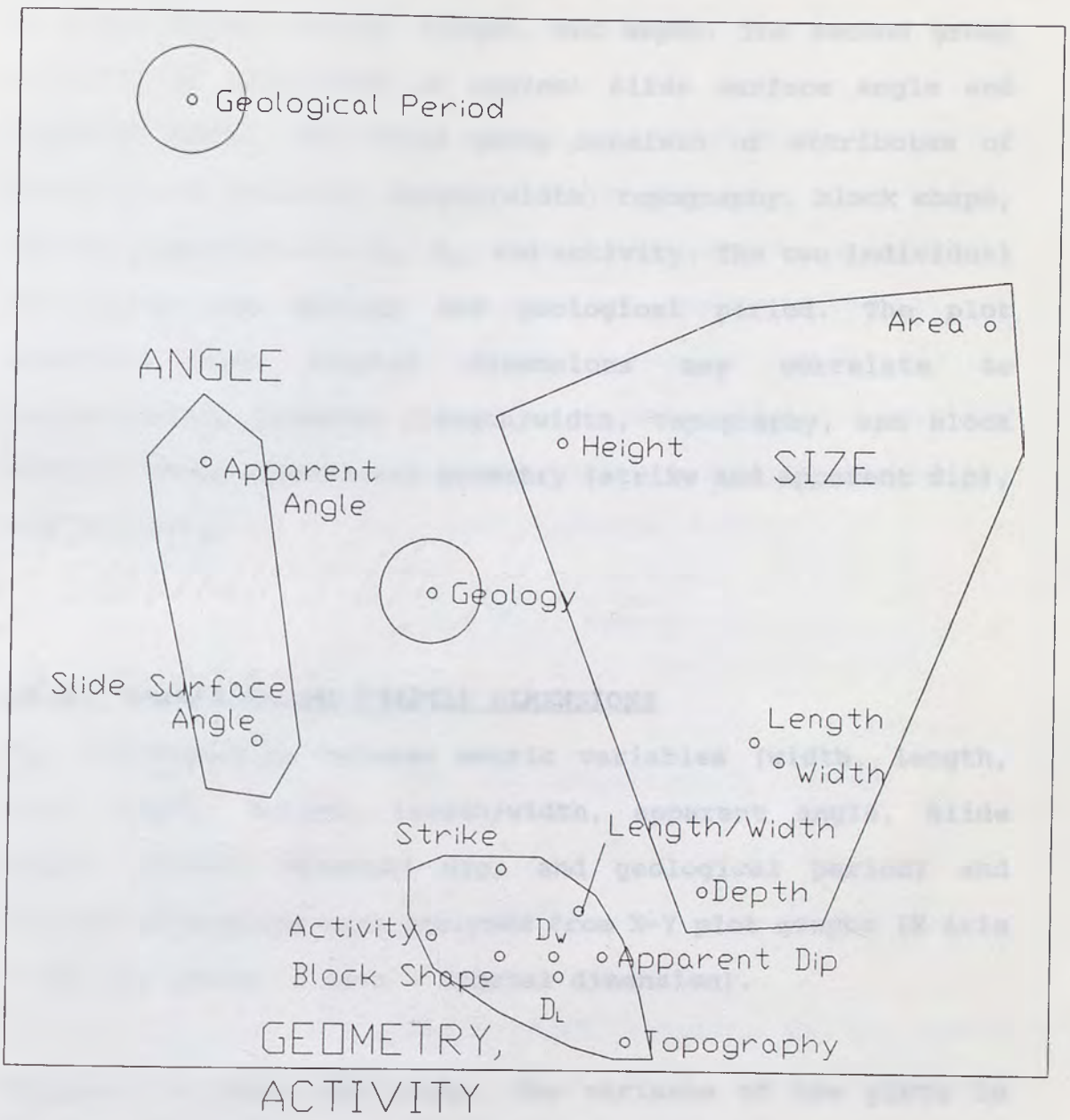

Figure 7.3 Correspondence analysis plot

From the plot, the attributes are classified into three groups and two independents. The first group consists of attributes of size: width, length, height, and depth. The second group consists of attributes of angles: slide surface angle and apparent angle. The third group consists of attributes of geometry and activity: length/width, topography, block shape, strike, apparent dip, D_W, D_L, and activity. The two individual attributes are geology and geological period. The plot suggests that fractal dimensions may correlate to topographical geometry (length/width, topography, and block shape), three dimensional geometry (strike and apparent dip), and activity.

METRIC VARIABLES AND FRACTAL DIMENSIONS

The relationships between metric variables (width, length, area, depth, height, length/width, apparent angle, slide angle, strike, apparent dip, and geological period) and fractal dimensions were analyzed from X-Y plot graphs (X axis - the variables, Y axis - fractal dimension).

Figures 7.4 shows the plots. The variance of the plots is great and the relationships are vague. The least square linear regression between each of the metric variables and the fractal dimensions were calculated. Because the variables consist different units, such as meter, kilometer, degree, and

none, all units were converted to percentages, i.e., the maximum value is 100% and the minimum value is 0%, for the least square linear regression calculation.

Least square linear regression is expressed generally as $Y = mX + b$, where m is X coefficient and b is the Y axis intercept. Figure 7.5 shows the X coefficient, m, and the absolute value of the correlation coefficients, r. By statistical t test, when the following inequation is satisfied, we can tell there is a correlation between the independent variables and dependent variables with a 90% confidence level (Devore, 1987; Satsuma, 1992):

$$\sqrt{\frac{(N-2)r^2}{1-r^2}} \geq 1.684$$

In this case, N is 39. When the inequation is solved:

$$|r| \geq 0.267$$

Length/width versus D_W; length/width versus D_L; and dip versus D_W satisfy this condition. This result agrees with the correspondence analysis (Figure 7.3).

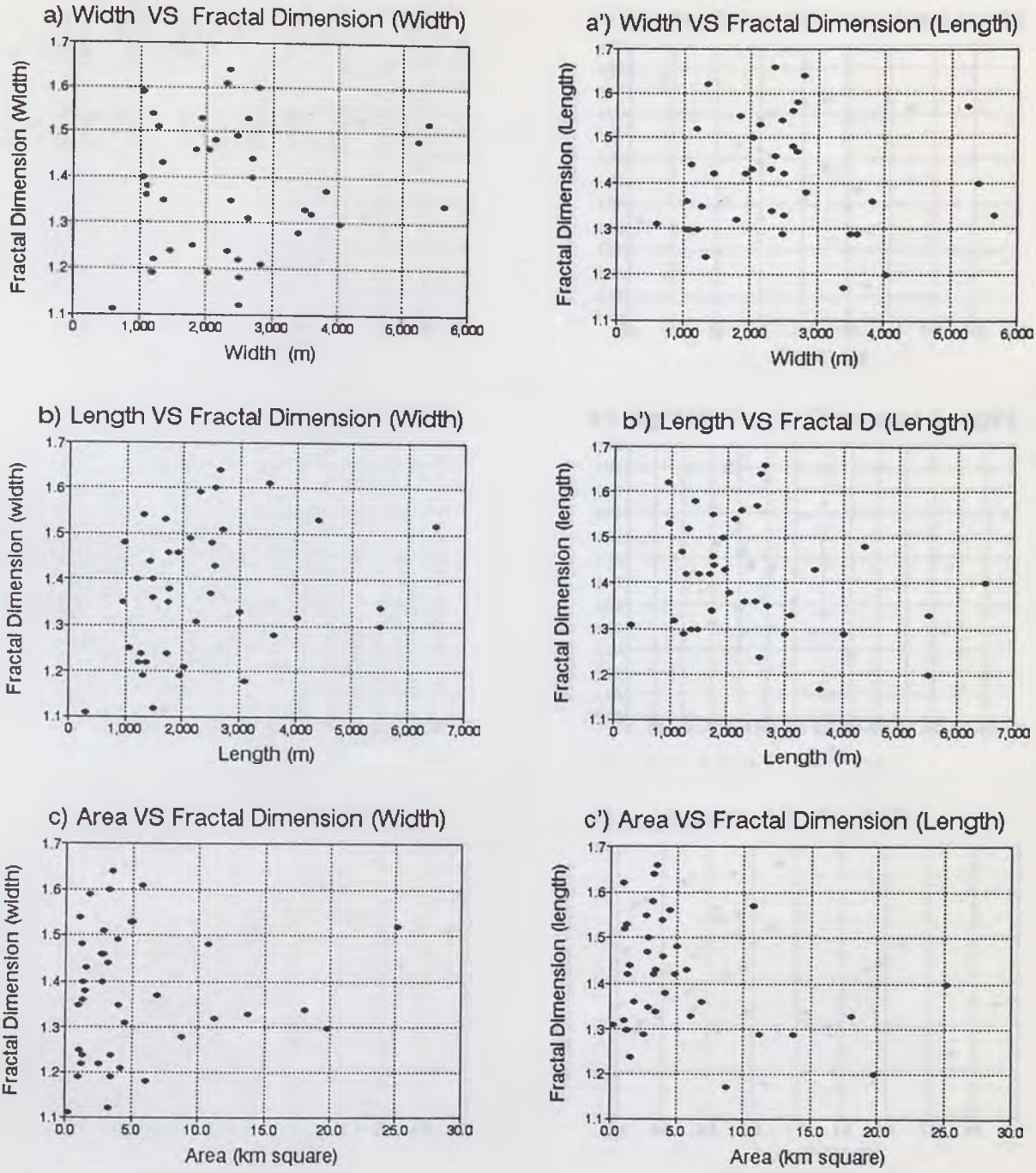

Figure 7.4 Metric attributes and fractal dimension plots

d) Depth VS Fractal Dimension (Width)

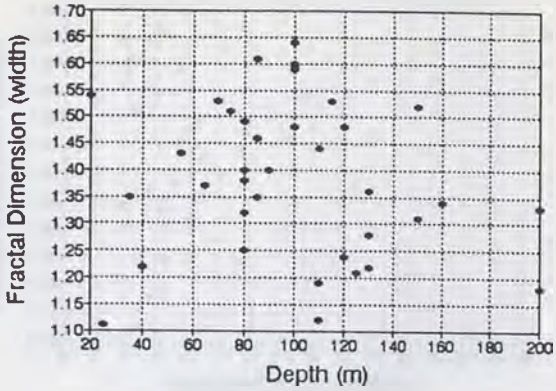

d') Depth VS Fractal Dimension (Length)

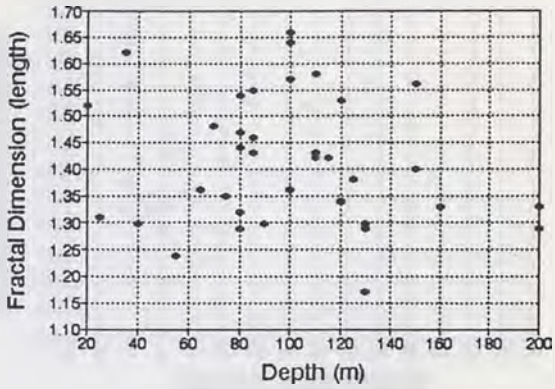

e) Hight VS Fractal Dimension (Width)

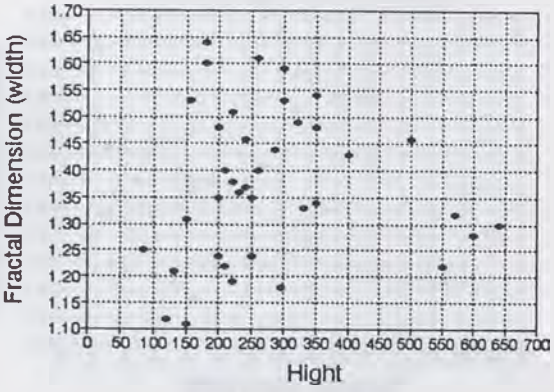

e') Hight VS Fractal Dimension (Length)

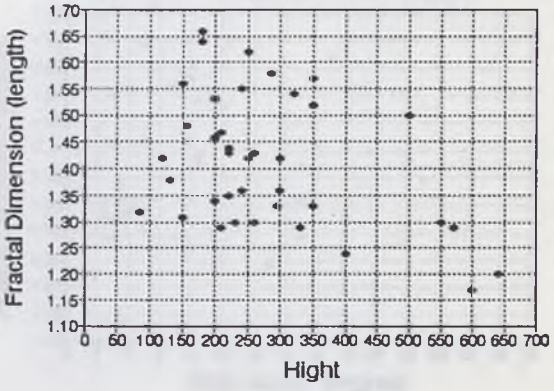

f) Legth/Width VS Fractal D (Width)

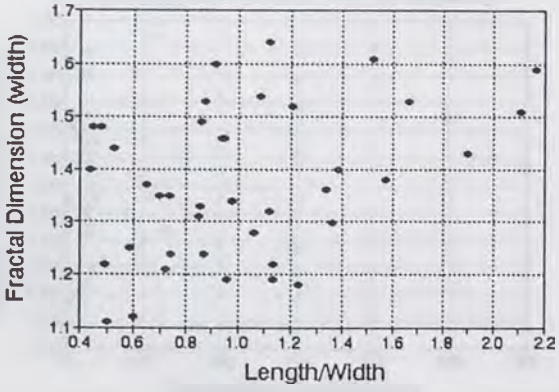

f') Legth/Width VS Fractal D (Length)

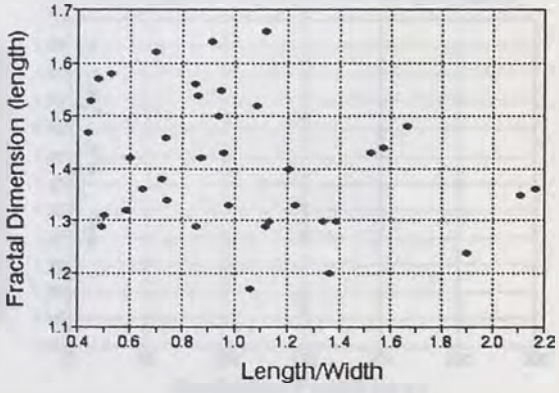

g) Apparent Angle VS D (Width)

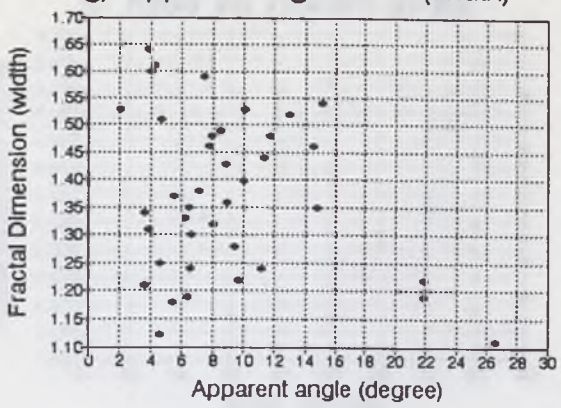

g') Apparent Angle VS D (Length)

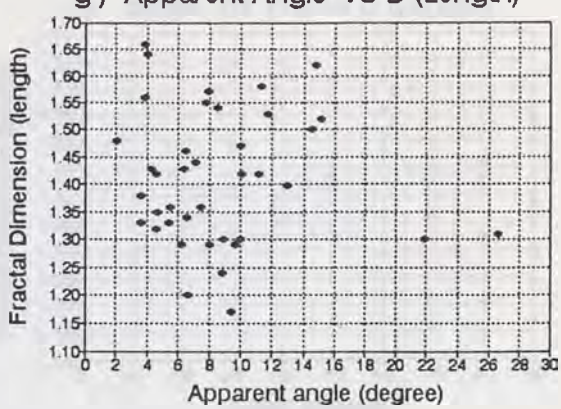

h) Slide Angle VS D(Width)

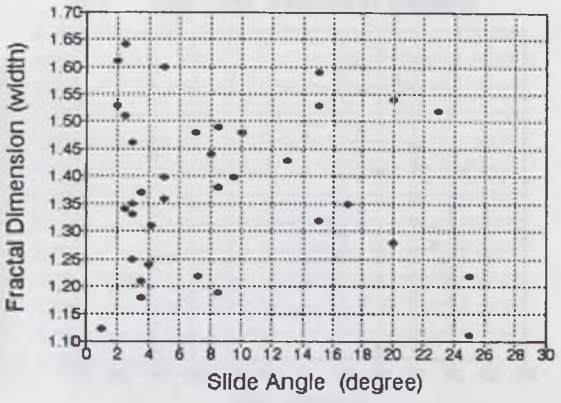

h') Slide Angle VS D (Length)

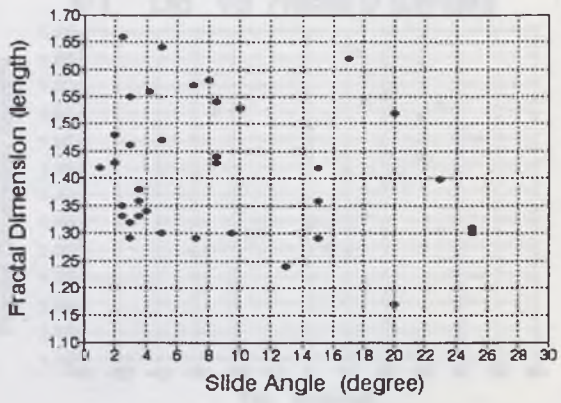

i) Geollogical Period VS D (Width)

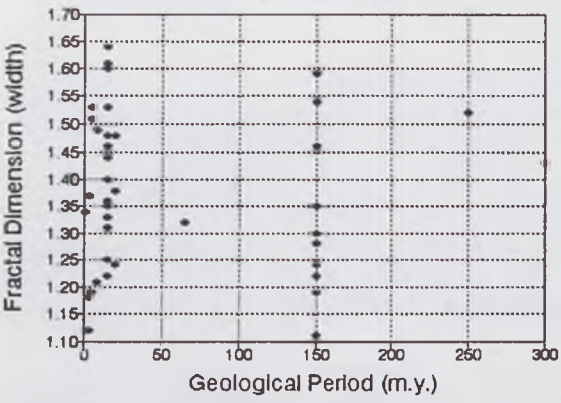

i') Geollogical Period VS D (Length)

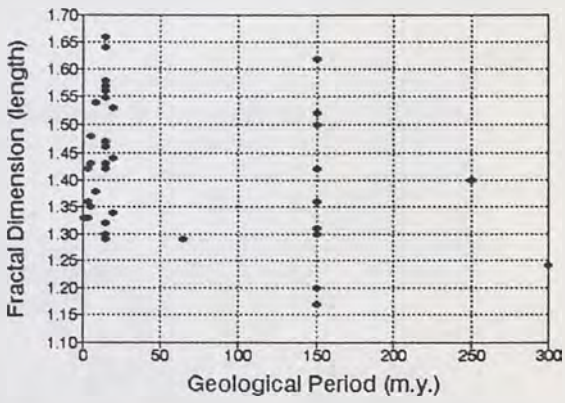

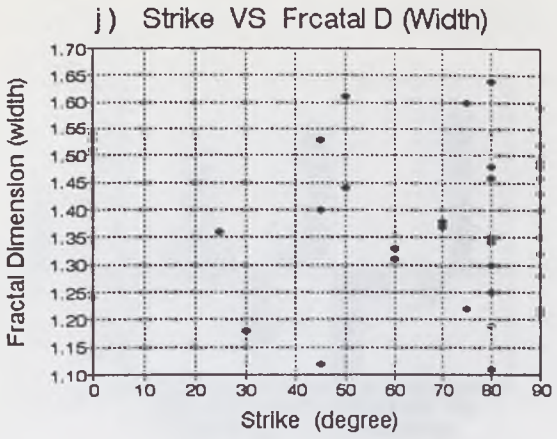
j) Strike VS Frcatal D (Width)
Fractal Dimension (width)
Strike (degree)

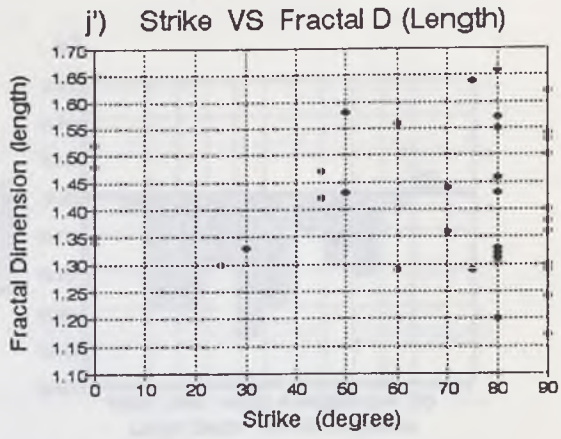
j') Strike VS Fractal D (Length)
Fractal Dimension (length)
Strike (degree)

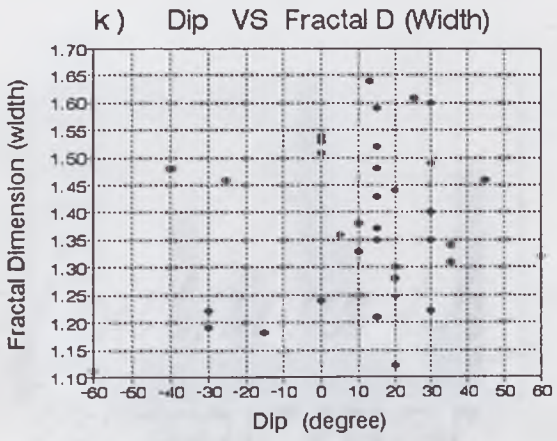
k) Dip VS Fractal D (Width)
Fractal Dimension (width)
Dip (degree)

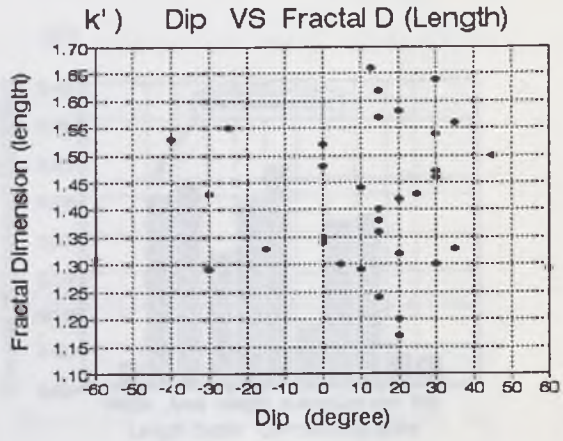
k') Dip VS Fractal D (Length)
Fractal Dimension (length)
Dip (degree)

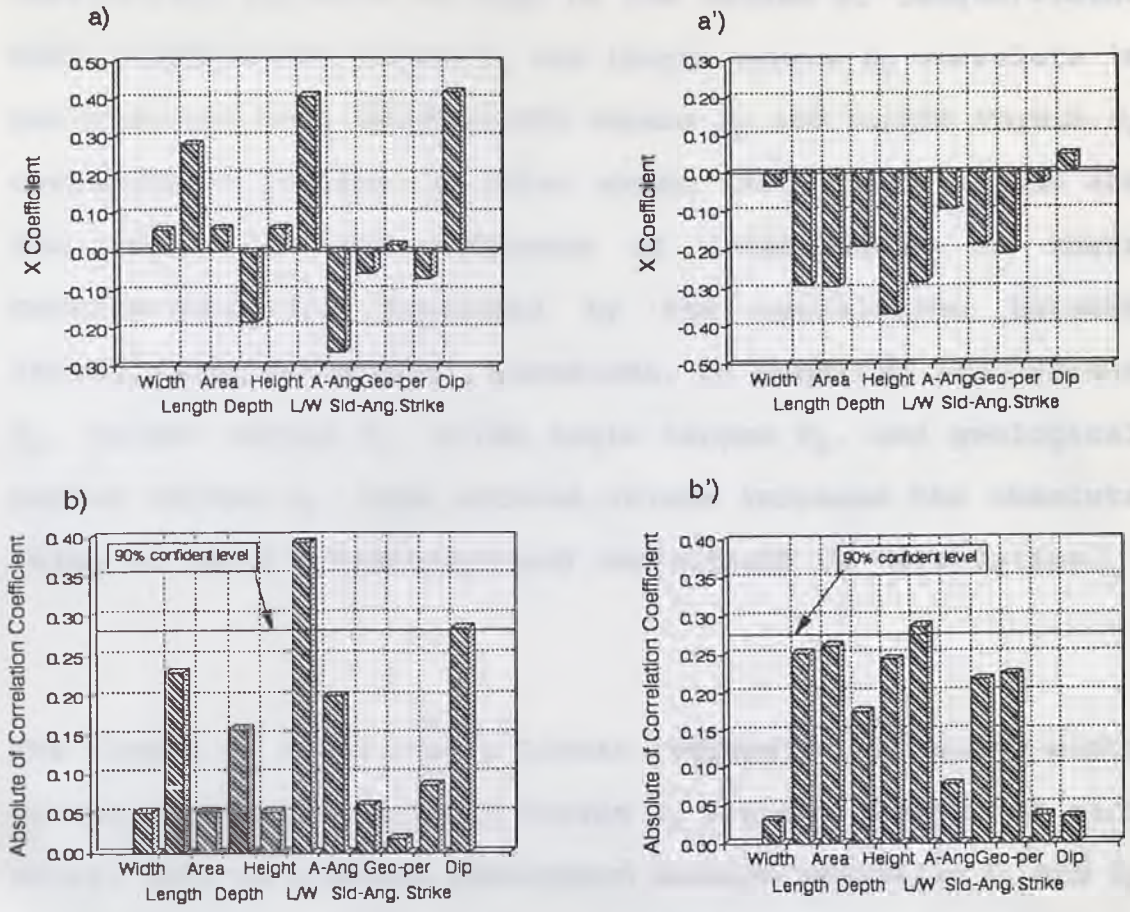

Figure 7.5 a) X coefficient and b) coefficient of correlation of metric attributes and fractal dimension of landslide blocks a) X coefficient of least square regression of metric attributes and D_W; a') X coefficient of least square regression of metric attributes and D_L; b) Coefficient of correlation of least square regression of metric attributes and D_W; b') Coefficient of correlation of least square regression of metric attributes and D_L

Length versus D_W and D_L, area versus D_L, height versus D_L, slide angle versus D_L, and geological period versus D_L show some correlation ($|r| > 0.2$). In graphs of length versus D_W and D_L (Figure 7.4.f and f'), plots which increase the absolute value of X coefficient and the coefficient of

correlation coincide to high or low values of length/width. Both length/width versus D_W and length versus D_W correlate in positive and both length/width versus D_L and length versus D_L correlate in inverse. In other words, their correlations are the result of the influence of length/width or their correlations are explained by the correlation between length/width and fractal dimensions. In graphs of area versus D_L, height versus D_L, slide angle versus D_L, and geological period versus D_L, some extreme values increase the absolute value of the X coefficient and coefficient of correlation.

The slopes of least square linear regression of length/width versus D_W and length/width versus D_L are the reverse of each other. This is a unique phenomenon because basically D_W and D_L are positively related (Figure 6.6, Section 6.3) and graph configurations of the other attributes versus D_W and D_L are similar. This phenomenon may be explained as follows. In a landslide whose width is wide and whose length is short (length/width is small), the variance of the width of the blocks becomes great (D_W is small) and the variance of the length of the blocks becomes small (D_L is great). In a landslide whose width is short and whose length is long (length/width is great), the variance of the width of the blocks becomes small (D_W is great) and the variance of the length of the blocks becomes great (D_L is small). Because

variance and fractal dimension are reversely related to each other (Figure 7.6).

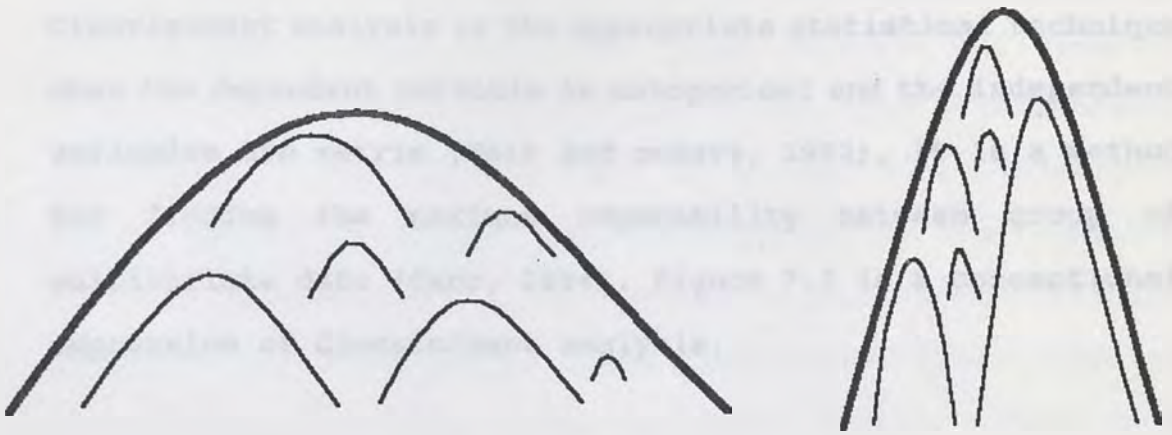

Figure 7.6 Conceptional picture for explanation of relationship between length/width and fractal dimension. a) length/width is small: variance of width (length) of blocks is great (small) = D_W (D_L) is relatively small (great) b) length/width is big: variance of width (length) of blocks is small (great) = D_W (D_L) is relatively great (small)

DISCRIMINANT ANALYSIS

The relationship between fractal dimension and each categorical attribute was analyzed using discriminant analysis. It is assumed that if an attribute influence the fractal dimensions, the data sets divided based on the attribute should be statistically separatable. Discriminant analysis indicates whether there is a statistically meaningful difference between two data sets which have more than one

attributes. The categorical attributes are geology, topography, block shape, apparent dip, and activity.

Method

Discriminant analysis is the appropriate statistical technique when the dependent variable is categorical and the independent variables are metric (Hair and others, 1992). It is a method for finding the maximum separability between group of multivariate data (Carr, 1994). Figure 7.7 is a conceptional expression of discriminant analysis.

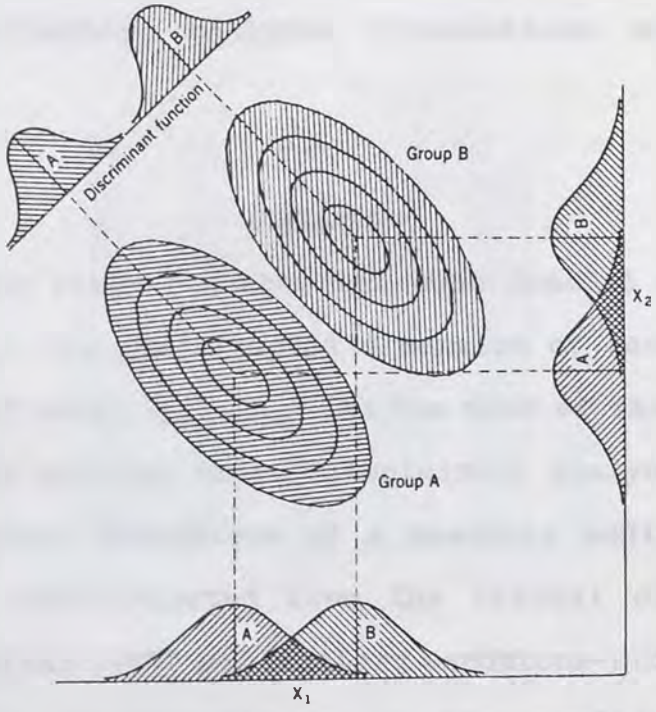

Figure 7.7 Plot of two bivariate distributions, showing overlap between group A and B along both variables X_1 and X_2. Groups can be distinguished by projecting members of the two groups onto the discriminant function line (Davis, 1986)

In a discriminant analysis of Group A and Group B, you first set a null hypothesis $R_A = R_B$ (R is the discriminant score). The analysis tells you whether the null hypothesis can be denied or not, and if it can be denied, the analysis tells you the confidence level (90%, 95%, 97.5%, or 99%). For example, discriminant analysis can tell you if the fractal dimensions (D_W and D_L) of mudstone area can be divided from the fractal dimensions of a schist area statistically. The computer software DISCRIM (Carr, 1994) was used to perform discriminant analysis. For a mathematical and quantitative description of discriminant analysis, refer to Davis (1986) and/or Carr (1994). Discriminant analysis calculations are shown in Appendix I.

GEOLOGY

Figure 7.8 and Table 7.1 show the mean fractal dimension of width, $D_{W\text{-}mean}$; the mean fractal dimension of length; $D_{L\text{-}mean}$, the average of both, $D_{Avg\text{-}mean}$; and the mean of length/width of each base rock geology area. Discriminant analysis indicates that the fractal dimensions of a Mesozoic sedimentary rock area can be discriminated from the fractal dimensions of Tertiary mudstone (95%) and Tertiary sandstone-mudstone (99%), areas (number in parentheses is the confidence level). Discriminant analysis did not deny the null hypothesis for any other combinations.

Table 7.1 Mean and standard deviation of fractal dimension of each geology

		D(width)	D(length)	D(average)
mudstone	# of landslides	11	11	
	mean	1.395	1.453	1.424
	std. deviation	0.166	0.100	0.133
ss, ms	# of landslides	7	7	
	mean	1.343	1.430	1.387
	std. deviation	0.122	0.106	0.114
tuff	# of landslides	5	5	
	mean	1.440	1.458	1.449
	std. deviation	0.084	0.140	0.112
volcanic	# of landslides	4	4	
	mean	1.370	1.373	1.372
	std. deviation	0.105	0.061	0.083
Mesozoic	# of landslides	5	5	
	mean	1.398	1.303	1.351
	std. deviation	0.091	0.081	0.086
schist	# of landslides	8	7	
	mean	1.309	1.418	1.364
	std. deviation	0.165	0.110	0.138

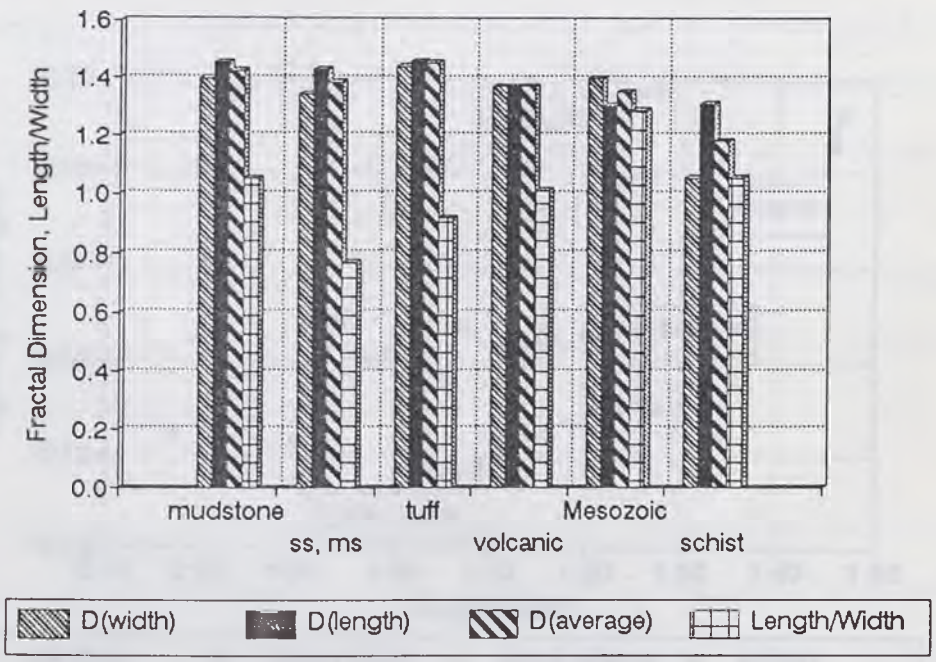

Figure 7.8 Mean of fractal dimensions and length/width of each geology. mudstone: Tertiary mudstone; ss, ms: Tertiary sandstone, mudstone, and conglomerate; tuff: Tertiary tuff and tuffaceous mudstone; volcanic: Tertiary andesite or latite; Mesozoic: Mesozoic sedimentary rock (sandstone, shale, limestone); Metamorphic: schist or greenstone

The mean of length/width of landslides in Mesozoic rock areas is much higher than the means of landslides in other geological areas. Figure 7.4.f,f' show that D_W is higher than D_L in landslides with high length/width. Figure 7.9 shows good positive correlation between the mean of length/width and D_W - D_L of each geological areas. A landslide in a Mesozoic rock area tends to have a big length/width ratio, so it indicates great D_W and small D_L. In other words, the relationship of geology and fractal dimensions is one variation of the relationship of length/width and fractal dimension. Yokoi and others (1995) indicated that fractal dimension is independent from base rock geology. My data support this indication.

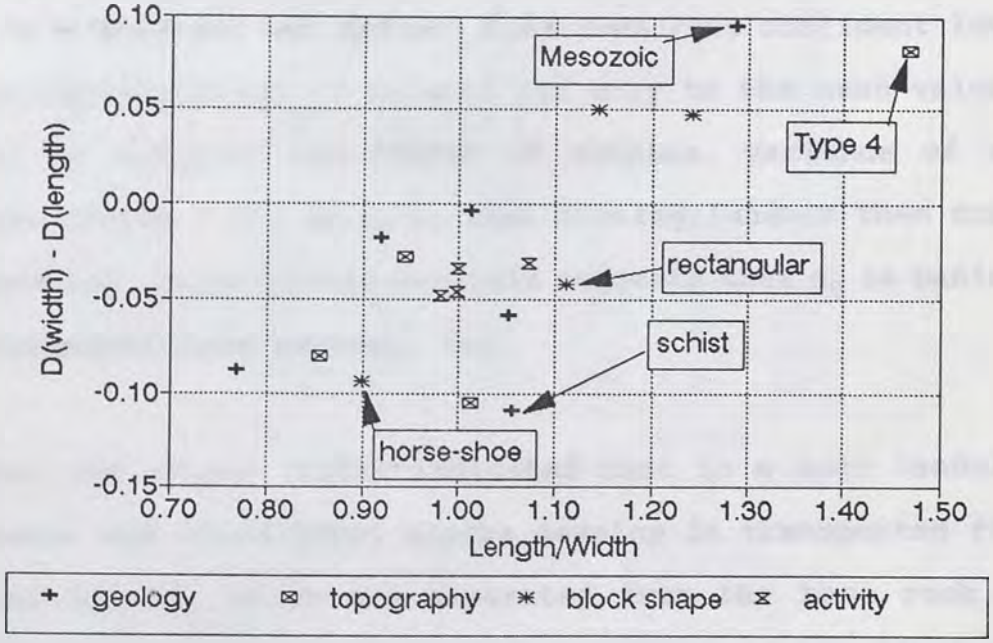

Figure 7.9 Relationship between mean of length/width and gap of $D_{W\text{-}mean}$ and $D_{L\text{-}mean}$.

Sasaki and others (1991) defined α as the Y axis intercept of $\log(N(r))$ versus $\log(r)$ plot or theoretical number of blocks whose width (length) is greater than one meter. Theoretical number of the blocks in the unit area, α_0, is obtained by α divided by the area of the landslide. The unit of α_0 is number/hectare in this thesis.

Figure 7.10 and Table 7.2 show mean α_0 of each base rock geology area. Yokoi and others (1995) suggested that α_0 of mudstone area is distinguished from α_0 of a schist area. Figure 7.12 shows the great difference of α_0 among different geologies; however, discriminant analysis indicated that only α_0 of Tertiary sandstone-mudstone area is distinguished from α_0 of a Mesozoic sedimentary rock area (90% confident level). Distinguishability is related not only to the mean value but also to variance and number of samples. Variance of α_0 is great (Table 7.2), so α_0 is less distinguishable than fractal dimension. Discriminate analysis suggests that α_0 is basically independent from geology, too.

Yokoi and others (1995) indicated that in a huge landslide, second- and third-level blocks develop in transported first-level blocks, which are separated from the base rock by a slide surface. So cracks made by movement of the first-level block or other discontinuities would be an important factor in the occurrence of second and third level blocks.

Table 7.2 Mean and standard deviation of α_0 of each geology

		alpha-0(Width)	alpha-0(Length)	alpha-0(average)
mudstone	# of landslides	11	11	
	mean	154.9	202.7	178.8
	std. deviation	133.9	169.5	151.7
ss, ms	# of landslides	7	7	
	mean	115.3	205.7	160.5
	std. deviation	112.5	157.5	135.0
tuff	# of landslides	5	5	
	mean	175.2	256.8	216.0
	std. deviation	116.2	195.5	155.9
volcanic	# of landslides	4	4	
	mean	66.3	103.0	84.7
	std. deviation	26.1	76.0	51.1
Mesozoic	# of landslides	5	5	
	mean	129.3	111.5	120.4
	std. deviation	134.0	137.6	135.8
schist	# of landslides	8	7	
	mean	134.7	265.0	199.9
	std. deviation	95.5	262.1	178.8

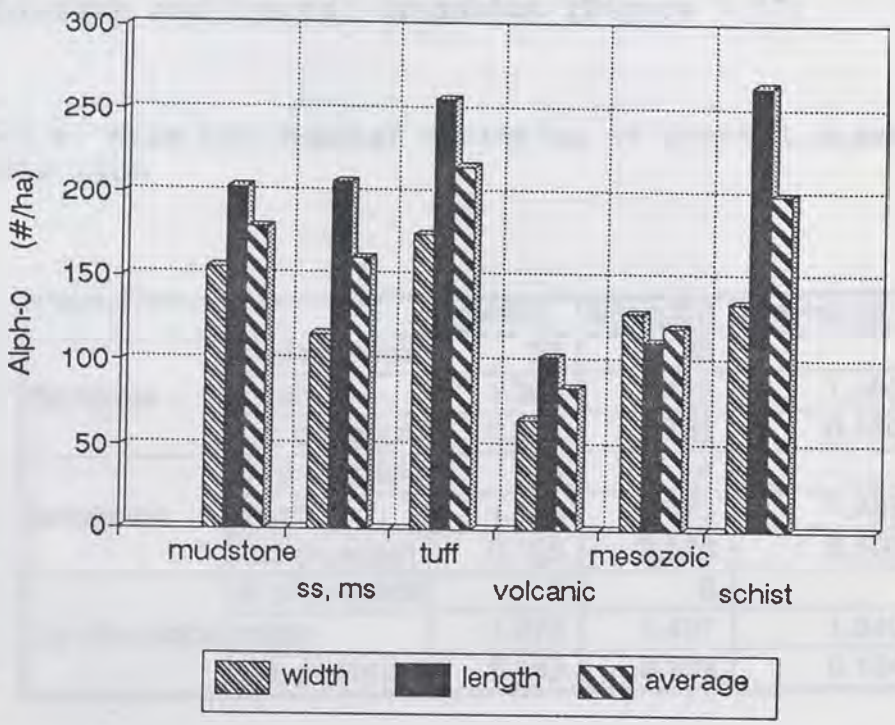

Figure 7.10 Mean of α_0 of each geology
mudstone: Tertiary mudstone; ss, ms: Tertiary sandstone, mudstone, and conglomerate; tuff: Tertiary tuff and tuffaceous mudstone; volcanic: Tertiary andesite or latite; Mesozoic: Mesozoic sedimentary rock (sandstone, shale, limestone); Metamorphic: schist or greenstone

APPARENT DIP OF BASE ROCK

Figure 7.11 and Table 7.3 show the mean fractal dimension of width, $D_{W\text{-}mean}$; the mean fractal dimension of length, $D_{L\text{-}mean}$; the average of both, $D_{Avg\text{-}mean}$; and the mean of length/width of dip slope landslides, horizontal dip landslides, and dipping into slope landslides. Discriminant analysis indicates that the fractal dimensions of dipping into slope are discriminated from the fractal dimensions of both dip slope (90%) and horizontal (90%). Dip and length/width don't show any correlation, so the correlation between apparent dip and fractal dimensions is not influenced by the correlation of length/width and fractal dimension (Figure 7.12)

Table 7.3 Mean and fractal deviation of fractal dimension of each dip type

		D(width)	D(length)	D(avearge)
dip slope	# of landslide	28	28	
	mean	1.396	1.413	1.405
	std. deviation	0.127	0.132	0.130
horizontal	# of landslide	4	4	
	mean	1.455	1.423	1.439
	std. deviation	0.125	0.079	0.102
dip into slope	# of landslide	6	6	
	mean	1.273	1.407	1.340
	std. deviation	0.143	0.104	0.124

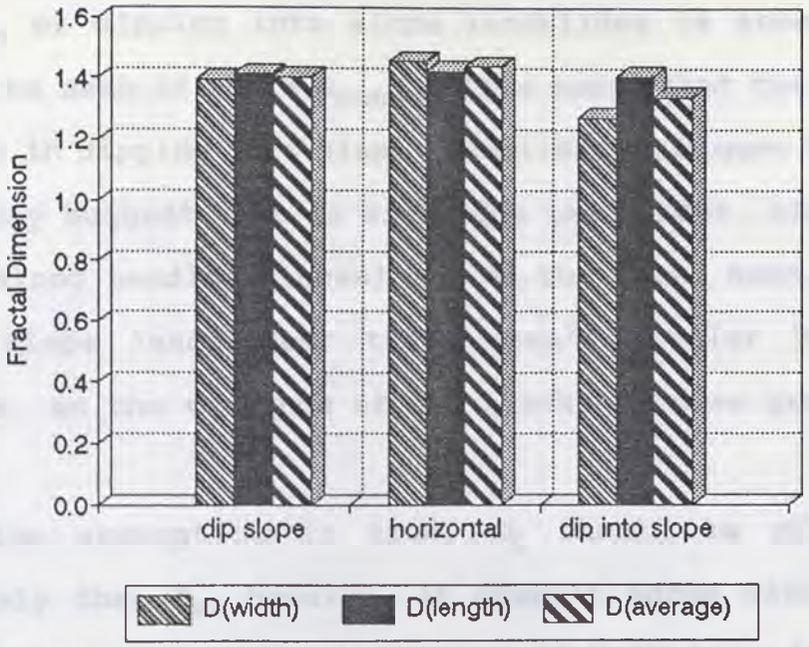

Figure 7.11 Mean of fractal dimensions of each dipping type of base rock. dip slope: base rock dip to same direction as slide; horizontal: apparent dip of base rock is horizontal in slide direction; dipping into slope: base rock dips to opposite direction of slide

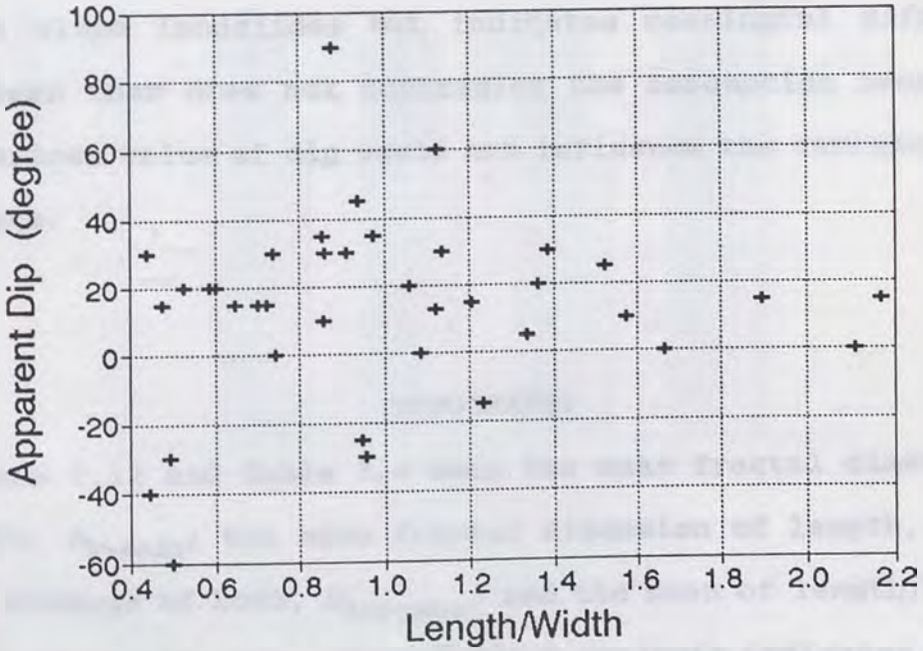

Figure 7.12 Relationship between apparent dip and length/width

$D_{W\text{-}mean}$ of dipping into slope landslides is about 10% lower than the mean of whole $D_{W\text{-}mean}$. This means that the variance of blocks in dipping into slope landslides is bigger than others. This may suggest that in dip slope landslides, blocks tend to fail along bedding planes; and on the other hand, in dipping into slope landslides, there aren't regular weak bedding planes, so the variance of the blocks becomes greater.

If this assumption is true, D_L should be affected more severely than D_W, however, it doesn't agree with the facts. The facts are that the difference of D_W is more influenced by dip and that dip correlates to D_W but not D_L (Figure 7.5). On the other hand, the fact that dip doesn't correlate to the fractal dimensions in either dip slope landslides nor dipping into slope landslides but indicates meaningful differences between them does not contradict the assumption because the numerical value of dip would not influence the variance of the blocks.

TOPOGRAPHY

Figure 7.12 and Table 7.4 show the mean fractal dimension of width, $D_{W\text{-}mean}$; the mean fractal dimension of length, $D_{L\text{-}mean}$; the average of both, $D_{Avg\text{-}mean}$; and the mean of length/width of each topography type. Discriminant analysis indicates that the fractal dimensions of type 4 are discriminated from those of

type 1 and type 3 (90% confident level).

Table 7.4 Mean and standard deviation of fractal dimension of each topography.

Topography		D (width)	D (length)	D (average)
Type 1	# of landslides	10	10	
	mean	1.334	1.439	1.387
	std. deviation	0.145	0.12	0.133
Type 2	# of landslides	4	4	
	mean	1.313	1.393	1.353
	std. deviation	0.088	0.062	0.075
Type 3	# of landslides	21	20	
	mean	1.398	1.426	1.412
	std. deviation	0.147	0.127	0.137
Type 4	# of landslides	5	5	
	mean	1.406	1.324	1.365
	std. deviation	0.095	0.092	0.094

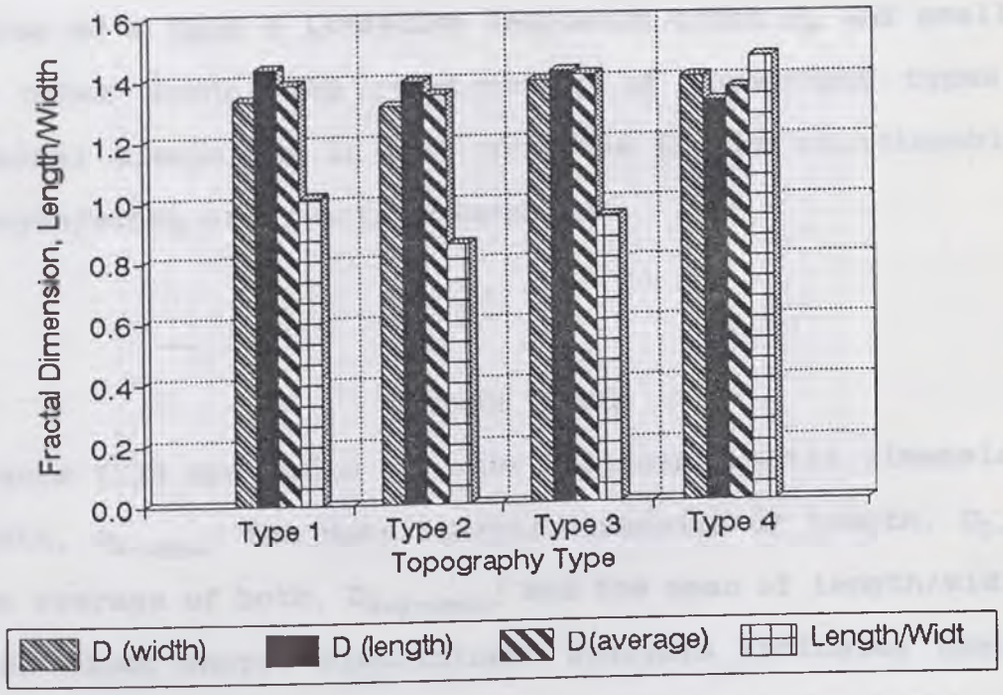

Figure 7.13 Mean of fractal dimensions and length/width of each topography type.

$D_{Avg\text{-}mean}$ of type 4 is similar to $D_{Avg\text{-}mean}$ of the other types. $D_{W\text{-}mean}$ of type 4 landslides is higher than its $D_{L\text{-}mean}$, on the other hand, $D_{W\text{-}mean}$ of other landslides is smaller than their $D_{L\text{-}mean}$. This means that the variance of block length is greater than the variance of block width in type 4 landslides.

The mean of length/width of type 4 is much higher than the means of other types. Figure 7.4.f,f' show that in a landslide with high length/width D_W is higher than D_L. Figure 7.9 shows positive correlation between mean of length/width and (D_W - D_L) of each topography type and both values of type 4 is distinguished from those of other types. Then, a type 4 landslide tends to have a great length/width ratio or vice versa so a type 4 landslide indicates great D_W and small D_L. In other words, the relationship of topography types and fractal dimensions is one variation of the relationship of length/width and fractal dimension.

BLOCK SHAPE

Figure 7.13 and Table 7.5 show the mean fractal dimension of width, $D_{W\text{-}mean}$; the mean fractal dimension of length, $D_{L\text{-}mean}$; the average of both, $D_{Avg\text{-}mean}$; and the mean of length/width of each block shape. Discriminant analysis indicates that the fractal dimensions of horse-shoe shaped landslides are discriminated from the fractal dimensions of rectangular

landslides (90% confidence level).

Table 7.5 Mean and standard deviation of fractal dimensions of each block shapes

Block Shape		D (width)	D (length)	D (average)
Triangle	# of landslides	3	3	
	mean	1.470	1.420	1.445
	std. deviation	0.110	0.070	0.090
Horse	# of landslides	20	19	
	mean	1.319	1.412	1.366
	std. deviation	0.148	0.137	0.143
Rectanglure	# of landslides	14	14	
	mean	1.431	1.429	1.430
	std. deviation	0.098	0.112	0.105
Bottle	# of landslides	3	3	
	mean	1.380	1.333	1.357
	std. deviation	0.123	0.047	0.085

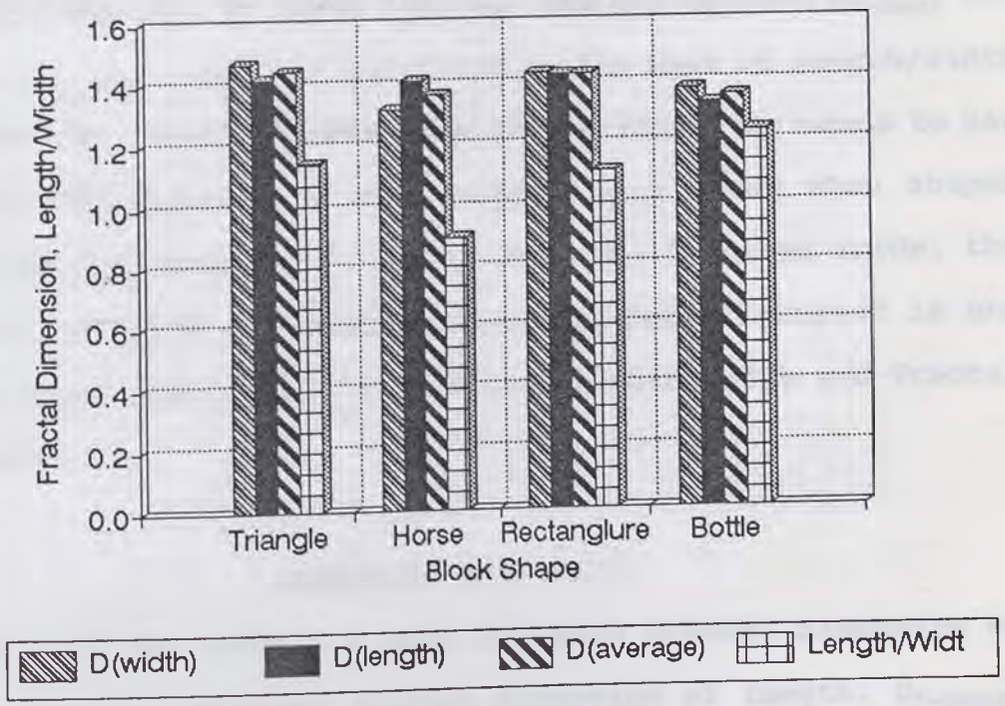

Figure 7.14 Mean of fractal dimensions and length/width of each block shape type.

$D_{Avg\text{-}mean}$ of horse-shoe shaped landslides is about 5% smaller than $D_{Avg\text{-}mean}$ of rectangular shaped landslides. $D_{L\text{-}mean}$ of horse-shoe shaped landslides is about 6% higher than its $D_{W\text{-}mean}$; on the other hand, the $D_{L\text{-}mean}$ of rectangular shaped landslides is similar to its $D_{W\text{-}mean}$. This means that the variance of blocks in a horse-shoe shaped landslide is greater than that in a rectangular shaped landslide. Also, the variance of block width is greater than the variance of block length in horse-shoe shaped landslides.

The mean of length/width of horse-shoe shaped landslides is about 17% smaller than the means of rectangular shaped landslides. Figure 7.4 shows that in landslides with small length/width, D_W, is lower than D_L. The gap between $D_{W\text{-}mean}$ and $D_{L\text{-}mean}$ ($D_{L\text{-}mean}$ - $D_{W\text{-}mean}$) correlate to the mean of length/width (Figure 7.9). Thus, a horse-shoe shaped landslide tends to has a small length/width or vice versa, so a horse shoe shaped landslide indicates small D_W and great D_L. In other words, the correlation between block shape and fractal dimension is one variation of the correlation between length/width and fractal dimension.

LANDSLIDE ACTIVITY

Figure 7.14 and Table 7.6 show the mean fractal dimension of width, $D_{W\text{-}mean}$; the mean fractal dimension of length, $D_{L\text{-}mean}$; the average of both, $D_{Avg\text{-}mean}$; and the mean of length/width of

each activity level. Although none of them can be discriminated from each other by discriminant analysis, the positive correlation between activity level and fractal dimensions is clear, i.e., the more active the landslide is, the higher the fractal dimension.

Length/width and (D_W - D_L) don't correlate to each other (Figure 7.9) so the relationship of activity and fractal dimension is not influenced by length/width.

Table 7.6 Mean and standard deviation of fractal dimension of each activity level

Activity		D (width)	D (length)	D (average)
ancient	# of landslides	6	6	
	mean	1.300	1.348	1.324
	std. sediation	0.155	0.086	0.121
stable	# of landslides	10	10	
	mean	1.361	1.395	1.378
	std. sediation	0.129	0.059	0.094
dormant	# of landslides	13	12	
	mean	1.388	1.419	1.404
	std. sediation	0.130	0.156	0.143
active	# of landslides	11	11	
	mean	1.414	1.460	1.437
	std. sediation	0.137	0.126	0.132

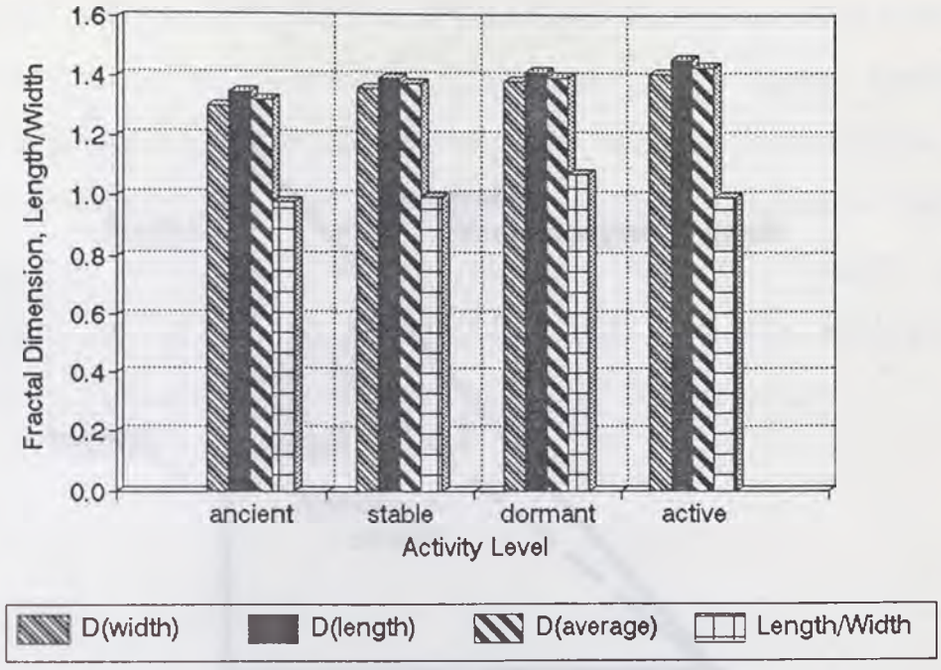

Figure 7.15 Mean of fractal dimensions and length/width of each activity level

The present block distribution is the result of interaction between block propagation and erosion. When block propagation stops, the number of blocks begins to decrease due to erosion. Erosion is fractal, too. Many small blocks are eroded while far fewer big blocks are eroded. In other words, the absolute value of the slope of $\log(N(r))$ versus $\log(r)$ plot, which is equivalent to the fractal dimension, decreases (Figure 7.15). Fractal dimension may be used as an index of activity or time since activity ended.

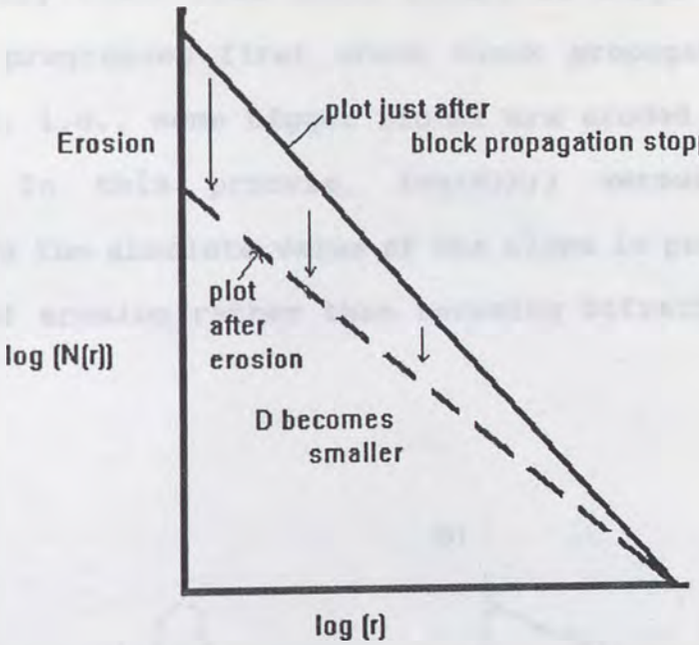

Figure 7.16 Conceptional illustration of log(*N(r)*) versus log(*r*) plot to explain how activity and fractal dimension correlate each other. When block propagation stops, number of blocks begin to decrease due to erosion. Therefore absolute value the slope of the plot (= fractal dimension) decrease.

Korvin (1992) discussed the fact that some coastlines are *bifractal*: their log(*N(r)*) versus log(*r*) plot is approximated as two straight lines, i.e., high *D* at large *r* portion and low *D* at small *r* portion (Figure 7.17). The low *D* is the result of the smoothing effect of erosion (Nakano, 1983; quoted in Korvin, 1992) (Figure 7.18). Few landslide block distributions are bifractal, however, they have no relation to activity (or erosion). In the case of landslides, block propagation doesn't

stop in all areas at the same time and some parts of the landslide often reactivates. Therefore, block erosion doesn't necessarily occur from small blocks to large ones; instead, erosion progresses first where block propagation stops the earliest, i.e., some bigger blocks are eroded before smaller blocks. In this process, $\log(N(r))$ versus $\log(r)$ plot decreases the absolute value of the slope in proportion to the degree of erosion rather than becoming bifractal.

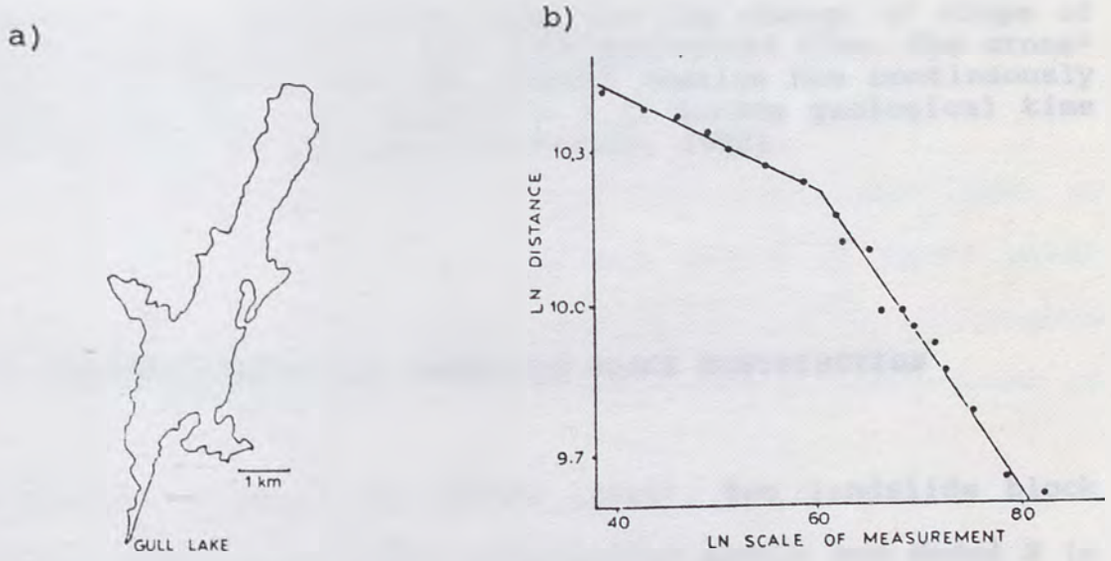

Figure 7.17 a) The Gull Lake, Ontario, Canada. b) The fractal analysis of its shoreline (Kent and Wong, 1982; reprinted from Korvin, 1992)

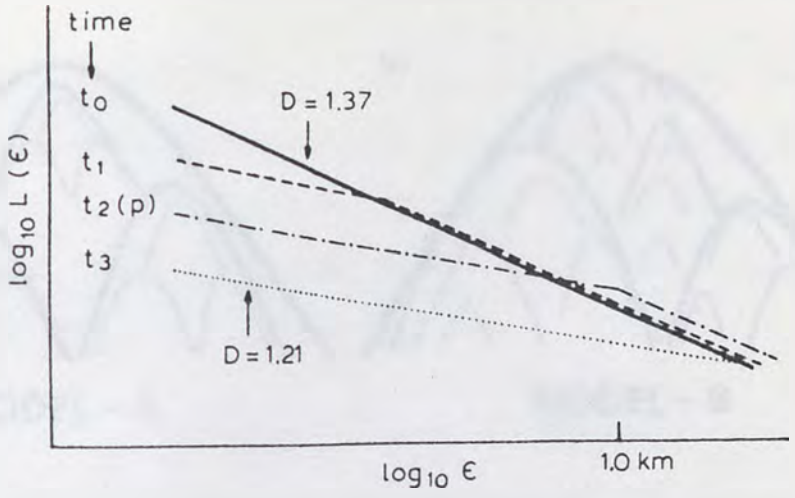

Figure 7.18 Hypothetical model for the change of slope of $\log(N(r))$ versus $\log(r)$ plot with geological time. The cross-over point between the two fractal domains has continuously moved from D = 1.37 toward D = 1.21 during geological time (Nakano, 1983; reprinted from Korvin, 1992).

7.3 FRACTAL MODELS FOR LANDSLIDE BLOCK DISTRIBUTION

According to Yokoi and others (1995), two landslide block models, Model A (an ideal self-similar model) and Model B (a combination of unique fractal dimensions of second and third level blocks yielding another fractal dimension), help in understanding the fractal character of landslide block distribution. The applicability of both models to the actual landslides was examined.

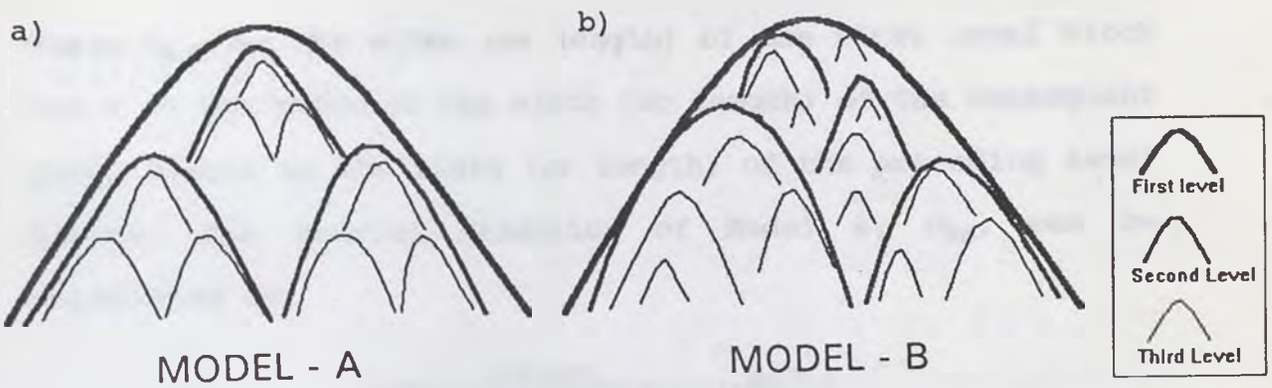

Figure 7.19 Conceptional illustration of a) Model A and b) Model B

MODEL A

In Model A, a certain number of second level blocks occur in the first level block and the same number of third level blocks occur in each second level block and so on (Figure 7.19.a). The fractal dimension of Model A is calculated as follows:

The number of first to n^{th} level blocks, *num*, can be calculated as:

$$num=\sum_{m=0}^{m=n} b^m=\frac{b^{n+1}}{b-1}+\frac{1}{1-b}=\frac{b^{n+1}-1}{b-1} \quad \ldots\ldots\ldots\ldots Eq.7.1$$

where b is the number of subsequent blocks in a preceding block. The n^{th} order width (or length), W_n is calculated as:

$$W_n = W_{max} s^n \ldots\ldots\ldots Eq.7.2$$

where W_{max} is the width (or length) of the first level block and s is the ratio of the width (or length) of the subsequent level blocks to the width (or length) of the preceding level blocks. The fractal dimension of Model A, D_{MA}, can be calculated as:

$$D_{MA} = \frac{\log(num)}{\log(W_{max}) - \log(W_n)} \ldots\ldots Eq.7.3$$

From Equations 7.1 and 7.2:

$$\log(num) = \log\left(\frac{b^{n+1}-1}{b-1}\right) = \log(b^{n+1}-1) - \log(b-1) \ldots\ldots Eq.7.4$$

$$\log(W_n) = \log(W_{max}) + n\log(s) = \log(W_{max}) - n\log(1/s) \ldots\ldots Eq.7.5$$

Put Equations 7.4 and 7.5 into equation 7.3:

$$D_{MA} = \frac{\log(b^{n+1}-1) - \log(b-1)}{n\log(1/s)} \ldots\ldots Eq.7.6$$

D_{MA} is asymptotic to D_S, where D_S is the similarity dimension, which is calculated as

$$D_S = \frac{\log(b)}{\log(1/s)} \ldots\ldots Eq.7.7$$

D_S is calculated using b and s (s_w, s_l), where b is the number

of subsequent level blocks inside the preceding level block; and s_w (s_l) is the mean of width (or length) of the subsequent level blocks divided by the width (or length) of the preceding level block.

Tables 7.7 and 7.8 show b, $1/s_w$, $1/s_l$, and self similar fractal dimension, D_S. The averages of b, $1/s_w$, $1/s_l$ of second level blocks in a first level block are 18.0, 6.23, 4.94 respectively and those of third level blocks in a second level block are 5.63, 9.07, 8.81 respectively. In other words, fewer and bigger blocks (relative to the preceding block) occur in first-level blocks than in second level blocks. $D_{SW(1-2)}$ ($D_{SL(1-2)}$) is an abbreviation of the self-similar fractal dimension calculated using data from first and second level blocks and $D_{SW(2-3)}$ ($D_{SL(2-3)}$) is an abbreviation of the self-similar fractal dimension calculated using data from second and third level blocks.

Figure 7.20 shows the relationship between self-similar fractal dimensions ($D_{SW(1-2)}$, $D_{SL(1-2)}$, $D_{SW(1-3)}$, $D_{SL(1-3)}$) and actual fractal dimensions (D_W, D_L). $D_{SW(1-3)}$ and $D_{SL(1-3)}$ are averages of $D_{SW(1-2)}$ and $D_{SW(2-3)}$; and $D_{SL(1-2)}$ and $D_{SL(2-3)}$ respectively. Although variances are high, self-similar fractal dimensions are in proportion to actual fractal dimensions. $D_{SW(1-3)}$ and $D_{SL(1-3)}$ correlate to actual fractal dimension better than $D_{SW(1-2)}$ and $D_{SL(1-2)}$.

Table 7. 7 Model A calculation

		1st - 2nd					2nd - 3rd				
		# of	1/s		Ds		# of	1/s		Ds	
		blocks	wid	len	wid	len	blocks	wid	len	wid	len
1	Midway Bridge	18	8.66	6.86	1.34	1.50	4.67	5.80	9.37	0.88	0.69
2	Boca Ridge	35	6.61	6.29	1.88	1.93	4.37	16.79	24.61	0.52	0.46
3	Palos Verdes	22	8.88	3.23	1.42	2.64	4.91	6.44	7.73	0.85	0.78
4	Bick Rock Mesa	43	12.13	5.32	1.51	2.25	6.60	10.31	11.69	0.81	0.77
5	Thristle	12	4.77	4.45	1.59	1.66	5.92	10.58	9.08	0.75	0.81
6	Lower Gross	11	3.77	3.89	1.81	1.76	6.45	8.54	13.23	0.87	0.72
7	Upper Gross	18	6.02	5.86	1.61	1.63	3.39	8.35	12.46	0.57	0.48
8	Meadow Mt.	12	4.54	5.16	1.64	1.52	5.50	7.50	6.91	0.85	0.88
9	Mayunmarca	13	4.91	3.86	1.61	1.90	6.08	8.64	6.82	0.84	0.94
10	La Frasse	14	3.50	5.97	2.11	1.48	3.71	5.67	3.91	0.76	0.96
11	Arvey	18	6.91	4.25	1.50	2.00	3.00	9.97	8.62	0.48	0.51
12	Kiritani	23	6.06	3.03	1.74	2.82	2.74	13.66	7.79	0.39	0.49
13	Katsurabara	6	3.11	3.13	1.58	1.57	20.67	10.53	12.18	1.29	1.21
14	Hitohane	57	11.46	9.96	1.66	1.76	5.39	12.82	8.51	0.66	0.79
15	Takisaka	27	6.02	7.52	1.84	1.63	5.26	13.17	16.52	0.64	0.59
16	Sakae	9	4.19	3.79	1.53	1.65	4.33	11.26	3.06	0.61	1.31
17	Mushigame	33	9.28	7.53	1.57	1.73	3.61	12.94	5.06	0.50	0.79
18	Higashinomyo	11	8.04	2.99	1.15	2.19	6.18	11.11	9.83	0.76	0.80
19	Karuizawa	17	4.89	5.51	1.79	1.66	6.59	5.70	8.01	1.08	0.91
20	Happoudai	15	4.65	3.08	1.76	2.41	3.67	10.10	6.99	0.56	0.67
21	Raiden	25	4.56	8.31	2.12	1.52	6.00	11.37	18.93	0.74	0.61
22	Nishinakanoho	11	2.86	5.39	2.28	1.42	4.55	5.78	4.97	0.86	0.94
23	Mizunashi	32	9.44	7.89	1.54	1.68	7.19	12.12	9.37	0.79	0.88
24	Kitaurata	14	4.62	4.86	1.72	1.67	5.29	11.19	5.30	0.69	1.00
25	Uenoyama	7	5.29	2.87	1.17	1.85	6.29	7.72	7.78	0.90	0.90
26	Nakatateyama	15	8.59	3.43	1.26	2.20	5.00	5.32	6.53	0.96	0.86
27	Yumoto	8	3.92	3.60	1.52	1.62	4.25	3.70	5.23	1.10	0.87
28	Yuyama	13	8.61	3.79	1.19	1.92	5.00	4.80	6.87	1.03	0.84
29	Kamatsuka	17	5.73	3.92	1.62	2.08	7.06	8.60	5.69	0.91	1.12
30	Maruyama	17	8.14	5.80	1.35	1.61	8.47	12.39	14.13	0.85	0.81
31	Maseguchi	20	7.31	5.52	1.51	1.75	4.60	5.77	7.21	0.87	0.77
32	Maruta	20	7.41	3.58	1.50	2.35	5.15	11.18	13.33	0.68	0.63
33	Kodomari	18	7.02	5.48	1.48	1.70	3.33	14.50	7.44	0.45	0.60
34	Ohbora	9	3.99	5.35	1.59	1.31	8.00	8.60	6.82	0.97	1.08
35	Urushinose	8	6.60	3.09	1.10	1.85	5.25	7.22	6.91	0.84	0.86
36	Nishinotani	27	6.04	5.95	1.83	1.85	5.07	7.48	7.85	0.81	0.79
37	Youne	8	3.79	2.62	1.56	2.16	4.88	5.80	4.21	0.90	1.10
38	Nuta	11	5.48	4.73	1.41	1.54	9.73	6.17	8.25	1.25	1.08
39	Nyuuya	9	5.24	4.78	1.33	1.40	2.11	4.05	4.43	0.53	0.50
40	Hikinota										
	Average	18.0	6.23	4.94	1.58	1.83	5.65	9.07	8.81	0.79	0.82
	std. Dev.	10.49	2.214	1.696	0.257	0.338	2.889	3.149	4.274	0.205	0.202

Table 7. 8 Fractal dimension of Model - A

No.	Landslide	Real D		Dma(1st-2nd)		Dma(2nd-3rd)		Dma(1st-2nd,2nd-3rd)	
		Whole	Length	width	length	width	length	width	length
1	Midway Bridge	1.53	1.42	1.34	1.50	0.88	0.69	1.11	1.09
2	Boca Ridge	1.33	1.29	1.88	1.93	0.52	0.46	1.20	1.20
3	Palos Verdes	1.48	1.57	1.42	2.64	0.85	0.78	1.14	1.71
4	Bick Rock Mesa	1.48	1.53	1.51	2.25	0.81	0.77	1.16	1.51
5	Thristle	1.32	1.29	1.59	1.66	0.75	0.81	1.17	1.24
6	Lower Gross	1.28	1.17	1.81	1.76	0.87	0.72	1.34	1.24
7	Upper Gross	1.30	1.20	1.61	1.63	0.57	0.48	1.09	1.06
8	Meadow Mt.	1.43	1.24	1.64	1.52	0.85	0.88	1.24	1.20
9	Mayunmarca	1.52	1.40	1.61	1.90	0.84	0.94	1.22	1.42
10	La Frasse	1.59	1.36	2.11	1.48	0.76	0.96	1.43	1.22
11	Arvey	1.24	1.42	1.50	2.00	0.48	0.51	0.99	1.25
12	Kiritani	1.24	1.34	1.74	2.82	0.39	0.49	1.06	1.66
13	Katsurabara	1.38	1.44	1.58	1.57	1.29	1.21	1.43	1.39
14	Hitohane	1.64	1.66	1.66	1.76	0.66	0.79	1.16	1.27
15	Takisaka	1.36	1.30	1.84	1.63	0.64	0.59	1.24	1.11
16	Sakae	1.12	1.42	1.53	1.65	0.61	1.31	1.07	1.48
17	Mushigame	1.31	1.56	1.57	1.73	0.50	0.79	1.04	1.26
18	Higashinomyo	1.22	1.29	1.15	2.19	0.76	0.80	0.95	1.49
19	Karuizawa	1.61	1.43	1.79	1.66	1.08	0.91	1.43	1.28
20	Happoudai	1.35	1.46	1.76	2.41	0.56	0.67	1.16	1.54
21	Raiden	1.53	1.48	2.12	1.52	0.74	0.61	1.43	1.06
22	Nishinakanoho	1.51	1.35	2.28	1.42	0.86	0.94	1.57	1.18
23	Mizunashi	1.60	1.64	1.54	1.68	0.79	0.88	1.17	1.28
24	Kitaurata	1.19	1.43	1.72	1.67	0.69	1.00	1.21	1.33
25	Uenoyama	1.25	1.32	1.17	1.85	0.90	0.90	1.03	1.37
26	Nakatateyama	1.44	1.58	1.26	2.20	0.96	0.86	1.11	1.53
27	Yumoto	1.40	1.30	1.52	1.62	1.10	0.87	1.31	1.25
28	Yuyama	1.40	1.47	1.19	1.92	1.03	0.84	1.11	1.38
29	Kamatsuka	1.46	1.55	1.62	2.08	0.91	1.12	1.27	1.60
30	Maruyama	1.34	1.33	1.35	1.61	0.85	0.81	1.10	1.21
31	Maseguchi	1.49	1.54	1.51	1.75	0.87	0.77	1.19	1.26
32	Maruta	1.37	1.36	1.50	2.35	0.68	0.63	1.09	1.49
33	Kodomari	1.21	1.38	1.48	1.70	0.45	0.60	0.97	1.15
34	Ohbora	1.18	1.33	1.59	1.31	0.97	1.08	1.28	1.20
35	Urushinose	1.11	1.31	1.10	1.85	0.84	0.86	0.97	1.35
36	Nishinotani	1.54	1.52	1.83	1.85	0.81	0.79	1.32	1.32
37	Youne	1.35	1.62	1.56	2.16	0.90	1.10	1.23	1.63
38	Nuta	1.46	1.50	1.41	1.54	1.25	1.08	1.33	1.31
39	Nyuuya	1.22	1.30	1.33	1.40	0.53	0.50	0.93	0.95
40	Hikinota	1.19							
	mean	1.38	1.41	1.58	1.83	0.79	0.82	1.19	1.32
	std. deviation	0.139	0.122	0.257	0.338	0.205	0.202	0.150	0.174

I redefined fractal dimensions of Model A as $D_{MAW} = D_{SW(1-3)}$ and $D_{MAL} = D_{SL(1-3)}$. Coefficient correlations ,r, of D_W versus D_{MAW} and D_L versus D_{MAL} are r = 0.568 and r = 0.421 respectively.

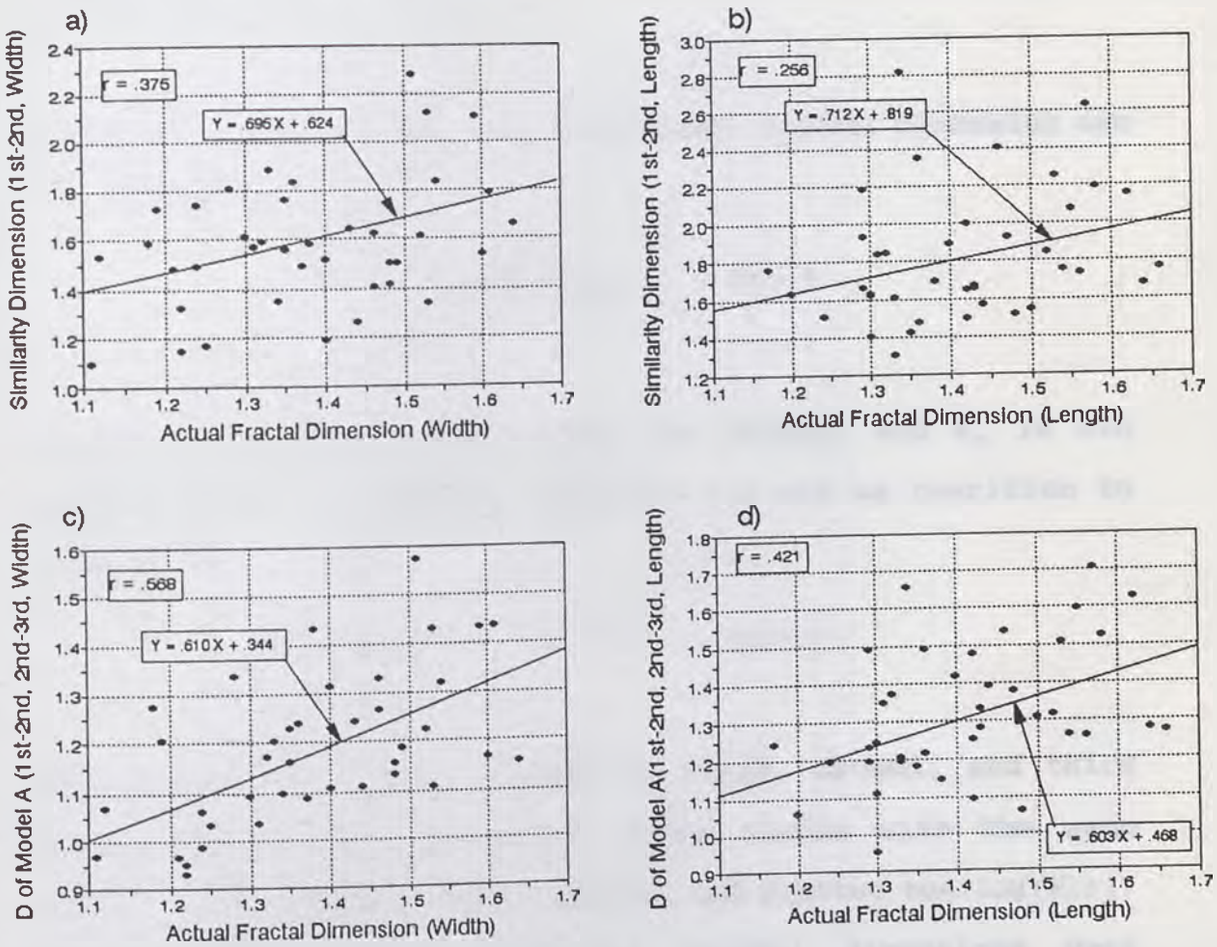

Figure 7.20 Relationship of fractal dimension of actual landslide and Model A a) D_W versus $D_{MAW(1-2)}$; b) D_L versus $D_{MAL(1-2)}$; c) D_W versus $D_{MAW(1-3)}$; d) D_L versus $D_{MAL(1-3)}$

MODEL B

In Model B, each of the second level blocks and the third level blocks has a unique fractal dimension and the combination of these blocks with the first level block yields another fractal dimension (Figure 7.19.b). The method of calculation of Model B fractal dimension, D_B, is as follows (Yokoi and others, 1995):

When there are n blocks, the theoretical fractal dimension can be calculated as:

$$D_n = \frac{\log(n)}{\log(W_1) - \log(w_n)} \quad \text{.....Eq.7.8}$$

where W_1 is the greatest width (or length) and W_n is nth block's width (or length). Equation 7.8 can be rewritten to become:

$$W_n = 10^{[\log(W_1) - (\log(n)/D_n)]} \quad \text{.....Eq.7.9}$$

The theoretical width (length) of first, second, and third level blocks were calculated. These blocks with the same number of real blocks were combined, and plotted the $\log(N(r))$ versus $\log(r)$ curve. Then the fractal dimensions were calculated as the negative of the slope of the least-squares linear regression.

Appendix D shows the $\log(N(r))$ - $\log(r)$ plots of Model B.

Table 7.9 shows actual and Model B fractal dimensions. Figure 7.21 shows the relationship between D_{MB} and the actual dimension (D_W and D_L). They correlate fairly well (coefficient correlation r are r = 0.672 (between D_{MB} and D_W) and r = 0.597 (between D_{MB} and D_L).

Table 7.9 Fractal dimension of Model B and actual D

No		D of Model B		Actual D	
		Width	Length	Width	Length
1	Midway Bridge	1.58	1.30	1.53	1.42
2	Boca Ridge	1.30	1.21	1.33	1.29
3	Palos Verdes	1.20	1.14	1.48	1.57
4	Big Rock Mesa	1.91	1.91	1.48	1.53
5	Thristle	1.22	1.25	1.32	1.29
6	Lower Gross	1.15	1.09	1.28	1.17
7	Upper Gros	1.44	1.24	1.30	1.20
8	Meadow	1.39	1.30	1.43	1.24
9	Mayunmarca	1.18	1.17	1.52	1.40
10	La Frassa	1.57	1.56	1.59	1.36
11	Arvey	1.13	1.38	1.24	1.42
12	Kiritani	1.18	1.59	1.24	1.34
13	Katsurabara	1.27	1.29	1.38	1.44
14	Hitohane	1.84	1.59	1.64	1.66
15	Takisaka	1.40	1.20	1.36	1.30
16	Sakae	1.02	1.06	1.12	1.42
17	Mushigame	1.25	1.68	1.31	1.56
18	Higashinomyo	1.15	1.24	1.22	1.29
19	Karuizawa	1.68	1.60	1.61	1.43
20	Happoudai	1.04	1.54	1.35	1.46
21	Raiden	1.90	1.68	1.53	1.48
22	Nishinakanoho	1.47	1.50	1.51	1.35
23	Mizunashi	1.81	1.76	1.60	1.64
24	Kitaurata	1.49	1.75	1.19	1.43
25	Uenoyama	1.09	1.44	1.25	1.32
26	Nakatateyama	1.58	1.54	1.44	1.58
27	Yumoto	1.47	1.33	1.40	1.30
28	Yuyama	1.44	1.65	1.40	1.47
29	Kamatsuka	1.39	1.53	1.46	1.55
30	Maruyama	1.50	1.39	1.34	1.33
31	Maseguchi	1.82	1.63	1.49	1.54
32	Maruta	1.38	1.28	1.37	1.36
33	Kodomari	1.12	1.35	1.21	1.38
34	Ohbora	1.29	1.35	1.18	1.33
35	Urushinose	1.49	1.50	1.11	1.31
36	Nishinotani	1.52	1.48	1.54	1.52
37	Youne	1.35	1.54	1.35	1.62
38	Nuta	1.72	1.73	1.46	1.50
39	Nyuya	1.17	1.15	1.22	1.30
40	Hikinota			1.19	
	mean	1.41	1.43	1.37	1.41
	std. deviation	0.24	0.21	0.14	0.12

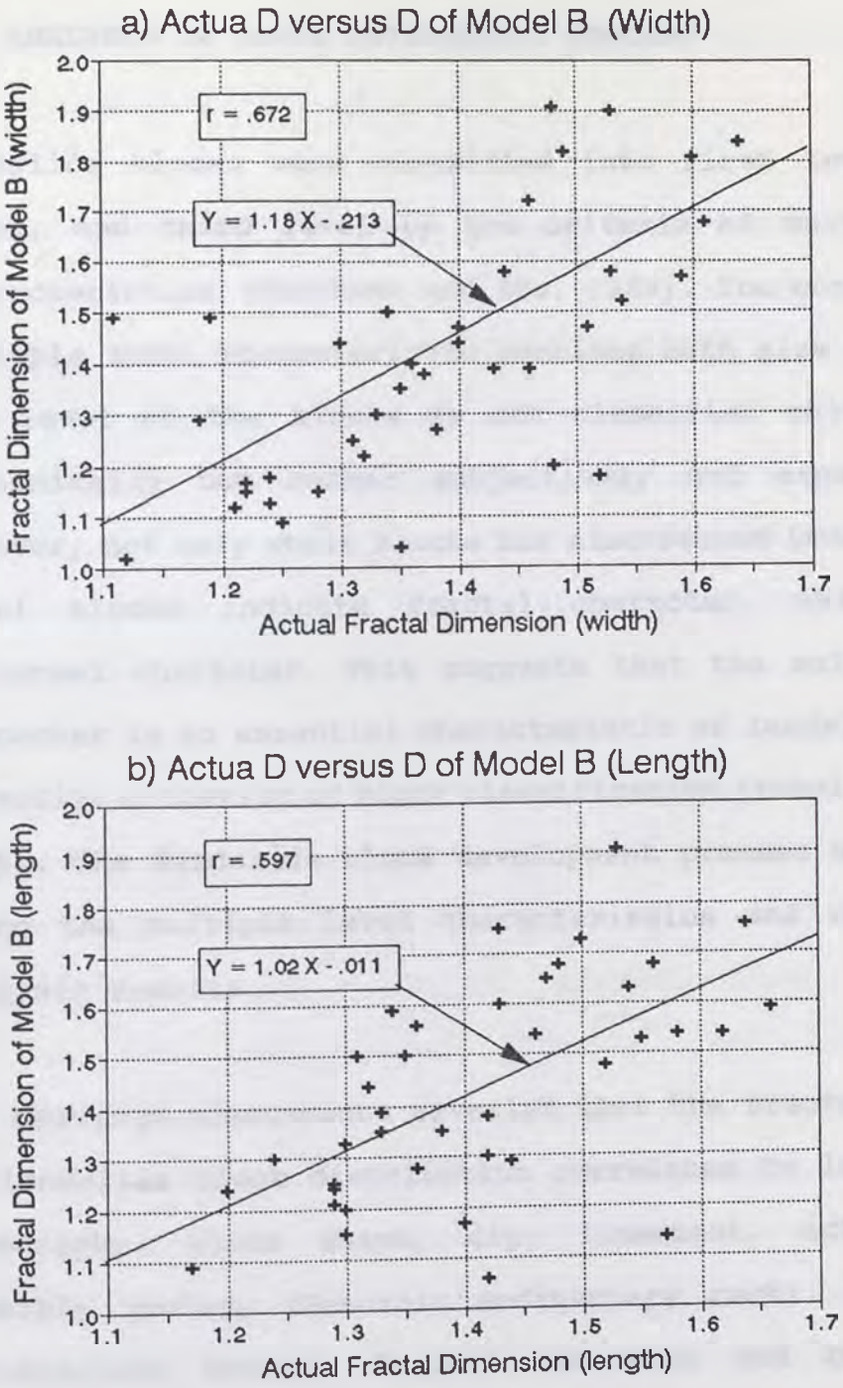

Figure 7.21 Relationship of fractal dimension of actual landslide and Model B a) D_W versus D_{MB}; b) D_L versus D_{MB}

7.4 ANALYSIS OF BLOCK DEVELOPMENT PROCESS

Landslide blocks were classified into first level, second level, and third level by the criteria of multiple level characteristics (Tahahama and Ito, 1989). The concept of the multiple level characteristic combines both size and age, so the level of the blocks is not classified objectively or mechanically but rather subjectively and experimentally. However, not only whole blocks but also second level and third level blocks indicate fractal character, which is the universal character. This suggests that the multiple level character is an essential characteristic of landslides and an effective criterion of block classification (Yokoi and others, 1995). The landslide block development process was analyzed using the multiple level characteristics and the previous analysis results.

The previous discussions revealed that the fractal dimension of landslide block distribution correlates to length/width, topography, block shape, dip, lineament, activity, and possibly geology (Mesozoic sedimentary rock). Among them, correlations between fractal dimension and block shape; topography; and geology, are explained as variations of correlation between fractal dimension and length/width. Dip and lineament are characterized as discontinuities. So the fractal dimension of landslide block distribution is

essentially influenced by landslide geometry (length/width), discontinuities, and activity.

The fact that the fractal dimensions of both Model A and Model B correlate closely with the actual fractal dimensions suggests that the actual landslide block distribution has characteristics of both Model A and Model B. In other words, the landslide blocks develop self-similarly, while at the same time, second and third level blocks develop independently and combined blocks come to have a self-similar character (Yokoi and others, 1995).

The present block distribution is the result of interaction between block propagation and erosion. As discussed previously, activity controls the time of erosion, and geometry and discontinuities control block propagation process. The self-similar (fractal) characteristics of landslide blocks can be explained by the influence of block geometry on block propagation. Under the influence of block geometry, self-similar subsequent blocks develop inside the preceding block. This process is idealized in Model A.

From the analysis of fractal dimension of lineament, it is revealed that lineaments influence second level block distribution but not third level. The fractal dimension of third level blocks is similar to the fractal dimension of

outcrop size fracture and rock fragments. In the process of Model A analysis, it is shown that first and second level blocks have higher b and lower $1/s$ than second and third level blocks. It is considered that different levels of discontinuities influence second level and third level block propagation separately. However, there aren't enough evidence about the influence of discontinuities on third level blocks. The difference of fractal dimension of second and third blocks might be due to differences of their mechanisms. Third level blocks fail as rotational failures while second level blocks fail as complex type (Varnes, 1978) i.e., rotational at head and translational at other part. Translational slide is heavily controlled by discontinuities. This process is idealized as Model B, which shows that second and third level blocks develop independently and combined blocks come to have a fractal character.

Landslide block distribution keeps its fractal character during the process of erosion, because erosion is a fractal process too, i.e., many small blocks are eroded while far fewer big blocks are eroded. As erosion progresses the absolute value of the slope of $\log(N(r))$ versus $\log(r)$ plot, which is equivalent to fractal dimension, decreases (Figure 7.20). The fractal dimension can be an index of activity or time passed since block propagation stopped.

The block development process of landslides is summarized as follows (Figure 7.22):

Stage 1: Initial (first level) slide occurred as a huge block.

Stage 2: Second-level blocks occur inside the initial blocks. They are controlled by the geometry of the initial block and by lineaments (discontinuities). Second-level block distribution has a unique fractal dimension, which relates to the fractal dimension of the lineaments.

Stage 3: Third-level blocks occur mainly inside the second-level blocks. They are controlled by the geometry of the second-level blocks and by cohesion and friction of soil and/or outcrop size fractures. Third-level block distribution has a unique fractal dimension which is similar to the fractal dimension of fractures and rock fragment. Whole block distribution has another unique fractal dimension.

Stage 4: Erosion starts where activity finished. Block distribution keep its fractal character during erosion; however, the fractal dimension decreases in proportion to the degree of erosion.

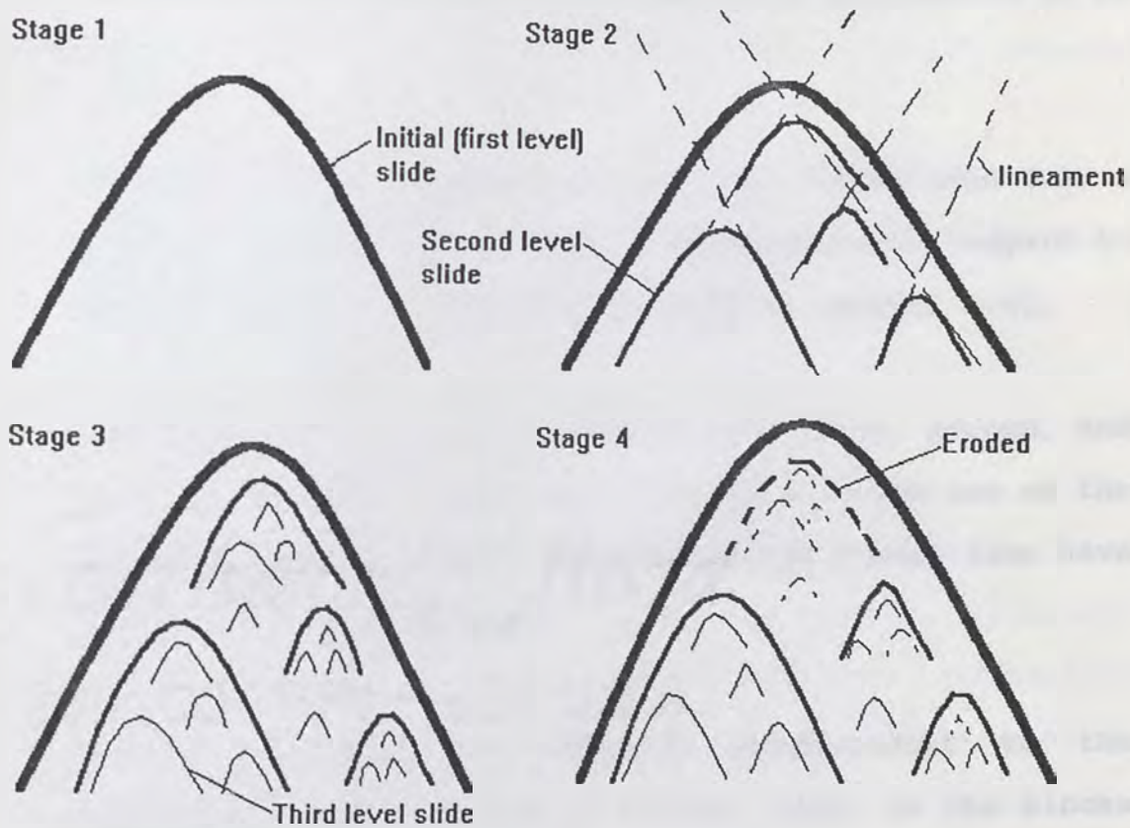

Figure 7.22 Conceptional landslide block development process

CHAPTER EIGHT: CONCLUSION AND FURTHER STUDY

The fractal characteristics of landslide block distribution were analyzed and the block development process was discussed using its fractal character. The summary of my research is as follows:

Landslide block distribution in huge landslides has a fractal character. Their fractal dimension with respect to width averages 1.37 and with respect to length, 1.41.

Huge landslides can be classified into first, second, and third level blocks based mainly on the size and age of the blocks. Second and third level landslide blocks also have unique fractal dimensions.

Fractal dimension is reversely proportional to the logarithm of the variance of blocks' size. So the blocks with greater variance have smaller fractal dimension and the blocks with smaller variance have greater fractal dimension.

Fractal dimension correlates to the geometry of landslide, discontinuities of base rock, and activity of the landslide. Fractal dimension is independent from size of the landslide, angle of the slide surface, and geology of

the base rock.

The fractal character of landslide block distribution can be explained by: 1) self-similar geometry (Model A); 2) unique fractal dimensions made by combining second and third level blocks (Model B); and 3) the fractal erosion process.

The self-similar (fractal) character of landslide blocks can be explained by the influence of block geometry on block propagation (a preceding block to subsequent blocks).

The unique fractal dimension of second and third level blocks is explained by the fractal dimension difference between lineament and fracture, or different mechanisms (second level blocks: rotational + transnational; third level blocks: rotational).

The activity of landslides correlated to the fractal dimension. Activity levels were defined with time passed since block propagation ended. As erosion progresses, the fractal dimension of the landslide block distribution decreases.

Data were collected on 40 landslides, however, field surveys were performed on only nine landslides of the 40. The quantity and quality of the data varies greatly. Analysis using data of uniformally high reliability would improve understanding of the fractal character of landslides.

The development process was analyzed of landslides which occurred as huge landslides in ancient times and includes smaller blocks inside the huge landslides. However, some other landslide development processes are known e.g., the retrogressive type, so analysis of the development process of other types will be important.

The block propagation process was analyzed using the two kinds of models. However, the erosion process, which also influences fractal dimensions, was analyzed only in terms of time. Degree of erosion depends on its energy, the resistance (strength) of the soil, and length of time. A proper model for erosion, taking into consideration its energy and the resistance of the soil, would help in better understanding the fractal character of landslide block distribution.

Many tragic landslide-related incidents have occurred all over the world. Many of them are caused by artificial work, e.g., construction or mining. They could be avoided if the potential for landslides had been recognized and mitigated properly.

Recognizing landslides, especially huge dormant or stable ones, is an important and basic task for the geotechnical engineer; it is also a difficult task. Even an experienced engineer sometimes misses recognizing landslides. Knowledge of the landslide block distribution pattern, which is fractal geometry, would help in recognizing potential landslides.

REFERENCES

American Geological Institute, 1976, *Dictionary of Geological Terms,* Anchor Press, Garden City, New York, p.472.

AVILES C. A.; SCHOLZ, C. H.; AND BOATWRIGHT, J., 1987, Fractal analysis applied to characteristic segments of the San Andreas Fault: *Journal of Geophysical Research,* Vol. 92, No. B1, pp. 331-344.

BARNSLEY, M. F., 1988, *Fractals Everywhere,* Academic Press, Boston, p. 394.

BEROCAL, J.; ESPINASA, A. F.; AND GALDOS, J, 1978, Seismological and geological aspects of the Mantaro landslide in Peru: *Nature,* Vol. 275, pp. 533-536.

CARR, J. R., 1990,CORSPOND: a portable FORTRAN-77 program for correspondence analysis: *Computers and Geosciences,* Vol. 16, No. 3, pp. 289-307.

CARR, J. R., 1994, *Numerical Analysis for the Geological Sciences,* Prentice hall, Englewood Cliffs, NJ, p. 592.

CARR, J. R. AND BENZER, W. B., 1991, On the practice of estimating fractal dimension: *Mathematical Geology,* Vol. 23, No. 7, pp. 945-958.

CARR, J. R. AND WARRINER, J. B., 1989, Relationship between the
fractal dimension and joint roughness coefficient: *Bulletin of the Association of Engineering Geologists,* Vol. 26, No. 2, pp. 253-263.

DARIN, D., 1993, *The Meadow Mountain Landslide Complex, Eagle County, Colorado*, unpubl. MS thesis, Machay School of Mines, University of Nevada, Reno, p. 142. John Wiley and sons, New York, p. 646.

DAVIS. D. C., 1986, *Statistics and Analysis in Geology*, John Wiley and sons, New York, p. 646.

DAVIS. W. M., 1923, The cycle of erosion and the summit level of Alps, *Jour. Geol.*, Vol. 31, pp. 1-41.

DAVORE. J. L., 1987, *Probability and Statistics for Engineering and the Sciences,* Cole Publishing Company, Monterey, California, p. 672.

DIETRICH F. H. AND KEARNS, T. J., 1989, *Basic Statistics*, Dellen Publishing Co., San Francisco, Collier Macmillan Publishers, London, p. 745.

FEDER, J., 1988, *Fractals*, Plenum Press, New York, p. 283.

GABUS, J. H.; BONNARD, CH.; NOVERRAZ, F.; AND PARRIAUX, A., 1988,
Arveyes, un glissement, une tentative de correction:In Bonnard, C. (editor), *Proceedings of the Fifth International Symposium on Landslides, Lausanne, Switzerland,* A.A. Balkema, Rotterdam. pp. 911-914.

GATES, W. C. B., 1994, *Regional Slope Stability of the Truckee*
River Canyon (Drainage Basin) from Tahoe City, California to Reno Nevada, unpubl. PhD thesis, Machay School of Mines, University of Nevada, Reno, p. 380.

GATES, W. C. B. AND WATTERS, R. J., 1992, Geology of Reno and Truckee Meadows, Nevada, United States of America: *Bulletin of the Association of Engineering Geologists,* Vol. XXIX, No. 3, pp. 229-298.

HAIR, J. F.; ANDERSON, R. E.; TATHAM, R. L.; AND BLACK, W. C., 1984, *Multivariate Data Analysis with Readings,* Macmillan, New York. p. 592.

HANSEN, M., 1984, Strategies for classification of landslides: In Brunsden, D. (editer), *Slope Instability,* John Wiley and Sons Ltd., New York. pp. 1-25.

HIGAKI, D.; UENO, T.; AND YOSHIMATSU, H., 1994, Progress level and fractal evolution of landslide slopes: *Proceedings of the Seventh International Symposium on Landslides, Lausanne, Switzerland,* A.A. Balkema, Rotterdam. pp. 83-88.

HUCHINSON, J. N., 1988, General report: morphological and geotechnical parameters of landslides in relation to geology and hydrogeology: In Bonnard, C. (editor), *Proceedings of the Fifth International Symposium on Landslides, Lausanne, Switzerland,* A.A. Balkema, Rotterdam. pp. 3-35.

IKEDA, 1984, A huge landslide reactivated due to snow melting (in Japanese): *Landslide*, Japan Landslide Society Kansai Branch, No.2, pp. 1-10.

KALISER, B. N. AND FLEMING, R. W., 1986, The 1983 landslide dam st Thistle, Utah. In Schuster, R. L. (editor):*Landslide Dams: processes, Risk, and Mitigation,* American Society of Civil Engineers, New York. pp. 59-83.

KOJAN, E. AND HUTCHINSON, J. N., 1978, Mayunmarca rockslide and debris flow, Peru. In Voight, B. (editor): *Rockslides and Avalanches,* Elsevier Scientific Pub., Amsterdam. pp. 315-361.

KONUKI, Y, 1973, *Introduction to Applied Geology,* Morikita Publisher Co., p. 308.

KORVIN, G., 1992, *Fractal Models in the Earth Sciences,* Elsevier, Amsterdam. p. 396.

LAUWERIER, H. A., 1991, *Fractals: Endlessly Repeated Geometrical Figures,* Princeton University Press, Princeton, New Jersey. p. 209.

LEE, K. AND DUNCAN, J. M., 1975, *Landslide on April 25, 1974 on the Mantaro River, Peru,* National Academy of Sciences, Washington D. C., p. 71.

MANDELBROT, B.B., 1967, How long is the coast of Britain? Statistical self-similarity and fractional dimension: *Science,* Vol. 156, pp. 636-638.

MANDELBROT, B.B., 1977, *Fractals; Form, Chance and Dimension,* W. H. Freeman, San Francisco, p. 365.

MANDELBROT, B.B., 1982, *The Fractal Geometry of Nature,* W. H. Freeman, New York, p. 468.

MANDELBROT, B.B., 1990, Fractal geometry: What is it, and what does it do?: In Fleischmann M., Tildesley, D. J., and Ball, R. C. (editors), *Fractals in Natural Sciences,* Princeton University Press, Princeton, NJ, pp. 3-16.

McGUIRE, M., 1991, *An Eye for Fractals,* Addison-Wesley Publishing Company, Redwood City, CA, p. 165.

MERCERON, T.; AND VELDE, B., 1991, Application of Cantor's Method
for fractal analysis of fractures in the Toyoha Mine, Hokkaido, Japan: *Journal of Geophysical Research,* Vol. 96, No. 10, pp. 16,641- 16,650.

MINISTRY OF AGRICULTURE, HOKUROKU BRANCH, 1993, , *Report of Special Landslide Mitigation in Hokuriku Region,* unpubl. circular, p.

MITCHELL, B. M., 1986, *An Engineering Analysis of the May 1983 Rock Slope Failure on Slide Mountain, Nevada,* unpbl. Master thesis, Machay School of Mines, University of Nevada, Reno, p. 176.

NOVERRAZ, F. AND BONNARD, Ch, 1988, Technical note on the visit of La Frasse Landslide: In Bonnard, C. (editor), *Proceedings of the Fifth International Symposium on Landslides, Lausanne, Switzerland,* A.A. Balkema, Rotterdam. pp. 1549-1554.

OKUSA, S.; TAKAHAMA, N.; AND FUJITA, Y., 1991, Landslide history in a Tertiary sedimentary basin in Quaternary in Japan: *Quaternary Engineering Geology,* Geological Society Engineering Geology Special Publication No.7, pp. 671-677.

OLESON, S. G., 1989, *A Multivariate Statistical Analysis of Selected Western Nevada Reservoirs: Implications for Ecology of Stillwater Lakes, Nevada,* unpbl. Master thesis, Machay School of Mines, University of Nevada, Reno, p. 157.

OLESON, S.G. AND CARR, J. R., 1989, A multivariate analysis of Stillwater Lakes, Nevada: *Proceedings of National Water Conference, IR and Wr Divs, ASCE, Newark, Delaware, July, 1989,* pp. 196-203.

OLESON, S.G. AND CARR, J. R., 1990, Correspondence analysis of water quality data: implications for fauna deaths at Stillwater Lakes, *Mathematical Geology,* Vol. 22, No. 6, pp. 665-698.

OLSHANSKY, R. B., 1990, *Landslide hazard in the United states: Case study,* p. 63.

PEITGEN, H-O.; MALETSKY, E.; PERCIANTE, T. H.; AND YUNKER, L. E., 1992, *Fractals for the classroom,* Vol.1, Springer-Verlag, New York, p. 450.

SASAKI, Y.; ABE, M.; AND HIRANO, I., 1991, Fractal of slope failure
size-number distribution (in Japanese with English abstruct): *Journal of the Japan Society of Engineering Geology,* Vol. 32, No. 3, pp. 1- 11.

SATSUMA, J, 1992, *Probability · statistics,* Iwanami shoten, p. 222.

SCHRODER, J. F., 1971, Landslide of Utah, *Utah Geological and Mineralogical Survey,* Blletin 90, pp. 1-51.

SCHUSTER, R. L., 1985, Landslide dams in the western United States, *Proceedings of the Forth International Symposium on Landslides, Tokyo, Japan,* A.A. Balkema, Rotterdam. p. 164.

SHARPE, C. F. S., 1938, *Landslides and Related Phenomena,* Columbia University Press, New York, p. 137

TAKAHAMA, N., 1983, Older large-scale primaly landslide (in Japanese): *Ann. Rep. Saigaiken,Niigata Univ.*, NO.5, pp.43-52.

TAKAHAMA, N., 1988, On the large-scale ancient primary landslide (In Japanese): *Ann. Rep. Saigaiken,Niigata Univ.*, NO.10, pp.43-52.

TAKAHAMA, N., 1991, Some problems on ancient primary landslide mass and "rockslide" (in Japanese): *Ann. Rep. Saigaiken,Niigata Univ.*, NO.13, pp.9-22.

TAKAHAMA, N., 1992, On the huge landslide (in Japanese): *Proceeding of the 2nd Symposium on Geo-Environments*, pp.187-192.

TAKAHAMA, N. AND ITO, Y., 1989: Relation between huge ancient primary landslides and present landslides -- Level and history of landslide activities -- (in Japaneses with English abstruct): *Annual Report of Saigai-ken, Niigata University, Japan,* No.11, pp.25-36.

TAKAHAMA, N. AND YAMAZAKI, K., 1987: Studies on the ancient primary landslide (1) --Case studies of Sakae Primary Landslide--(in Japaneses): *Annual Report of Saigai-ken, Niigata University, Japan,* No.9, pp.85-90.

TAKAHAMA, N.; HAYAKAWA, K.; KATAGIRI, S.; AND FUKUMOTO, Y., 1991, Higashi-nomyo Landslide --Part 1, Landslide history and ground water--(in Japanese): *Journal of Japan Landslide Society*, Vol. 28, pp. 40-47.

TAKAHAMA, N. AND HAYAKAWA, in print, Presently active landslides in ancient primary slid mass at Higashinomyo, Niigata, Central Japan (in Japanese): *Journal of Japan Landslide Society*.

TAKAHAMA, N.; UDA, T.; NOZAKI, T.; YOKOI, Y.; AND SUZUKI, K., 1992, Hazard and environmental geology of northern part of Fossa Magna and southern part of Northeast Japan: *Proceeding of 29th IGC Field Trip C16,* pp. 1-33.

TAKAYASU, H., 1991, *Fractals in the Physical Sciences*, Wiley, New York, pp. 170.

TURCOTTE, D. L., 1986, Fractal and fragmentation: *Journal of Geophysical research*, Vol. 91, No. B2, pp. 1,921-1,926.

TURCOTTE, D. L., 1992, *Fractals and Chaos in Geology and Geophysics,* Cambridge University Press, Cambridge, New York, p. 221.

UENO, T.; YOSHIMATSU, H.; AND NISHI, M., 1993, Fractal property and hierarchy of landslides in fractured zones (In Japanese): *Proceedings of Japan Landslide Society Symposium on Some Problems about Geomorphology of landslides,* pp. 114-121.

VARNES, D. J., 1978, Slope movement types and processes. In: *Landslides: Analysis and Control,* Transportation Res. Board Nat. Ac. Sci. Washington Spec. Rep. 176, pp. 11-33.

VARNES, D. J., 1984, *Landslide hazard zonation: a review of principles and practice,* International Association of Engineering Geology, Unesco, Paris, p. 63.

VOIGHT, B., 1978, Lower Gros Ventre Slide, Wyoming, U.S.A., Voight, B. (editor): *Rockslides and Avalanches,* Elsevier Scientific Pub., Amsterdam. pp. 113-166.

VONDER, L. AND LINDVALL, C. E., 1982, The Portuguese Bend Landslide, In Cooper, J. D. (editer):*Landslide and Landslide Abatement, Palos Verdes Peninsula, Southern California,* Assoc. of Engineering Geologists, Southern California Section, Anaheim, pp. 49-56.

VOSS, R. F., 1988, Fractals in nature: From characterization to
simulation. In Peitgen H.-O. and Saupe, D. (editors):*The Science of Fractal Images,* Springer-Verlag, New York. pp. 21-70.

WATARI, M., 1977, A couple of problems about slope failure: *Soil and Foundation,* No 26, No. 6. pp. 3-8.

WATTERS, R. J., 1983, A Landslide Induced Waterflood-Debris Flow:
Bulletin of the International Association of Engineering Geology, No 28, pp. 12-17.

WATTERS, R. J.; CARR, J. R. AND CHUCK, D.M., 1990, New techniques in rock mass classification: application to welded tuffs at the Nevada Yucca Mountain, *International Journal of Mining and Geological Engineering,* Vol. 8. pp. 241-260.

WILLIAM COTTON AND ASSOCIATES, 1994, *Geological Map of the Big Rock Mesa Landslide.*

YOKOI, Y.; CARR, J. R.; AND WATTERS, R. J., 1995, Fractal character of landslides: *Bulletin of the Association of Engineering Geologists,* in press.

ZARUBA, Q. AND MENCL, V., 1982, *Landslides and their Control,* Elsevier, Amsterdam, p. 324.

APPENDIX A:

OUTLINE OF LANDSLIDES, BLOCK DISTRIBUTION MAPS, LINEAMENT MAPS, AND SAMPLING MAPS

OUTLINE OF LANDSLIDES

NO.1 MIDWAY BRIDGE LANDSLIDE

INVESTIGATION

Field investigation (from June to September, 1994), Areal photography interpretation, Map interpretation, literature (Gates, 1994)

LOCATION

39° 12' N; 120° 12' W

GEOMORPHIC EXPRESSION

First level block is rectanglar shaped. Main scarp is very distinguished (80 m).

There are several sags on the head of main slide.

Toe of slide has been oversteepend by recent erosion from the Truckee River.

Clear second and third level blocks exist.

MECHANICAL TYPE OF SLIDE

First Level Block is Rotational (Gates, 1994).

Many second and third level rotational slides has occurred.

Rock fall has occurred at the main scarp.

GEOLOGY

Surfacial Deposits: colluvium and landslide debris. Various angular to subrounded cobbles and boulders in matrix of sand and clay (Gates, 1994).

Base Rock: Tertiary andesite with steep dipping joints sets with striking NW-SE, NE-SW, and E-W (Gates, 1994).

PRIMARY CAUSE OF FAILURE

Flooding and rapid drawdown Lake Tahoe (Gates, 1994)

HISTORY OF LANDSLIDE

Relative minimum age of landslide: 60 ka ± 18 ka BP (Gates, 1994)

Two separate failure events might have occurred.

STABILITY

Factor of safety of main slide: about 1.2 (Gates, 1994)

Some small rotational slides are unstable (there are fresh scarps and tilting trees)

NO. 2 BOCA RIDGE LANDSLIDE

INVESTIGATION

Field investigation (from June to September, 1994), Areal photography interpretation, Map interpretation, literature (Gates, 1994)

LOCATION

39° 3' N; 120° 4' W

GEOMORPHIC EXPRESSION

Boca Ridge Landslide is complex of four Huge slides: Central-North (C-N), Central-South (C-S), West-North (W-N), and West-South (W-S).

Sags exist at the head of C-N, C-S, and W-N blocks. C-S and W-S blocks have steep toes which has been eroded Truckee River. Second and third level blocks are eroded and difficult to be recognized.

MECHANICAL TYPE OF SLIDE

C-N Block: Regressive rotational slide (Gates, 1994)

C-S and W-N Block: Rotational at head and traslational at middle and toe zone.

W-S Block: rotational

Many second and third level slides has occurred. Rock fall has occurred at the main and minor scarps of the blocks.

GEOLOGY

Surfacial Deposits: Colluvium and landslide debris. Angular to subangular cobbles and boulders exist in matrix of sand and clay (Gates, 1994).

Base Rock: At the toe the slide debris has overrun older Tahoe outwash deposits. At south slide debris overlaps diatomaceous and tuffaceous sandstone and shale of Tertiary Truckee Formation. Rocks at main scarp of C-N and W-N blocks is Tertiary Boca Ridge Latite.

Strike and dip of Truckee Formation is N56°E 22°E (Dip slope). A normal fault exists at head scarp of C-S and W-N block (Gates, 1994).

PRIMARY CAUSE OF FAILURE

Under cutting by flood (Gates, 1994), Fault at head scarp. Seismicity?

HISTORY OF LANDSLIDE

Relative minimum age of landslide: 60 ka ± 18 ka BP (Gates, 1994).

Two or three separate failure events might have occurred (Gates, 1994). Gates (1994) suggested that the landslide have developed retrogressively. It is considered that C-S, W-N, W-S

blocks occurred as initial slide first and then second and third level slides occurred. Because these blocks has clear main scarps and flanks; and the main scarps of C-S and W-N blocks coincide the fault. It is considered that C-N block developed retrogressively because clear normal fault like gaps occurred in the block.

STABILITY

The landslide is very stable. No sliding occurred when toe was cut with I-80 construction and sand pits.

NO. 3 PALOS VERDES LANDSLIDE

INVESTIGATION

Field investigation (July, 1994), Areal photography interpretation, Map interpretation, literature (Vonder Linden and Lindvall, 1982)

LOCATION

33° 45' N; 118° 21' W

GEOMORPHIC EXPRESSION

First level block is rectanglar shaped. The toe of slide has been steepened by erosion from Pacific Ocean.

Depression occurred at head. Clear second and third level blocks exist.

MECHANICAL TYPE OF SLIDE

First and second level slides: Rotational at head and traslational at middle and toe zone.

Third Level slides: rotational

GEOLOGY

First Level Block: Folding sedimentary rocks and basalt.

Second Level Blocks: Sedimentary rocks and basalt with complex faulting and folding.

Third level blocks: Colluvial and landslide debris.

Base Rock: Miocene sandstone, mudstone, tuff, and basalt. Dip slope (Vonder Linden and Lindvall, 1982)

PRIMARY CAUSE OF FAILURE

Erosion by ocean, Weak tufaceous layer, Seismicity.

HISTORY OF LANDSLIDE

The main (first level) slide is considered to occur in Pleistocene (Vonder Linden and Lindvall, 1982). Second and

third level slides followed the main slide.

STABILITY
A part of Portuguese Bend landslide is presently active. A part of Abalone Cove landslide had been active in 1960s and was stopped by mitigation.

MITIGATION
Horizontal drainage boring, Piles, Removal of landslide debris

NO. 4 BIG ROCK MESA LANDSLIDE

INVESTIGATION
Field investigation (July, 1994), Areal photography interpretation, Map interpretation, literature (Olshansky, 1990)

LOCATION
34° 2' N; 118° 38' W

GEOMORPHIC EXPRESSION
First level block is horse-shoe shaped. The toe of slide has been steepened by erosion from Pacific Ocean. Clear second and third level blocks exist except resident area.

MECHANICAL TYPE OF SLIDE
First and second level slides: Rotational at head and traslational at middle and toe zone.
Third Level slides: Rotational

GEOLOGY
Surfacial Deposits: Colluvial and landslide debris.
Base Rock: Eocene to Miocene sandstone and mudstone which are strongly folded and faulted by low angle trust faults, and dipping into slope with 25° to 65° (Olshansky, 1990).

PRIMARY CAUSE OF FAILURE
Erosion by ocean, Seismicity, Sewage water

HISTORY OF LANDSLIDE
The main (first level) slide is considered to occur prehistoric age. The landslide reactivated in 1983.

STABILITY
Landslide in 1983 was due to groundwater primary from residential septic systems (Olshanski, 1990). The slide has ceased due to dewatering. The slide didn't reactivate by Northrigde Earthquake on January, 1994.

NO.5 THISTLE LANDSLIDE

INVESTIGATION

Areal photography interpretation, Map interpretation, Literature (Schroder, 1991; Olshansky, 1990; Schuster, 1985; Ikeda, 1984; Kaliser and Fleming, 1986)

LOCATION

40° 0' N; 111° 31' W

GEOMORPHIC EXPRESSION

First level block is horse-shoe shaped. The flanks forms streams.

Second and third level blocks occur mainly at the sides and the toe of the slide. Some depression and sags occur at head of the slide.

MECHANICAL TYPE OF SLIDE

First and second level slides: Rotational at head and traslational at middle and toe zone.

Third Level slides: Rotational

GEOLOGY

Surfacial Deposits: A moderately plastic gravelly clay (Kaliser and Fleming, 1986).

Base Rock: Conglomerate, sandstone, and red shale of the North Horn Formation of Cretaceous-Tertiary age, which is overlain by Tertiary limestone, shale, and sandstone of the Flaggstaff Formation and conglomarate and red beds of the Colton Formation, also of Tertiary age (Schroder, 1971).

PRIMARY CAUSE OF FAILURE

Poorly consolidated sedimentary rock, Rapid drawdown of Lake Benneville, Erosion by the River.

HISTORY OF LANDSLIDE

The initial slide may have occurred approximately 14,000 years ago (Anderson and others, 1984; quoted in Olshansky, 1990).

A part of the landslide (2.2×10^6 m^3) reactivated on April 1983 due to heavy rain. The landslide formed a natural dam blocking the Spanish Fork River (Kaliser and Fleming, 1985).

STABILITY

The landslide is presently stable.

MITIGATION

A drainage tunnel in the dam, Reinforcement for the dam.

NO.6 LOWER GROS VENTRE LANDSLIDE

INVESTIGATION
Map interpretation, Literature (Voight, 1978).

LOCATION
43° 38' N; 110° 33' W

GEOMORPHIC EXPRESSION
The landslide can be divided into eastern part and western part by a stream. The eastern part is horse-shoe shaped, and has steep slope at the head and gentle slope at the toe. The toe forms a natural dam for Lower Gros Lake. The western part is triangle shaped and has NE-SW direction scarps and sags at the head. The gros Ventre River meanders very much at the toe of the slide. Clear second and third level blocks exist.

MECHANICAL TYPE OF SLIDE
First and second level slides: Rotational at head and traslational at middle and toe zone.

Third Level slides: Rotational

GEOLOGY
Surfacial Deposits: Weathered sandstone and Limestone, Clay-rich debris

Base Rock: Dolomite, shale, and sandstone of the Amsden Formation (Mississippian-Pennsylvanian); and Tensleep Sandstone (Pennsylvanian), Dip Slope (20°).

PRIMARY CAUSE OF FAILURE
Weathering, Heavy precipitation , and Seismicity

HISTORY OF LANDSLIDE
The initial slide occurred in prehistoric age. The eastern part (40×10^6 m^3) reactivated in June 23, 1925 due to heavy rain and earthquake. The slide dam formed Lower Gros Lake.

STABILITY
The landslide is presently stable.

NO.7 UPPER GROS VENTRE LANDSLIDE

INVESTIGATION
Aerial photography interpretation, Map interpretation.

LOCATION
43° 35' N; 110° 23' W

GEOMORPHIC EXPRESSION
First level block is rectangular shaped. The main scarp has been eroded and the flanks forms streams. Second level slides occurred mainly at the sides and the toe of the first level slide. It is difficult to recognize second and third level blocks.

GEOLOGY
Base Rock: Mesozoic sedimentary rocks. Dip slope.

PRIMARY CAUSE OF FAILURE
Weathering, Heavy precipitation , Seismicity

NO.8 MEADOW MOUNTAIN LANDSLIDE

INVESTIGATION
Map interpretation, Literature (Duran, 1993).

LOCATION
39° 37' N; 106° 27' W

GEOMORPHIC EXPRESSION
First slide is horse-shoe shaped. The main scarp is not clear. The right flank forms a stream. The left flank forms a steep slope. The slide area is used to be used for agriculture but it is presently used for a recreation area. Clear second and third level blocks exist.

MECHANICAL TYPE OF SLIDE
First level slide: Traslational.
Second level slides: Rotational at head and translational at middle and toe zone.
Third Level slides: Rotational

GEOLOGY
Surfacial Deposits: Colluvium, landslide debris; and weathered sandstone and shale.
Base Rock: Sandstone, shale, limestone, and dolomite of Minturn Formation (Pennsylvanian). Dip slope (15°).

PRIMARY CAUSE OF FAILURE
Alternation of base rock, faults, and erosion by Eagle River.

HISTORY OF LANDSLIDE
The initial slide is considered younger than 120-150

thousand years before present (stratigraphically) and older than 8,400 years before present (C^{14}).

STABILITY

A part of landslide (12 million ft^3) at the toe reactivated on April 1985. Adjust region (12,000 ft^3) reactivated in spring 1992. The landslide is presently stable.

MITIGATION

Removal of slide material, surface drainage, rock buttress.

NO.9 MAYUNMARCA LANDSLIDE

INVESTIGATION

Literature (Kojan and Huchinson, 1978; Lee and Duncan, 1975; Berrocal and others, 1978).

LOCATION

12° 40' S; 174° 40' W

GEOMORPHIC EXPRESSION

First level slide is bottle-neck shaped. The main scarp has been eroded. The flanks forms steep slopes.

MECHANICAL TYPE OF SLIDE

First level slide: Traslational.

Second level slides: Rotational at head and translational at middle and toe zone.

Third Level slides: Rotational

GEOLOGY

Surfacial Deposits: Widely graded material, e.g., clay size particle to blocks on the order of 10^2 m^3 (Kojan and Huchinson, 1978).

Base Rock: Permian sandstone and shale lying on Paleozoic schist and phylites. Sandstone and shale are overlain by glacial deposits or by unconsolidated weathered permeable Quaternary alluvium (Berrocal and others, 1978).

PRIMARY CAUSE OF FAILURE

Ground water, Dip slope.

HISTORY OF LANDSLIDE

The initial slide occurred prehistoric age. Reactivation of a part of slide have been recorded in 1930, on August 1945 (5×10^6), in 1960, in 1972, and in 1974. Reactivation in 1974 was gigantic catastrophic one, which resulted 51 deaths and large amount of economic damage.

NO.10 LA FRASSE LANDSLIDE

INVESTIGATION
Literature (Noverraz and Bonnard, 1988).

LOCATION
46° 20' N; 7° 0' E

GEOMORPHIC EXPRESSION
First level slide is long rectangular shaped. The landslide flows in an approximately 500 m wide channel and then spreads in the zone of the toe.

MECHANICAL TYPE OF SLIDE
First level slide: Traslational.
Second level slides: Rotational at head and translational at middle zone.
Third Level slides: Rotational

GEOLOGY
Surfacial Deposits: Soil and decomposed rock.
Base Rock: Clayey schistic rocks. Dip slope.

HISTORY OF LANDSLIDE
The initial slide might have occurred slightly after glacier retreat. Reactivation occurred during 1913-1919, 1966, 1981-1982.

NO.11 ARVEYES LANDSLIDE

INVESTIGATION
Literature (Gabus and others, 1988).

LOCATION
46° 9' N; 7° 2' E

GEOMORPHIC EXPRESSION
First level slide is horse-shoe shaped. The main scarp is clear. The head zone is flat and used for residential land. The slope of toe zone is steep.

MECHANICAL TYPE OF SLIDE
First and second level slides: rotational at head and translational at middle zone.
Third Level slides: Rotational

GEOLOGY
Base Rock: Schist

STABILITY
A part of landslide reactivates.

No. 12 KIRITANI LANDSLIDE

INVESTIGATION
Field Investigation, Drilling, Aerial photography interpretation, Topographic map interpretation.
Investigations wsre performed during 1985 to 1988 as projects of Toyama Prefectual Government. Nittoc Construction Co., of which I was an employee, was contractor of that investigation.

LOCATION
36° 33' N; 137° 11' E

GEOMORPHIC EXPRESSION
Shape of first level block is horse shoe.
There is a steep main scarp (60 m) which consists of andesite lava and tuff breccia. Slope of the landslide is gentle and used to be used for rice fields. Clear second and third blocks exist.

TYPE OF SLIDE
First and Second Level Slide: Rotational at head and translational at middle and toe zone.
Third Level Slide: Rotational

GEOLOGY
Surfacial Deposits: Colluvium and landslide debris. Angular to subround cobbles and boulders (maximum diameter 20 m) in matrix of tuffaceous clay.
Base Rock: Miocene tuff breccia, tuff, mudstone, sandstone.

Strike and dip is approximately EW 20°N. Apparent angle to the slope is horizontal.

PRIMARY CAUSE OF FAILURE
Weak tuff including montmorillonite. Erosion by a river. Seismicity.

HISTORY OF LANDSLIDE
First level slide might have occurred in Pleistocene and then second and third level slides followed. Historical and geographical evidences indicate that northern part of landslide moved more than 1,000 years ago and dammed the river.

STABILITY
First and second level slides are stable due to high permeability and low water table, however, some small rotational slides occurred in last decade.

MITIGATION
Surface drainage, Horizontal drainage boring, Vertical drainage wells.

NO. 13 KATSURABARA LANDSLIDE

INVESTIGATION
Field Investigation, Geotechnical boring, Aerial photography interpretation, Topographic map interpretation.
Investigation was performed during 1985 to 1988 as projects of Toyama Prefectual Government. Nittoc Construction Co.,of which I was an employee, was contractor of that investigation.

LOCATION
36° 30' N; 137° 7' E

GEOMORPHIC EXPRESSION
Shape of first level block is rectangular. There is a very steep main scarp (200 m) which consists of andesite lava and tuff breccia. Slope of the landslide is 6.6° in average and used for rice fields and forest. Clear second and third level blocks exist.

TYPE OF SLIDE
First and Second Level Slide: Rotational at head and translational at middle and toe zone.
Third Level Slide: Rotational

GEOLOGY
Surfacial Deposits: Colluvium and landslide debris. Angular to subround cobbles and boulders in matrix of tuffaceous clay.

Base Rock: Miocene tuff breccia, tuff, mudstone, sandstone.

Strike and dip is approximately EW 20°N. Apparent angle to slope is horizontal.

PRIMARY CAUSE OF FAILURE
Weak tuff including montmorillonite. Erosion by a river. Seismicity.

HISTORY OF LANDSLIDE
One or same huge rock avalanches occurred probably in Pleistocene. The accumulation of the debris is the landslide

body. Carbon 14 test suggest second level slide activity at 24,760 ± 240 y BP, of which sample was obtained from 18.9 m deep, and third level slide activity at 2,610 ± 100 y BP, of which sample was obtained from 6.1 m deep.

STABILITY
First and second level slides are stable. Small rotational slides and a debris flow occurred in this century. No activity is recorded after mitigation.

MITIGATION
Surface drainage, Horizontal drainage boring, Vertical drainage wells.

NO. 14 HITOHANE LANDSLIDE

INVESTIGATION
Field Investigation, Geotechnical boring, Aerial photography interpretation, Topographic map interpretation.
Investigation was performed during 1985 to 1988 as projects of Toyama Prefectual Government. Nittoc Construction Co., of which I was an employee, was contractor of that investigation.

LOCATION
36° 55' N; 136° 55' E

GEOMORPHIC EXPRESSION
First level block is horse shoe shape. Slope of the landslide is 3.9° in average and used for rice fields. Clear second and third level blocks exist.

TYPE OF SLIDE
First and Second Level Slide: Rotational at head and translational at middle and toe zone.
Third Level Slide: Rotational

GEOLOGY
Surfacial Deposits: Colluvium and landslide debris. Tuffaceous clay.
Base Rock: Miocene mudstone and tuff. Dip slope (apparent angle is 13°)

PRIMARY CAUSE OF FAILURE
Weak tuff including montmorillonite. Erosion by a river. Seismicity. Snow (maximum accumulation is 3-5 m)

HISTORY OF LANDSLIDE
First level slide might have occurred in Pleistocene and then, second and third level block followed. A small

rotational slide (about 1 ha) occurred on june, 1985 due to heavy rain.

STABILITY
First and second level slides are stable. Small rotational slides occurred in this century. No activity is recorded after mitigation.

MITIGATION
Surface drainage, Horizontal drainage boring, Vertical drainage wells, Piles.

NO. 15 TAKISAKA LANDSLIDE

INVESTIGATION
Field trip (29th IGC C16, 1992), Aerial photography and topographic map interpretation

LOCATION
37° 40' N; 139° 30' E

GEOMORPHIC EXPRESSION
The landslide can be divided into northern part and southern part. The southern part has many scarps and a steepened toe. The northern part moves toward the southern part. Slope of the landslide is 8.9° in average and covered with forest. Clear second and third level blocks exist.

TYPE OF SLIDE
Rotational

GEOLOGY
Surfacial Deposits: Colluvium and landslide debris.
Base Rock: Miocene tuff, mudstone, and sandstone wraps unconformally the pre-Tertiary granodiorite. A complicated structural framework of fault system was formed. Dip slope.

PRIMARY CAUSE OF FAILURE
Weak tuff including montmorillonite. Erosion by a river. Seismicity. Snow (maximum accumulation is 3-5 m)

HISTORY OF LANDSLIDE
There are activity records in late 19th and early 20th century.

STABILITY
Both northern and southern slide have been moving very slowly since 1957. Average displacement is about 1 m/year.

MITIGATION
Surface drainage, Horizontal drainage boring, Vertical drainage wells.

NO. 16 SAKAE LANDSLIDE

INVESTIGATION
Literature (Takahama, 1988; Takahama and Ito, 1989; Takahama and Yamazaki, 1987; Ministry of Agriculture of Japan, Hokuriku Branch, 1993).

LOCATION
37.7° 40' N; 139° 0' E

GEOMORPHIC EXPRESSION
Main scarp is eroded and flanks form streams. Second and third level blocks are not very clear. Slope of the landslide is used for forest and rice fields.

TYPE OF SLIDE
First and Second Level Slide: Rotational at head and translational at middle and toe zone.
Third Level Slide: Rotational

GEOLOGY
Surfacial Deposits: Colluvium and landslide debris.
Base Rock: Late pliocene mudstone. Dip slope.

PRIMARY CAUSE OF FAILURE
Weak tuff including montmorillonite. Seismicity. Snow (maximum accumulation is 4-6 m)

HISTORY
There is no record of activity.

NO. 17 MUSHIGAME LANDSLIDE

INVESTIGATION
Literature (Okusa and others, 1991; Takahama, 1991; Takahama and others, 1992; Ministry of Agriculture of Japan, Hokuriku Branch, 1993).

LOCATION
37° 20' N; 138° 53' E

GEOMORPHIC EXPRESSION
First level block is horse-shoe shaped. Main scarp and flanks forms valleys. Clear second and third level blocks exist. Slope of the landslide is used for forest and rice fields.

TYPE OF SLIDE
First and Second Level Slide: Rotational at head and translational at middle and toe zone.
Third Level Slide: Rotational

GEOLOGY
Surfacial Deposits: Colluvium and landslide debris.
Base Rock: Middle Miocene mudstone. Dip slope.

PRIMARY CAUSE OF FAILURE
Weak tuff including montmorillonite. Seismicity. Snow (maximum accumulation is 4-6 m)

HISTORY
Initial slide might have occurred in Late Pleistocene. A part of slide (200m wide, 1,500m long, and 20m deep) reactivated in 1980 due to thawing water leaking.

STABILITY
The landslide is presently stable.

NO. 18 HIGASHINOMYO LANDSLIDE

INVESTIGATION
Literature (Takahama and others, 1991; Takahama and Hayakawa, in print; Ministry of Agriculture of Japan, Hokuriku Branch, 1993).

LOCATION
37° 30' N; 139° 5' E

GEOMORPHIC EXPRESSION
First level block is rectangular shaped. Main scarp forms steep slope. Clear second and third level blocks exist. Slope of the landslide is used for forest and rice fields.

TYPE OF SLIDE
First and Second Level Slide: Rotational at head and translational at middle and toe zone.
Third Level Slide: Rotational

GEOLOGY
Surfacial Deposits: Colluvium and landslide debris.
Base Rock: Middle Miocene mudstone interbedded with tuff. Dipping into slope.

PRIMARY CAUSE OF FAILURE
Weak tuff including montmorillonite. Seismicity. Snow (maximum accumulation is 4-6 m)

HISTORY
Initial slide have occurred more than 50,000 B.P.(stratigraphically). Parts of the slide have reactivated intermediately.

STABILITY
The landslide is presently active.

MITIGATION
Vertical and horizontal drainage boring, drainage tunnel, piles.

NO. 19 KARUIZAWA LANDSLIDE

INVESTIGATION
Literature (Ministry of Agriculture of Japan, Hokuriku Branch, 1993), Topographic map interpretation

LOCATION
37° 26' N; 138° 57' E

GEOMORPHIC EXPRESSION
There is a clear steep main scarp (30 m). Flanks are not clear. Slope of the landslide is 4.2° in average and used for rice fields and orchards. Second and third level blocks are not very clear.

TYPE OF SLIDE
First and Second Level Slide: Rotational at head and translational at middle and toe zone.
Third Level Slide: Rotational

GEOLOGY
Surfacial Deposits: Colluvium and landslide debris.
Base Rock: Miocene mudstone. Dip slope.

PRIMARY CAUSE OF FAILURE
Weak tuff including montmorillonite. Seismicity. Snow (maximum accumulation is 4-6 m)

STABILITY
There is no record of activity.

NO. 20 HAPPOUDAI LANDSLIDE

INVESTIGATION
Literature (Ministry of Agriculture of Japan, Hokuriku Branch, 1993), Topographic map interpretation

LOCATION
37° 30' N; 138° 57' E

GEOMORPHIC EXPRESSION
There is a clear steep main scarp (50 m). Flanks are not clear. Slope of the landslide is 6.5° in average and used for rice fields and orchards. Clear second and third blocks exist.

TYPE OF SLIDE
First and Second Level Slide: Rotational at head and translational at middle and toe zone.
Third Level Slide: Rotational

GEOLOGY
Surfacial Deposits: Colluvium and landslide debris.
Base Rock: Miocene mudstone. Dip slope.

PRIMARY CAUSE OF FAILURE
Weak tuff including montmorillonite. Seismicity. Snow (maximum accumulation is 4-6 m)

STABILITY
There is no record of activity.

NO. 21 RAIDEN LANDSLIDE

INVESTIGATION
Literature (Ministry of Agriculture of Japan, Hokuriku Branch, 1993), Topographic map interpretation

LOCATION
37° 30' N; 139° 0' E

GEOMORPHIC EXPRESSION
There is a clear steep main scarp (30-70 m). Flanks form streams. Slope of the landslide is 2.0° in average and used for rice fields, orchards, and forest. Clear second and third

level blocks exist.

TYPE OF SLIDE
First and Second Level Slide: Rotational at head and translational at middle part and toe
Third Level Slide: Rotational

GEOLOGY
Surfacial Deposits: Colluvium and landslide debris.
Base Rock: Upper Pliocene mudstone. Apparent dip is horizontal.

PRIMARY CAUSE OF FAILURE
Weak tuff including montmorillonite. Seismicity. Snow (maximum accumulation is 4-6 m)

STABILITY
There is no record of activity.

NO. 22 NISHINAKANOHO LANDSLIDE

INVESTIGATION
Literature (Ministry of Agriculture of Japan, Hokuriku Branch, 1993), Topographic map interpretation

LOCATION
37° 23' N; 138° 50' E

GEOMORPHIC EXPRESSION
There is a clear steep main scarp (120 m). Flanks forms streams. Slope of the landslide is 4.7° in average and used for rice fields and residential land. Clear second and third level blocks exist.

TYPE OF SLIDE
First and Second Level Slide: Rotational at head and translational at middle part and toe
Third Level Slide: Rotational

GEOLOGY
Surfacial Deposits: Colluvium and landslide debris.
Base Rock: Upper Pliocene mudstone. Apparent dip is horizontal.

PRIMARY CAUSE OF FAILURE
Weak tuff including montmorillonite. Seismicity. Snow (maximum accumulation is 4-6 m)

STABILITY
There is no record of activity.

NO. 23 MIZUNASHI LANDSLIDE

INVESTIGATION
Literature (Ministry of Agriculture of Japan, Hokuriku Branch, 1993)

LOCATION
37° 6' N; 138° 36' E

GEOMORPHIC EXPRESSION
There is a clear steep main scarp (50 m). Flanks forms streams. Slope of the landslide is 4.0° in average and used for rice fields, orchards, and houses. Clear second and third level blocks exist.

TYPE OF SLIDE
First and Second Level Slide: Rotational at head and translational at middle and toe zone.
Third Level Slide: Rotational

GEOLOGY
Surfacial Deposits: Colluvium and landslide debris. tuffaceous clay.
Base Rock: Upper Pliocene tuff and mudstone. Dip slope (30°).

PRIMARY CAUSE OF FAILURE
Weak tuff including montmorillonite. Seismicity. Snow (maximum accumulation is 4-6 m)

HISTORY OF LANDSLIDE
First level slide might have occurred in Pleistocene and then, second and third level block followed. Carbon 14 and pollen analysis suggest activity at 5,770 ± 190 y BP and 7,000 y BP respectively. The landslide reactivated during 1960s and 1980s.

STABILITY
Activity of the landslide decreased. Factor of safety is 0.95-1.15.

MITIGATION
Surface drainage, Horizontal drainage boring, Vertical drainage wells.

NO. 24 KITAURATA LANDSLIDE

INVESTIGATION
Literature (Ministry of Agriculture of Japan, Hokuriku Branch, 1993), Topographic map interpretation

LOCATION
37° 4' N; 138° 33' E

GEOMORPHIC EXPRESSION
Right flank is very leaner and left one is circular. Slope of the landslide is 6.4° in average and used for orchards and forest. Second and third level blocks are not very clear.

TYPE OF SLIDE
First and Second Level Slide: Rotational at head and translational at middle and toe zone.
Third Level Slide: Rotational

GEOLOGY
Surfacial Deposits: Colluvium and landslide debris. Tuffaceous clay.
Base Rock: upper Pliocene mudstone. Bedding Dips into slope (30°).

PRIMARY CAUSE OF FAILURE
Weak tuff including montmorillonite. Seismicity. Snow (maximum accumulation is 4-6 m)

HISTORY OF LANDSLIDE
There is no record of activity.

STABILITY
The landslide is presently stable.

NO. 25 UENOYAMA LANDSLIDE

INVESTIGATION
Literature (Ministry of Agriculture, Hokuriku Branch, 1993), Topographic map interpretation

LOCATION
37° 5' N; 138° 34' E

GEOMORPHIC EXPRESSION
First level slide is horse-shoe shaped. The main scarp has been eroded. The slope of slide is used for orchard and residential land. Second and third level blocks are not very

clear.

TYPE OF SLIDE
First Level Slide: Rotational at head and translational at middle and toe zone.
Second and third Level Slides: Rotational.

GEOLOGY
Surfacial Deposits: Colluvium and landslide debris.
Base Rock: Middle Miocene sandstone and mudstone. Dip slope (20°).

PRIMARY CAUSE OF FAILURE
Weak tuff including montmorillonite. Seismicity. Snow (maximum accumulation is 4-6 m)

HISTORY OF LANDSLIDE
There are records of miner activities.

STABILITY
The landslide is presently stable.

NO. 26 NAKATATEYAMA LANDSLIDE

INVESTIGATION
Literature (Ministry of Agriculture, Hokuriku Branch, 1993), Topographic map interpretation

LOCATION
37° 3' N; 138° 34' E

GEOMORPHIC EXPRESSION
First level slide is wide rectangular shaped. The main scarp is 50-100 m high steep slope. The slope of slide is used for orchard and forest. Clear second and third level blocks exist.

TYPE OF SLIDE
First and Second Level slides: Rotational at head and traslational at middle and toe zone.
Third Level slides: Rotational.

GEOLOGY
Surfacial Deposits: Colluvium and landslide debris.
Base Rock: Middle Miocene tuff. Dip slope (20°).

PRIMARY CAUSE OF FAILURE
Weak tuff including montmorillonite. Seismicity. Snow (maximum accumulation is 4-6 m)

HISTORY OF LANDSLIDE
A part of slide (100 x 250 m) reactivated in 1976.
STABILITY
The landslide is presently stable.

NO. 27 YUMOTO LANDSLIDE

INVESTIGATION
Literature (Ministry of Agriculture, Hokuriku Branch, 1993), Topographic map interpretation.

LOCATION
37° 3' N; 138° 36' E

GEOMORPHIC EXPRESSION
First level slide is bottle-neck shaped. The main scarp is about 20 m high steep slope. Sags and depression occurs at the head. The slope of slide is used for residential land, orchard, and forest. Clear second and third level blocks exist.

TYPE OF SLIDE
First and Second Level slides: Rotational at head and traslational at middle and toe zone.
Third Level slides: Rotational.

GEOLOGY
Surfacial Deposits: Colluvium and landslide debris.
Base Rock: Middle Miocene mudstone and tuff. Dip slope (30°).

PRIMARY CAUSE OF FAILURE
Weak tuff including montmorillonite. Seismicity. Snow (maximum accumulation is 4-6 m)

HISTORY OF LANDSLIDE
A part of slide reactivated late 19th century and in 1952.

STABILITY
The landslide is presently stable.

NO. 28 YUYAMA LANDSLIDE

INVESTIGATION
Literature (Ministry of Agriculture, Hokuriku Branch, 1993), Topographic map interpretation.

LOCATION
37° 4' N; 138° 37' E

GEOMORPHIC EXPRESSION
First level slide is wide rectangular shaped. The main scarp is clear. The slope of slide is used for residential land, orchard, and forest. Clear second and third level blocks exist.

TYPE OF SLIDE
First and Second Level slides: Rotational at head and traslational at middle and toe zone.
Third Level slides: Rotational.

GEOLOGY
Surfacial Deposits: Colluvium and landslide debris.
Base Rock: Middle Miocene mudstone and tuff. Dip slope (30°).

PRIMARY CAUSE OF FAILURE
Weak tuff including montmorillonite. Seismicity. Snow (maximum accumulation is 4-6 m)

STABILITY
The landslide is presently stable.

NO.29 KAMATSUKA LANDSLIDE

INVESTIGATION
Literature (Ministry of Agriculture, Hokuriku Branch, 1993)

GEOMORPHIC EXPRESSION
First level slide is square shaped. The main scarp is clear steep slope. The slope of slide is used for residential land and orchard. Clear second and third level blocks exist.

TYPE OF SLIDE
First and Second Level slides: Rotational at head and traslational at middle and toe zone.
Third Level slides: Rotational.

GEOLOGY
Surfacial Deposits: Colluvium and landslide debris.
Base Rock: Middle Miocene mudstone and sandstone. Dipping into slope (25°).

PRIMARY CAUSE OF FAILURE
Weak tuff including montmorillonite. Seismicity. Snow (maximum accumulation is 4-6 m)

HISTORY
Parts of landslide have reactivated many times.

STABILITY
The landslide is presently stable.

NO.30 MARUYAMA LANDSLIDE

INVESTIGATION
Literature (Ministry of Agriculture, Hokuriku Branch, 1993), Topographic map interpretation.

LOCATION
37° N; 138.6° E

GEOMORPHIC EXPRESSION
First level slide is triangle shaped. The main scarp is clear. The river meanders in front of the slide. Clear second and third level blocks exist. The slope of slide is used for rice field and orchard.

TYPE OF SLIDE
First and Second Level slides: Rotational at head and traslational at middle and toe zone.
Third Level slides: Rotational.

GEOLOGY
Surfacial Deposits: Colluvium and landslide debris.
Base Rock: Pleistocene sandstone and conglomerate. Dip slope (35°).

PRIMARY CAUSE OF FAILURE
Weathered rocks, Seismicity, Snow (maximum accumulation is 4-6 m)

HISTORY
The initial slide may have occurred late Pliocene.

STABILITY
The landslide is presently stable.

NO.31 MASEGUCHI LANDSLIDE

INVESTIGATION
Literature (Takahama and others, 1992; Ministry of Agriculture, Hokuriku Branch, 1993), Topographic map interpretation.

LOCATION
37° 2' N; 138° 4'

GEOMORPHIC EXPRESSION
First level slide is wide rectangular shaped. The main scarp forms distinctive steep slope. Clear second and third level blocks exist. The slope of slide is used for rice field and residential land.

TYPE OF SLIDE
First and Second Level slides: Rotational at head and traslational at middle and toe zone.
Third Level slides: Rotational.

GEOLOGY
Surfacial Deposits: Colluvium and landslide debris.
Base Rock: Late Miocene mudstone. Dip slope (30°).

PRIMARY CAUSE OF FAILURE
Weak tuff layer, Seismicity, Snow (maximum accumulation is 4-6 m)

HISTORY
The initial slide may have occurred 25 to 45 thousands years ago. Parts of landslide reactivated repeatedly, e.g., in 1490, 1862, 1868, 1923, 1927, 1931, 1932, 1934, and 1942.

STABILITY
The southern part of the slide is presently active (3.3 m in 80 years).

NO.32 MARUTA LANDSLIDE

INVESTIGATION
Literature (Ministry of Agriculture, Hokuriku Branch, 1993), Topographic map interpretation.

LOCATION
37° 8' N; 138° 6' E

GEOMORPHIC EXPRESSION
First level slide is horse-shoe shaped. The main scarp has been eroded. The flanks form streams. Clear second and third level blocks exist. The slope of slide is used for rice field, forest, and residential land.

TYPE OF SLIDE
First and Second Level slides: Rotational at head and traslational at middle and toe zone.

Third Level slides: Rotational.

GEOLOGY
Surfacial Deposits: Colluvium and landslide debris.
Base Rock: Late Pliocene mudstone. Dip slope (15°).

PRIMARY CAUSE OF FAILURE
Weathered mudstone layer, Seismicity, Snow (maximum accumulation is 4-5 m)

STABILITY
Presently stable.

NO.33 KODOMARI LANDSLIDE

INVESTIGATION
Literature (Ministry of Agriculture, Hokuriku Branch, 1993), Topographic map interpretation.

LOCATION
37° 6' N; 138° 0' E

GEOMORPHIC EXPRESSION
First level slide is horse-shoe shaped. The main scarp has been eroded. Clear second and third level blocks exist. The slope of slide is used for orchard, forest, and residential land.

TYPE OF SLIDE
First and Second Level slides: Rotational at head and traslational at middle and toe zone.
Third Level slides: Rotational.

GEOLOGY
Surfacial Deposits: Colluvium and landslide debris.
Base Rock: Late Miocene mudstone and sandstone. Dip slope (15°).

PRIMARY CAUSE OF FAILURE
Weathered mudstone layer, Seismicity, Snow (maximum accumulation is 2-3 m)

STABILITY
Presently stable.

NO.34 OHBORA LANDSLIDE

INVESTIGATION
Literature (Takahama and Ito, 1988; Ministry of Agriculture, Hokuriku Branch, 1993), Topographic map interpretation.

LOCATION
37° 7' N; 138° 4' E

GEOMORPHIC EXPRESSION
First level slide is horse-shoe shaped. The main scarp is not very clear. Clear second and third level blocks exist. The slope of slide is used for rice field, forest, and residential land.

TYPE OF SLIDE
First and Second Level slides: Rotational at head and traslational at middle and toe zone.
Third Level slides: Rotational.

GEOLOGY
Surfacial Deposits: Colluvium and landslide debris.
Base Rock: Late Pliocene mudstone and sandstone. Dipping into slope (15°).

PRIMARY CAUSE OF FAILURE
Weathered mudstone, Seismicity, Snow (maximum accumulation is 2-3 m)

HISTORY
A part of slide reactivated in early 20th century.

STABILITY
Presently stable (dormant).

NO.35 URUSHINOSE LANDSLIDE

INVESTIGATION
Field investigation (From 1989 - 1990), Geotechnical boring, Topographic map interpretation.

LOCATION
33.9° N; 134.1° E

GEOMORPHIC EXPRESSION
First level slide is horse-shoe shaped. The main scarp forms distinctive steep slope. Clear second and third level blocks exist. The slope of slide is used for farm field and

residential land.

TYPE OF SLIDE
First and Second Level slides: Rotational at head and traslational at middle and toe zone.
Third Level slides: Rotational.

GEOLOGY
Surfacial Deposits: Colluvium and landslide debris. Clayish debris including schist blocks (maximum two meters).
Base Rock: Weathered black schist. Dipping into slope (60°).

PRIMARY CAUSE OF FAILURE
Weathered clayish schist, Seismicity, Rain and Snow (maximum accumulation is 2-3 m)

STABILITY
Presently stable (dormant).

Mitigation
Vertical and horizontal drainage.

NO.36 NISHINOTANI LANDSLIDE

INVESTIGATION
Field investigation, Geotechnical boring, Aerial photography and topographic map interpretation.

LOCATION
33° 33' N; 133° 4' E

GEOMORPHIC EXPRESSION
First level slide is horse-shoe shaped. The main scarp is not very clear. Clear second and third level blocks exist. The slope of slide is used for rice field, orchard, and residential land.

TYPE OF SLIDE
First and Second Level slides: Rotational at head and traslational at middle and toe zone.
Third Level slides: Rotational.

GEOLOGY
Surfacial Deposits: Colluvium and landslide debris. Clayish debris including schist blocks (maximum 2 meters).
Base Rock: Weathered sandstone, chart, shale, limestone.

PRIMARY CAUSE OF FAILURE
Weathered rocks, Seismicity, Heavy rain and Snow (maximum accumulation is 2-3 m).

HISTORY
Parts of the slide reactivated in 1963, 1965, 1975, and 1976.

STABILITY
The slide is presently active, however, the movement is very slow.

Mitigation
Vertical and horizontal drainage, Piles

NO.37 YOUNE LANDSLIDE

INVESTIGATION
Aerial photography and topographic map interpretation, Literature (Ueno and others, 1993; Higaki and others, 1994).

LOCATION
33° 46' N; 133° 47' E

GEOMORPHIC EXPRESSION
First level slide is horse-shoe shaped. The main scarp is clear steep slope. Clear second and third level blocks exist. The slope of slide is used for rice field.

TYPE OF SLIDE
First and Second Level slides: Rotational at head and traslational at middle and toe zone.
Third Level slides: Rotational.

GEOLOGY
Surfacial Deposits: Colluvium and landslide debris.
Base Rock: Fractured greenstone.

PRIMARY CAUSE OF FAILURE
Weathered rock, Seismicity, Heavy rain and Snow (maximum accumulation is 2-3 m).

STABILITY
The slide is presently active, however, the movement is very slow (50 mm/year).

Mitigation
Vertical and horizontal drainage.

NO.38 NUTA LANDSLIDE

INVESTIGATION
Aerial photography and topographical map interpretation, Literature (Higaki and others, 1994).

LOCATION
33° 47' N; 133° 47' E

GEOMORPHIC EXPRESSION
First level slide is horse-shoe shaped. The main scarp is clear steep slope. The slope of slide is used for rice field. Clear second and third level blocks exist.

TYPE OF SLIDE
First and Second Level slides: Rotational at head and traslational at middle and toe zone.
Third Level slides: Rotational.

GEOLOGY
Surfacial Deposits: Colluvium and landslide debris.
Base Rock: Fractured greenstone.

PRIMARY CAUSE OF FAILURE
Weathered rock, Seismicity, Heavy rain and Snow (maximum accumulation is 2-3 m).

NO.39 NYUYA LANDSLIDE

INVESTIGATION
Aerial photography and topographycal map interpretation, Literature (Ueno and others, 1993; Higaki and others, 1994).

LOCATION
35° 34' N; 138° 3' E

GEOMORPHIC EXPRESSION
First level slide is bottle-neck shaped. The main scarp is clear steep slope. The slope of slide is used for rice field and residential land. Clear second and third level blocks exist.

TYPE OF SLIDE
First and Second Level slides: Rotational at head and traslational at middle and toe zone.
Third Level slides: Rotational.

GEOLOGY
Surfacial Deposits: Colluvium and landslide debris.
Base Rock: Fractured black schist and green schist; and serpentinite.

PRIMARY CAUSE OF FAILURE
Weathered weak layer (serpentinite), Seismicity, Heavy rain and Snow (maximum accumulation is 2-3 m).

STABILITY
The slide is presently active, however, the movement is very slow (10 mm/year).

MITIGATION
Vertical and horizontal drainage.

NO.40 HIKINOTA LANDSLIDE

INVESTIGATION
Literature (Higaki and others, 1994).

LOCATION
35° 32' N; 138° 2' E

GEOMORPHIC EXPRESSION
First level slide is horse-shoe shaped. The main scarp is clear steep slope. The slope of slide is used for rice field and residential land. Clear second and third level blocks exist.

GEOLOGY
Surfacial Deposits: Colluvium and landslide debris.
Base Rock: Fractured black and green schist; and serpentinite.

PRIMARY CAUSE OF FAILURE
Weathered weak layer (serpentinite), Seismicity, Heavy rain and Snow (maximum accumulation is 2-3 m).

SLIDE MOUNTAIN

Slide Mountain is part of the Carson Range, which is an offshoot of the Sierra Nevada. Slide Mountain is composed of Cretaceous granodiorite. On May 30, 1983, a mass of about 720,000 m^3 of rock failed from the south-east side of Slide Mountain. One of the triggers was high pore pressure due to rapid snow melting. Four zones were identified: an almost intact slide mass; a rock avalanche zone; sand flow; and a region of displaced rock and soil, trees, and organic. Saturated landslide debris ran down the Ophir Creek canyon as a debris flow. The volume of the debris is at least 100,000-150,000 m^3 (Watters, 1983; Mitchell, 1986).

LANDSLIDE BLOCK MAPS

NO. 1 MIDWAY BRIDGE LANDSLIDE

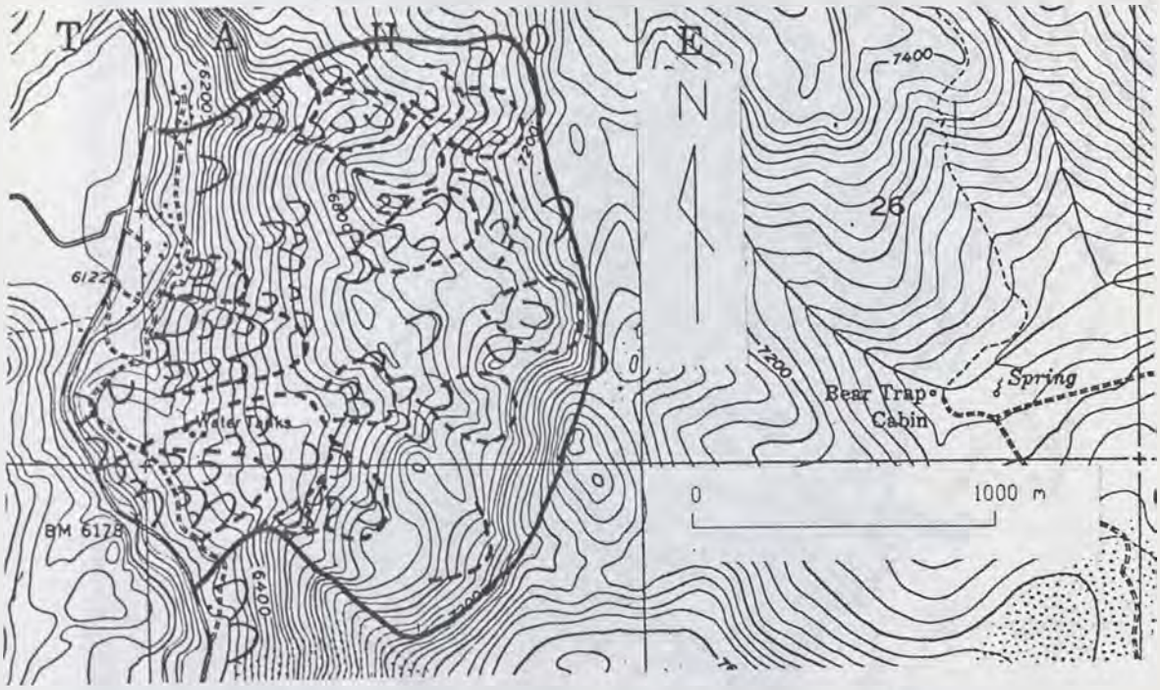

NO. 2 BOCA RIDGE LANDSLIDE

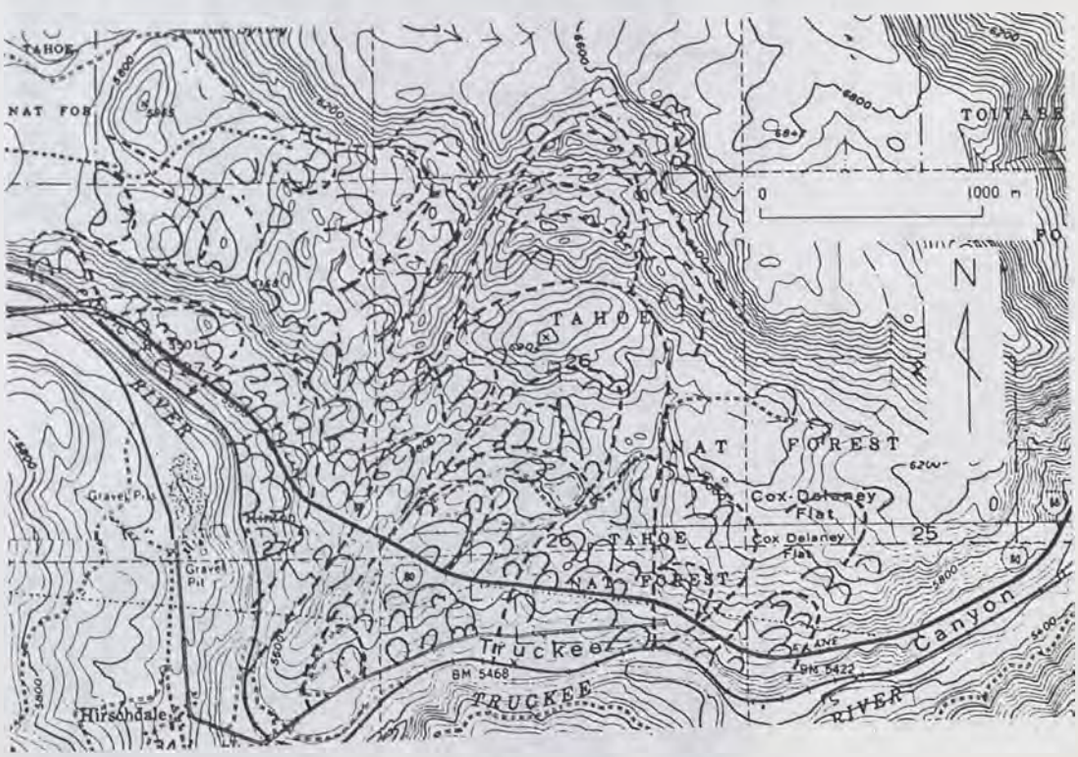

NO. 3 PALOS VERDES LANDSLIDE

NO. 4 BIG ROCK MESA LANDSLIDE

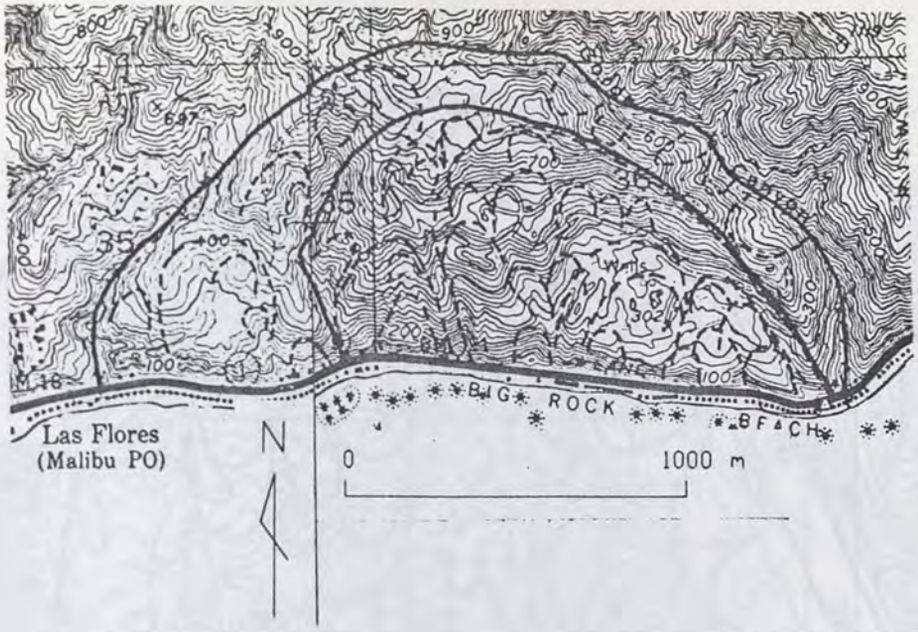

NO. 6 LOWER GROS VENTRE LANDSLIDE

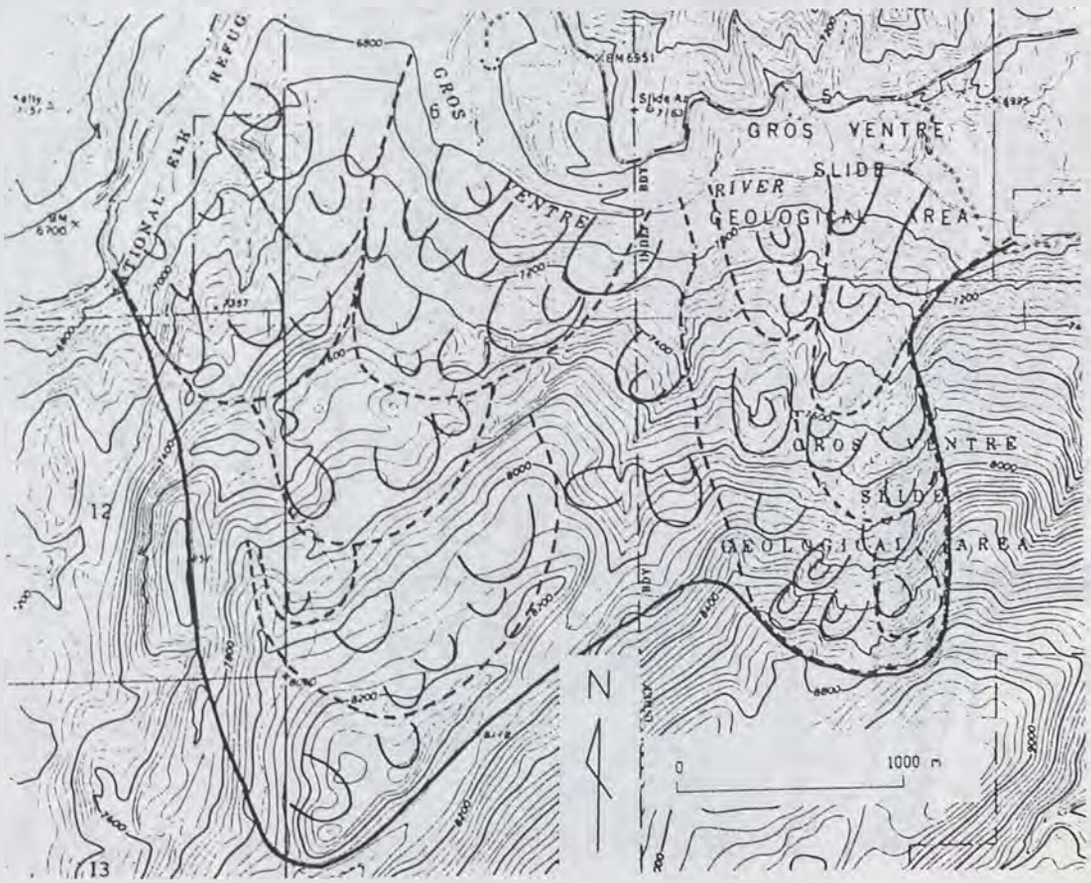

NO. 5 THRISTLE LANDSLIDE

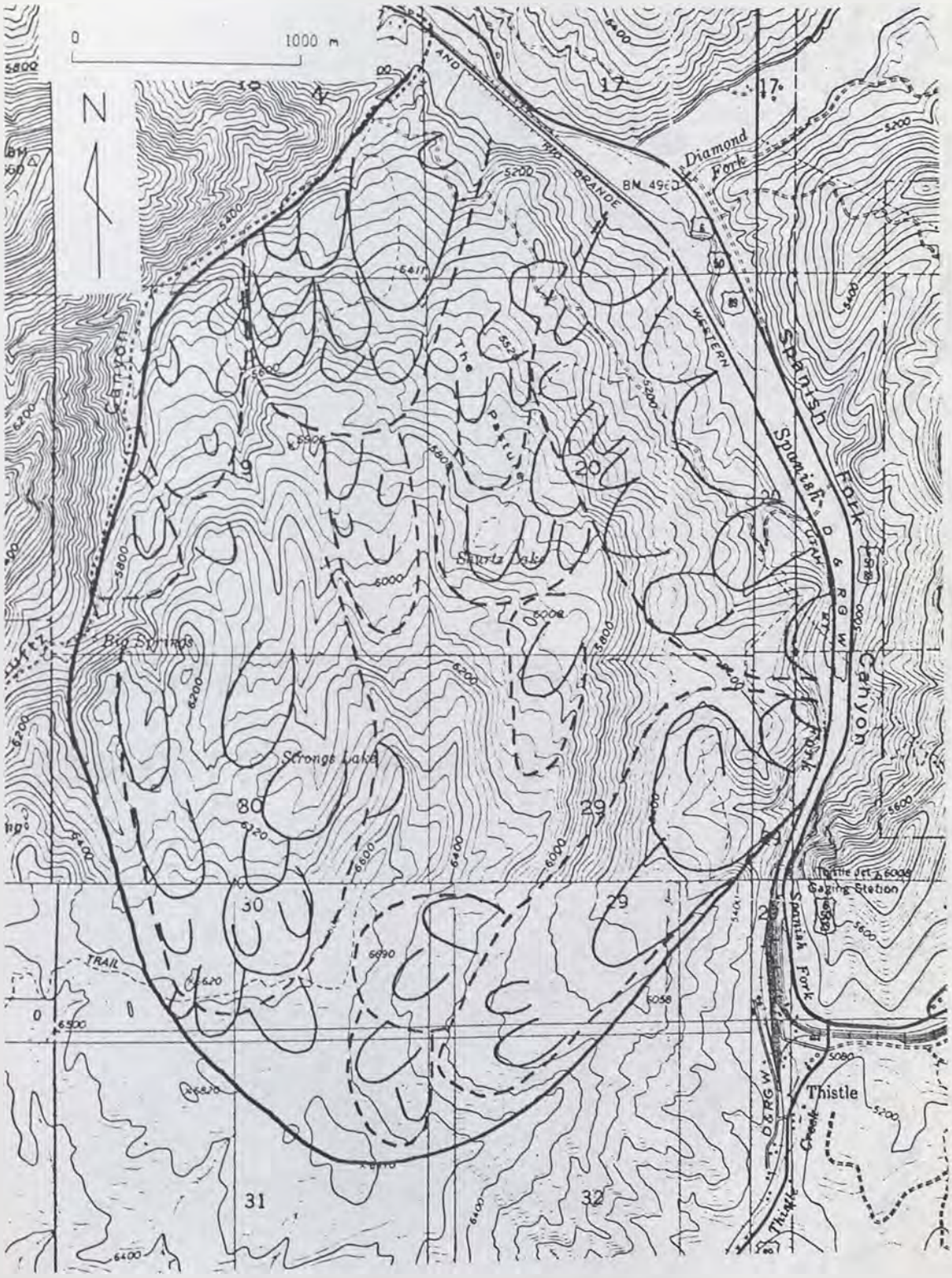

NO. 7 UPPER GROS VENTRE LANDSLIDE

NO. 8 MEADOW MOUNTAIN LANDSLIDE

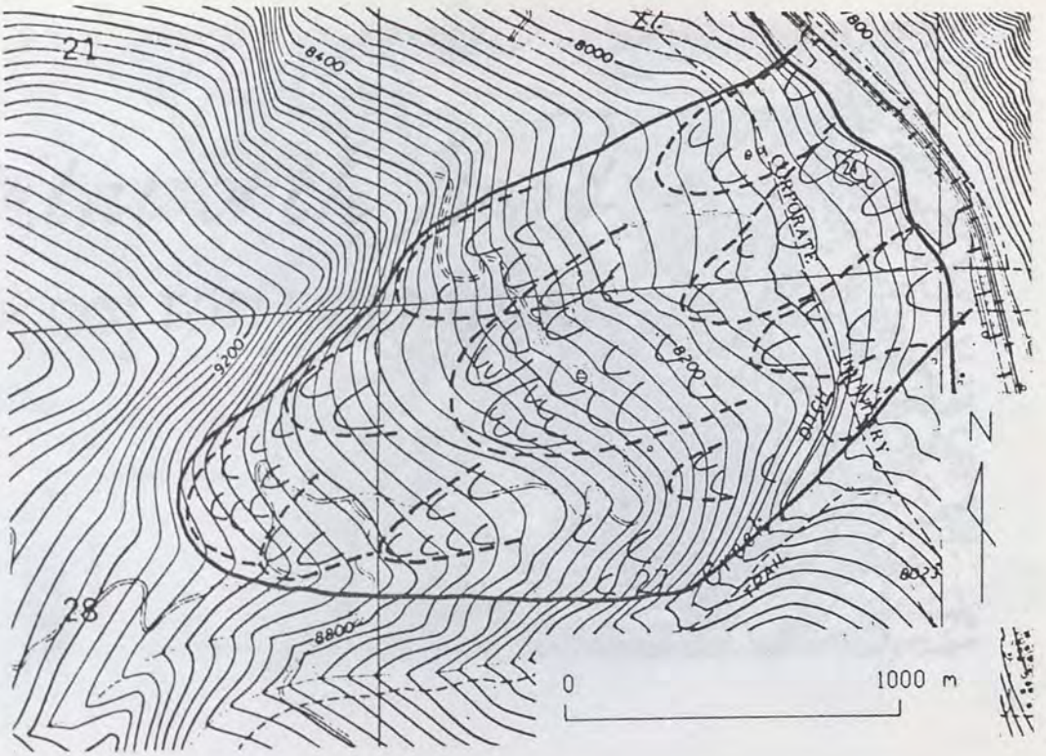

NO. 9 MAYUNMARCA LANDSLIDE

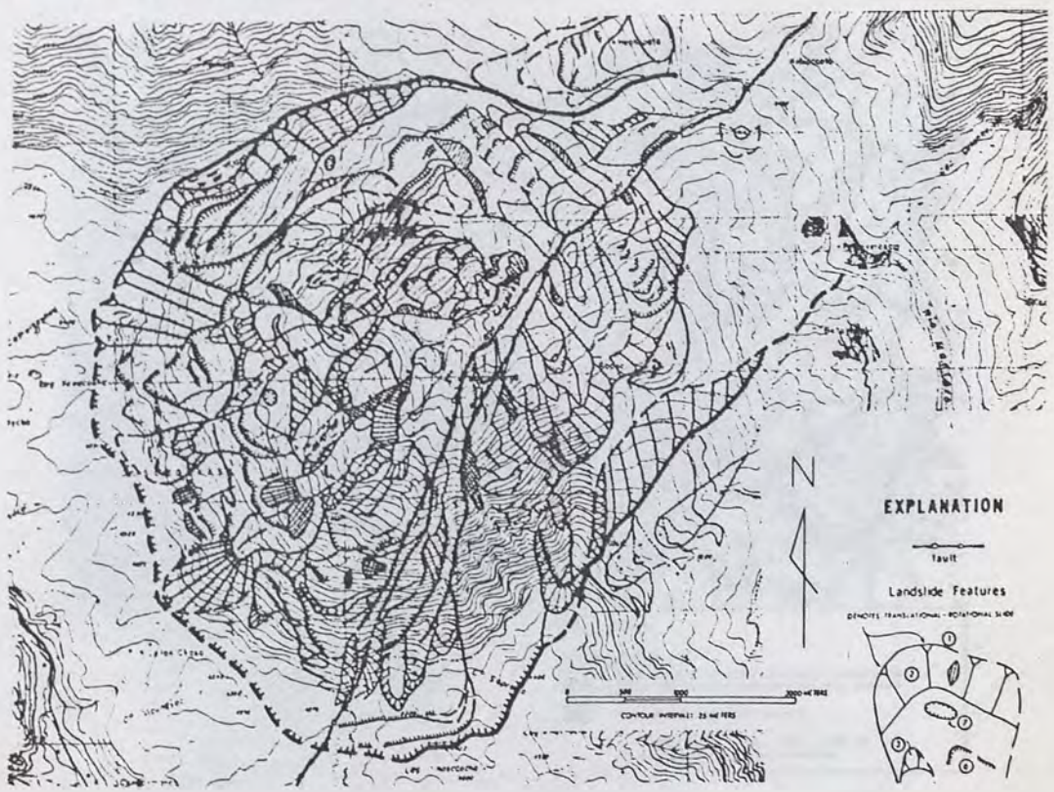

NO. 10 LA FRASSE LANDSLIDE

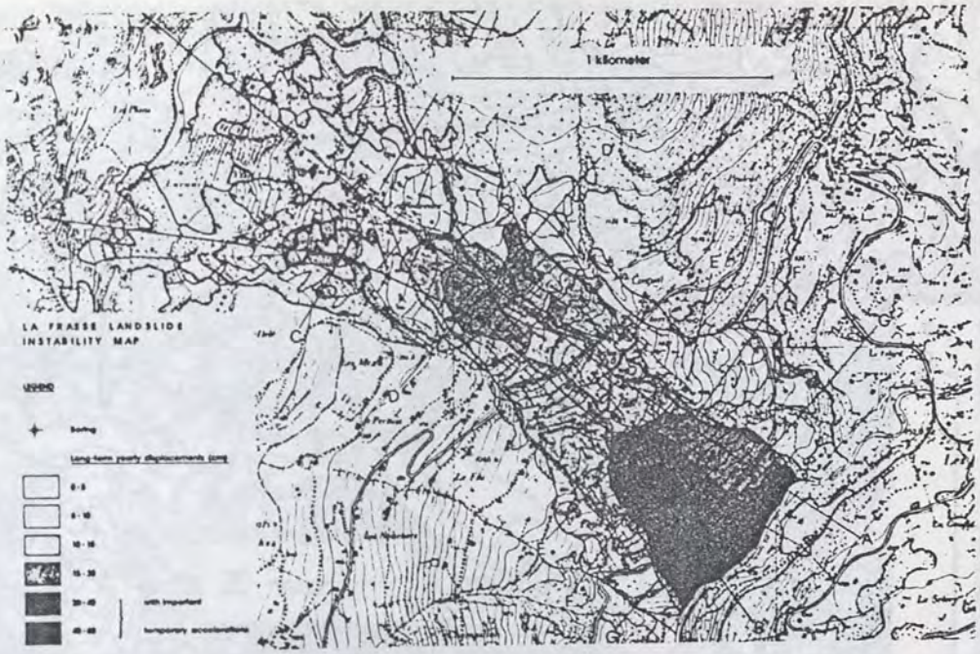

NO. 11 ARVEY LANDSLIDE

NO. 12 KIRITANI LANDSLIDE

NO. 13 KATSURABARA LANDSLIDE

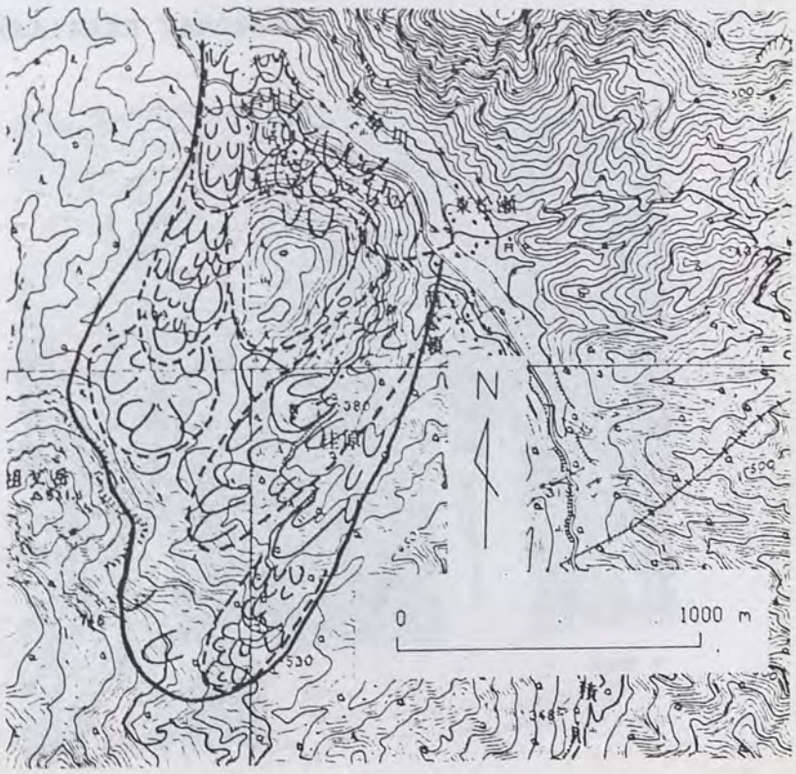

NO. 14 HITOHANE LANDSLIDE

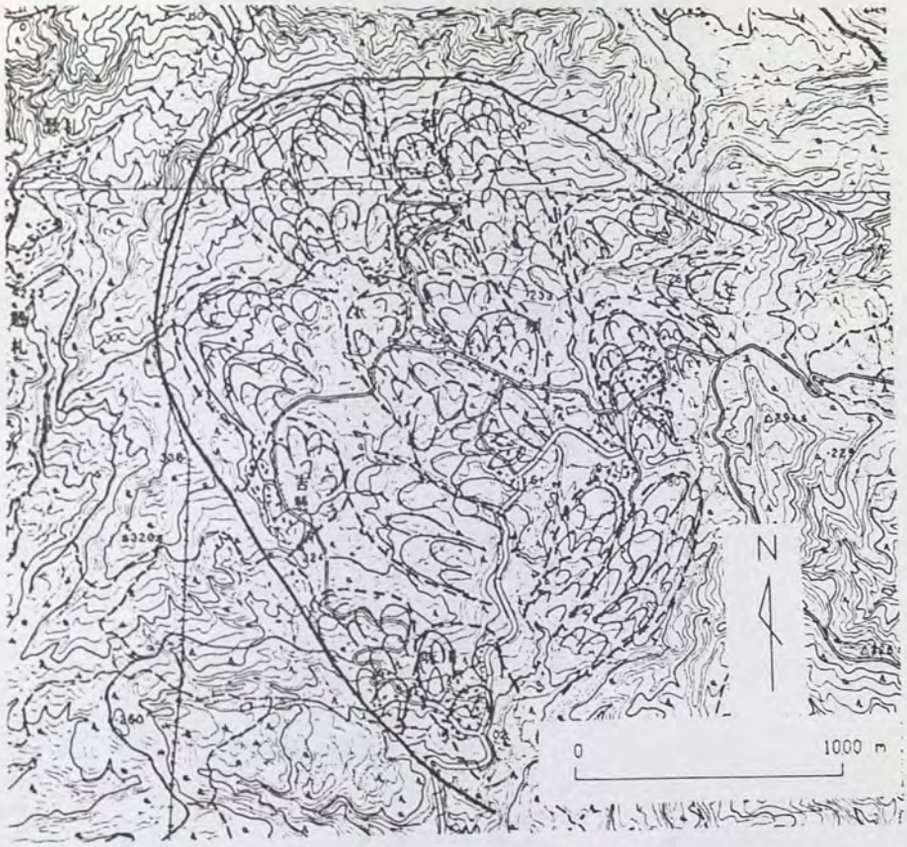

NO. 15 TAKISAKA LANDSLIDE

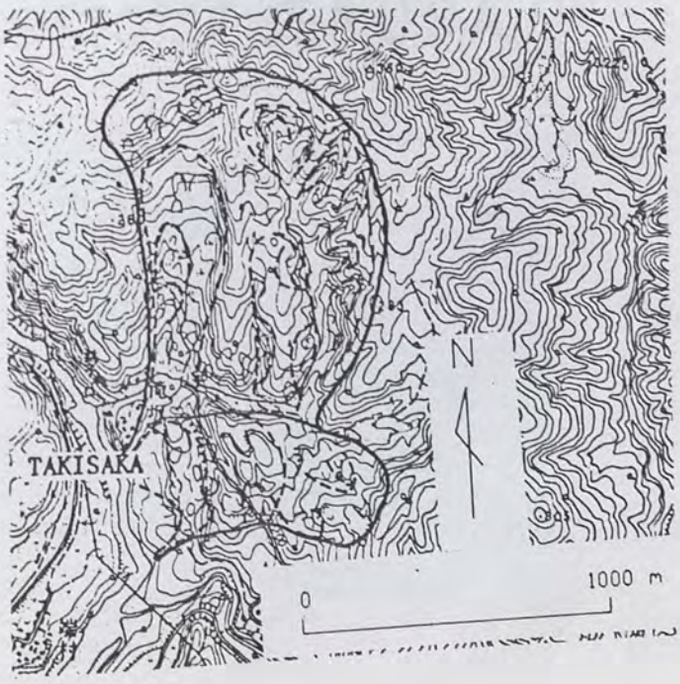

NO. 16 SAKAE LANDSLIDE

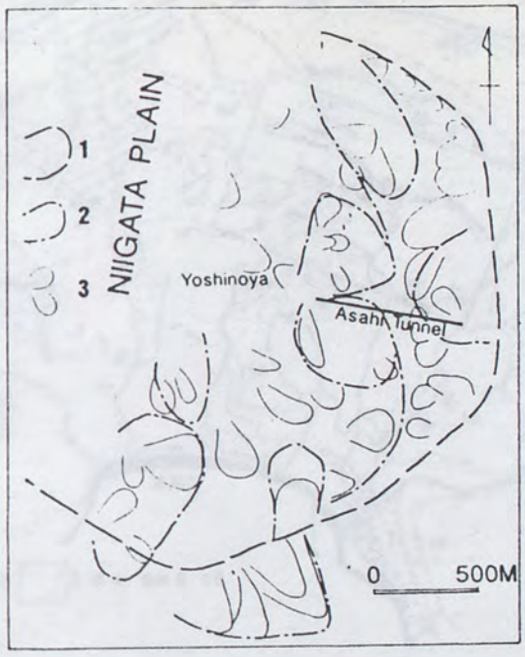

NO. 17 MUSHIGAME LANDSLIDE

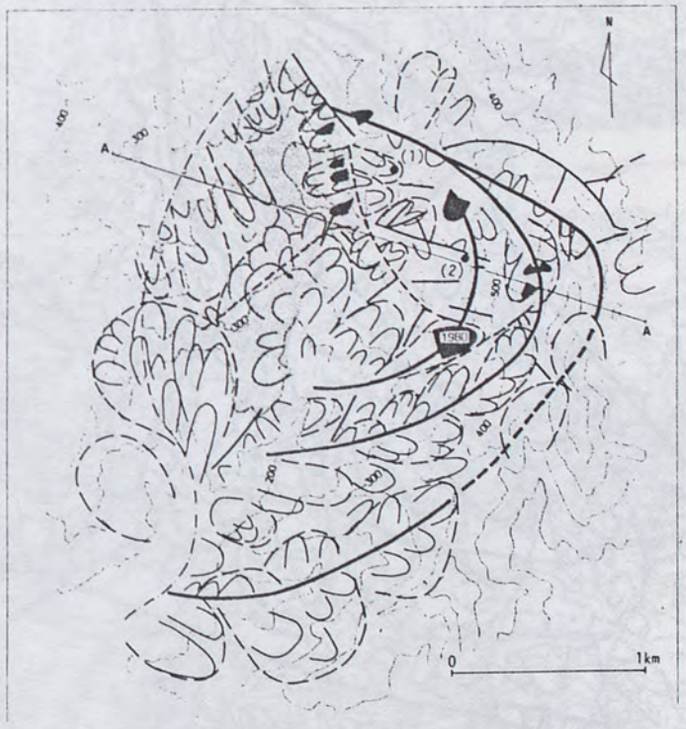

NO. 18 HIGASHINOMYO LANDSLIDE

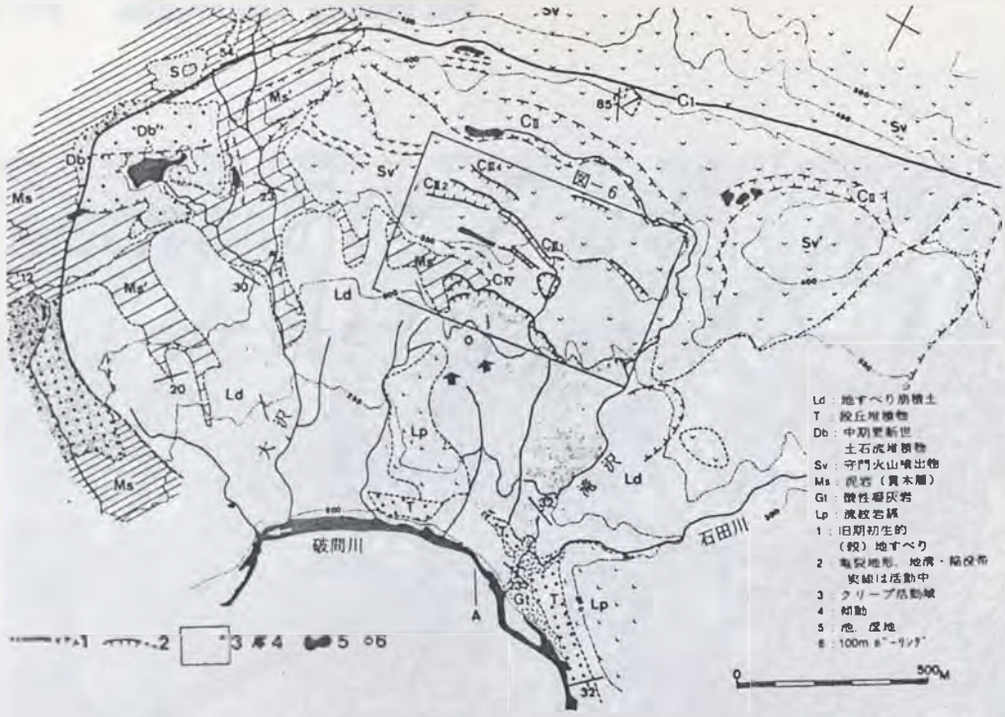

NO. 19 KARUIZAWA LANDSLIDE

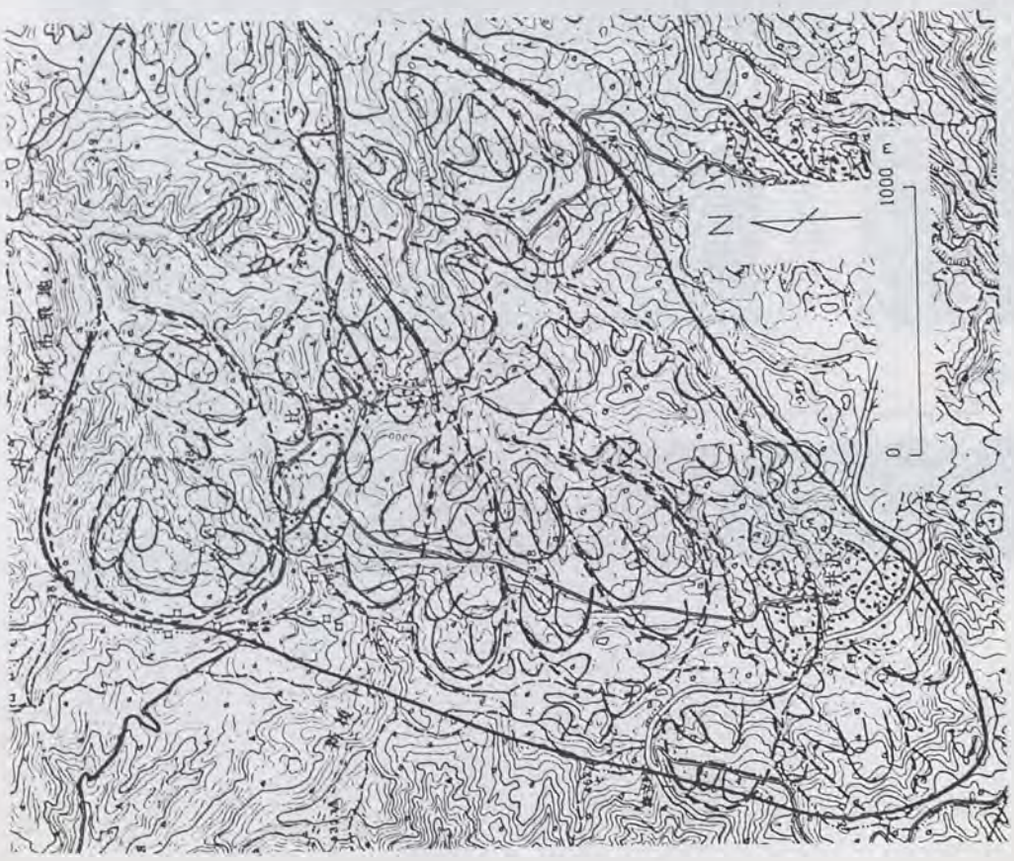

NO. 20 HAPPOUDAI LANDSLIDE

NO. 21 RAIDEN LANDSLIDE

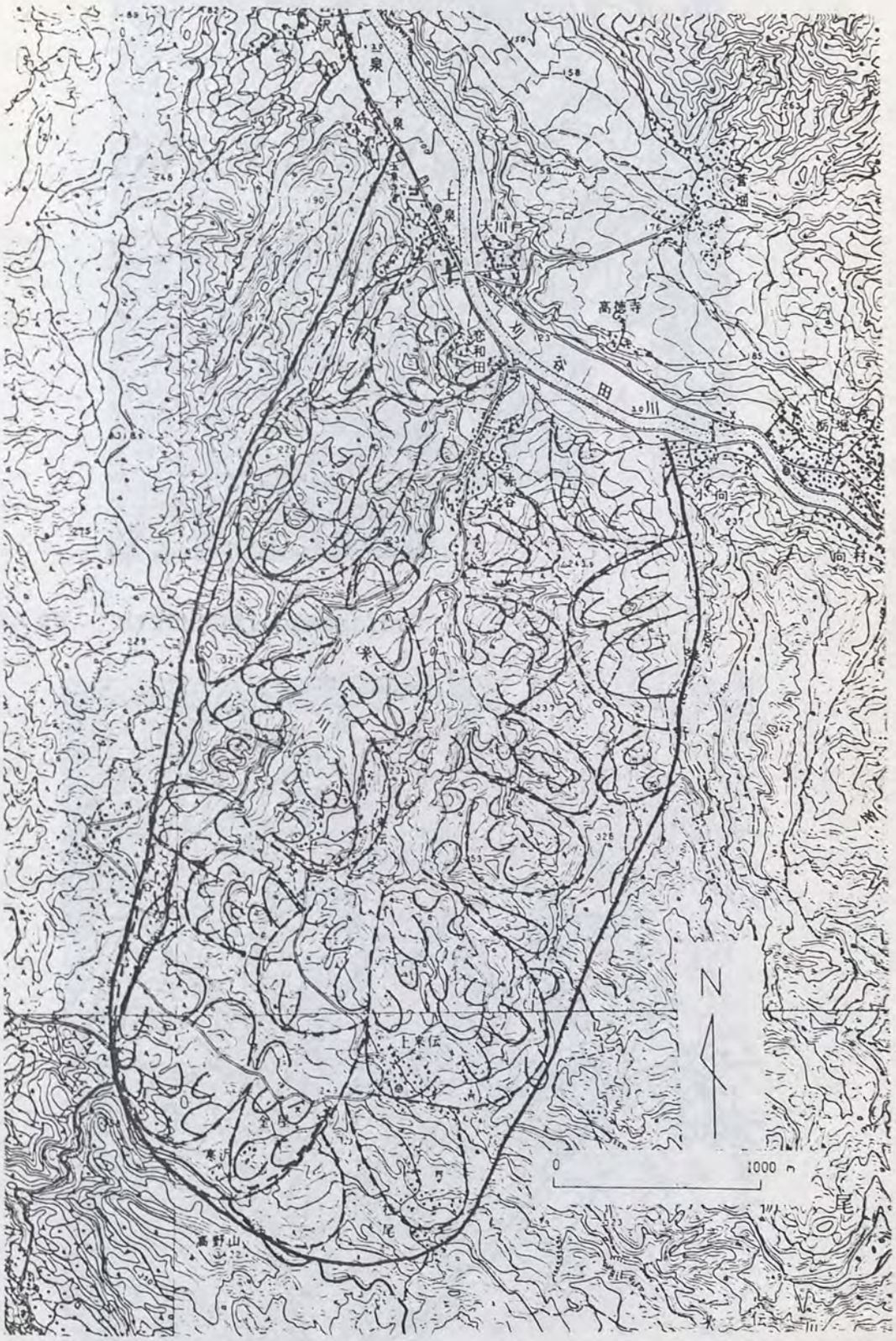

NO. 22 NISHINAKANOHO LANDSLIDE

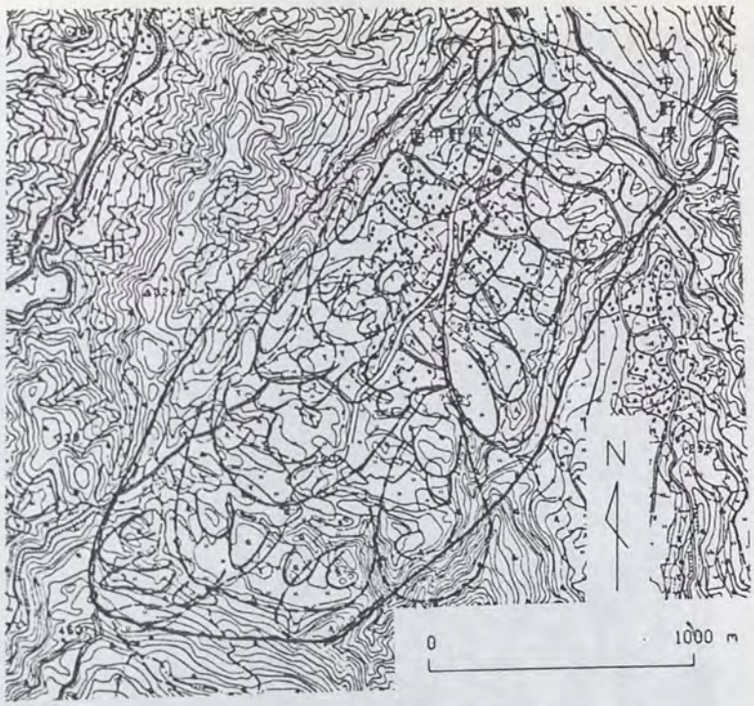

NO. 23 MIZUNASHI LANDSLIDE

NO. 24 KITAURATA LANDSLIDE

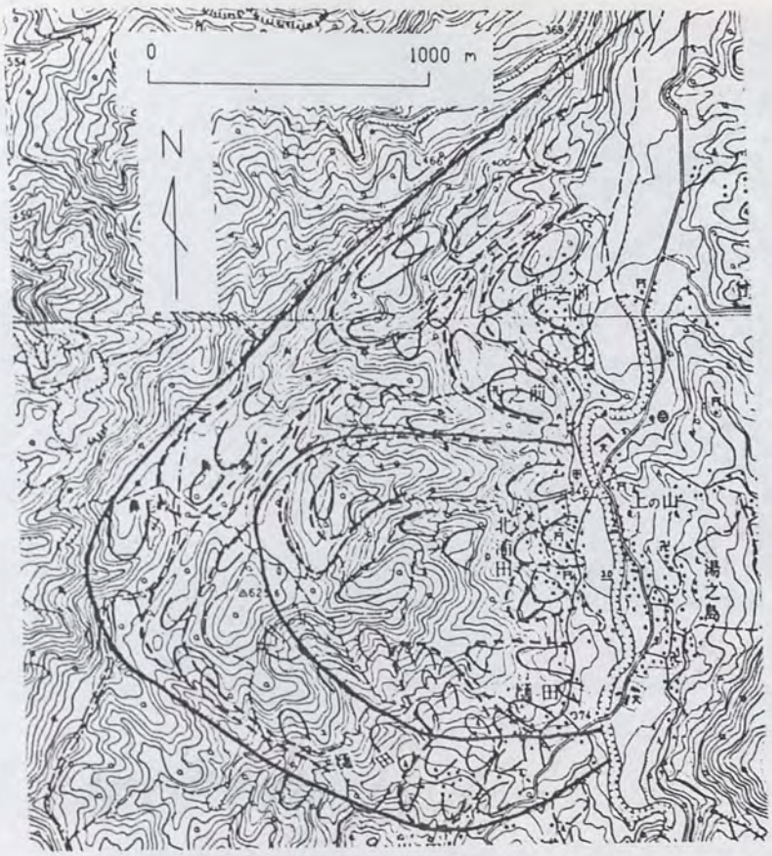

NO. 25 UENOYAMA LANDSLIDE

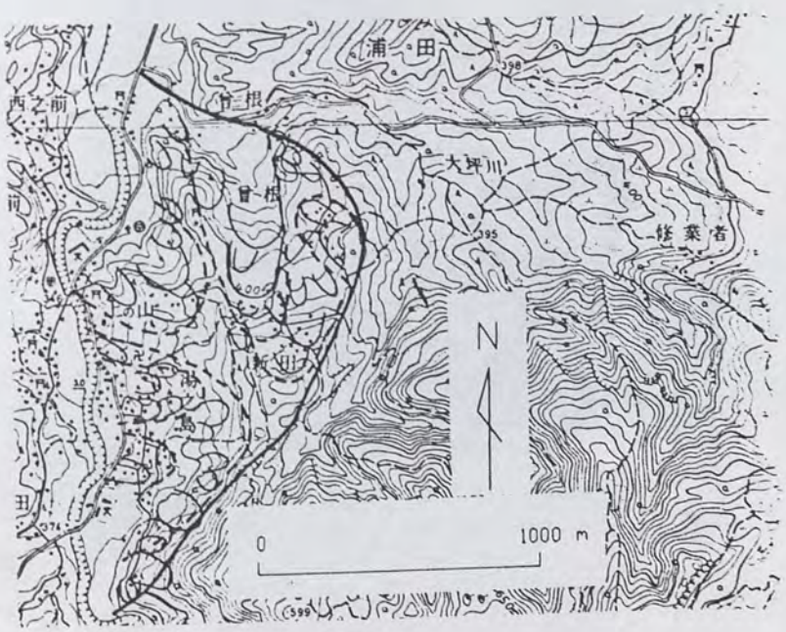

NO. 26 NAKATATEYAMA LANDSLIDE

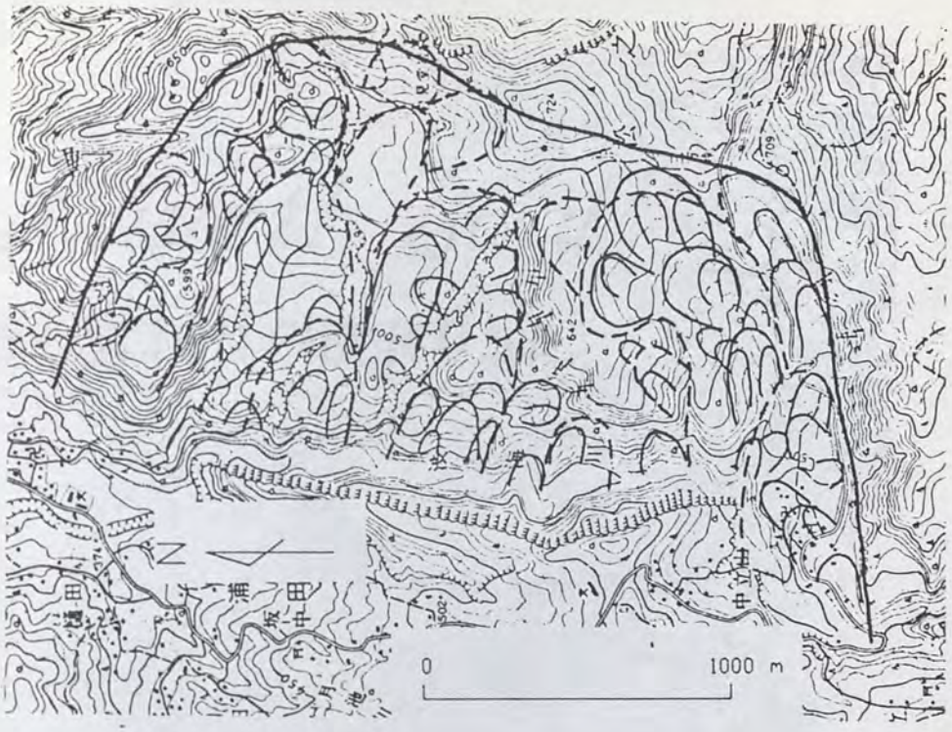

NO. 27 YUMOTO LANDSLIDE

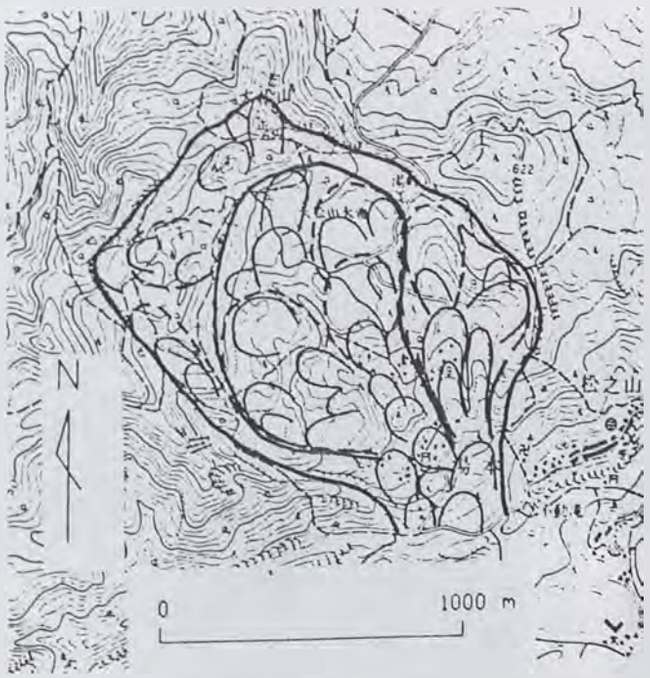

NO. 28 YUYAMA LANDSLIDE

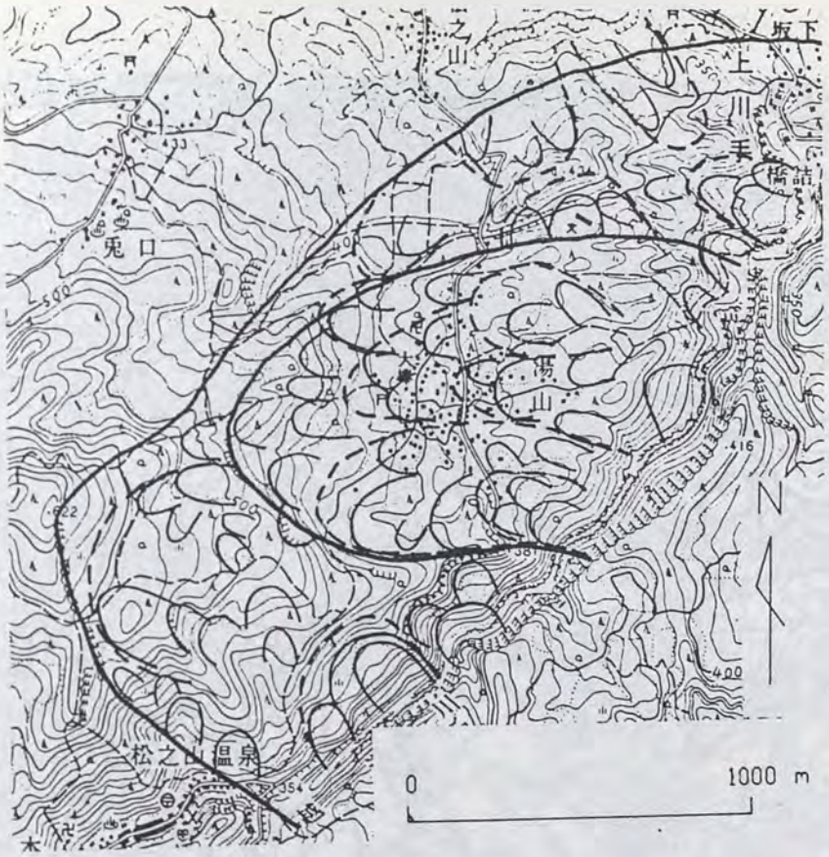

NO. 29 KAMATSUKA LANDSLIDE

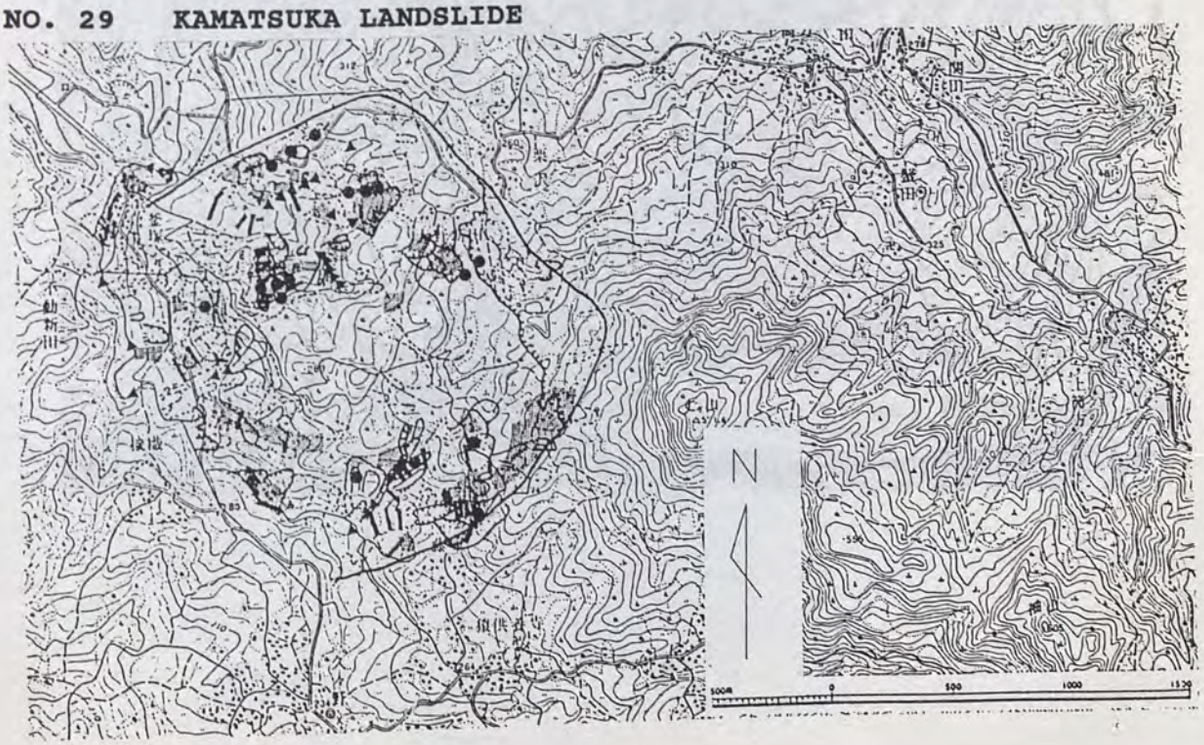

NO. 30 MARUYAMA LANDSLIDE

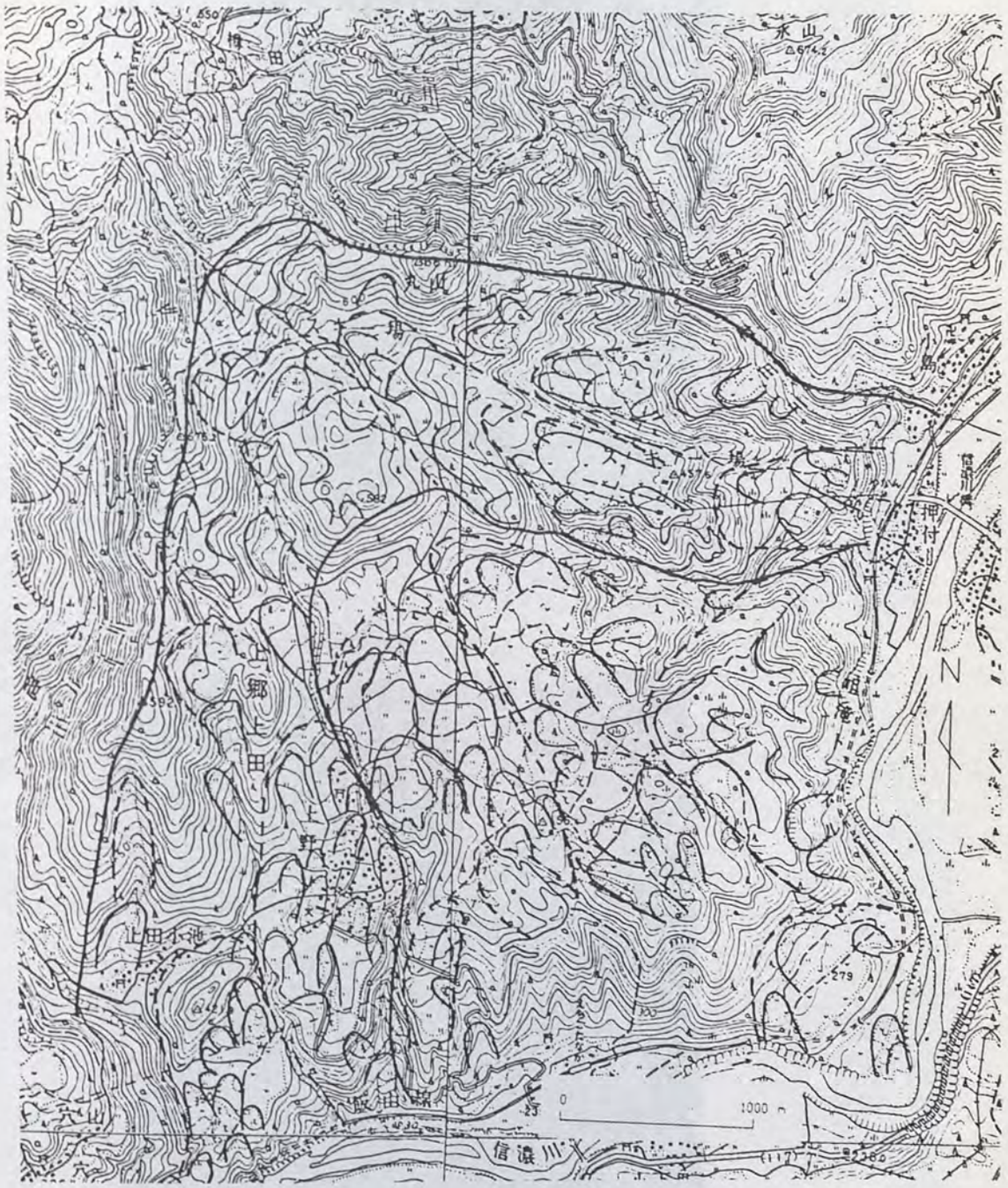

NO. 31 MASEGUCHI LANDSLIDE

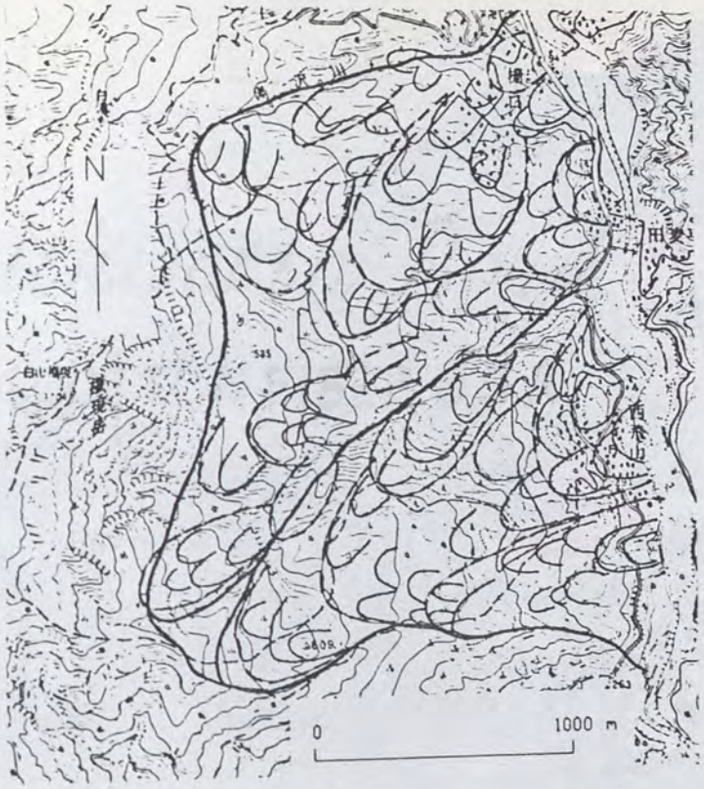

NO. 32 MARUTA LANDSLIDE

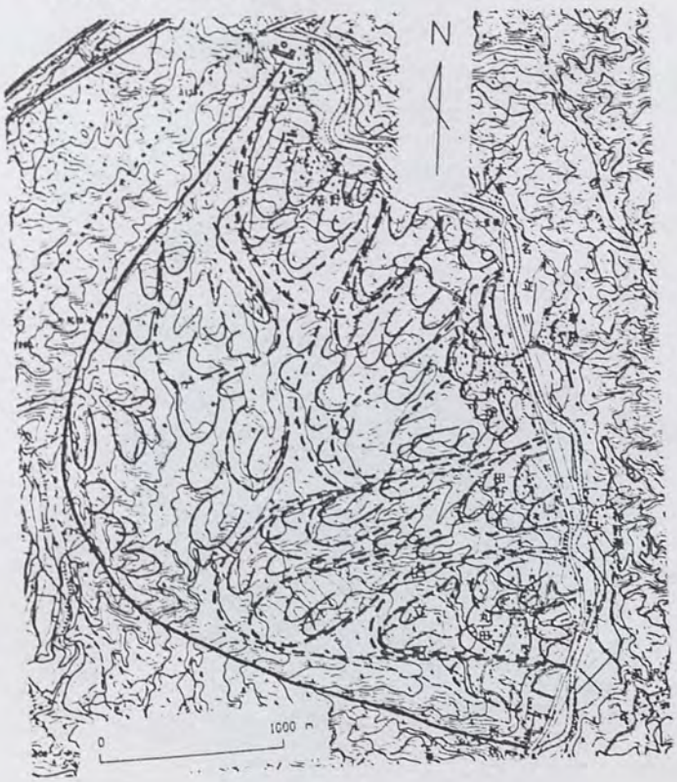

NO. 33 KODOMARI LANDSLIDE

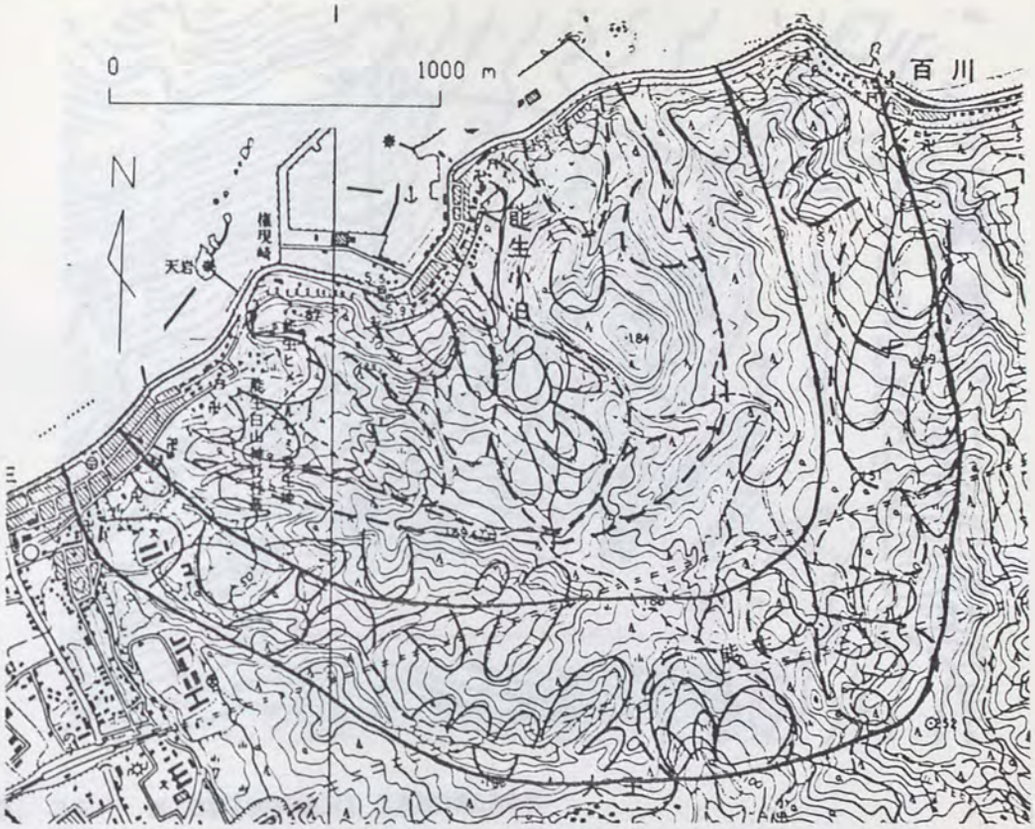

NO. 34 OHBORA LANDSLIDE

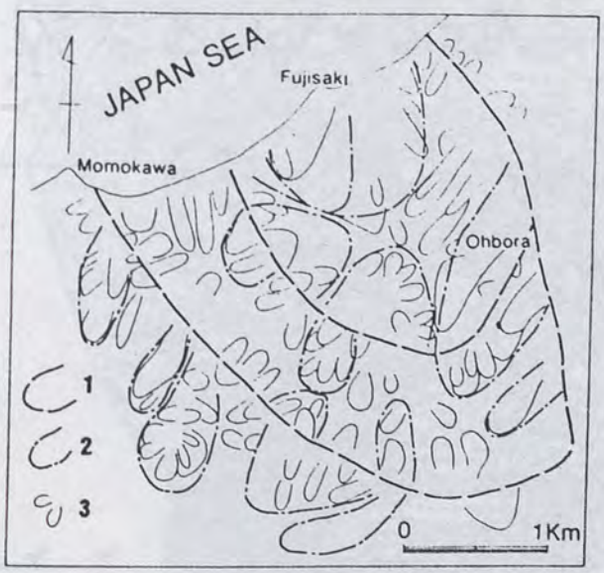

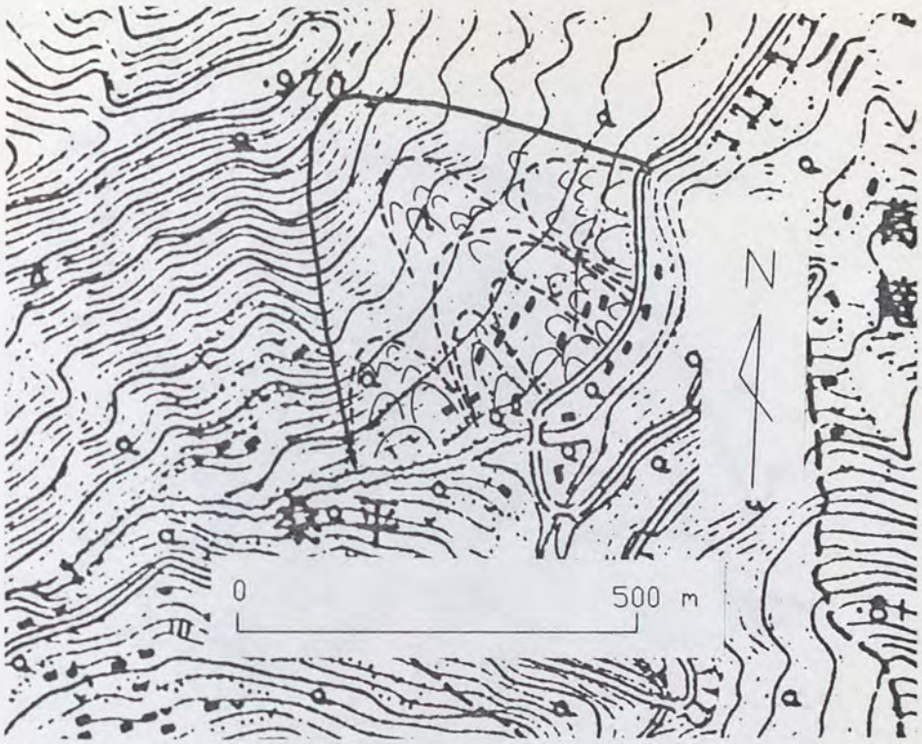

NO. 36 NISHINOTANI LANDSLIDE

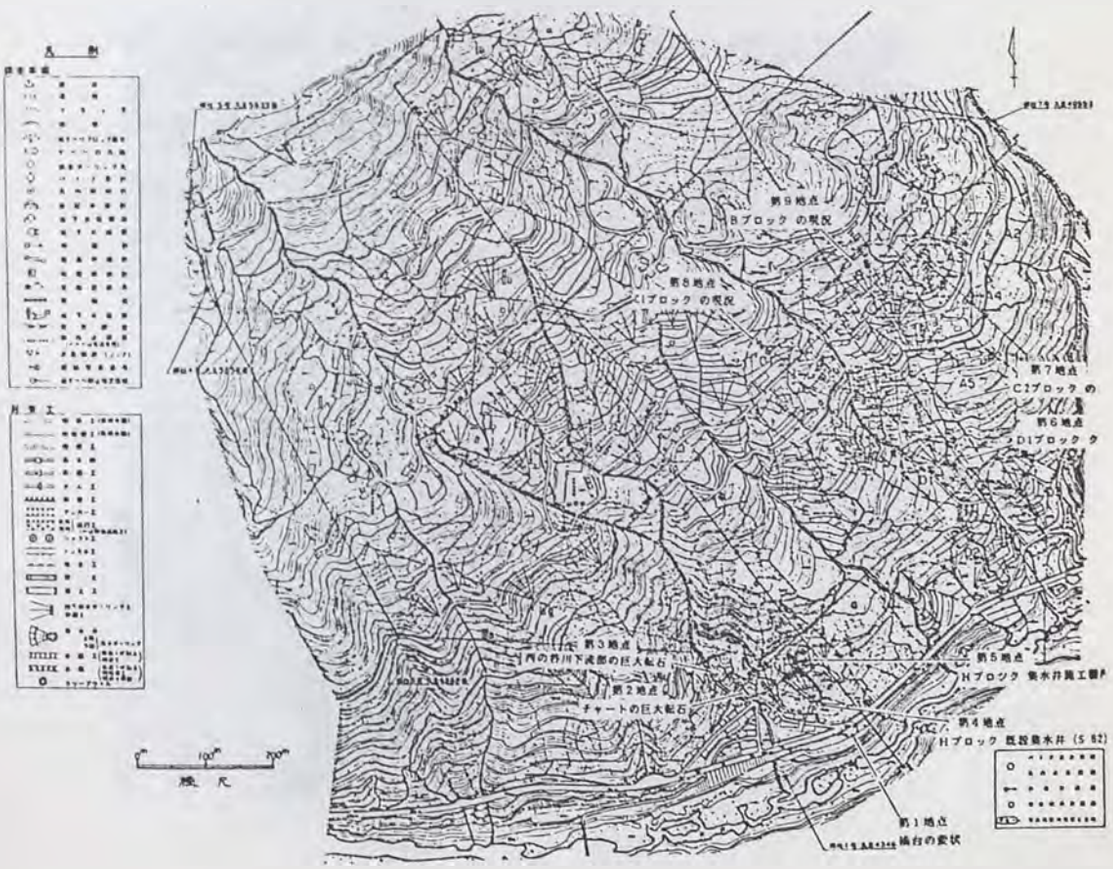

NO. 37 YOUNE LANDSLIDE

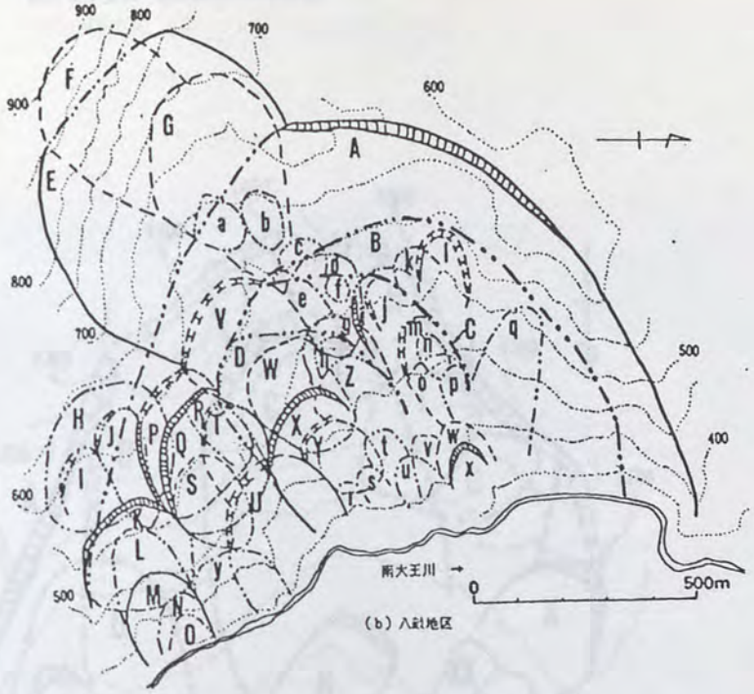

(b) 八釈地区

NO. 38 NUTA LANDSLIDE

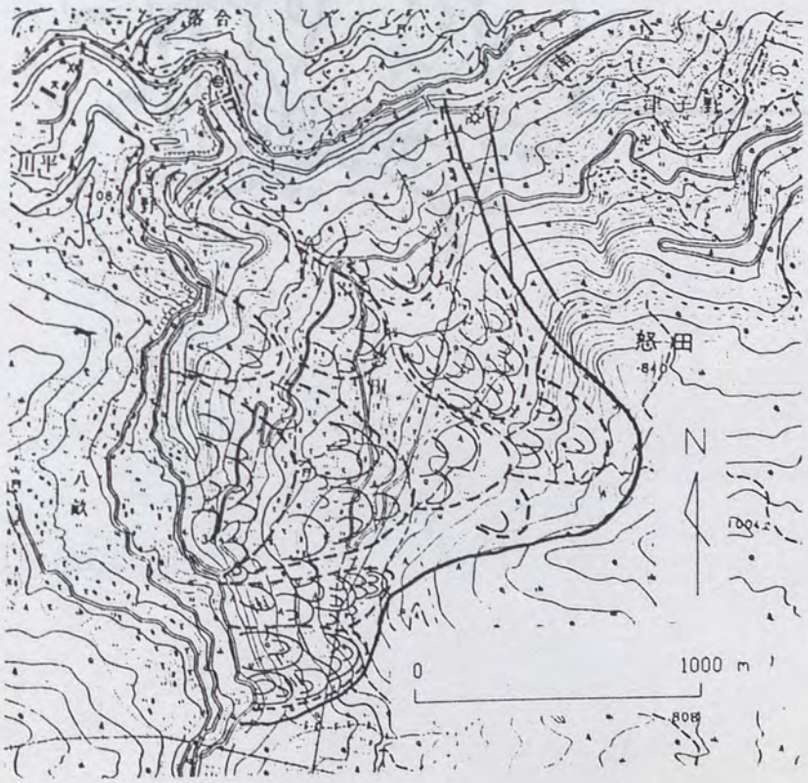

NO. 39 NYUUYA LANDSLIDE

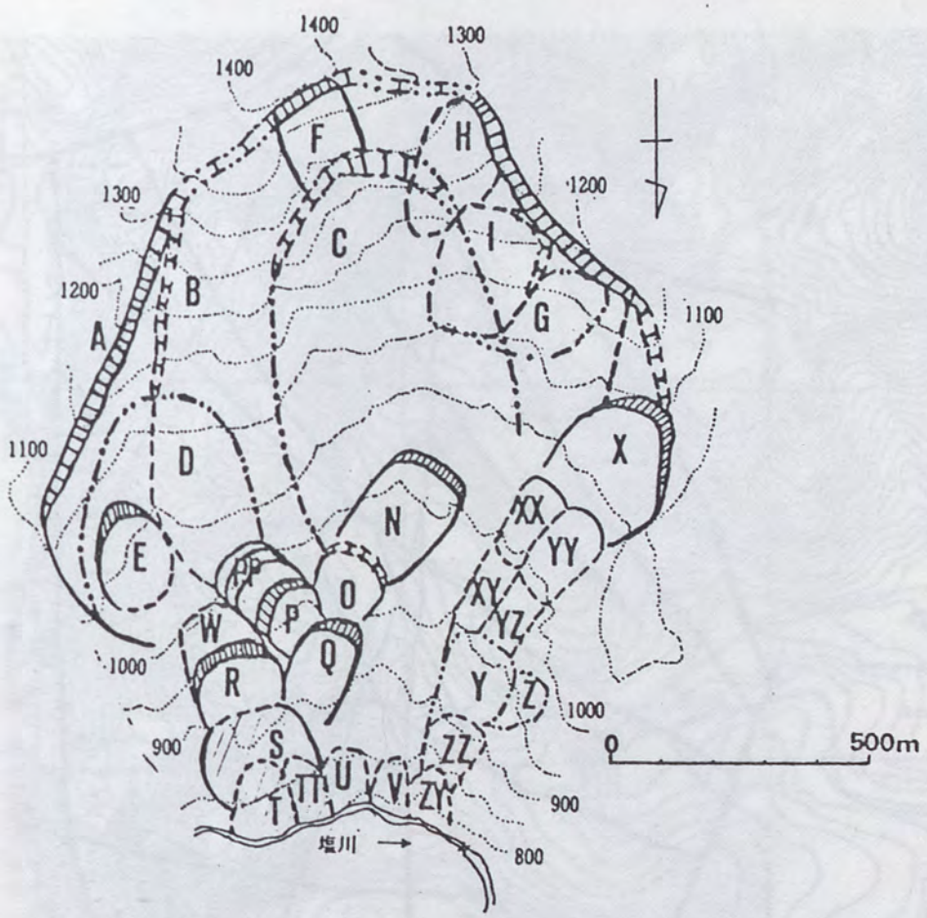

LINEAMENT MAPS

NO. 1 MIDWAY BRIDGE LANDSLIDE

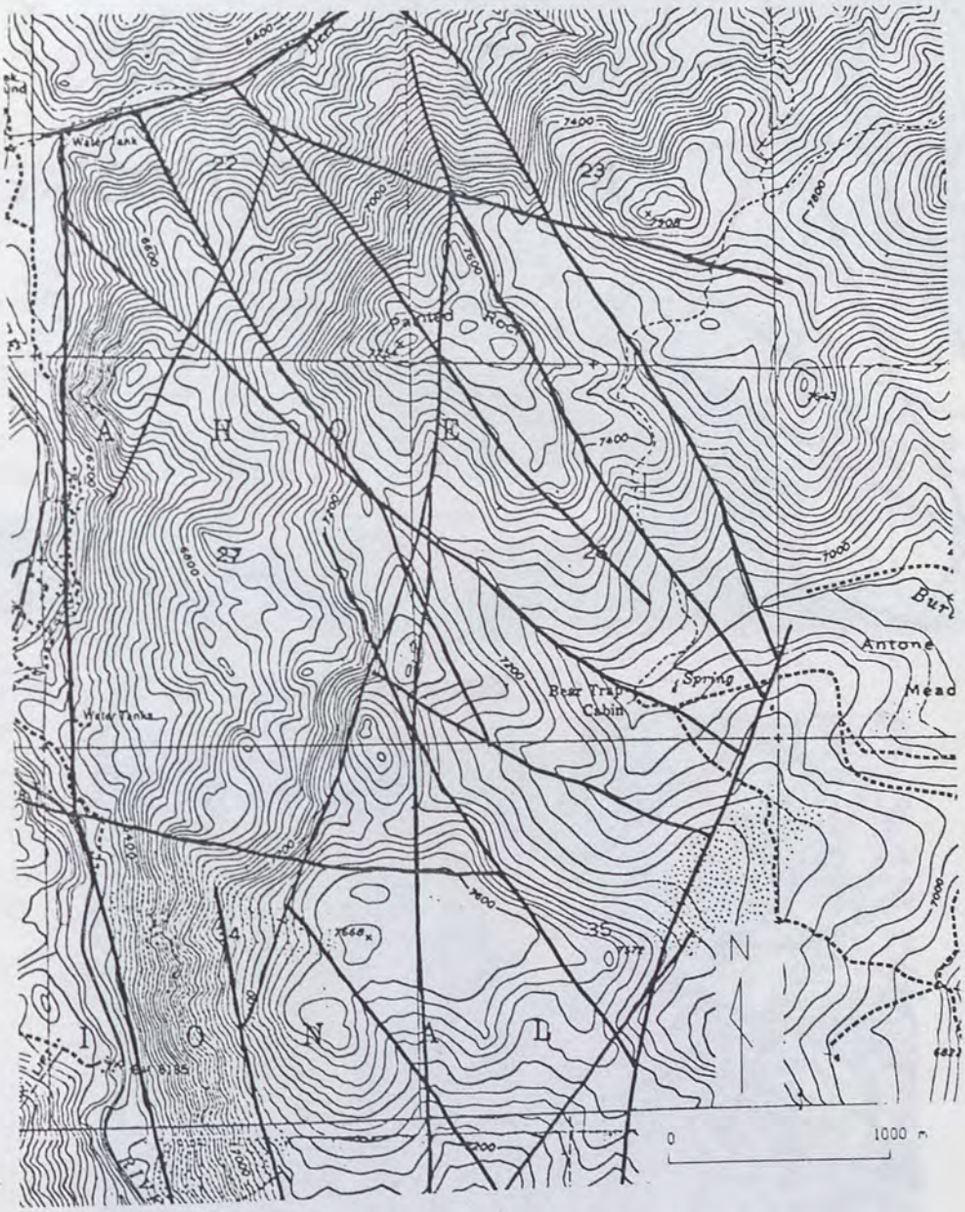

NO. 2 BOCA RIDGE LANDSLIDE

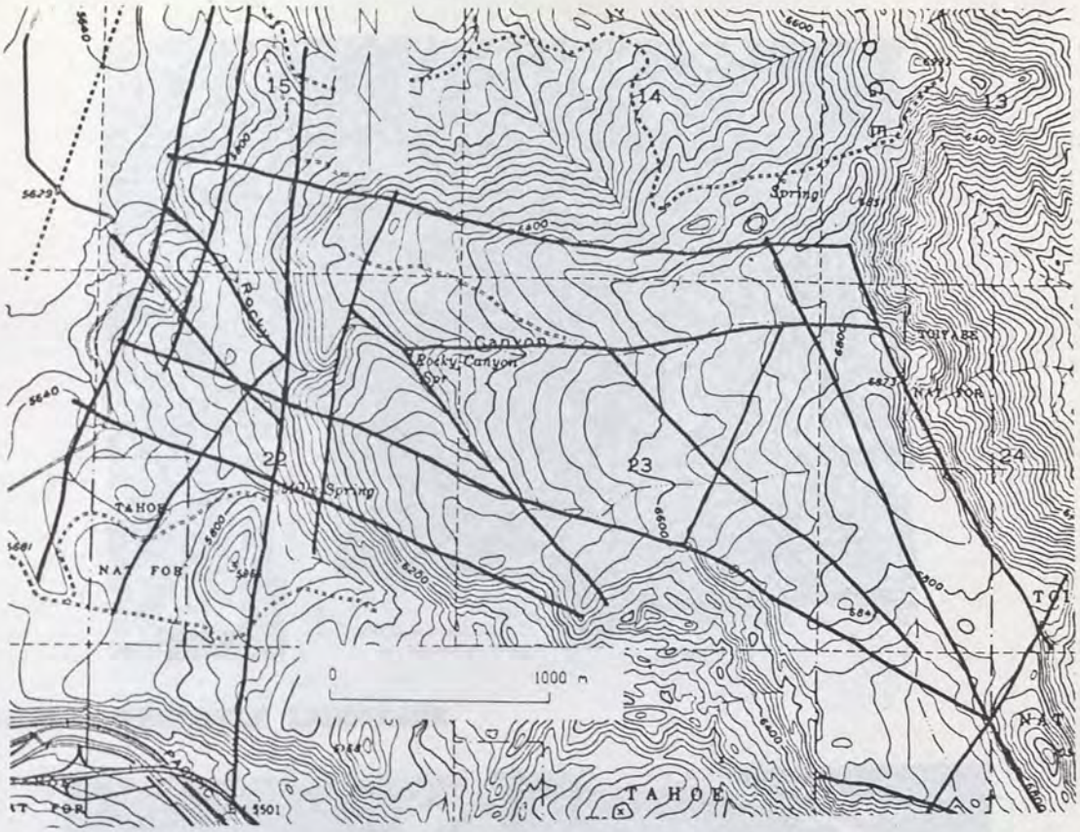

NO. 3 PALOS VERDES LANDSLIDE

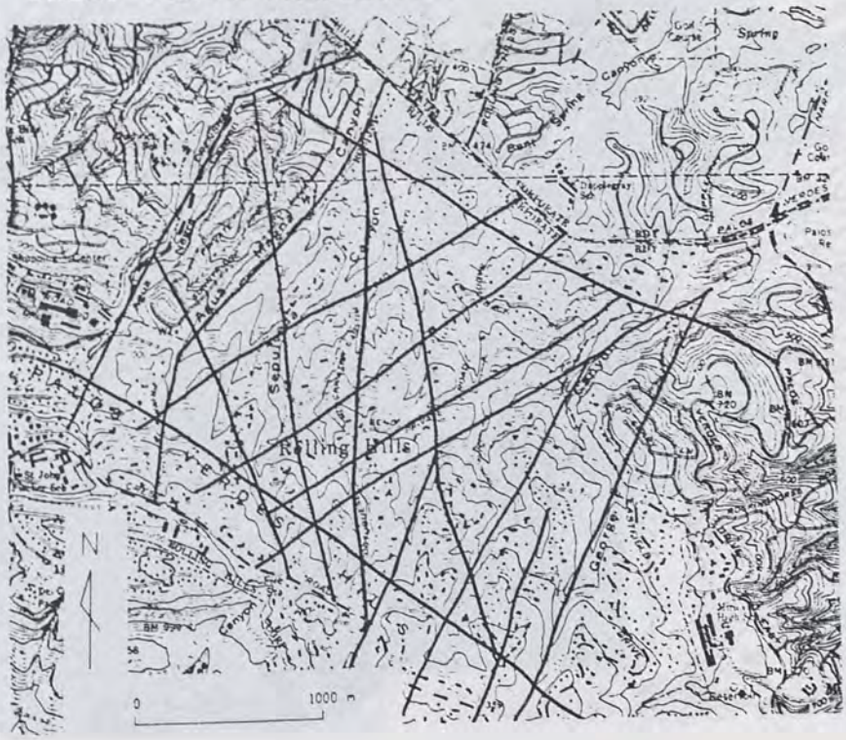

NO. 4 BIG ROCK MESA LANDSLIDE

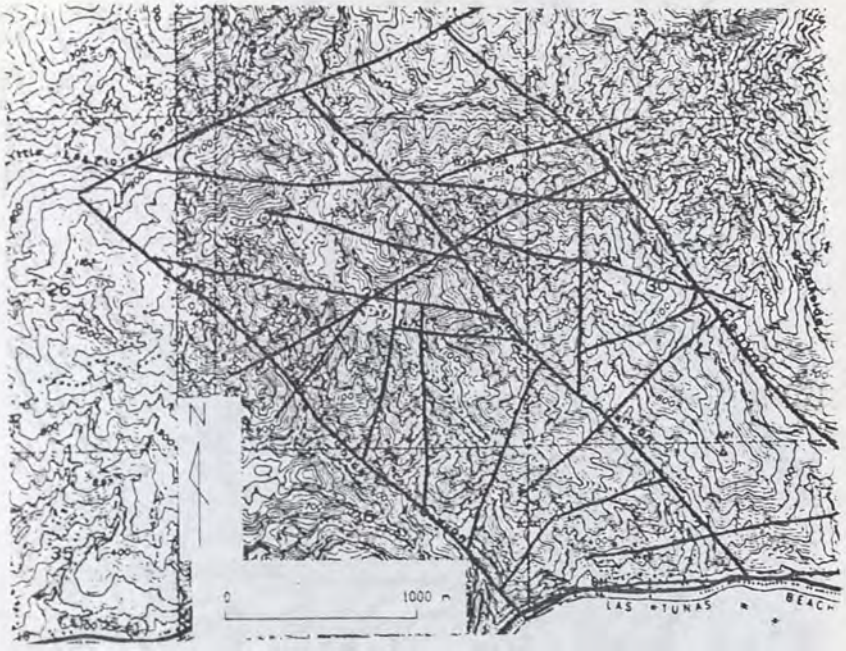

NO. 5 THRISTLE LANDSLIDE

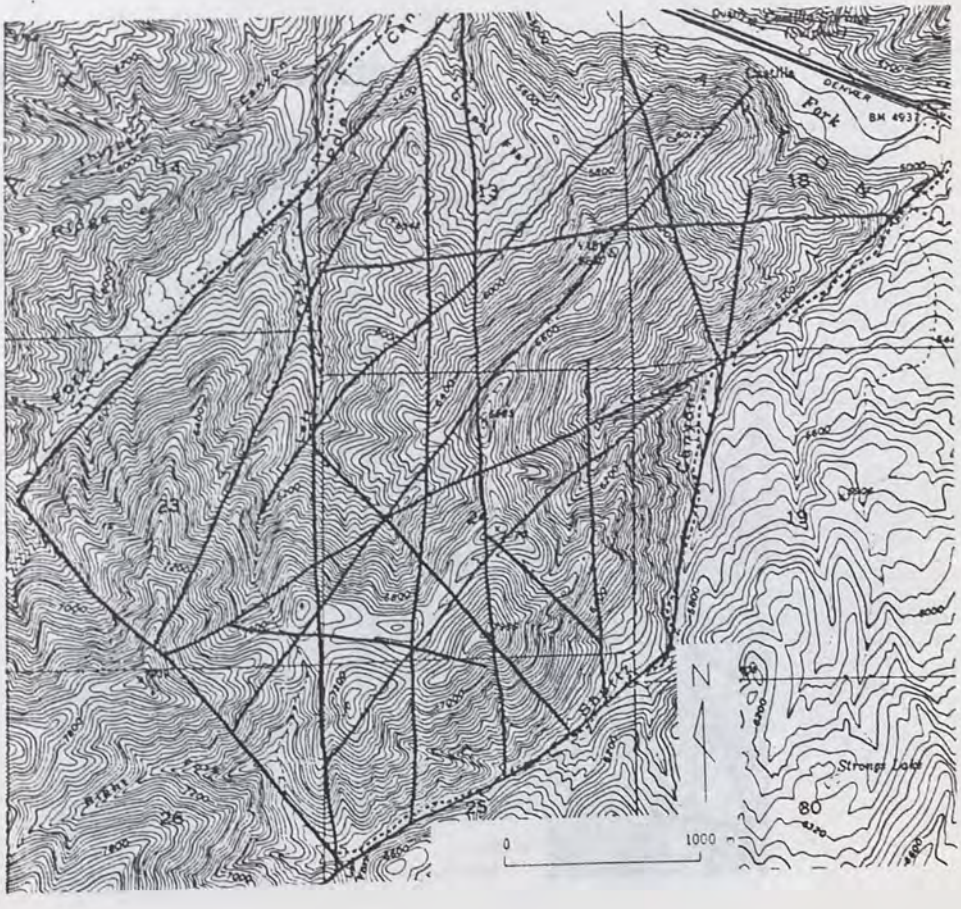

NO. 7 UPPER GROS VENTRE LANDSLIDE

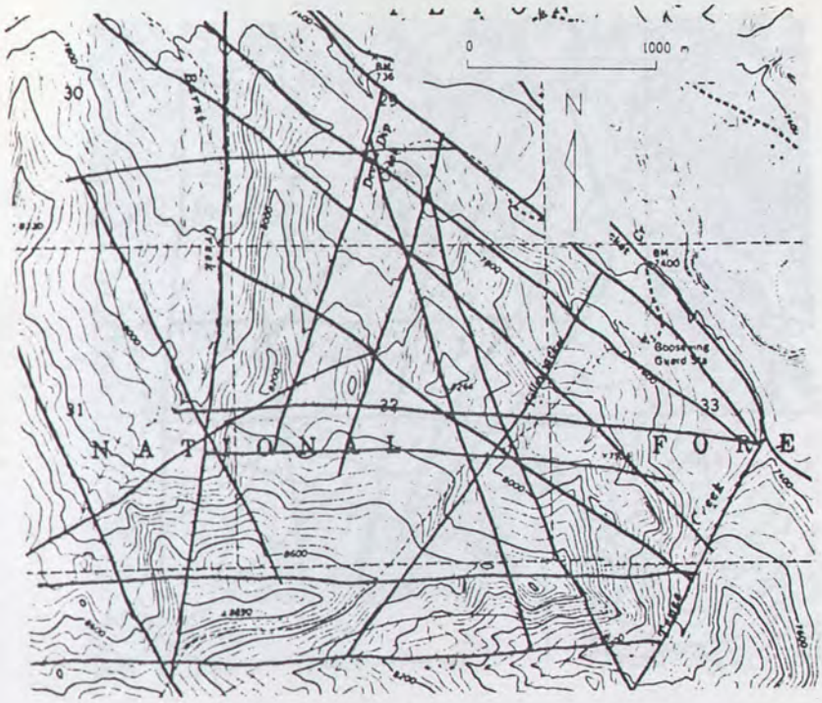

NO. 12 KIRITANI LANDSLIDE

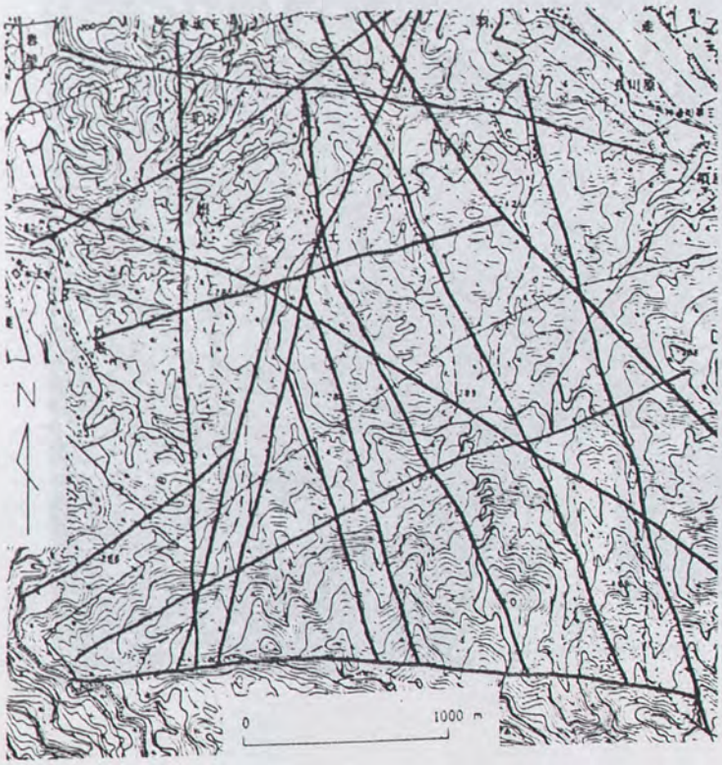

NO. 13 KATSURABARA LANDSLIDE

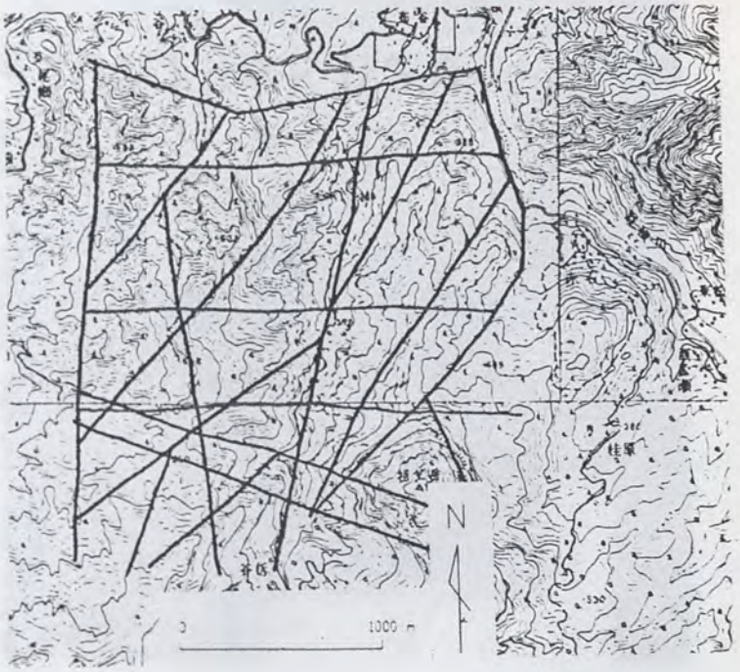

NO. 15 TAKISAKA LANDSLIDE

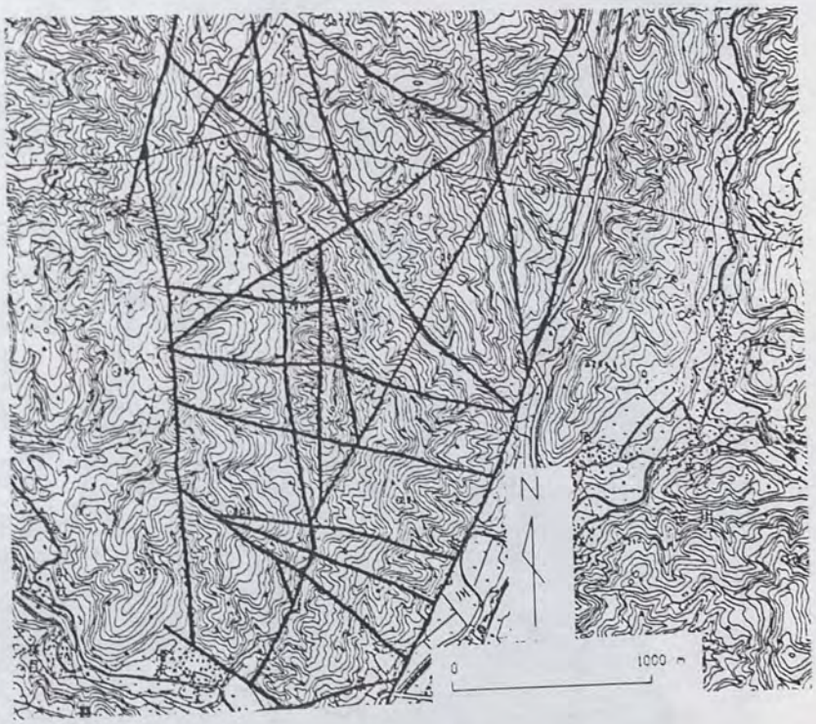

NO. 17 MUSHIGAME LANDSLIDE

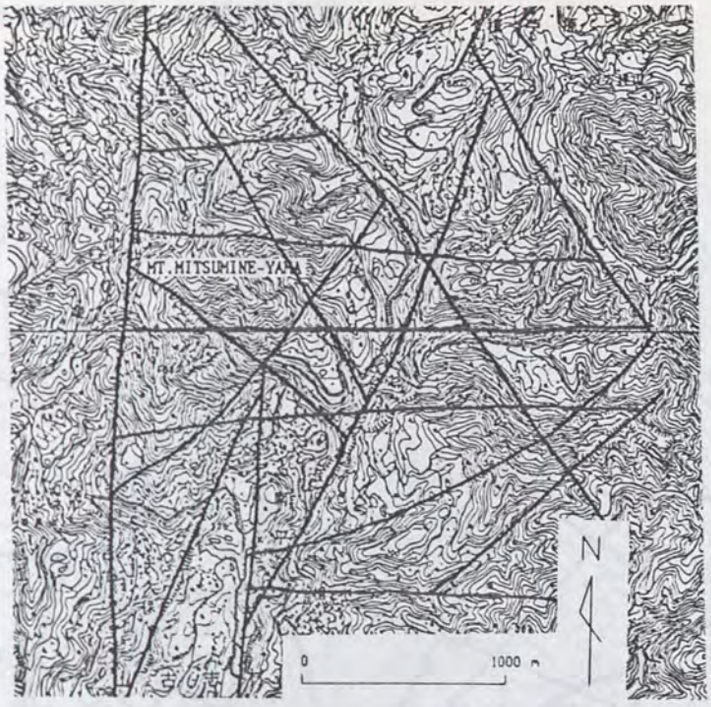

NO. 21 RAIDEN LANDSLIDE

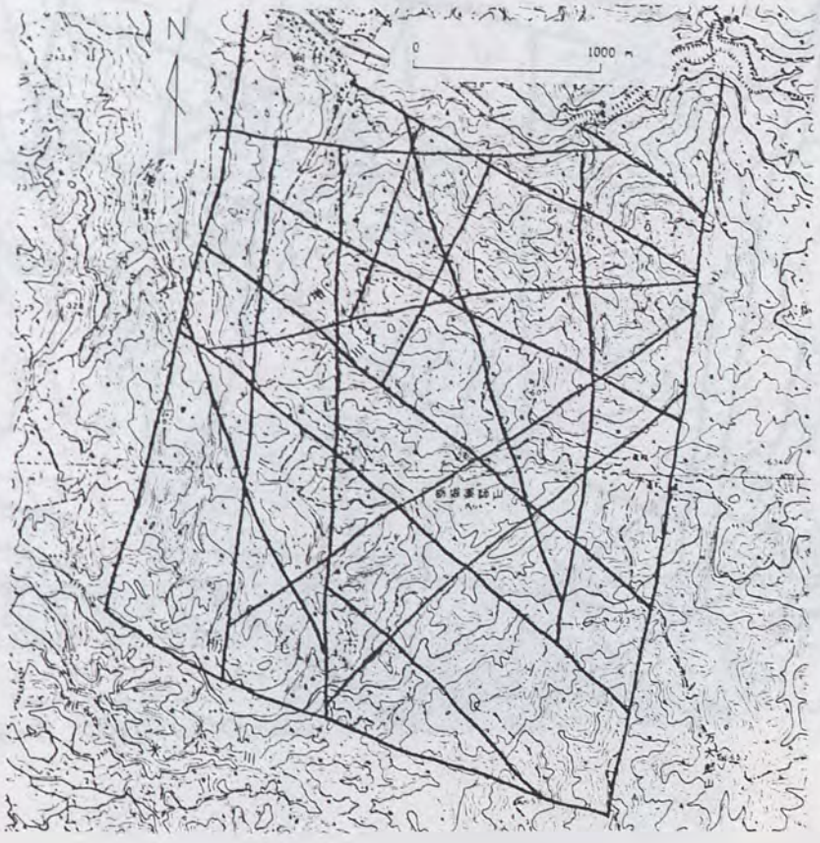

NO. 19 KARUIZAWA LANDSLIDE
NO. 20 HAPPOUDAI LANDSLIDE

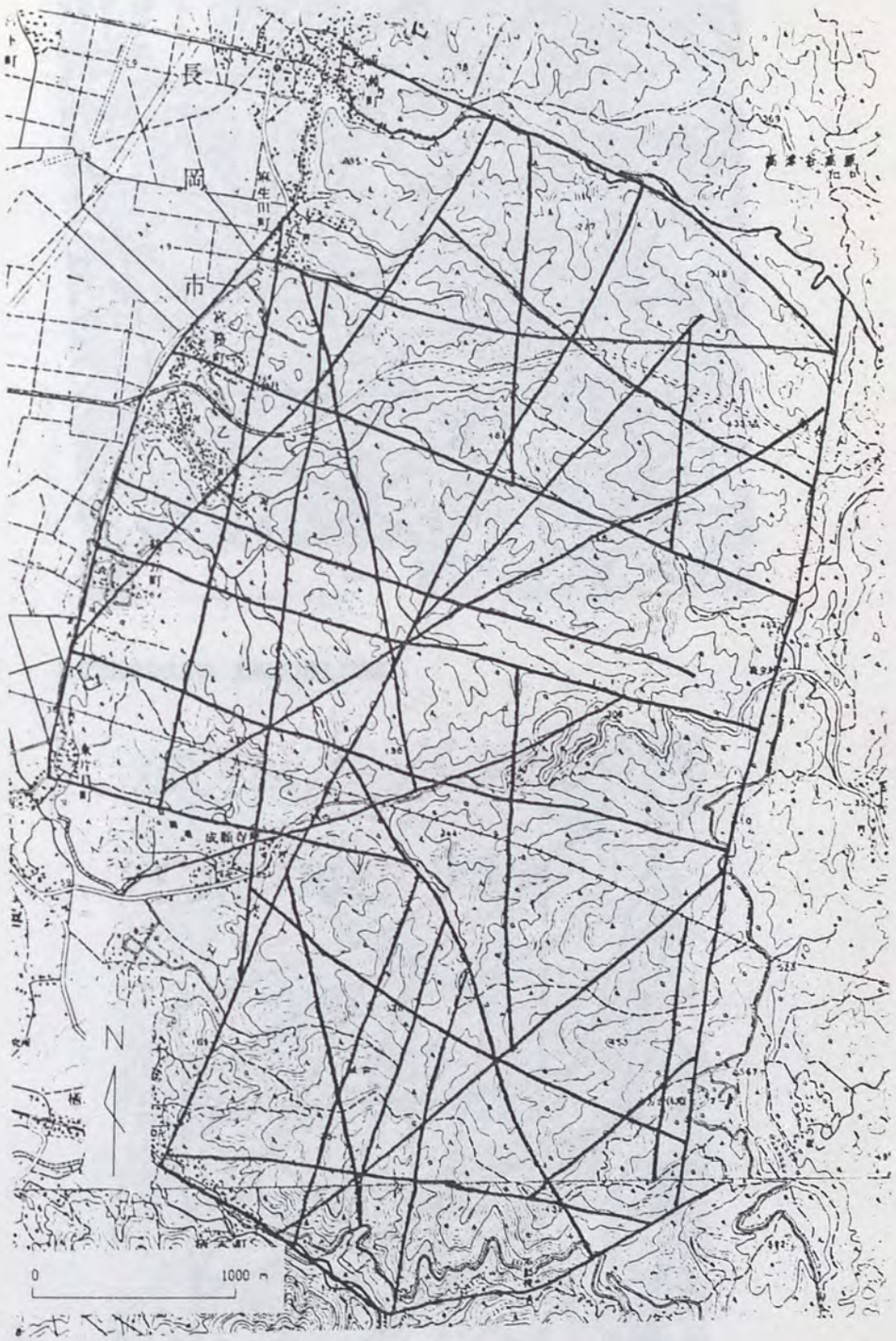

NO. 22 NISHINAKANOHO LANDSLIDE

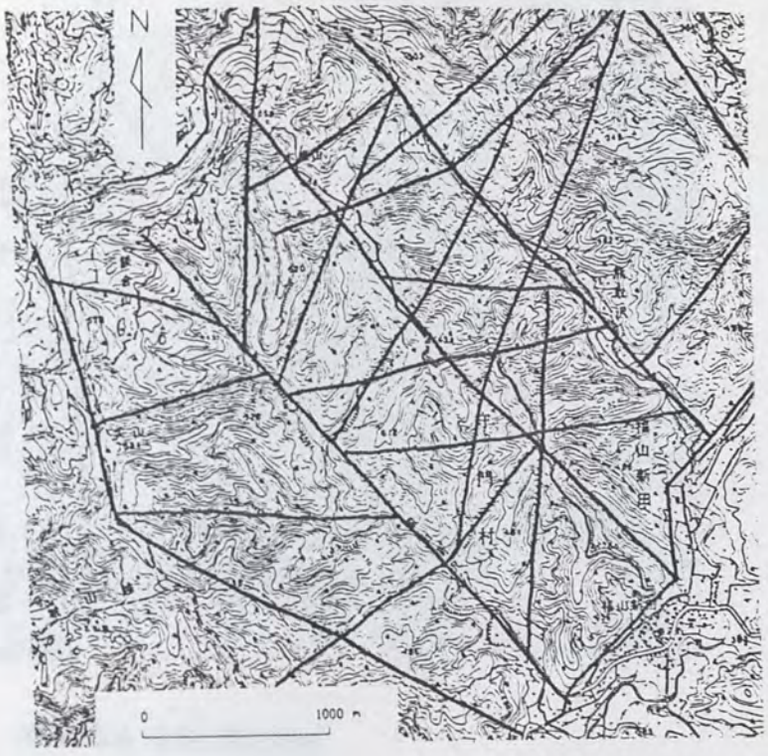

NO. 24 KITAURATA LANDSLIDE

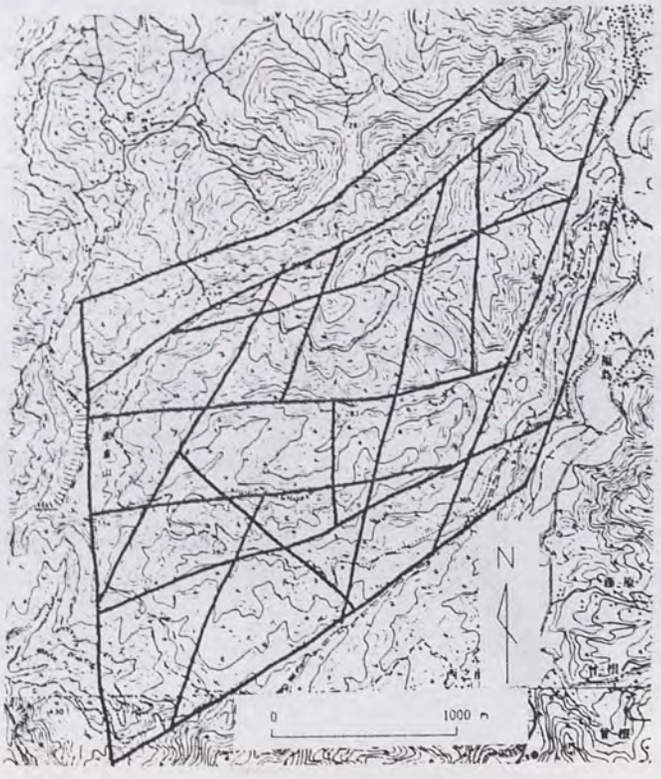

NO. 31 MASEGUCHI LANDSLIDE

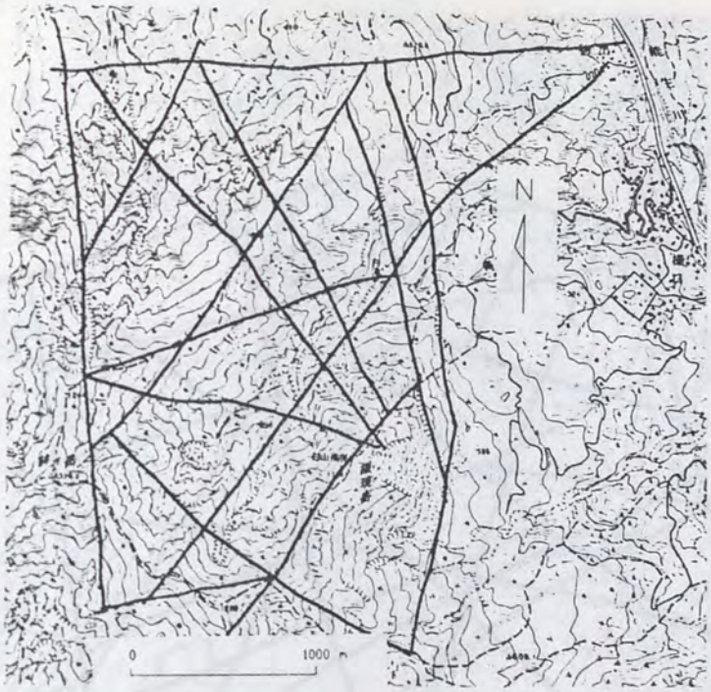

NO. 32 MARUTA LANDSLIDE

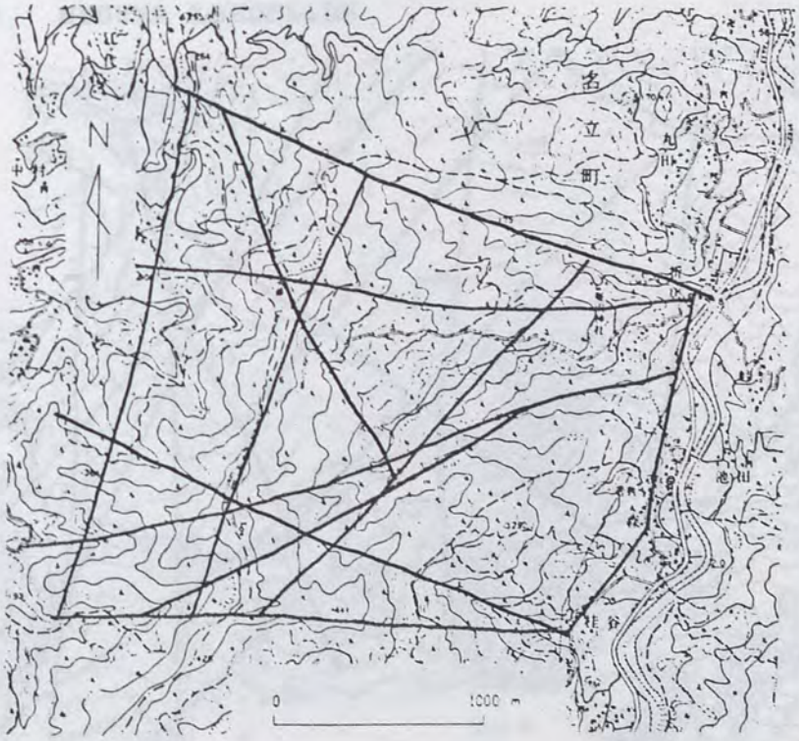

NO. 37 YOUNE LANDSLIDE

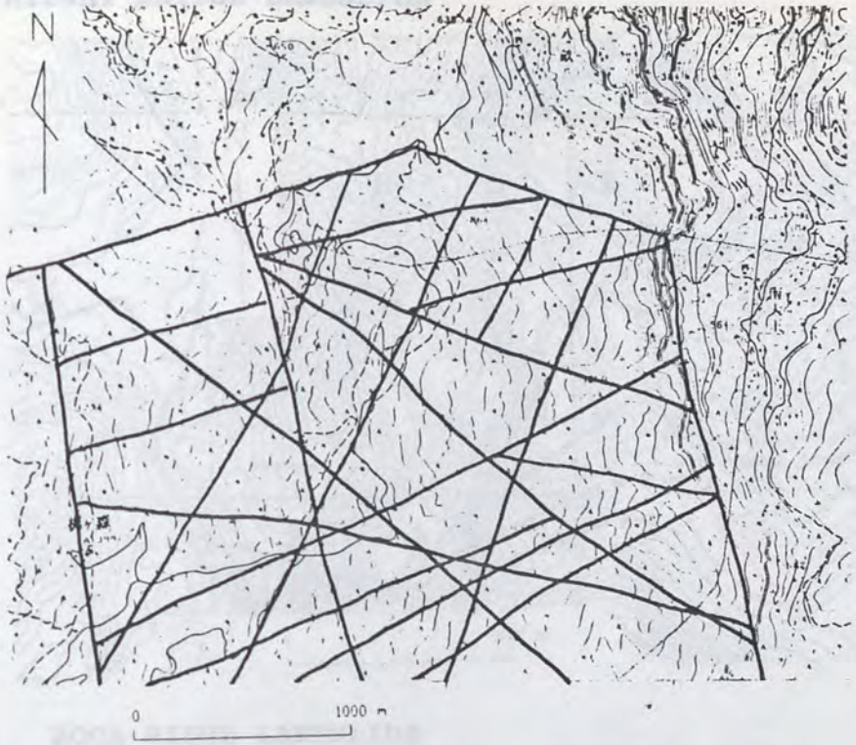

NO. 39 NYUUYA LANDSLIDE

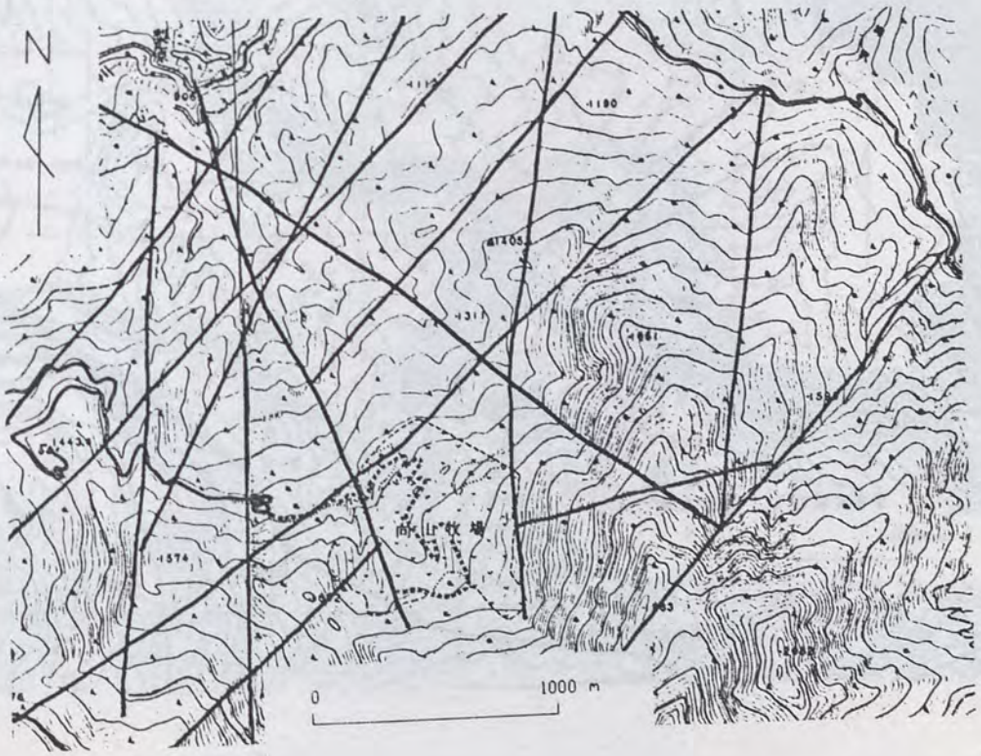

ROCK FRAGMENTS AND FRACTURES DATA COLLECTION LOCATIONS

NO.1 MIDWAY BRIDGE LANDSLIDE

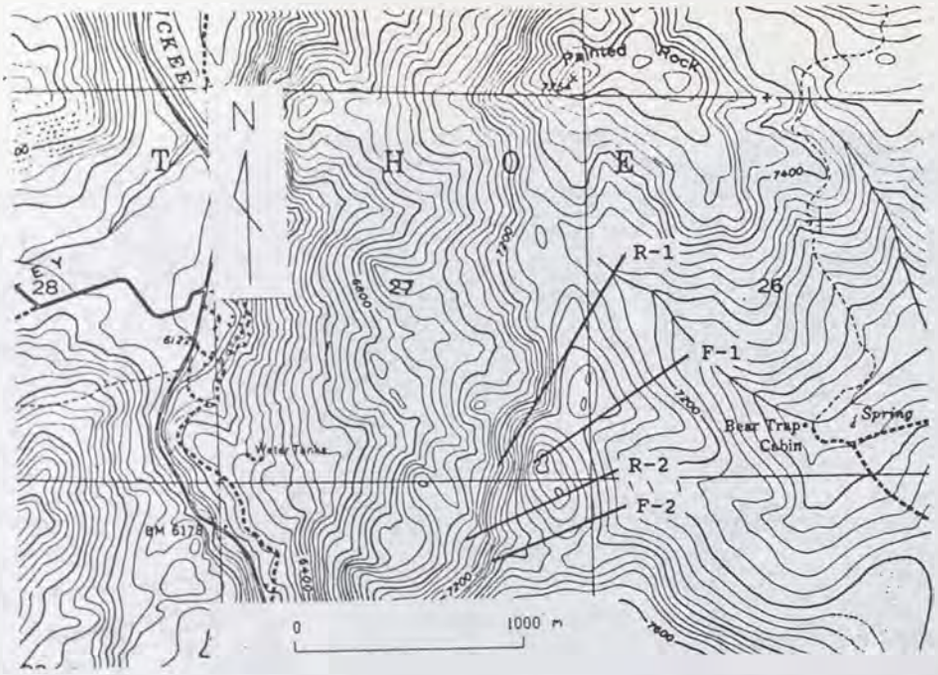

NO. 2 BOCA RIDGE LANDSLIDE

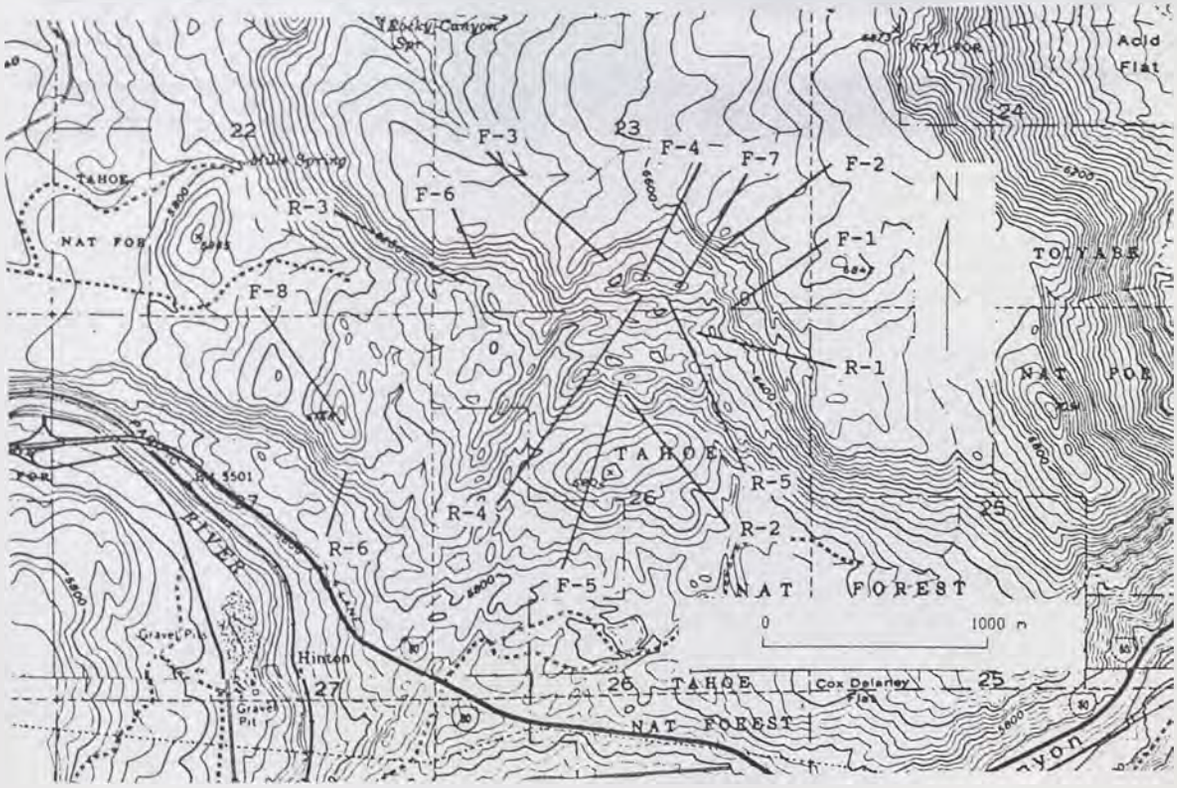

SLIDE MOUNTAIN

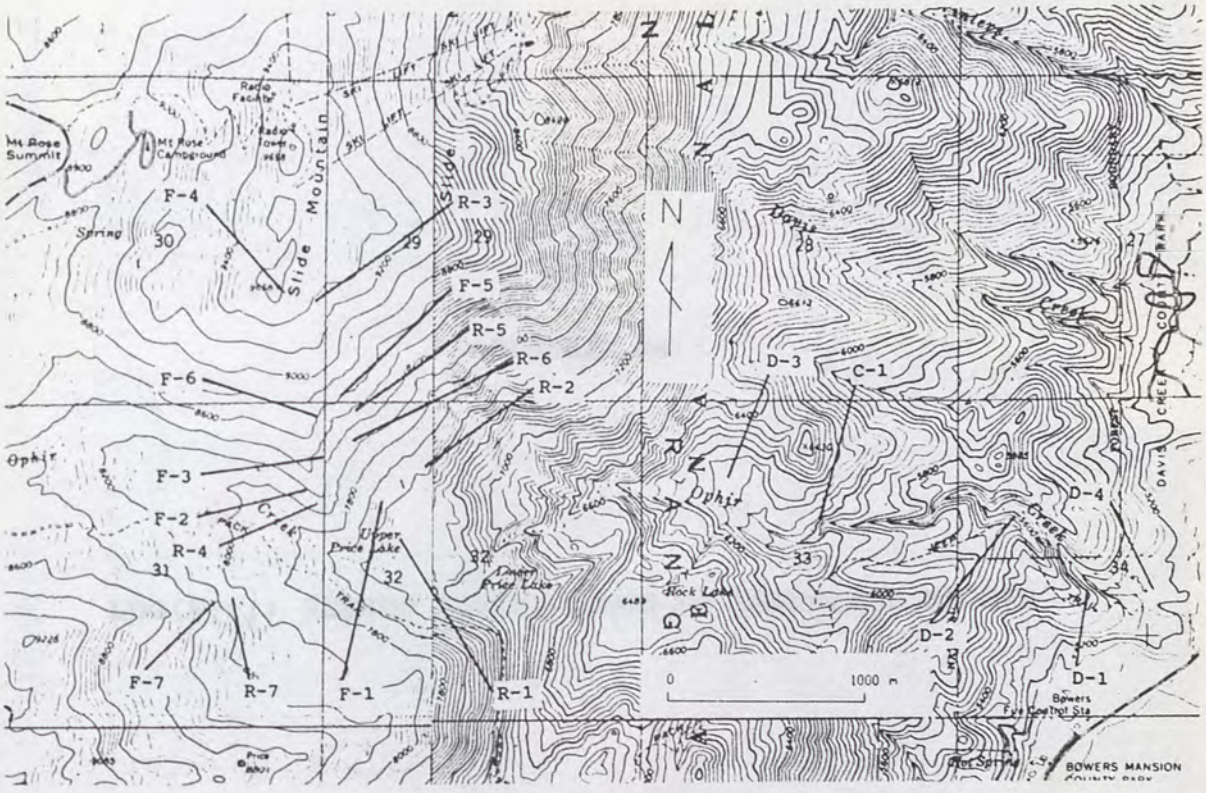

APPENDIX B:

LOG($N(r)$) VERSUS LOG(r) PLOTS OF LANDSLIDE BLOCKS

No.1 Midway Ridge Landslide
Whole Blocks Ruler - Width

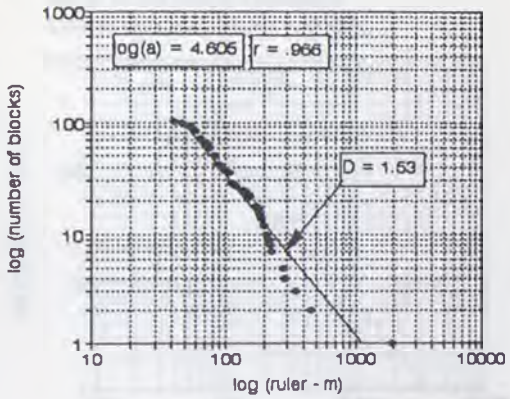

No.1 Midway Ridge Landslide
whole blocks ruler - length

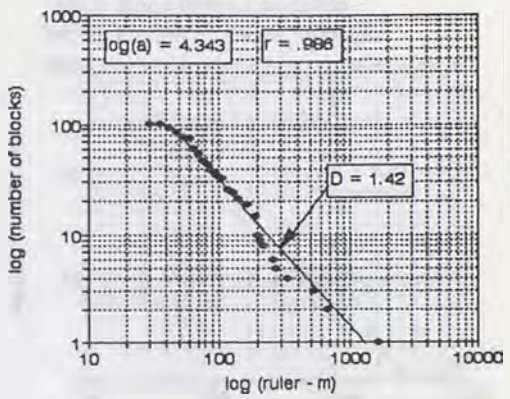

Midway Ridge Landslide
2nd level blocks ruler - width

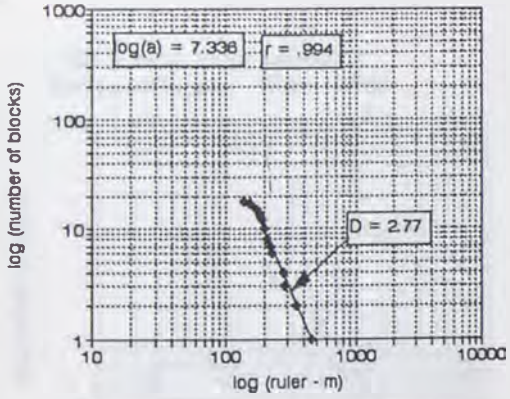

No.1 Midway Ridge Landslide
2nd level blocks ruler - length

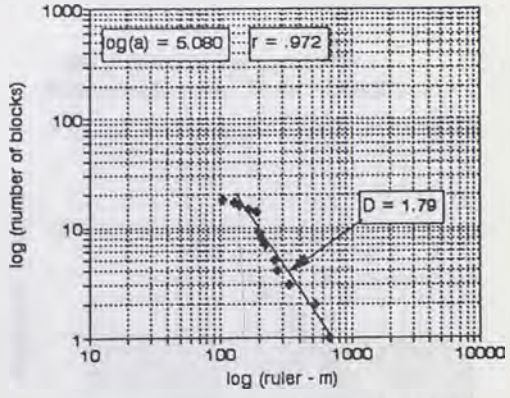

No.1 Midway Ridge Landslide
3nd level blocks ruler - length

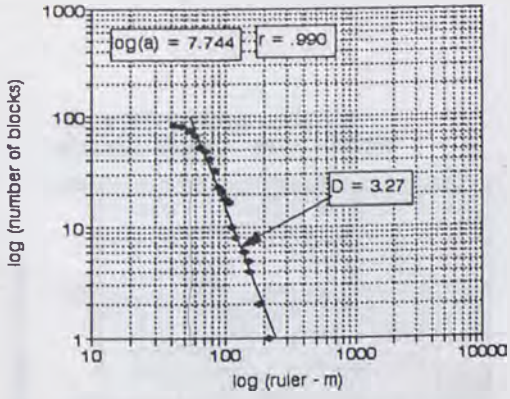

No.1 Midway Ridge Landslide
3nd level blocks ruler - length

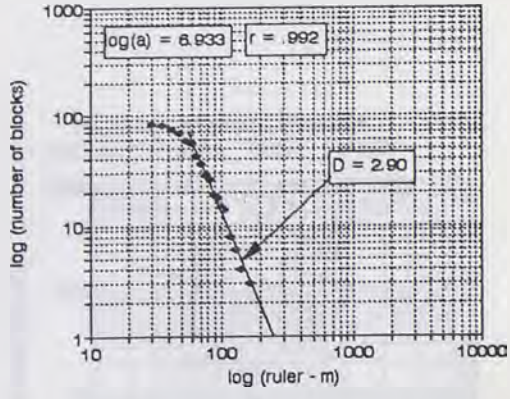

No.2 Boca Ridge Landslide
Whole Blocks Ruler - Width

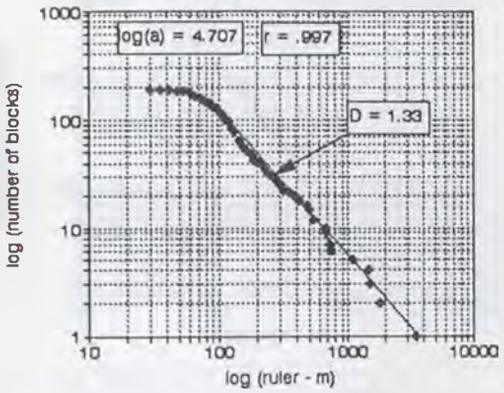

No.2 Boca Ridge Landslide
Whole Blocks Ruler - Length

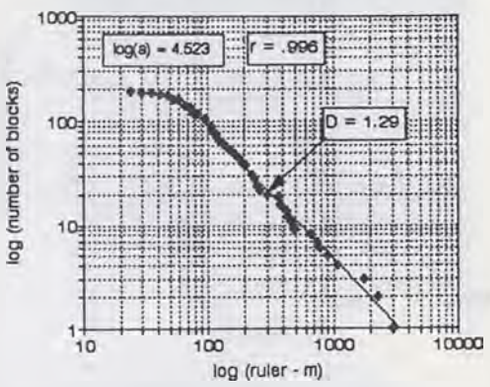

No.2 Boca Ridge Landslide
2nd Level Blocks Ruler - Width

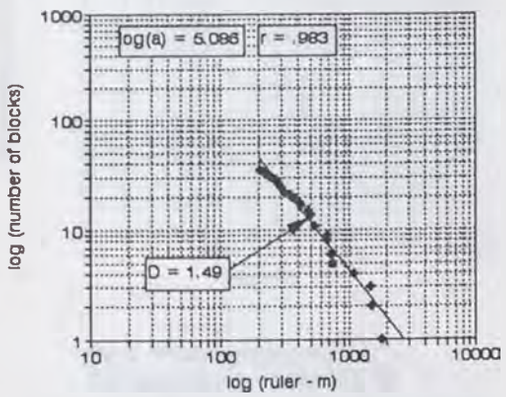

No.2 Boca Ridge Landslide
2nd Level Blocks Ruler - Length

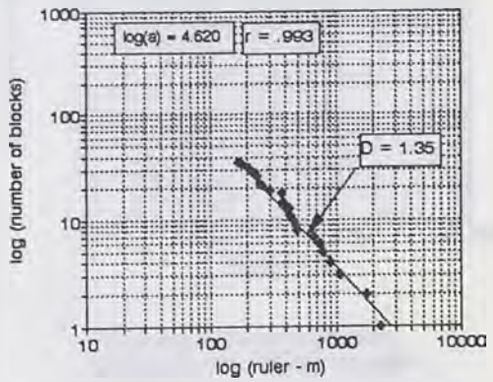

No.2 Boca Ridge Landslide
3rd Level Blocks Ruler - Width

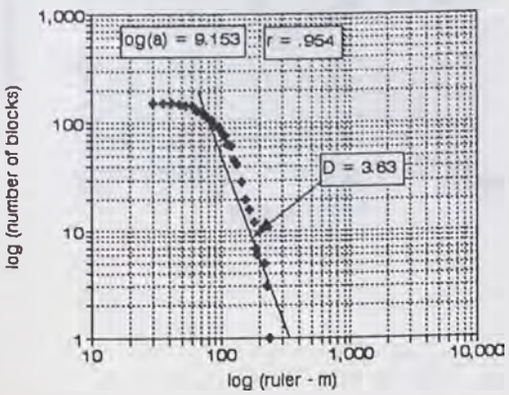

No.2 Boca Ridge Landslide
3rd Level Blocks Ruler - Length

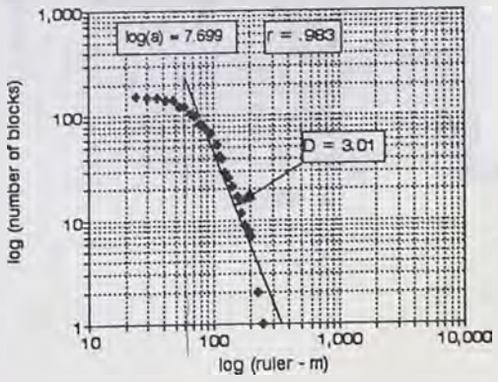

No.3 Palos Verdes Landslide
Whole Blocks Ruler - Width

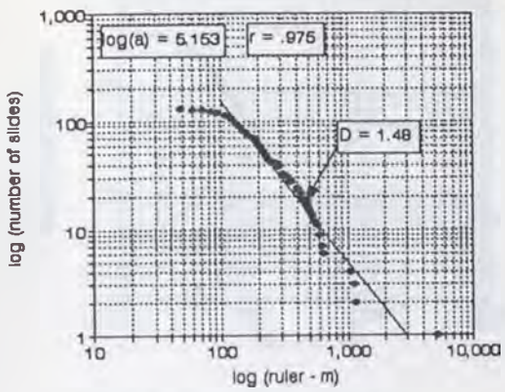

No.3 Palos Verdes Landslide
Wlole Blocks Ruler - Length

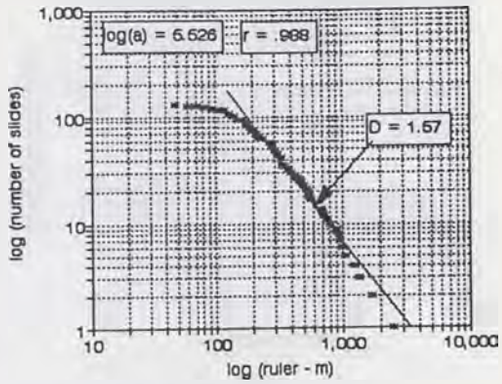

No.3 Palos Verdes Landslide
2rd level blocks Ruler - width

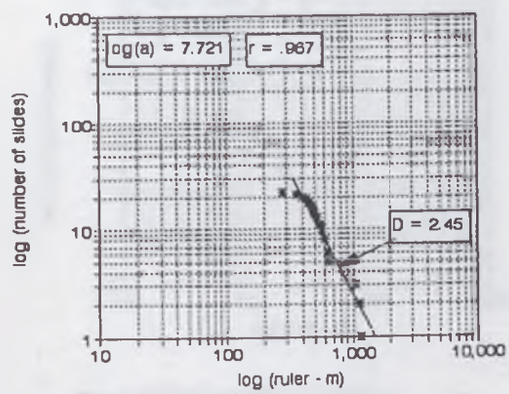

No.3 Palos Verdes Landslide
2rd level blocks Ruler - Length

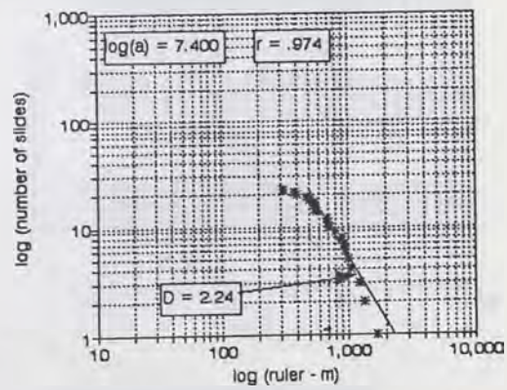

No.3 Palos Verdes Landslide
3rd level blocks Ruler - width

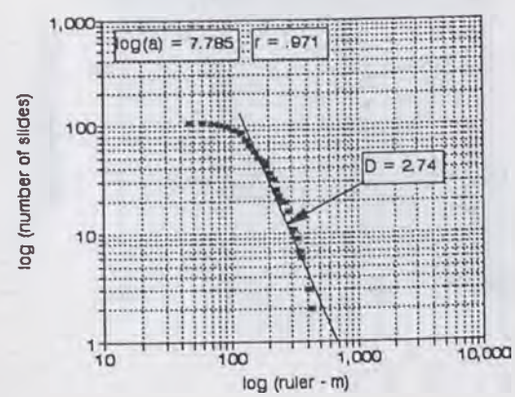

No.3 Palos Verdes Landslide
3rd level blocks Ruler - Length

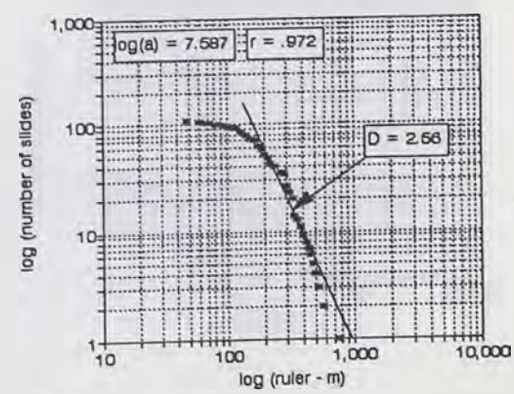

No.4 Big Rock Mesa Landslide
Whole Blocks Ruler - Width

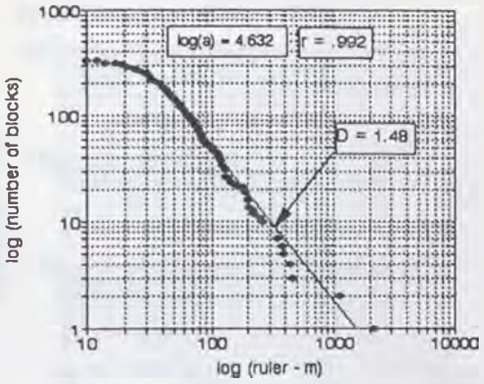

No.4 Big Rock Mesa Landslide
Whole Blocks Ruler - Length

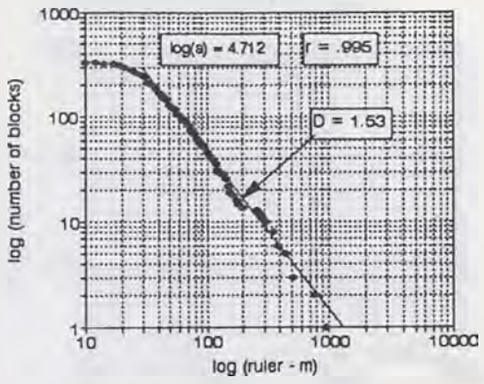

No.4 Big Rock Mesa Landslide
2nd Level Blocks Ruler - Width

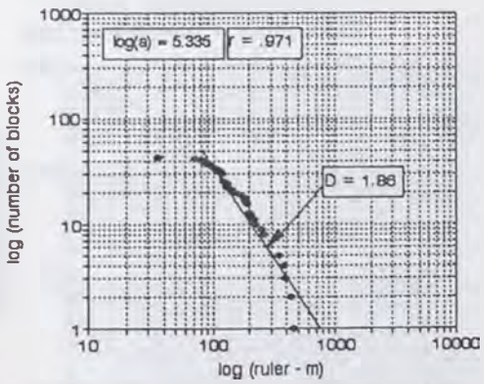

No.4 Big Rock Mesa Landslide
2nd Level Blocks Ruler - Length

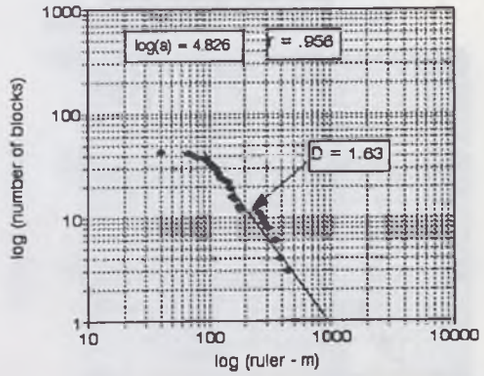

No.4 Big Rock Mesa Landslide
3rd Level Blocks Ruler - Width

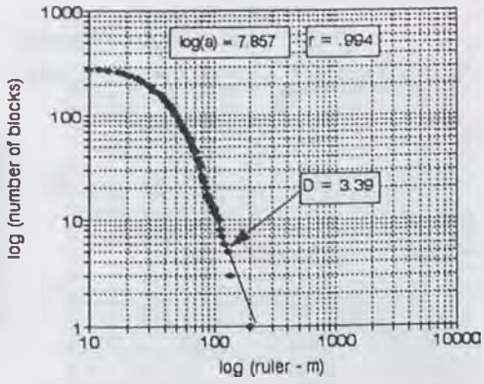

No.4 Big Rock Mesa Landslide
3rd Level Blocks Ruler - Length

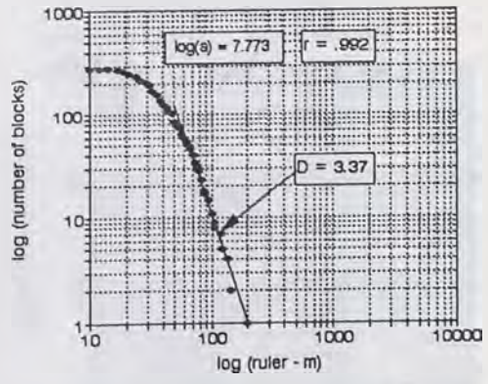

No.5 Thistle Landslide
Whole Blocks Ruler - Width

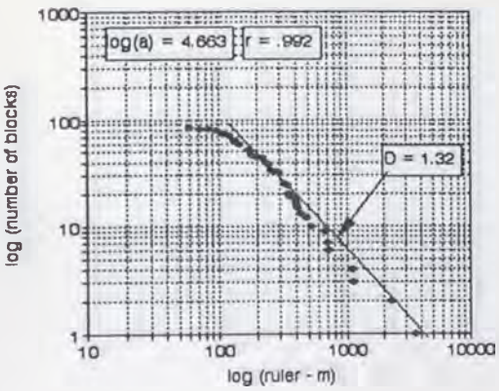

No.5 Thistle Landslide
Whole Blocks Ruler - Length

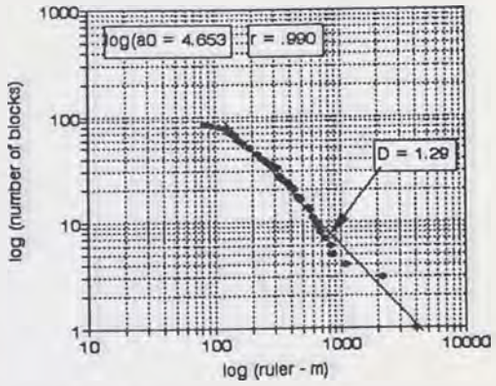

No.5 Thistle Landslide
2nd Level Blocks Ruler - Width

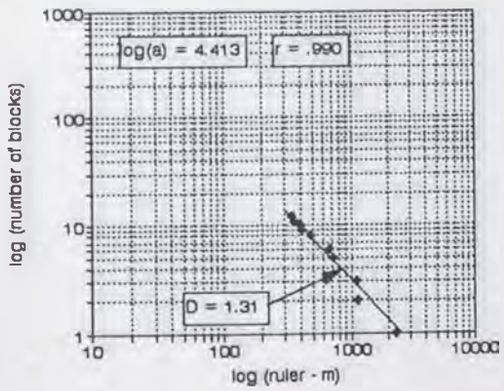

No.5 Thistle Landslide
2nd Level Blocks Ruler - Length

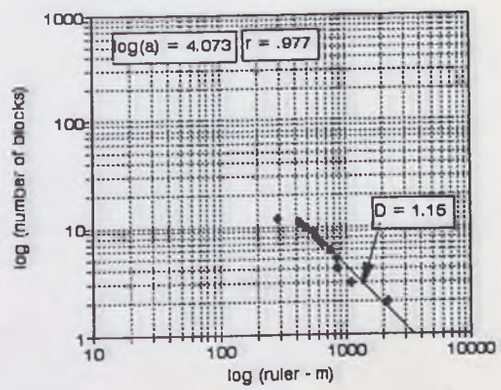

No.5 Thistle Landslide
3rd Level Blocks Ruler - Width

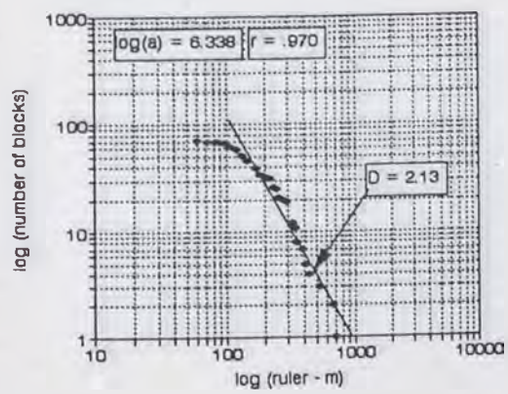

No.5 Thistle Landslide
3rd Level Blocks Ruler - Length

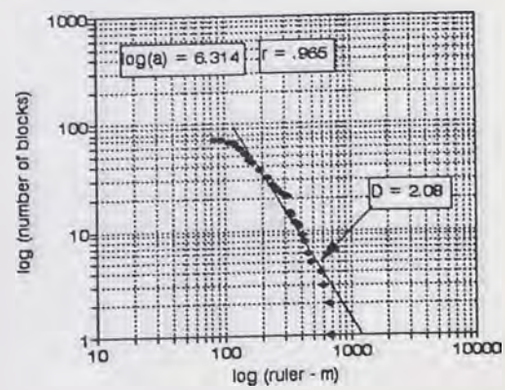

No.6 Lower Gros Ventre Landslide
Whole Blocks Ruler - Width

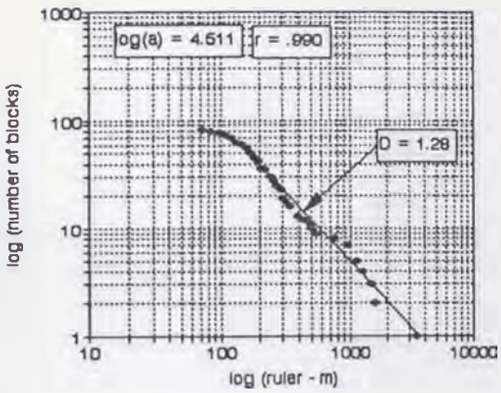

No.6 Lower Gros Ventre Landslide
Whole Blocks Ruler - Length

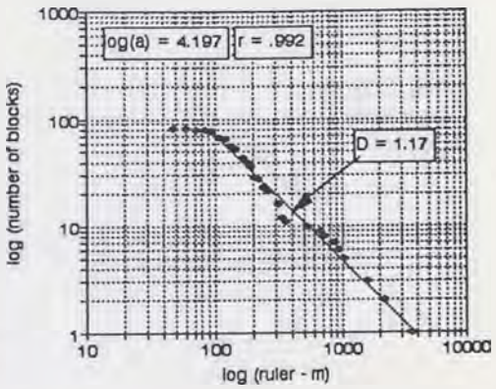

No.6 Lower Gros Ventre Landslide
2nd Level Blocks Ruler - Width

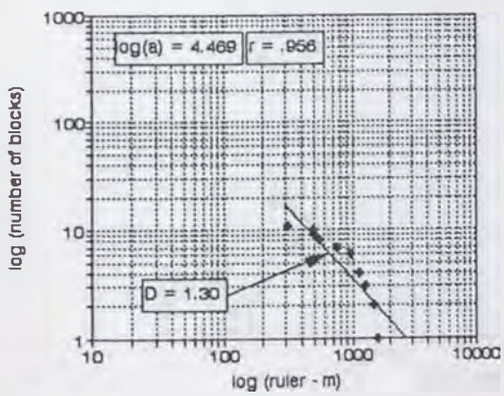

No.6 Lower Gros Ventre Landslide
2nd Level Blocks Ruler - Length

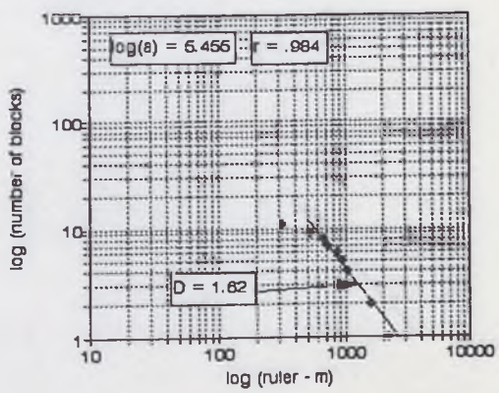

No.6 Lower Gros Ventre Landslide
3rd Level Blocks Ruler - Width

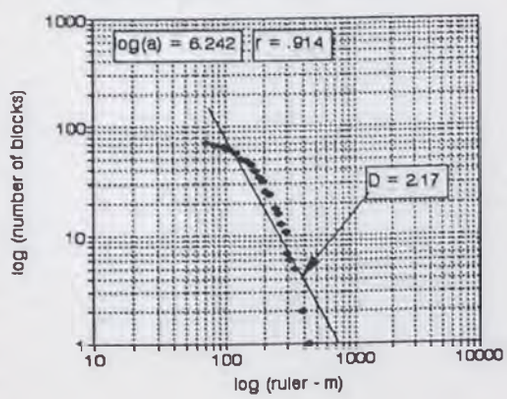

No.6 Lower Gros Ventre Landslide
3rd Level Blocks Ruler - Length

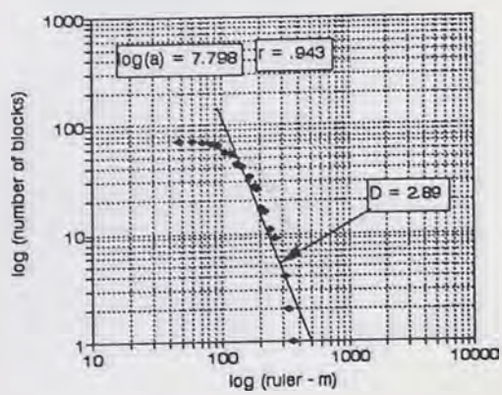

No.7 Upper Gros Ventre Landslide
Whole Blocks Ruler - Width

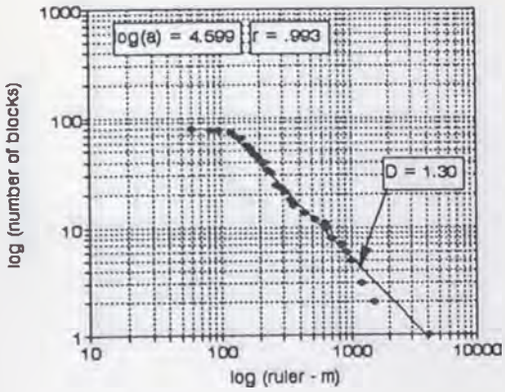

No.7 Upper Gros Ventre Landslide
Whole Blocks Ruler - Length

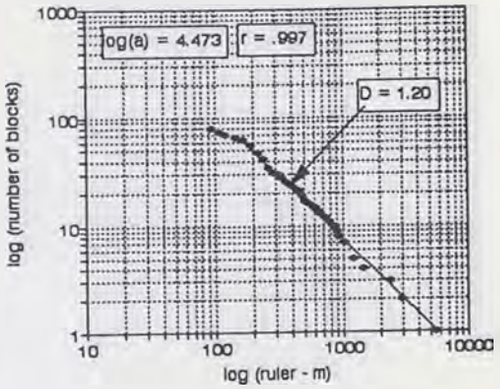

No.7 Upper Gros Ventrte Landslide
2nd Level Blocks Ruler - Width

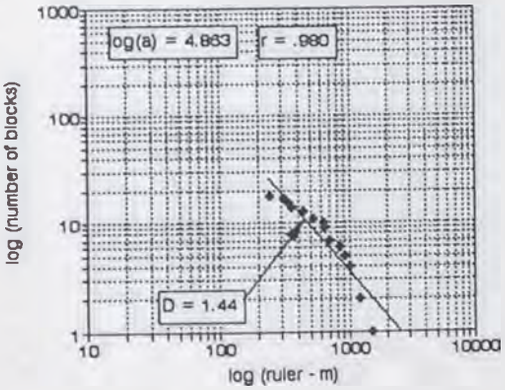

No.7 Upper Gros Ventre Landslide
2nd Level Blocks Ruler - Length

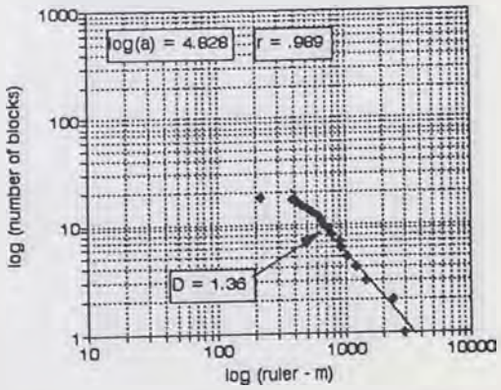

No.7 Upper Gros Ventre Landslide
3rd Level Blocks Ruler - Width

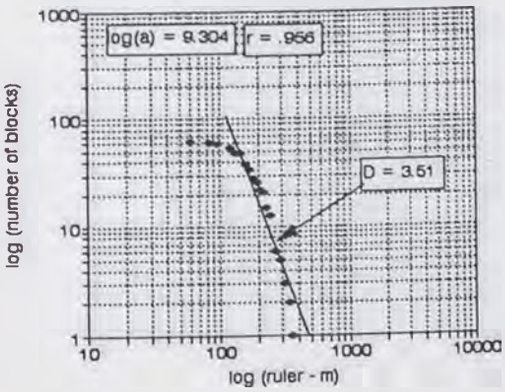

No.7 Upper Gros Ventre Landslide
3rd Level Blocks Ruler - Length

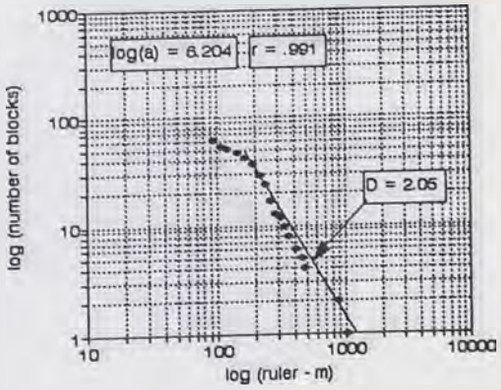

No.8 Meadow Mountain Landslide
Whole Blocks Ruler - Width

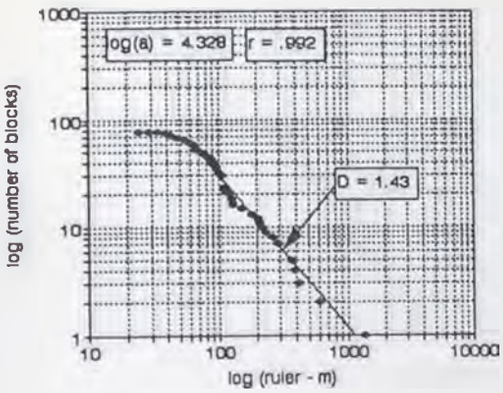

No.8 Meadow Mountain Landslide
Whole Blocks Ruler - Length

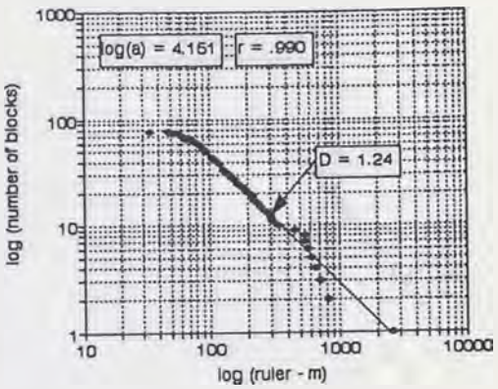

No.8 Meadow Mountain Landslide
2nd Level Blocks Ruler - Width

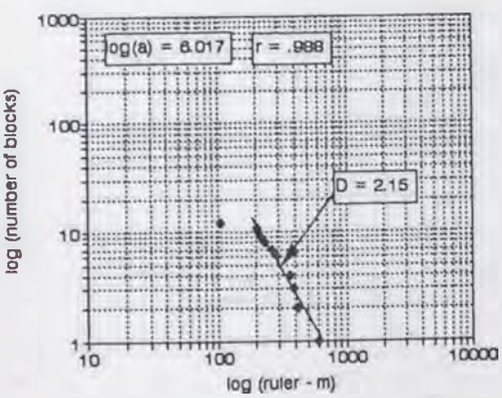

No.8 Meadow Mountain Landslide
2nd Level Blocks Ruler - Length

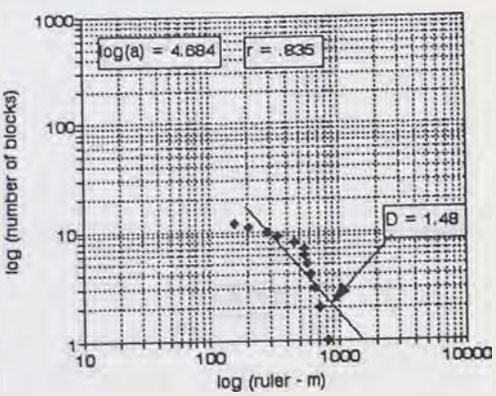

No.8 Meadow Mountain Landslide
3rd Level Blocks Ruler - Width

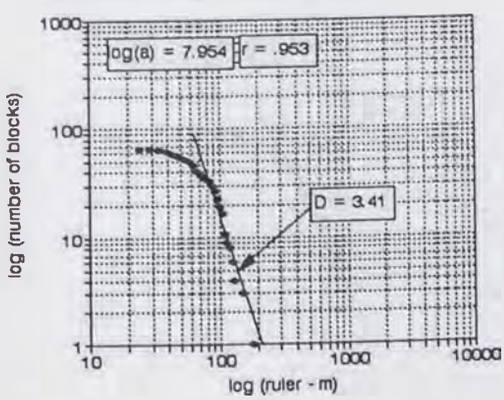

No.8 Meadow Mountain Landslide
3rd Level Blocks Ruler - Length

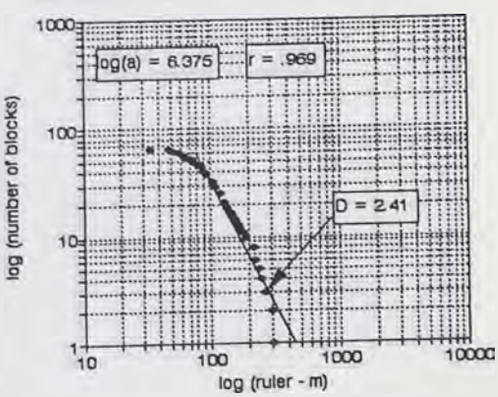

No.9 Mayunmarca Landslide
Whole Blocks Ruler - Width

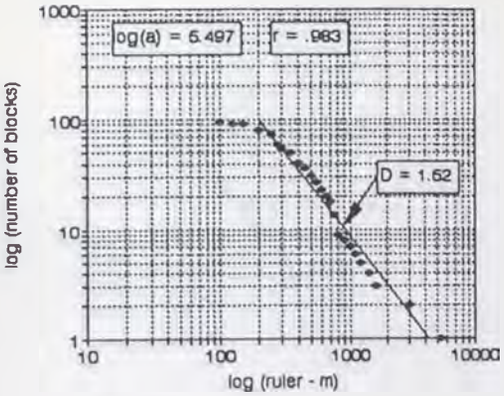

No.9 Mayunmarca Landslide
Whole Blocks Ruler - Length

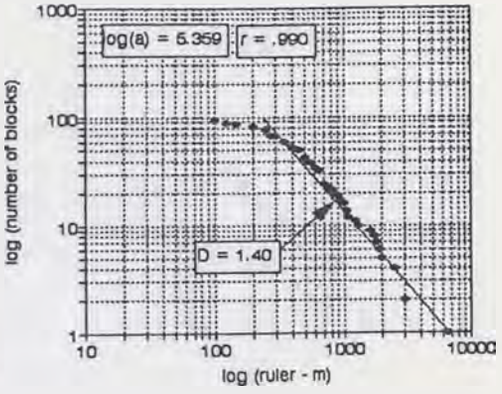

No.9 Mayunmarca Landslide
2nd Level Blocks Ruler - Width

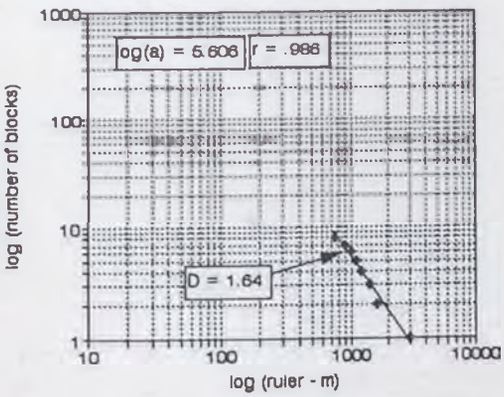

No.9 Mayunmarca Landslide
2nd Level Blocks Ruler - Length

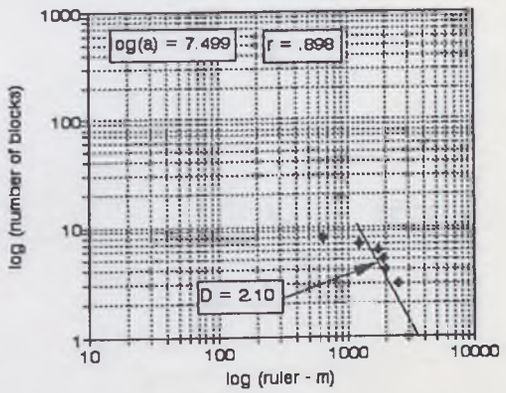

No.9 Mayunmarca Landslide
3rd Level Blocks Ruler - Width

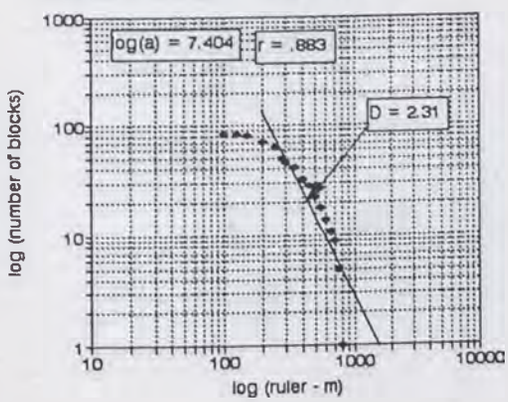

No.9 Mayunmarca Landslide
3rd Level Blocks Ruler - Length

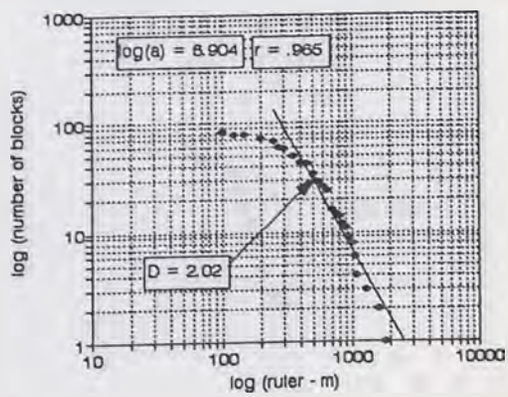

No.10 La Frasse Landslide
Whole Blocks Ruler - Width

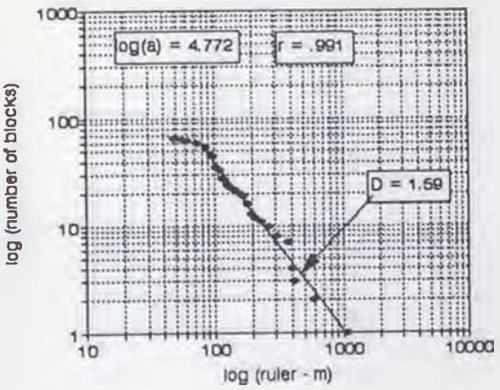

No.10 La Frasse Landslide
Whole Blocks Ruler - Length

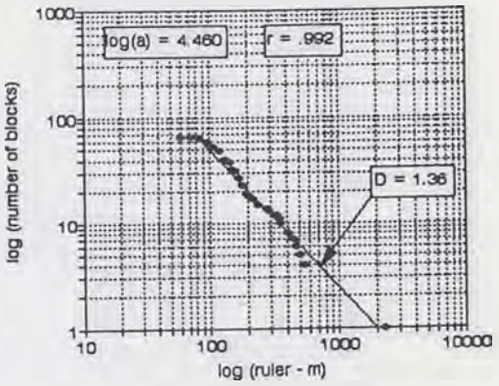

No.10 La Frasse Landslide
2nd Level Blocks Ruler - Width

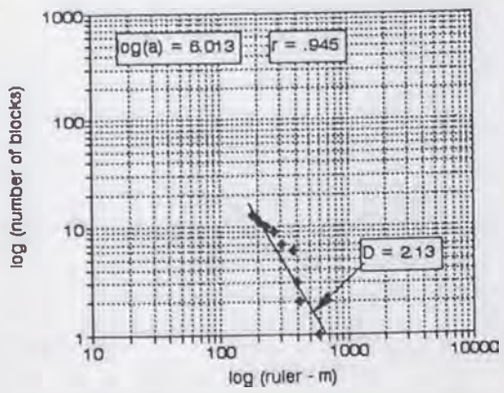

No.10 La Frasse Landslide
2nd Level Blocks Ruler - Length

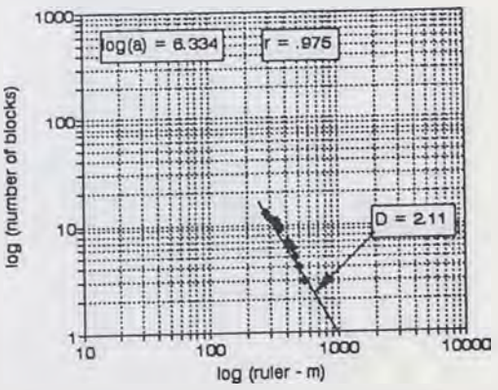

No.10 La Frasse Landslide
3nd Level Blocks Ruler - Width

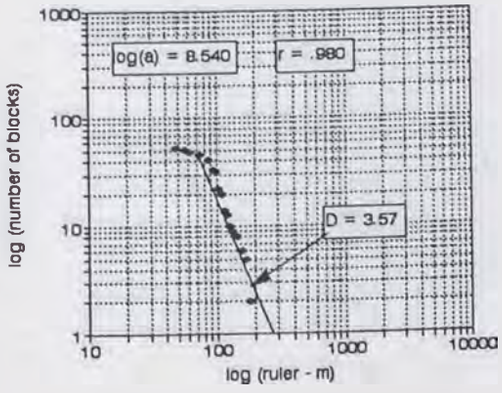

La Frasse Landslide
3nd level blocks ruler - length

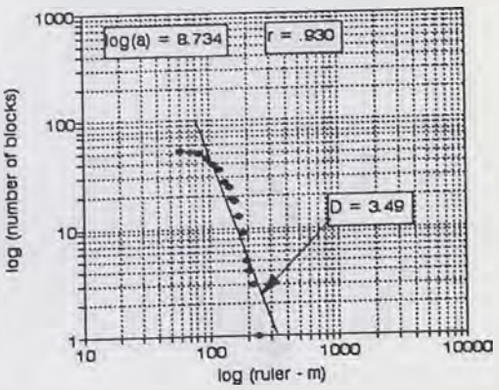

No.11 Arveys Landslide
Whole Blocks Ruler - Width

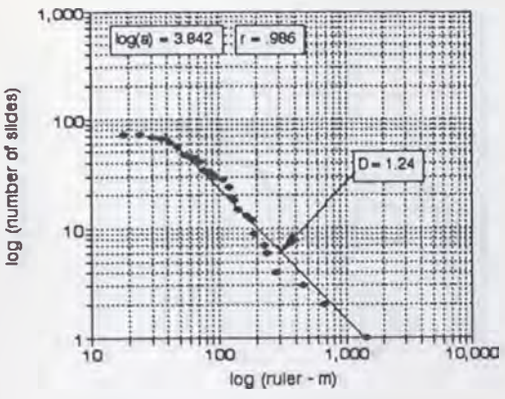

No.11 Arveys Landslide
Whole Blocks Ruler - Length

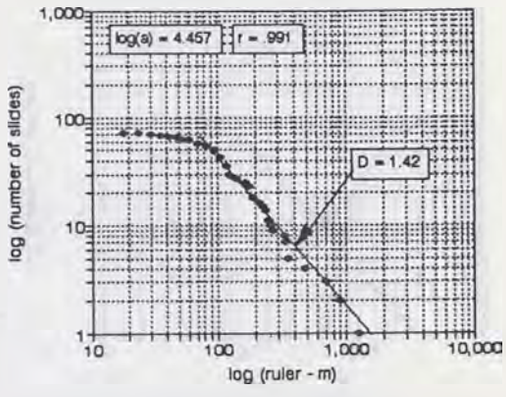

No.11 Arveys Landslide
2nd Level Blocks Ruler - Width

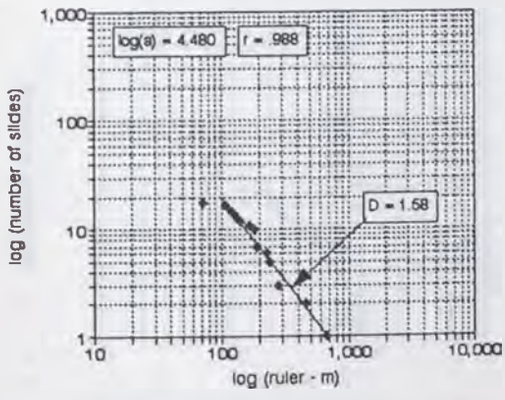

No.11 Arveys Landslide
2nd Level Blocks Ruler - Length

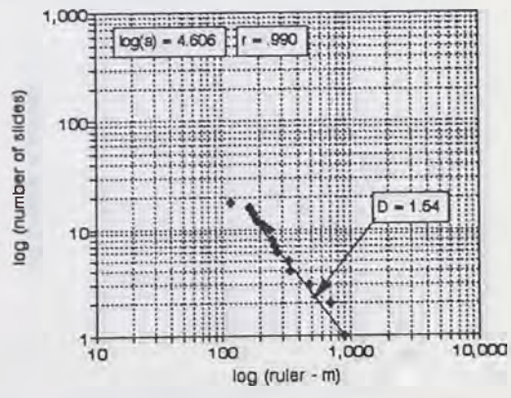

No.11 Arveys Landslide
3rd Level Blocks Ruler - Width

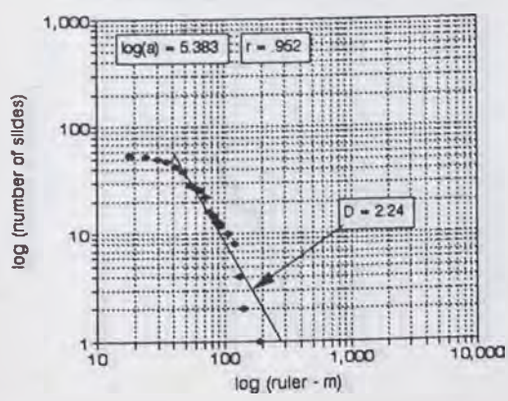

No.11 Arveys Landslide
3rd Level Blocks Ruler - Length

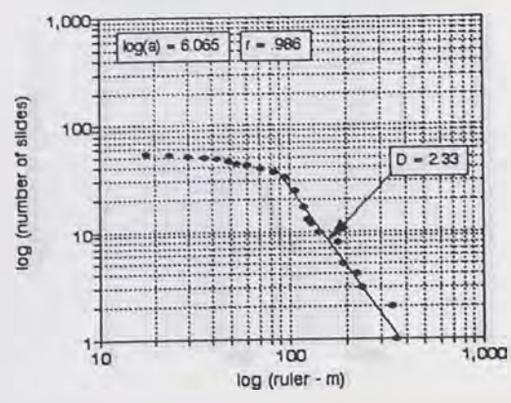

No.12 Kiritani Landslide
Whole Blocks Ruler - Width

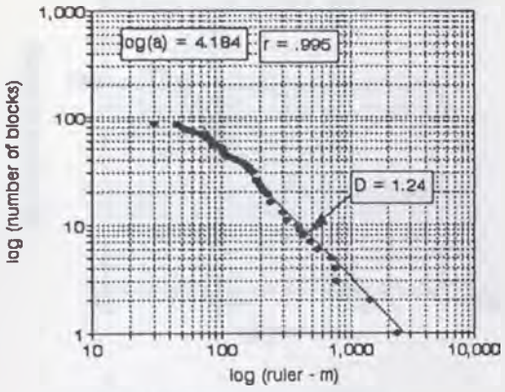

No.12 Kiritani Landslide
Whole Blocks Ruler - Length

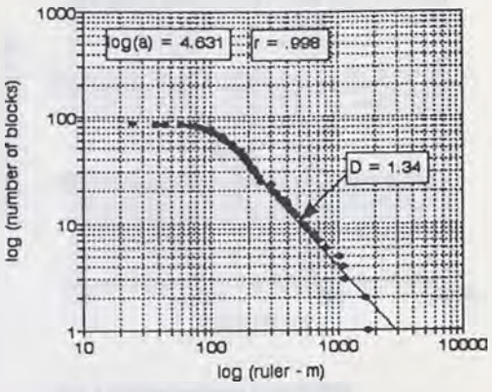

No.12 Kiritani Landslide
2nd Level Blocks Ruler - Width

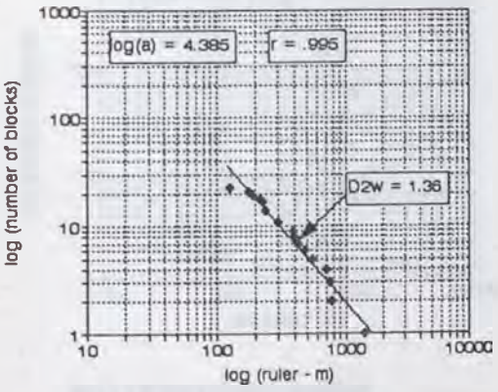

No.12 Kiritani Landslide
2nd Level Blocks Ruler - Length

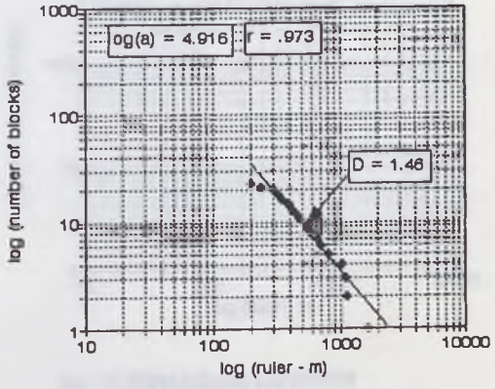

No.12 Kiritani Landslide
3rd Level Blocks Ruler - Width

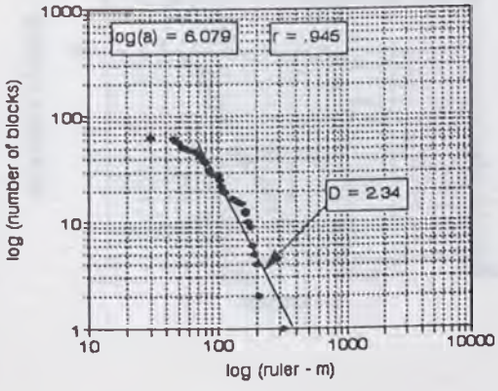

Kiritani Landslide
3rd Level Blocks Ruler - Length

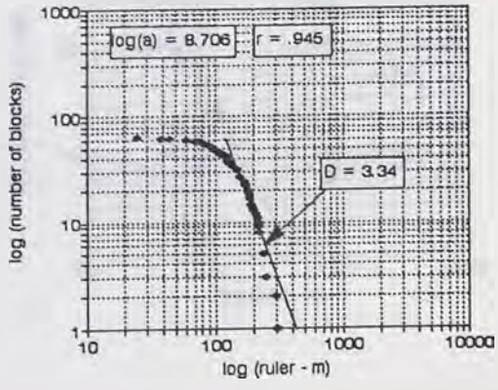

No.13 Katsurabara Landslide
Whole Blocks Ruler - Width

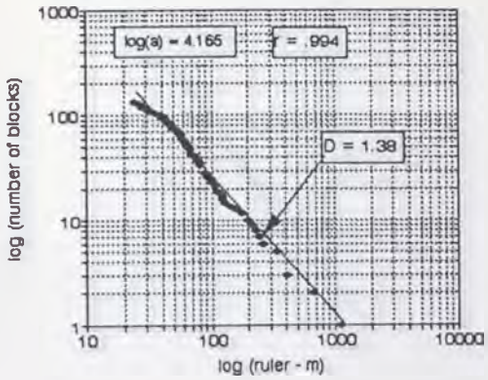

No.13 Katsurabara Landslide
Whole Blocks Ruler - Length

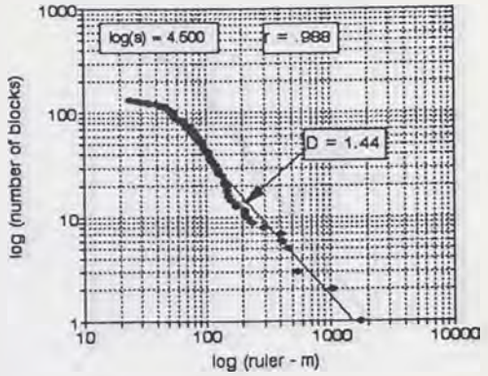

No.13 Katsurabara Landslide
2nd Level Blocks Ruler - Width

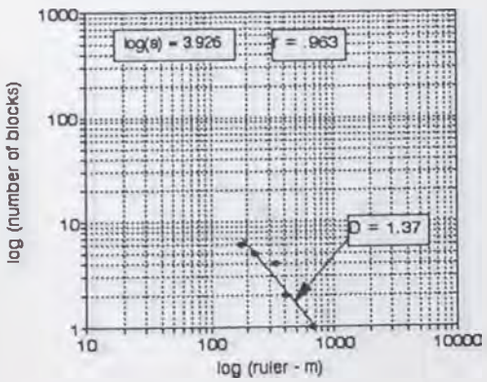

No.13 Katsurabara Landslide
2nd Level Blocks Ruler - Length

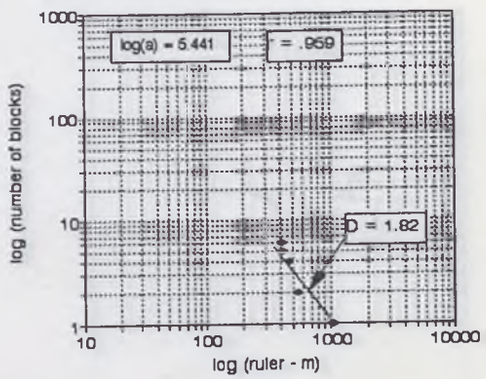

No.13 Katsurabara Landslide
3rd Level Blocks Ruler - Width

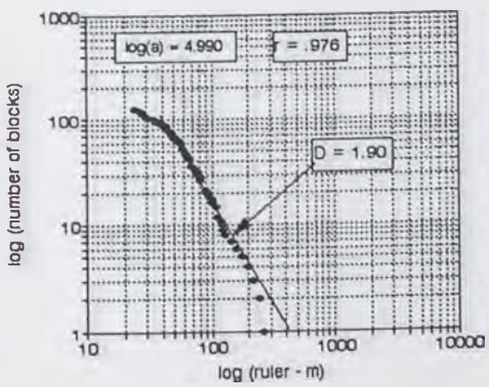

No.13 Katsurabara Landslide
3rd Level Blocks Ruler - Length

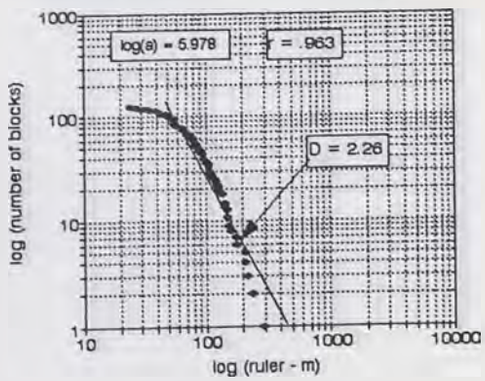

No.14 Hitohane Landslide
Whole Blocks Ruler - Width

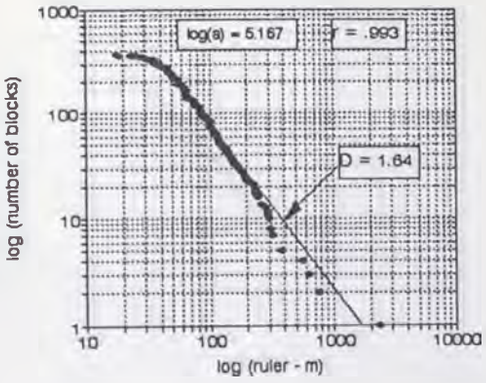

No.14 Hitohane Landslide
Whole Blocks Ruler - Length

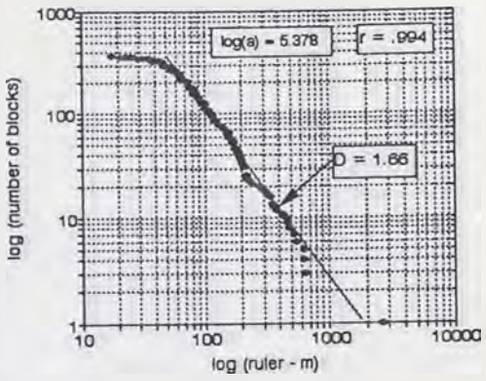

Hitohane Landslide
2nd Level Blocks Ruler - Width

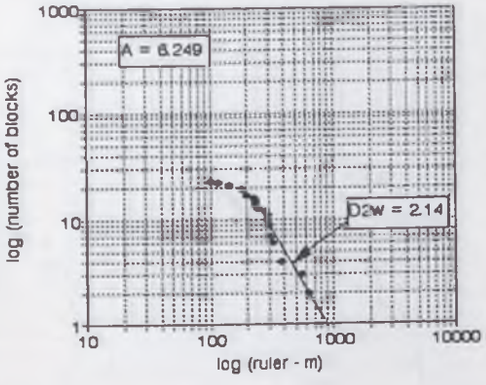

Hitohane Landslide
2nd Level Blocks Ruler - Length

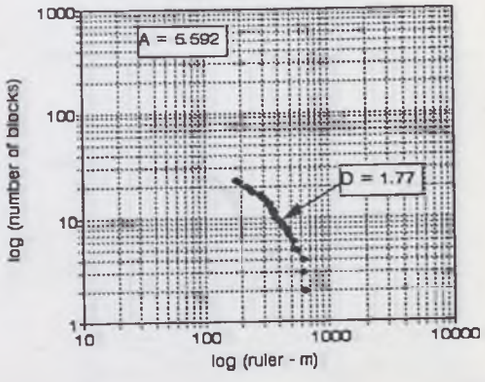

No.14 Hitohane Landslide
3rd Level Blocks Ruler - Width

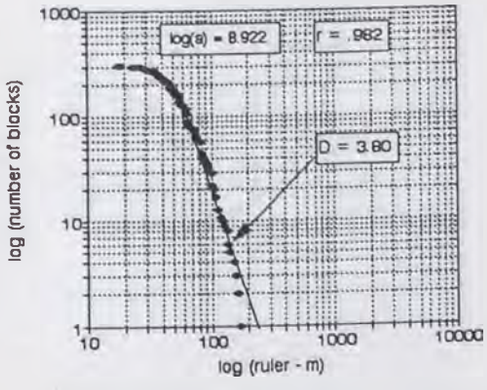

Hitohane Landslide
3rd Level Blocks Ruler - Length

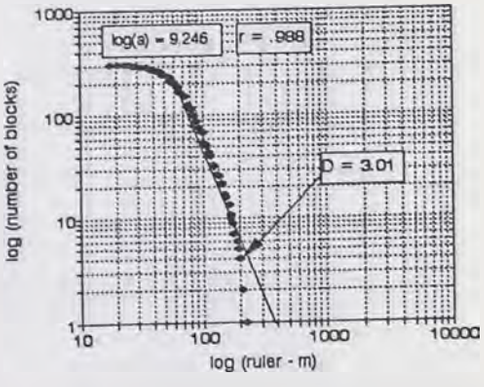

No.15 Takisaka Landslide
Whole Blocks Ruler - Width

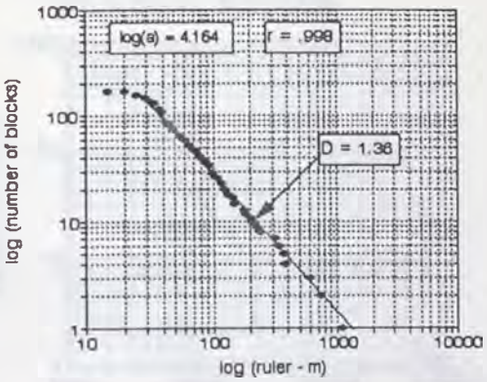

No.15 Takisaka Landslide
Whole Blocks Ruler - Length

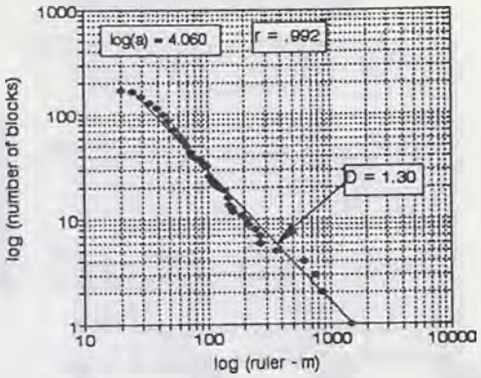

No.15 Takisaka Landslide
2nd Level Blocks Ruler - Width

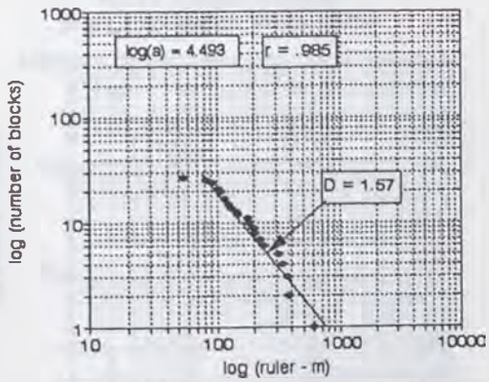

No.15 Takisaka Landslide
2nd Level Blocks Ruler - Length

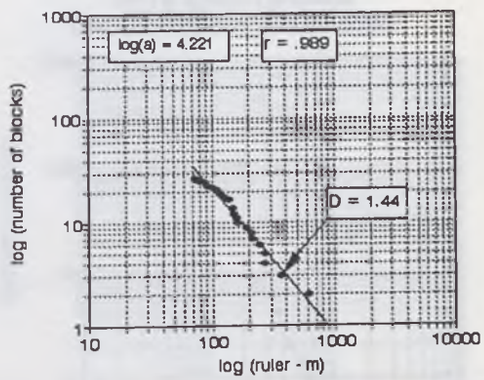

Takisaka Landslide
3rd Level Blocks Ruler - Width

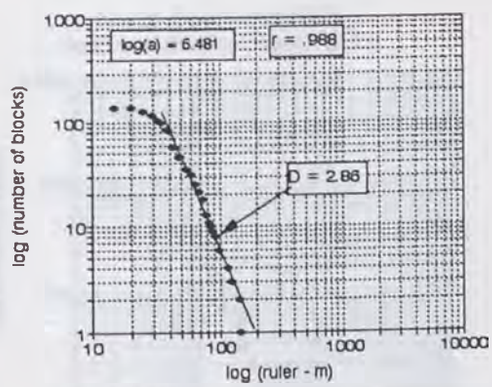

Takisaka Landslide
3rd Level Blocks Ruler - Length

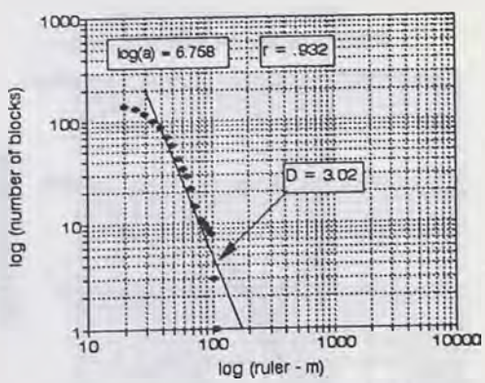

No.16 Sakae Landslide
Whole Blocks Ruler-Width

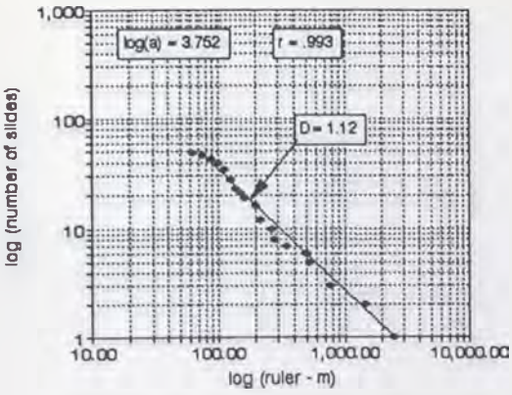

No.16 Sakae Landslide
Whole Blocks Ruler-Length

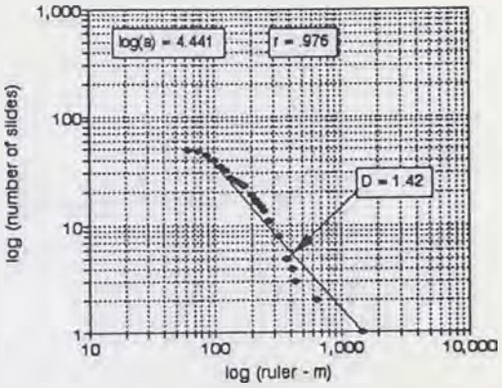

No.16 Sakae Landslide
2nd Level Blocks Ruler-Width

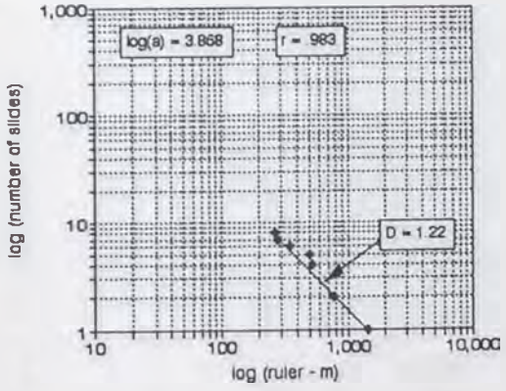

No.16 Sakae Landslide
2nd Level Blocks Ruler-Length

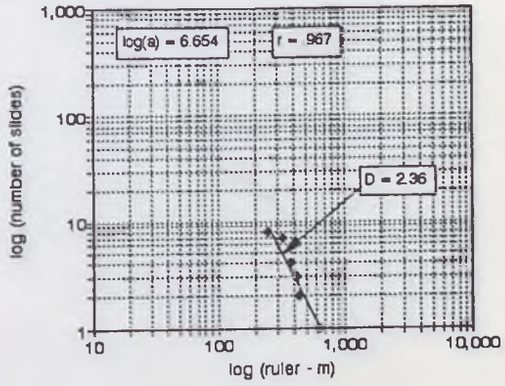

No.16 Sakae Landslide
3rd Level Blocks Ruler-Width

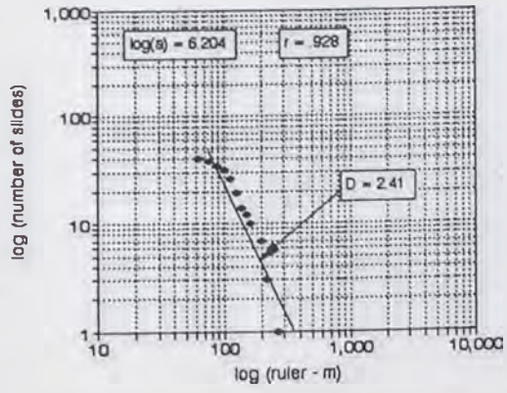

No.16 Sakae Landslide
3rd Level Blocks Ruler-Length

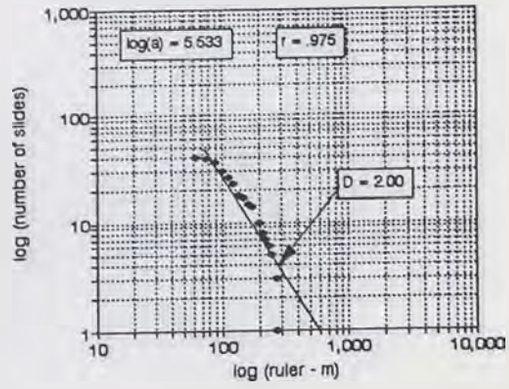

No.17 Mushigame Landslide
Whole Blocks Ruler-Width

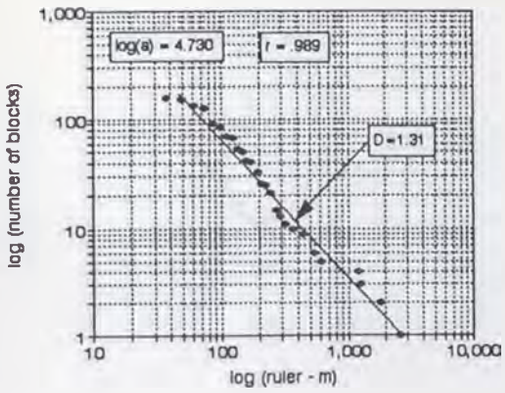

No.17 Mushigame Landslide
Whole Blocks Ruler-Length

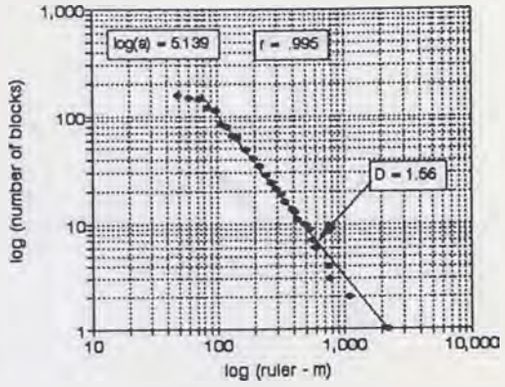

No.17 Mushigame Landslide
2nd Level Blocks Ruler-Width

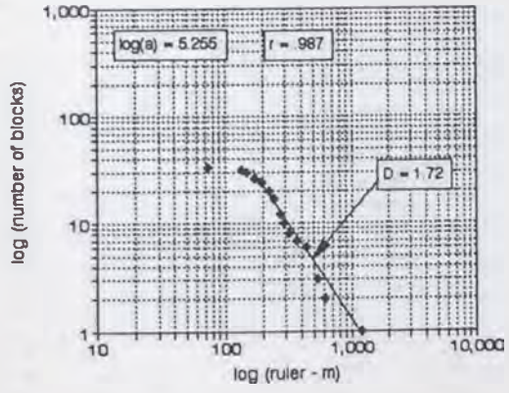

No.17 Mushigame Landslide
2nd Level Blocks Ruler-Length

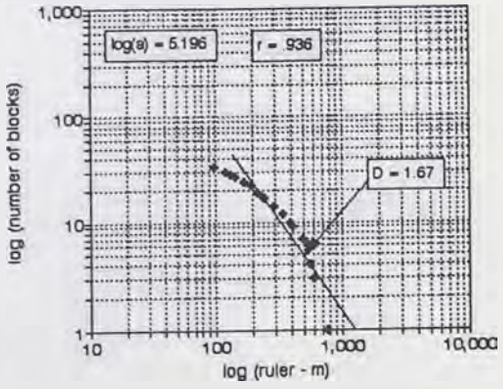

No.17 Mushigame Landslide
3rd Level Blocks Ruler-Width

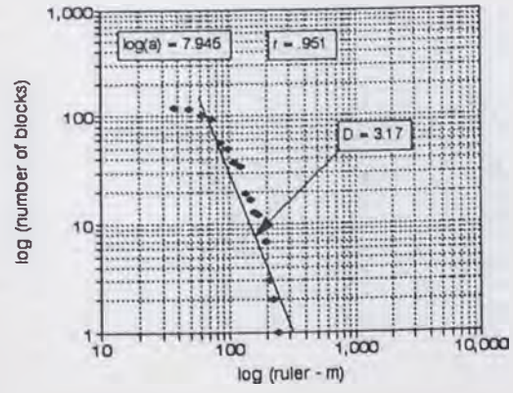

No.17 Mushigame Landslide
3rd Level Blocks Ruler-Length

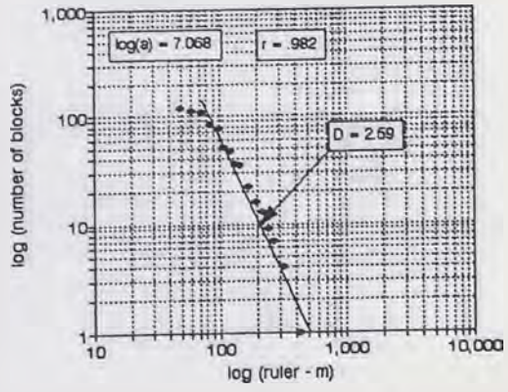

No.18 Higashinomyo Landslide
Whole Blocks Ruler - Width

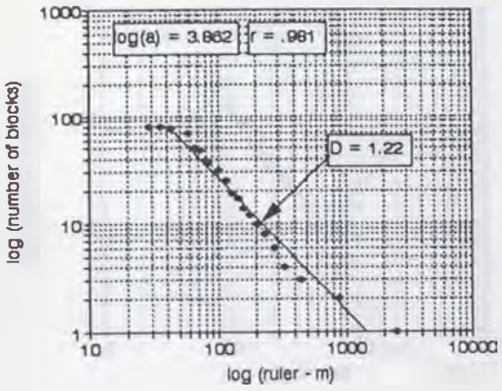

No.18 Higashinomyo Landslide
Whole Blocks Ruler - Length

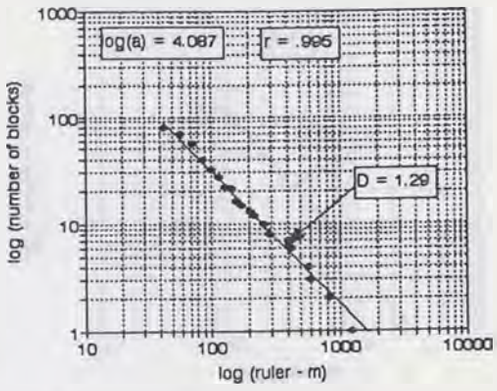

No.18 Higashinomyo Landslide
2nd Level Blocks Ruler - Width

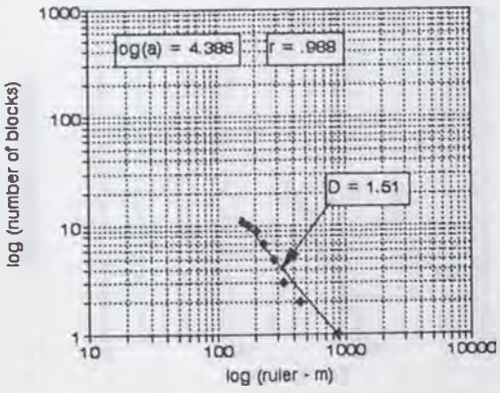

No.18 Higashinomyo Landslide
2nd Level Blocks Ruler - Length

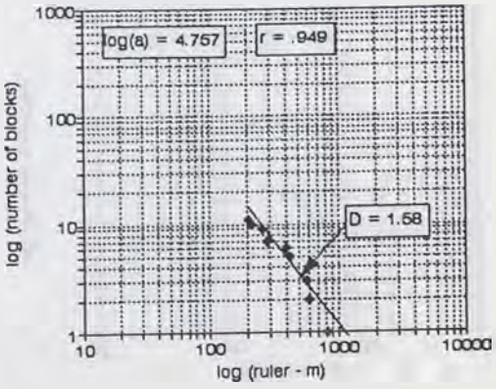

Higashinomyo Landslide
3rd Level Blocks Ruler - Width

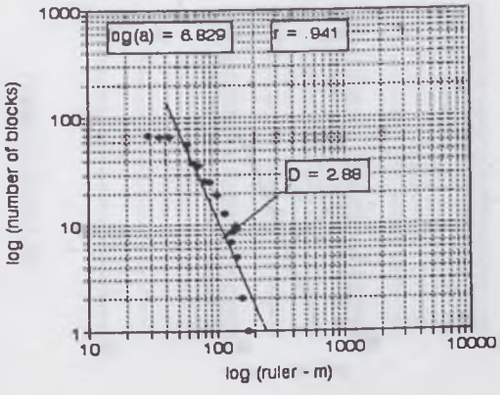

Higashinomyo Landslide
3rd Level Blocks Ruler - Length

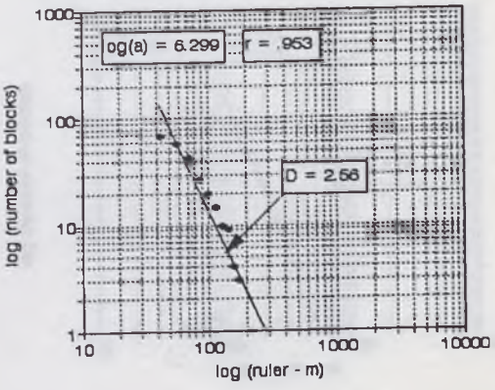

No.19 Karuizawa Landslide
Whole Blocks Ruler - Width

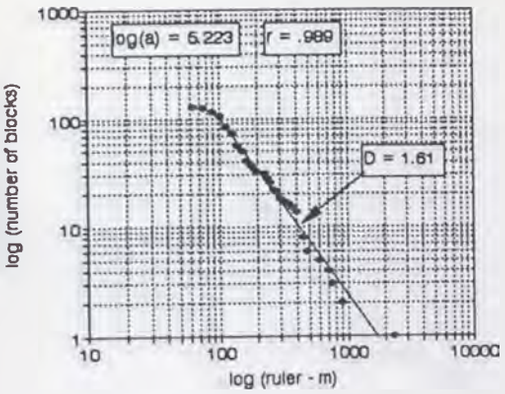

No.19 Karuizawa Landslide
Whole Blocks Ruler - Length

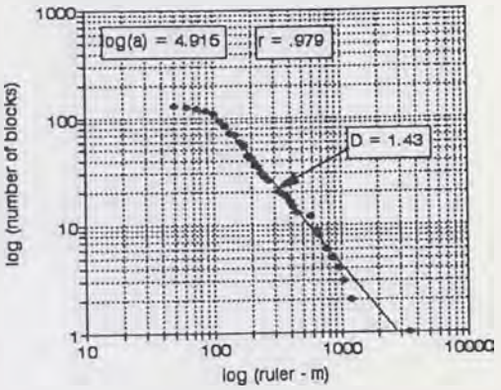

No.19 Karuizawa Landslide
2nd Level Blocks Ruler - Width

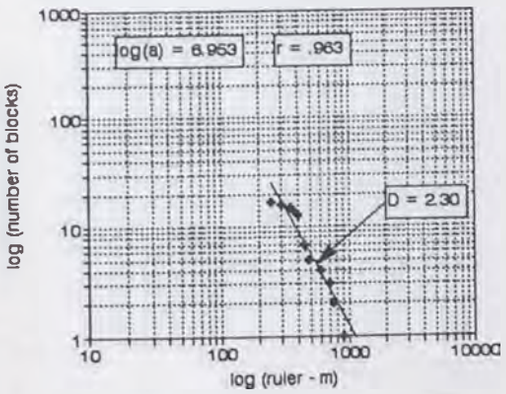

No.19 Karuizawa Landslide
2nd Level Blocks Ruler - Length

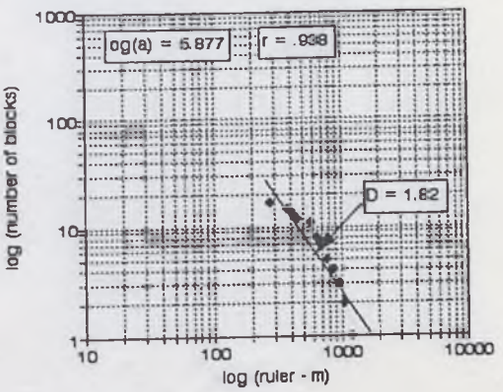

No.19 Karuizawa Landslide
3rd Level Blocks Ruler - Width

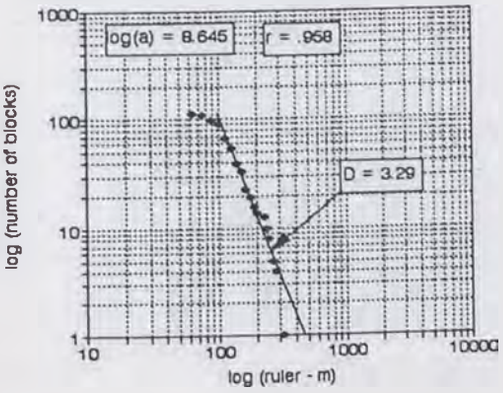

Karuizawa Landslide
3rd Level Blocks Ruler - Length

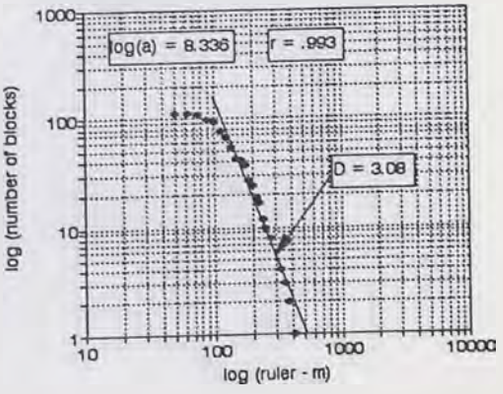

No.20 Happoudal Landslide
Whole Blocks Ruler - Width

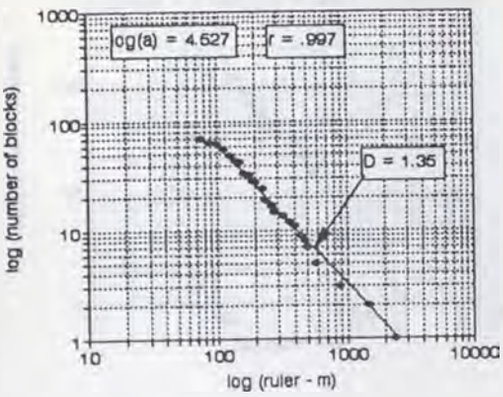

No.20 Happoudal Landslide
Whole Blocks Ruler - Length

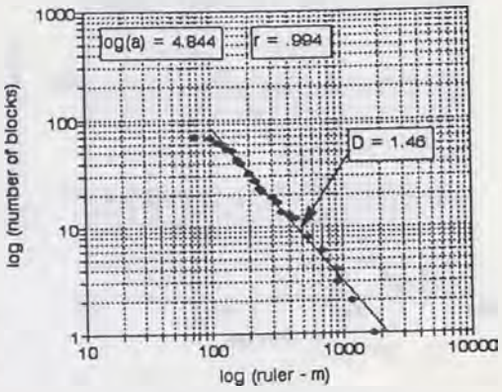

No.20 Happoudal Landslide
2nd Level Blocks Ruler - Width

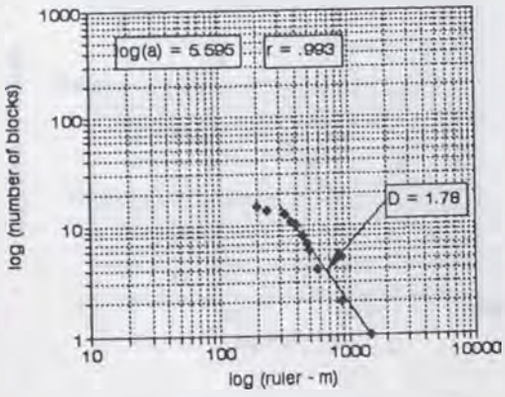

No.20 Happoudal Landslide
2nd Level Blocks Ruler - Length

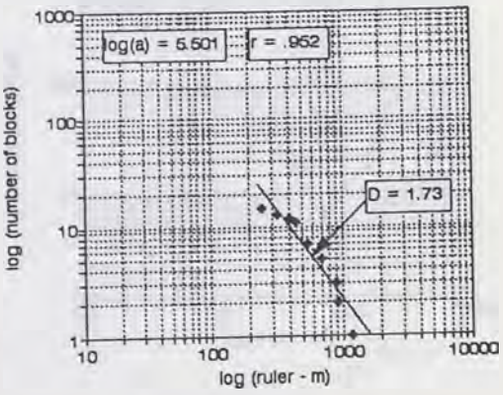

No.20 Happoudal Landslide
3rd Level Blocks Ruler - Width

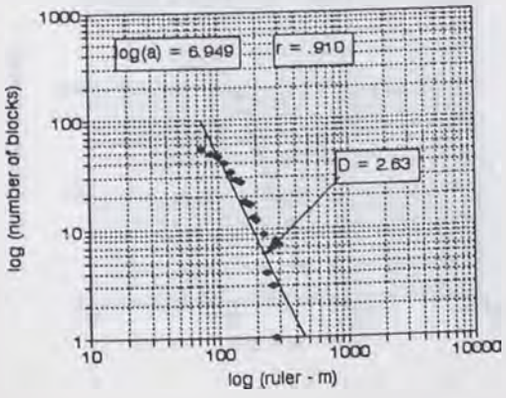

Happoudal Landslide
3rd Level Blocks Ruler - Length

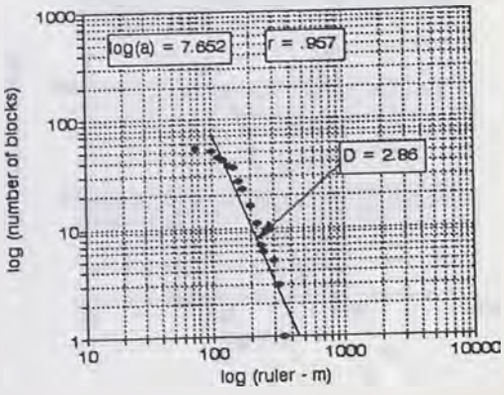

No.21 Ralden Landslide
Whole Blocks Ruler - Width

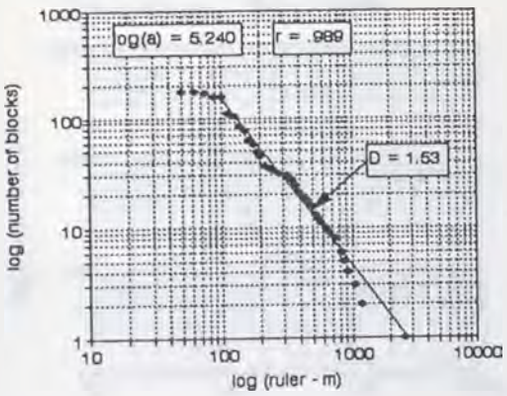

No.21 Ralden Landslide
Whole Blocks Ruler - Length

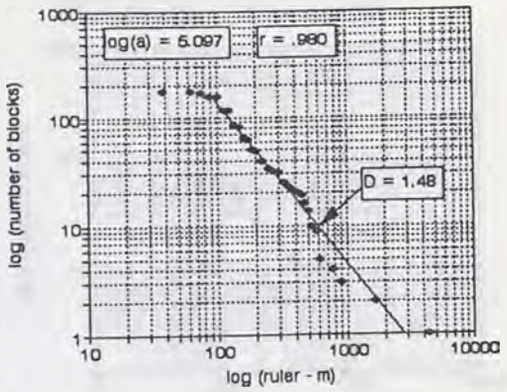

No.21 Ralden Landslide
2nd Level Blocks Ruler - Width

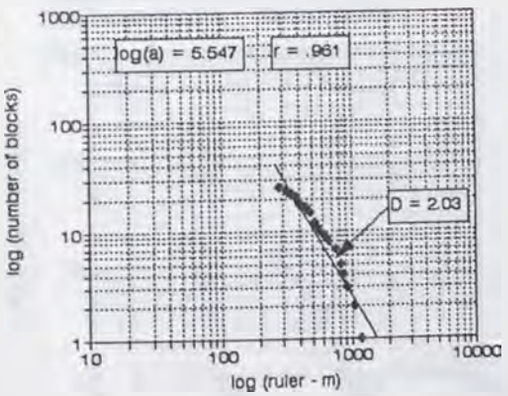

No.21 Ralden Landslide
2nd Level Blocks Ruler - Length

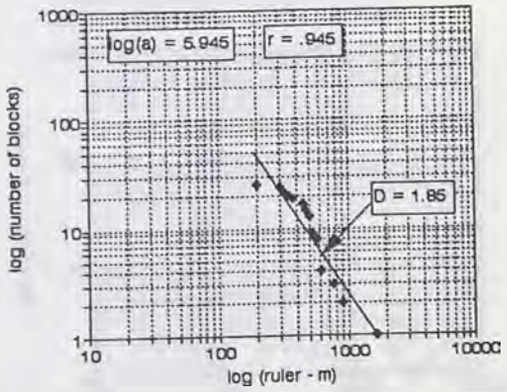

No.21 Ralden Landslide
3rd mLevel Blocks Ruler - Width

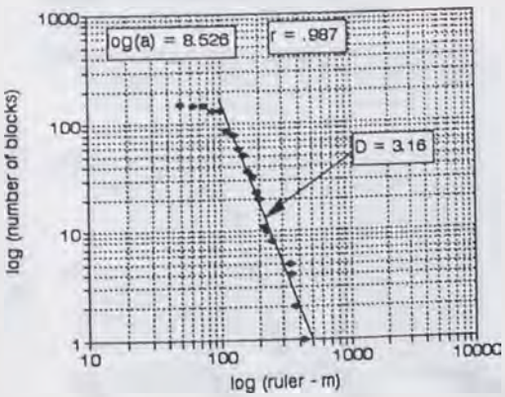

Ralden Landslide
3rd Level Blocks Ruler - Length

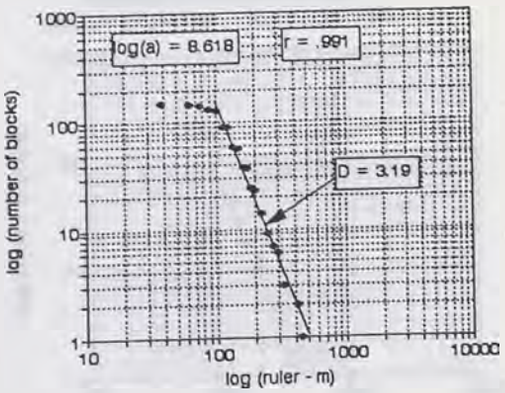

No.22 Nishinakanoho Landslide
Whole Blocks Ruler - Width

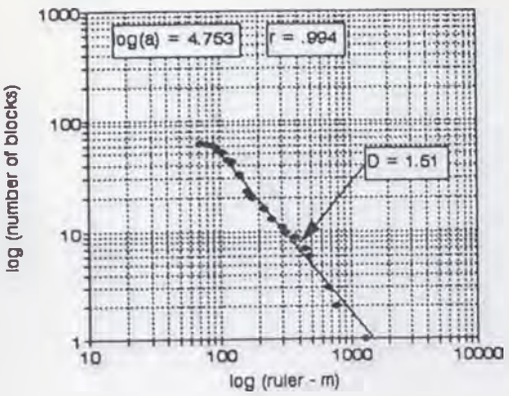

No.22 Nishinakanoho Landslide
Whole Blocks Ruler - Length

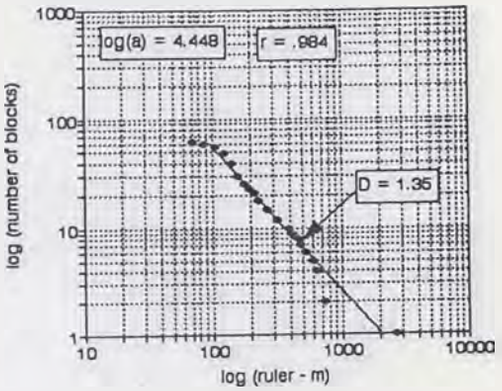

No.22 Nishinakanoho Landslide
2nd Level Blocks Ruler - Width

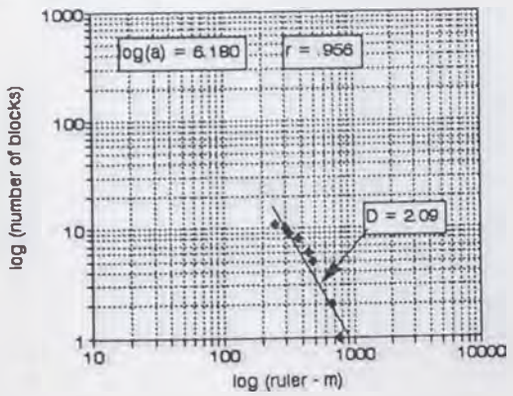

No.22 Nishinakanoho Landslide
2nd Level Blocks Ruler - Length

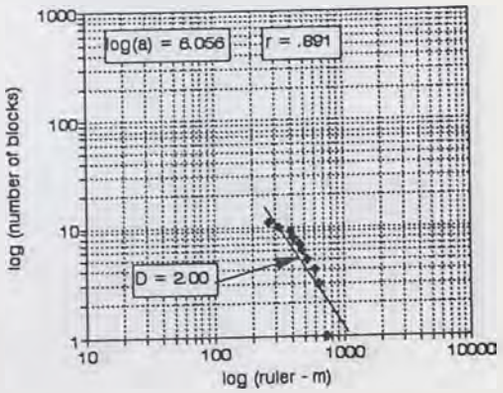

No.22 Nishinakanoho Landslide
3rd mLevel Blocks Ruler - Width

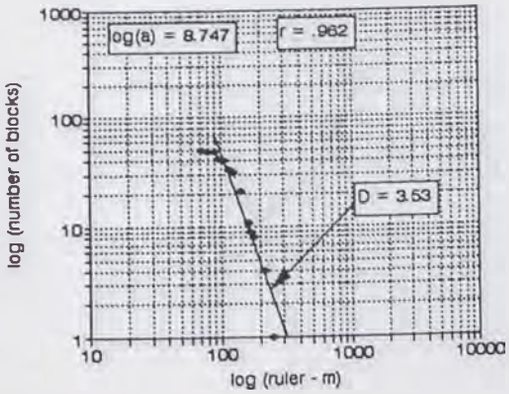

Nishinakanoho Landslide
3rd Level Blocks Ruler - Length

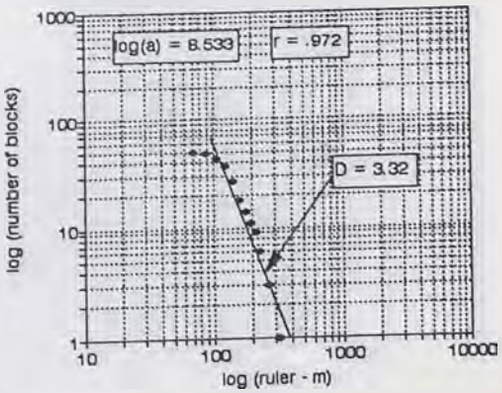

No.23 Mizunashi Landslide
Whole Blocks Ruler - Width

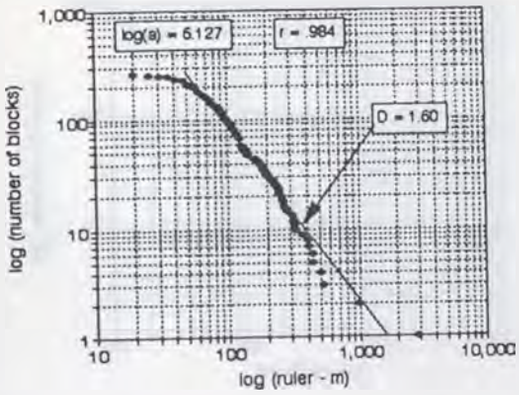

No.23 Mizugame Landslide
Whole Blocks Ruler - Length

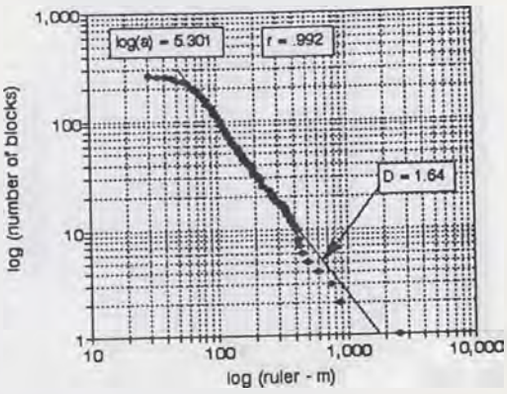

No.23 Mizunashi Landslide
2nd Level Blocks Ruler - Width

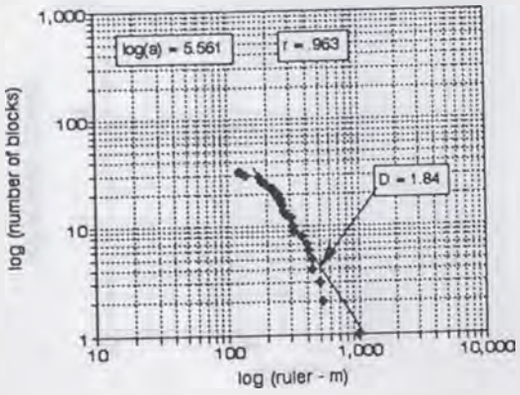

No.23 Mizunashi Landslide
2nd Level Blocks Ruler - Length

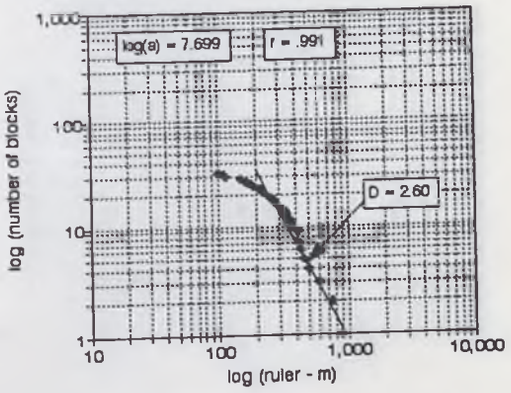

No.23 Mizunashi Landslide
3rd Level Blocks Ruler - Width

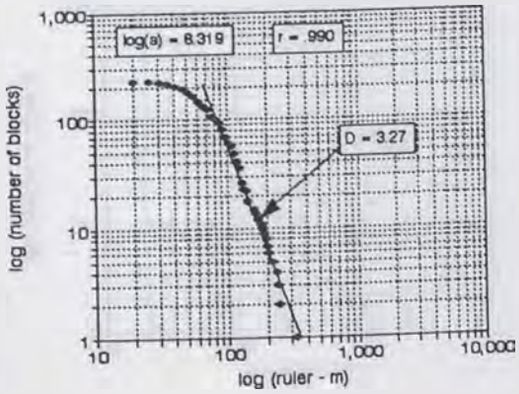

No.23 Mizunashi Landslide
3rd Level Blocks Ruler - Length

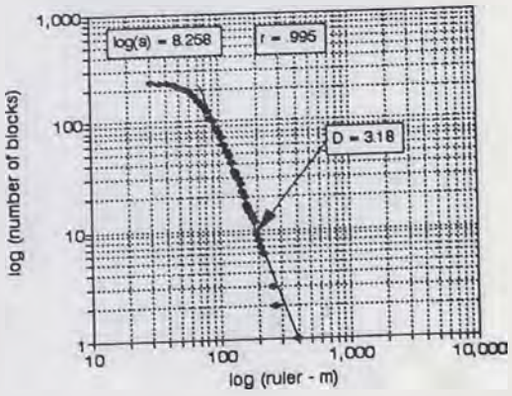

No.24 Kitaurata Landslide
Whole Blocks Ruler - Width

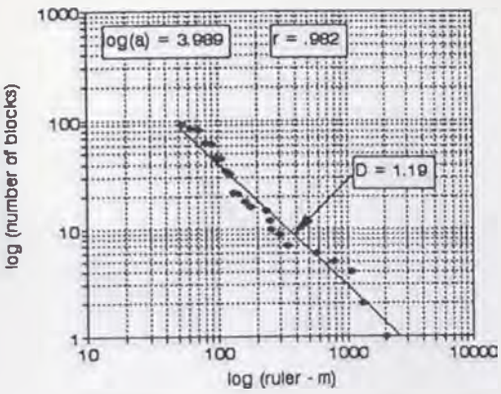

No.24 Kitaurata Landslide
Whole Blocks Ruler - Length

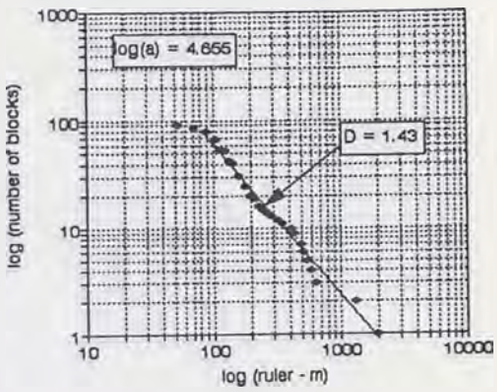

No.24 Kitaurata Landslide
2nd Level Blocks Ruler - Width

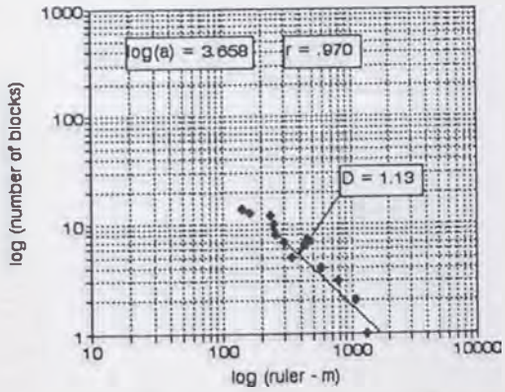

No.24 Kitaurata Landslide
2nd Level Blocks Ruler - Length

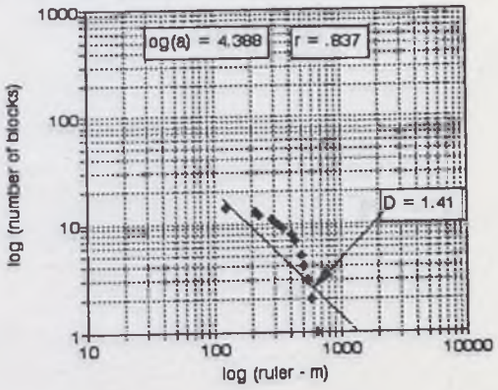

No.24 Kitaurata Landslide
3rd Level Blocks Ruler - Width

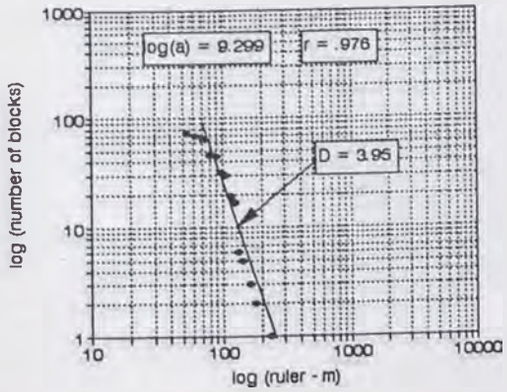

Kitaurata Landslide
3rd Level Blocks Ruler - Length

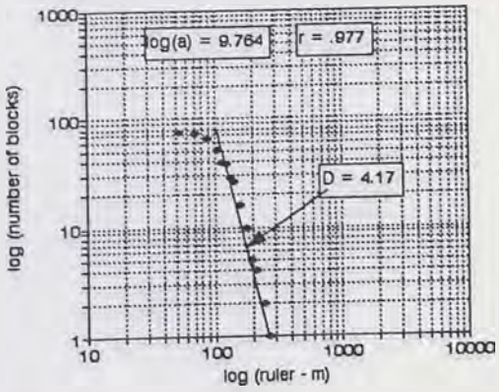

No.25 Uenoyama Landslide
Whole Blocks Ruler - Width

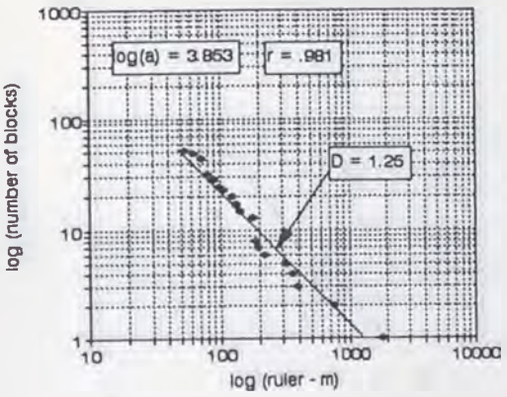

No.25 Uenoyama Landslide
Whole Blocks Ruler - Length

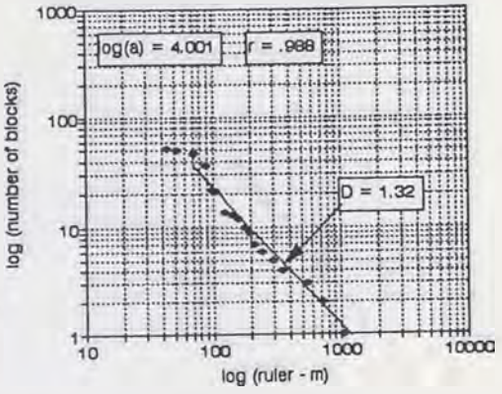

No.25 Uenoyama Landslide
2nd Level Blocks Ruler - Width

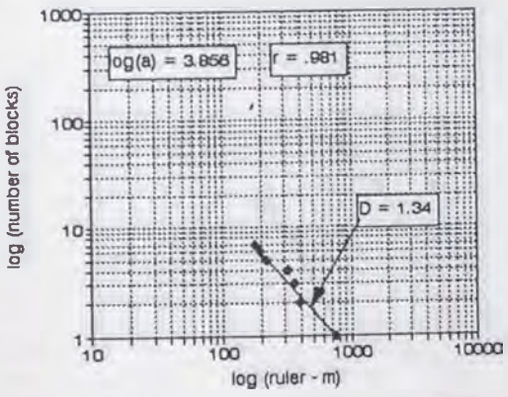

No.25 Uenoyama Landslide
2nd Level Blocks Ruler - Length

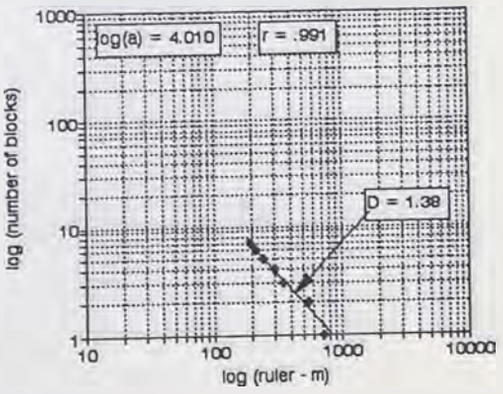

No.25 Uenoyama Landslide
3rd Level Blocks Ruler - Width

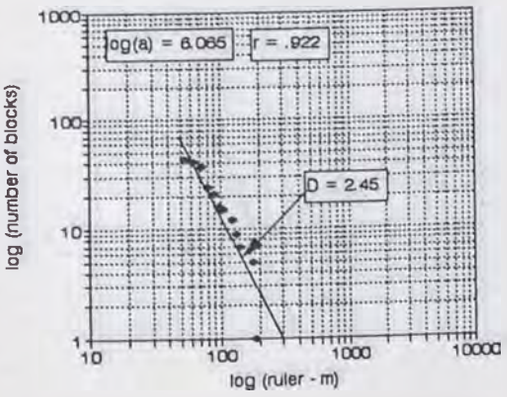

Uenoyama Landslide
3rd Level Blocks Ruler - Length

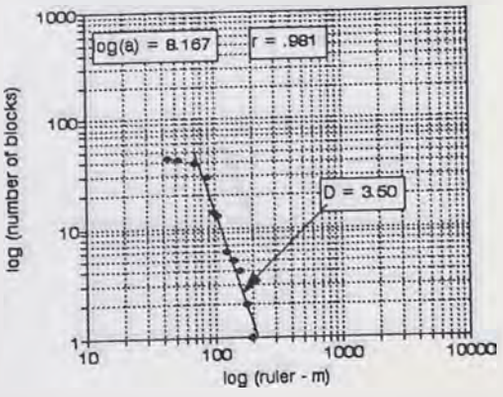

No.26 Nakatateyama Landslide
Whole Blocks Ruler - Width

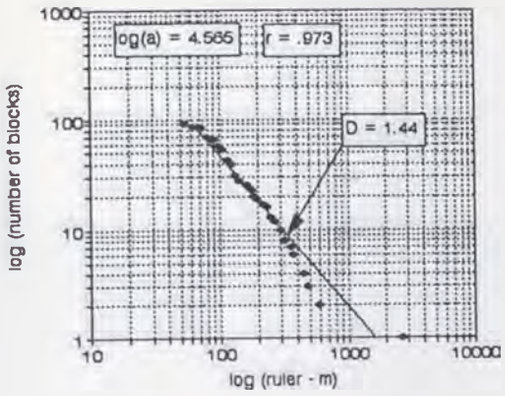

No.26 Nakatateyama Landslide
Whole Blocks Ruler - Length

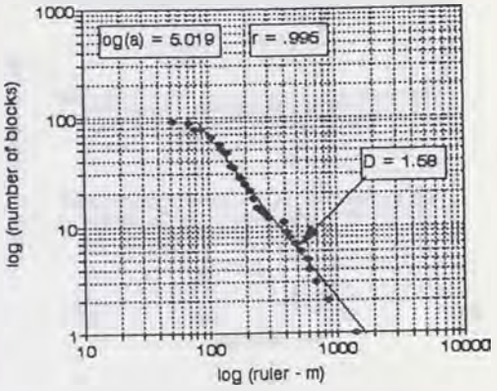

No.26 Nakatateyama Landslide
2nd Level Blocks Ruler - Width

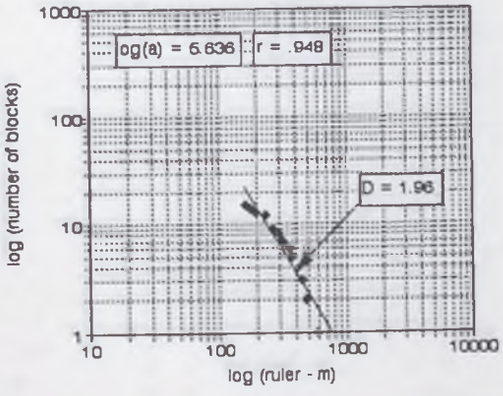

No.26 Nakatateyama Landslide
2nd Level Blocks Ruler - Length

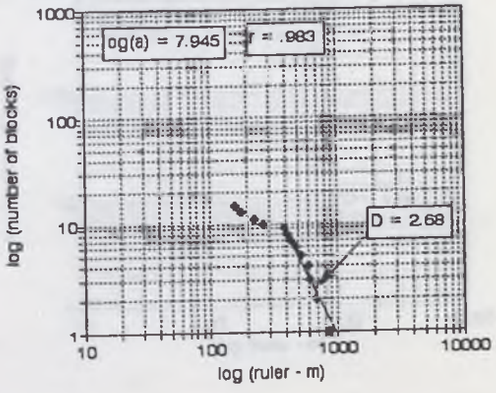

No.26 Nakatateyama Landslide
3rd Level Blocks Ruler - Width

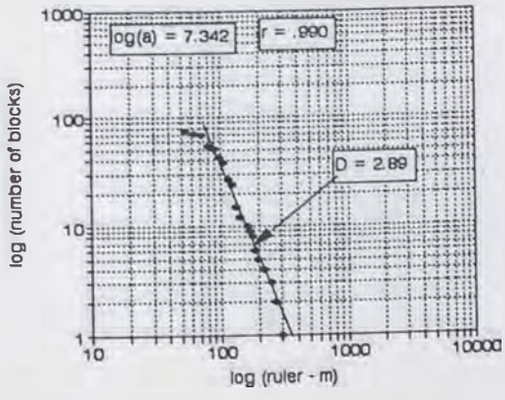

Nakatateyama Landslide
3rd Level Blocks Ruler - Length

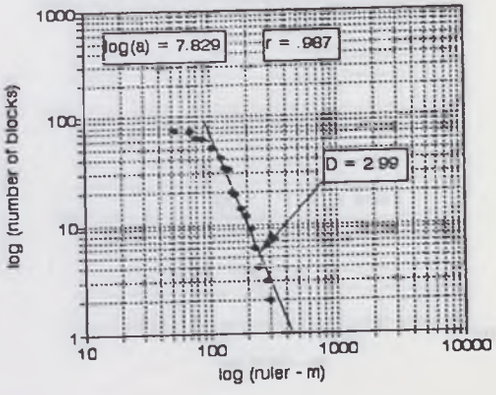

No.27 Yumoto Landslide
Whole Blocks Ruler - Width

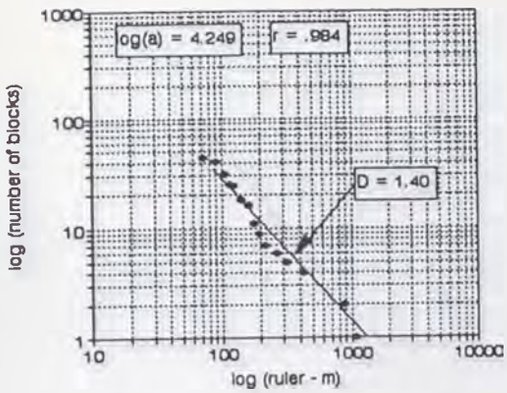

No.27 Yumoto Landslide
Whole Blocks Ruler - Length

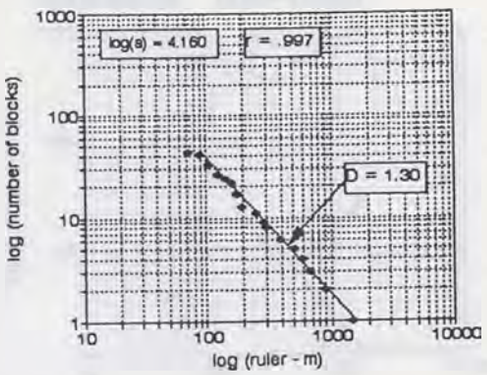

No.27 Yumoto Landslide
2nd Level Blocks Ruler - Width

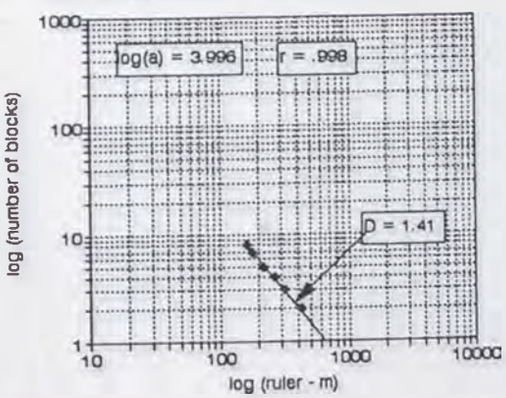

No.27 Yumoto Landslide
2nd Level Blocks Ruler - Length

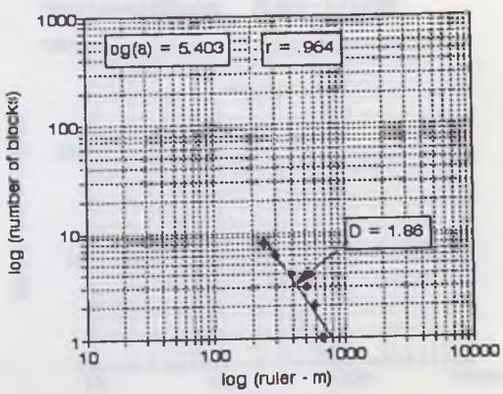

No.27 Yumoto Landslide
3rd mLevel Blocks Ruler - Width

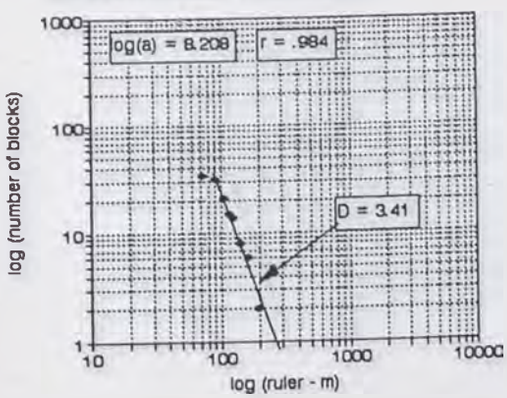

Yumoto Landslide
3rd Level Blocks Ruler - Length

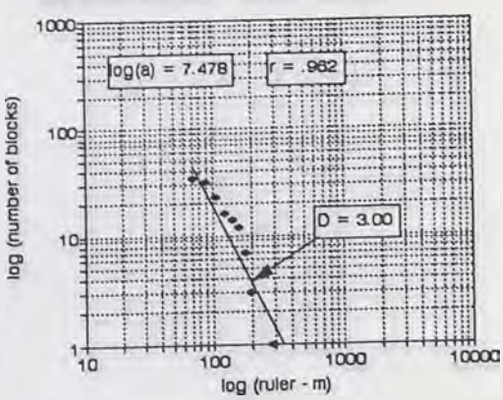

No.28 Yuyama Landslide
Whole Blocks Ruler - Width

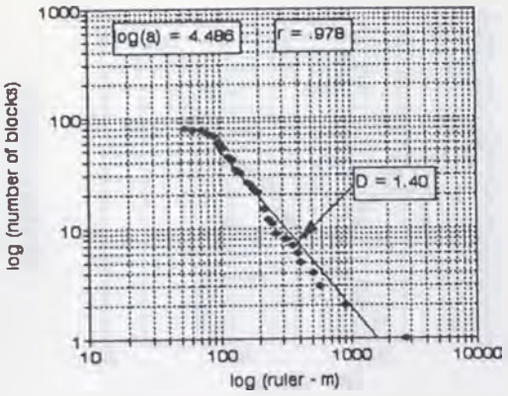

No.28 Yuyama Landslide
Whole Blocks Ruler - Length

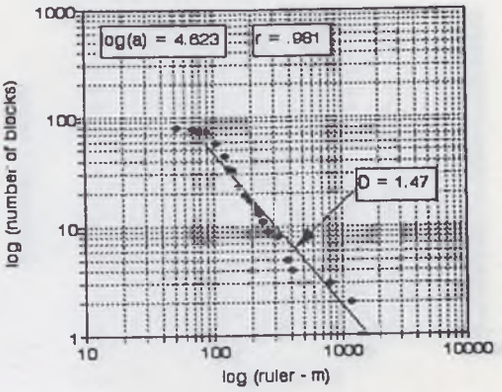

No.28 Yuyama Landslide
2nd Level Blocks Ruler - Width

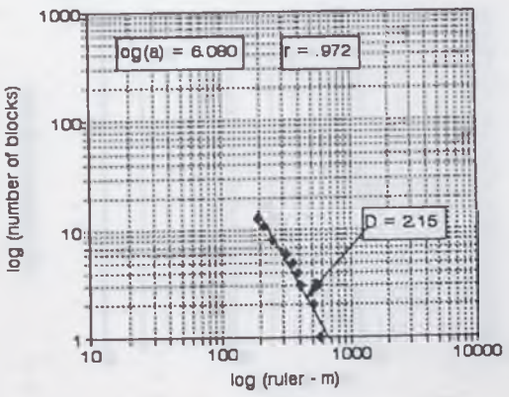

No.28 Yuyama Landslide
2nd Level Blocks Ruler - Length

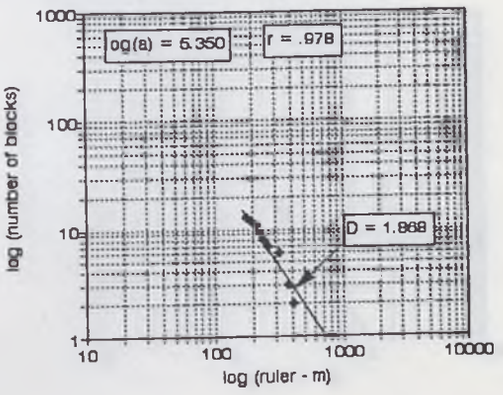

No.28 Yuyama Landslide
3rd Level Blocks Ruler - Width

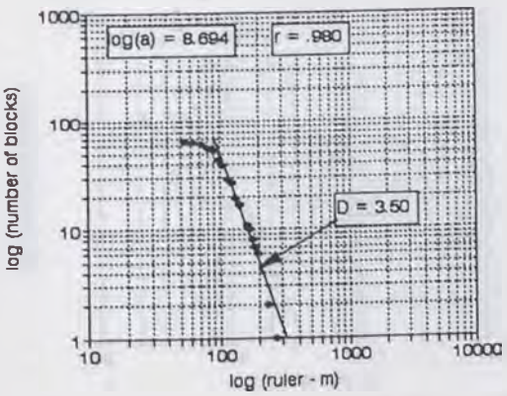

No.28 Yuyama Landslide
3rd Level Blocks Ruler - Length

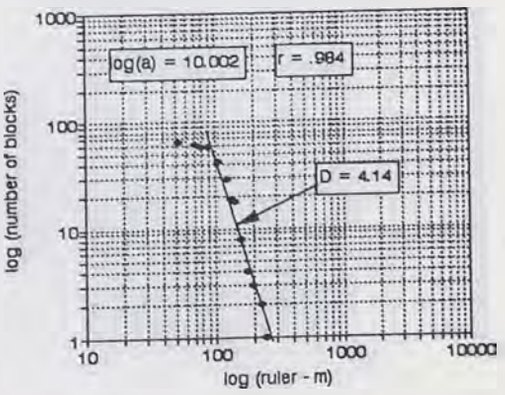

No.29 Kamatsuka Landslide
Whole Blocks Ruler - Width

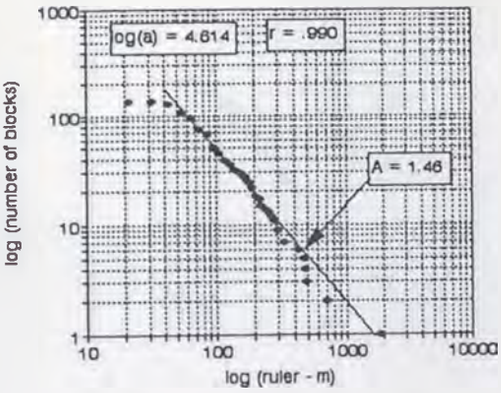

No.29 Kamatsuka Landslide
Whole Blocks Ruler - Length

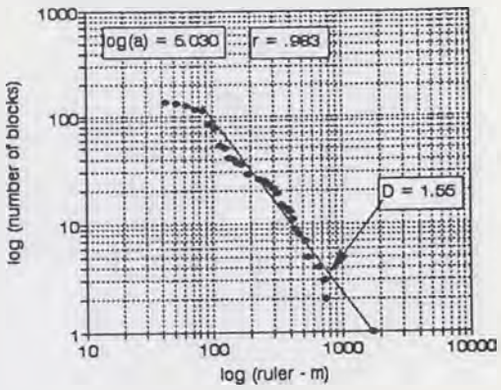

No.29 Kamatsuka Landslide
2nd Level Blocks Ruler - Width

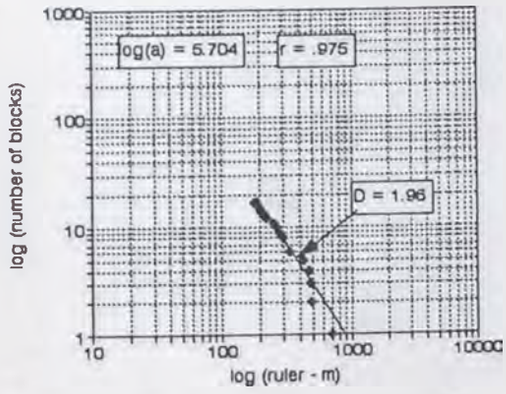

No.29 Kamatsuka Landslide
2nd Level Blocks Ruler - Length

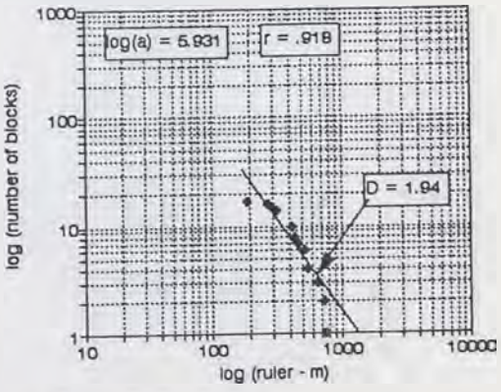

No.29 Kamatsuka Landslide
3rd Level Blocks Ruler - Width

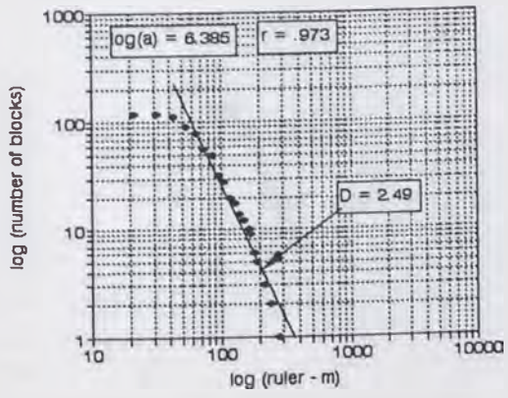

Kamatsuka Landslide
3rd Level Blocks Ruler - Length

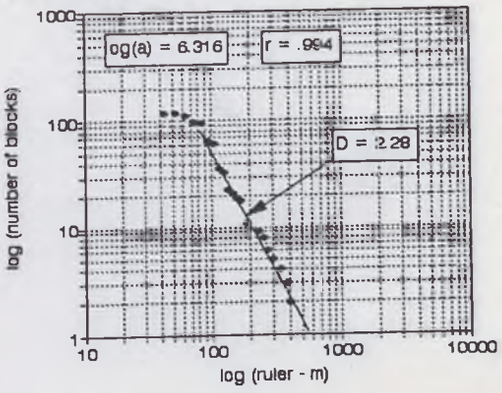

No.30 Maruyama Landslide
Whole Blocks Ruler - Width

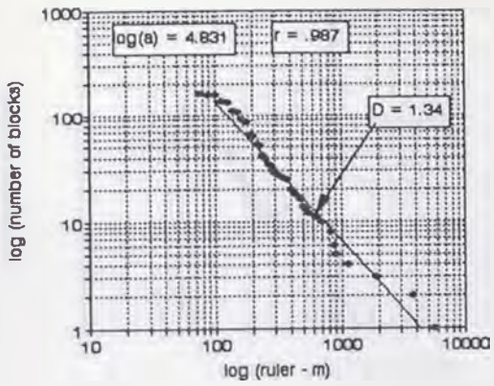

No.30 Maruyama Landslide
Whole Blocks Ruler - Length

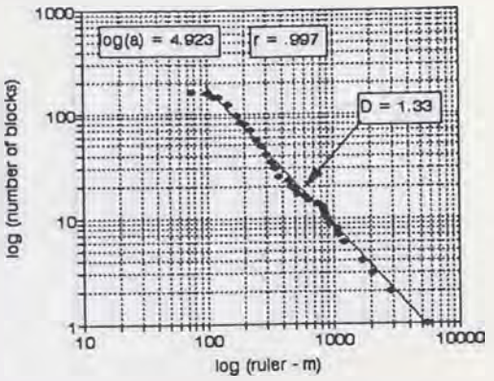

No.30 Maruyama Landslide
2nd Level Blocks Ruler - Width

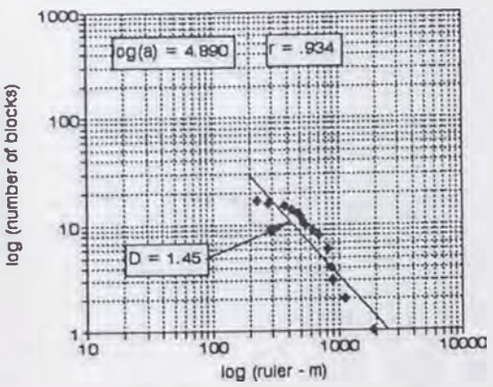

No.30 Maruyama Landslide
2nd Level Blocks Ruler - Length

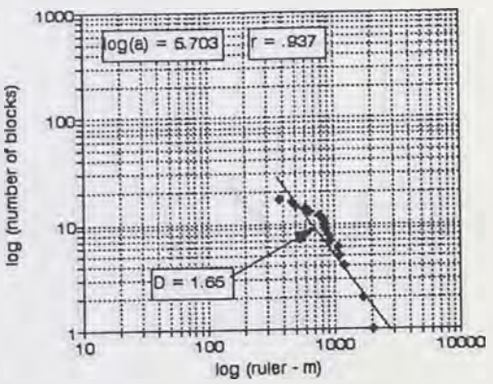

No.30 Maruyama Landslide
3rd Level Blocks Ruler - Width

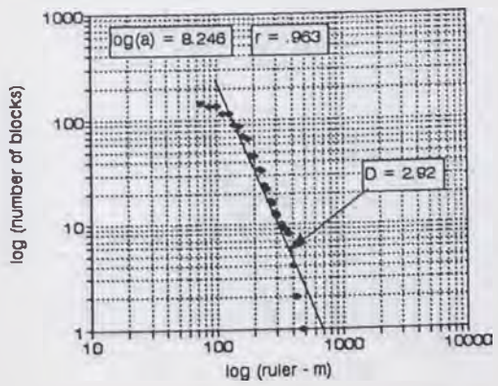

No.30 Maruyama Landslide
3rd Level Blocks Ruler - Length

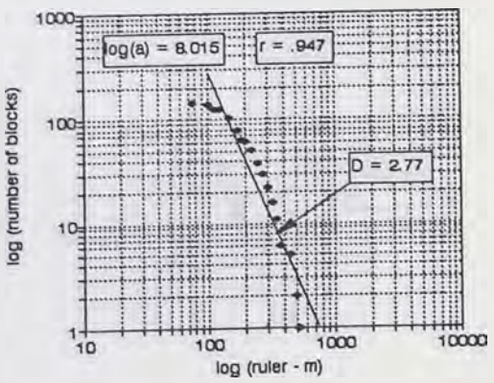

No.31 Maseguchi Landslide
Whole Blocks Ruler - Width

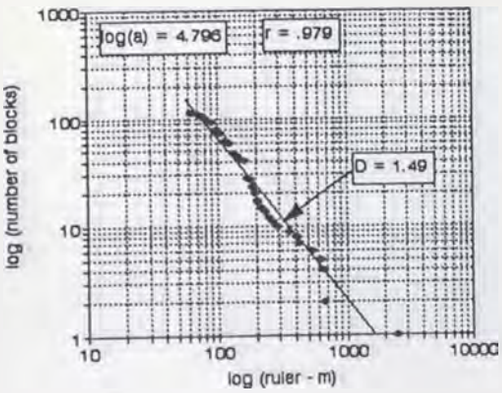

No.31 Maseguchi Landslide
Whole Blocks Ruler - Length

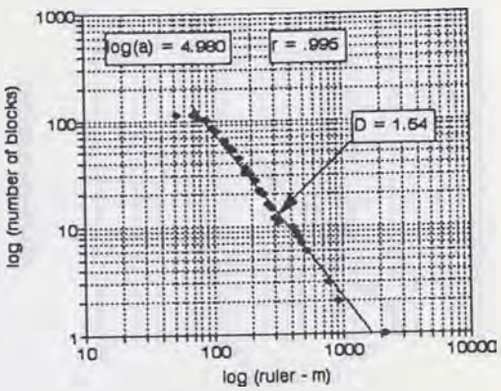

No.31 Maseguchi Landslide
2nd Level Blocks Ruler - Width

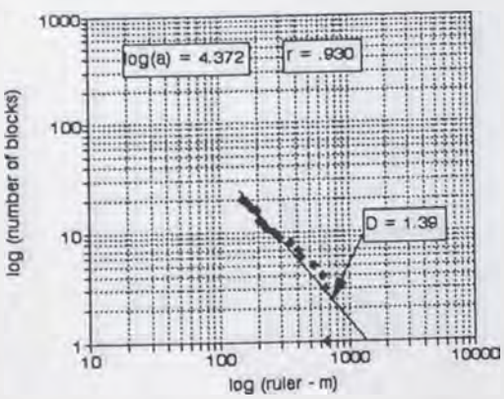

No.31 Maseguchi Landslide
2nd Level Blocks Ruler - Length

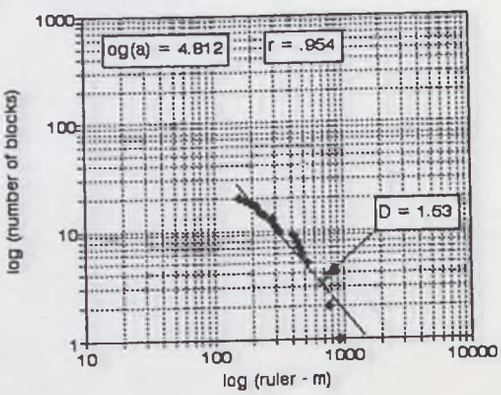

No.31 Maseguchi Landslide
3rd Level Blocks Ruler - Width

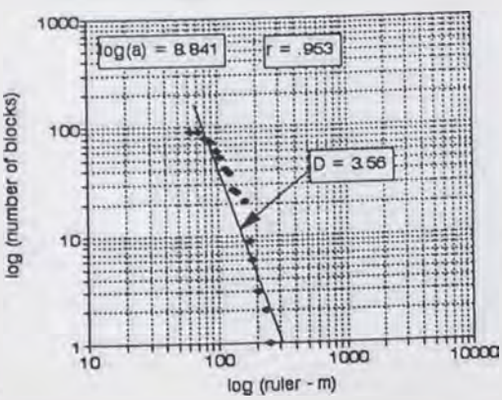

Maseguchi Landslide
3rd Level Blocks Ruler - Length

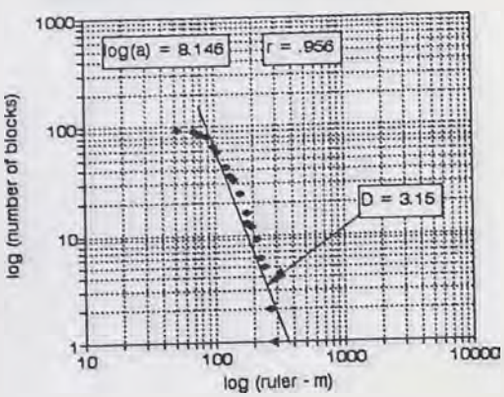

No.32 Maruta Landslide
Whole Blocks Ruler - Width

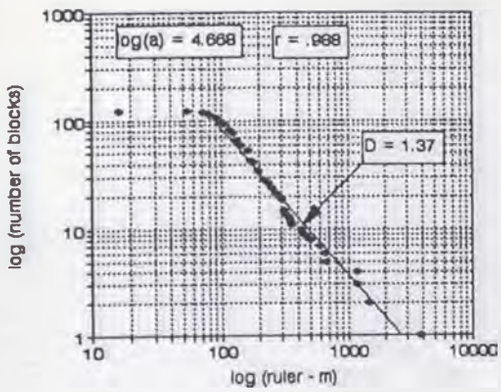

No.32 Maruta Landslide
Whole Blocks Ruler - Length

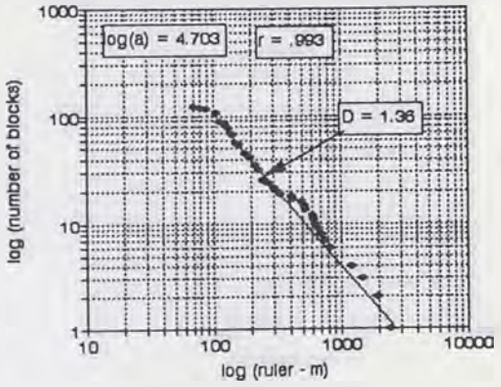

No.32 Maruta Landslide
2nd Level Blocks Ruler - Width

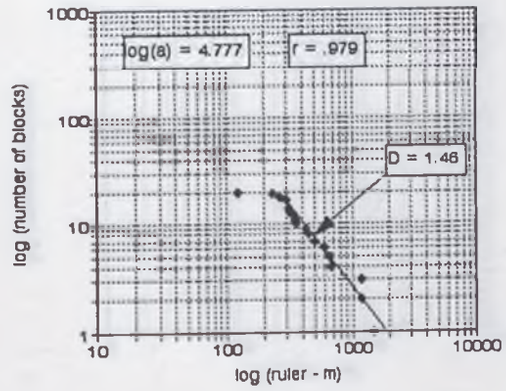

No.32 Maruta Landslide
2nd Level Blocks Ruler - Length

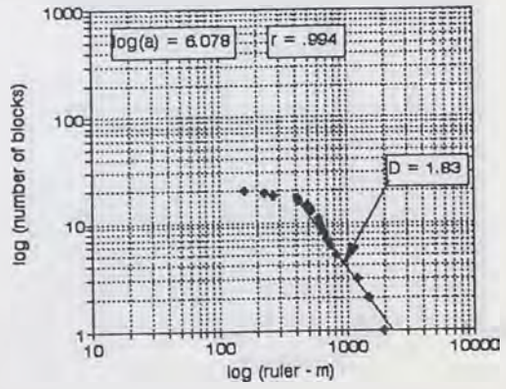

No.32 Maruta Landslide
3rd Level Blocks Ruler - Width

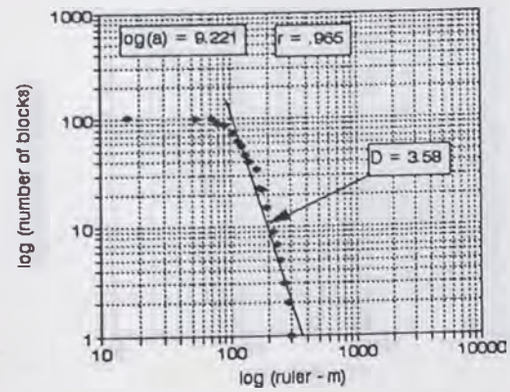

Maruta Landslide
3rd Level Blocks Ruler - Length

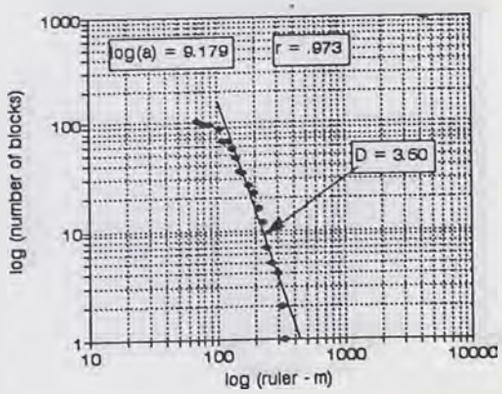

No.33 Kodomari Landslide
Whole Blocks Ruler - Width

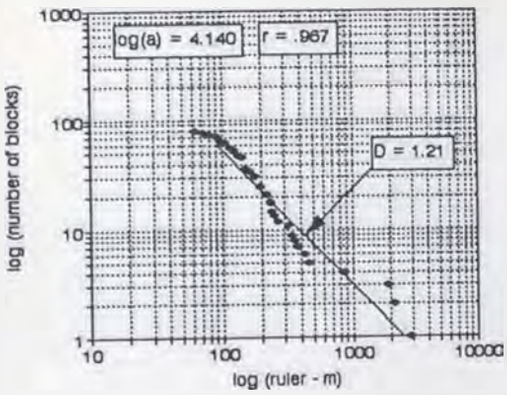

No.33 Kodomari Landslide
Whole Blocks Ruler - Length

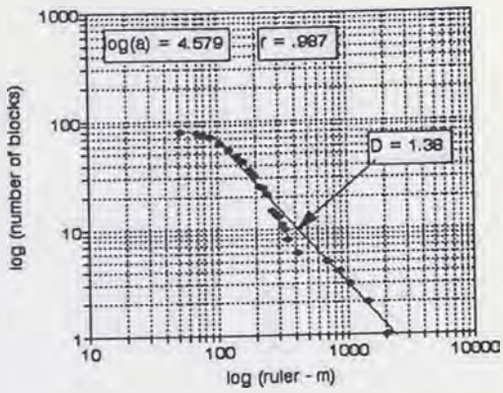

No.33 Kodomari Landslide
2nd Level Blocks Ruler - Width

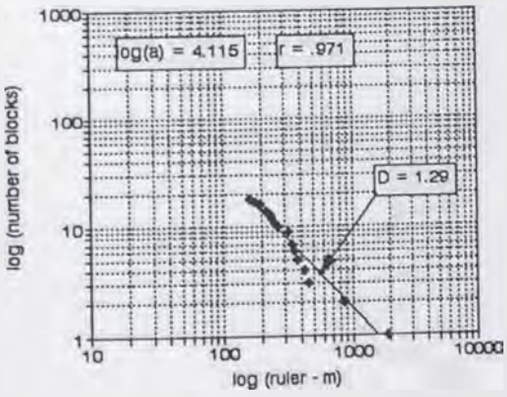

No.33 Kodomari Landslide
2nd Level Blocks Ruler - Length

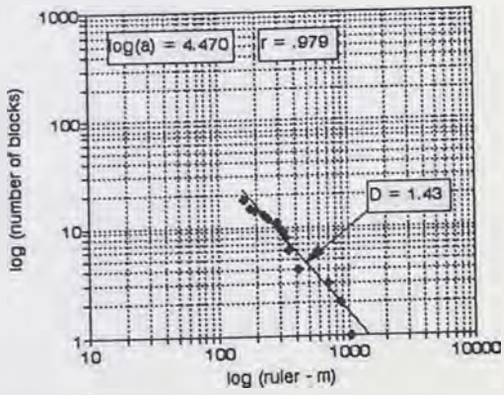

No.33 Kodomari Landslide
3rd mLevel Blocks Ruler - Width

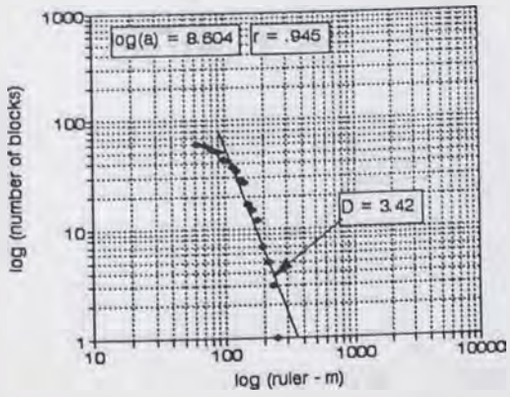

No.33 Kodomari Landslide
3rd Level Blocks Ruler - Length

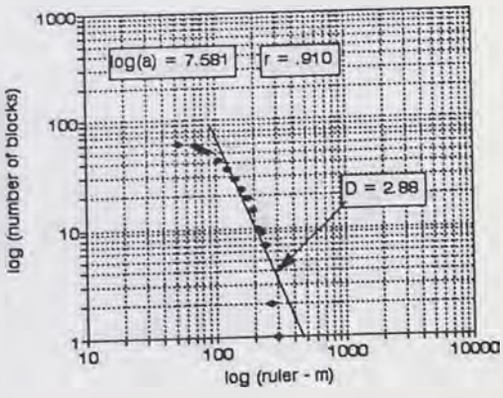

No.34 Ohbora Landslide
Whole Blocks Ruler-Width

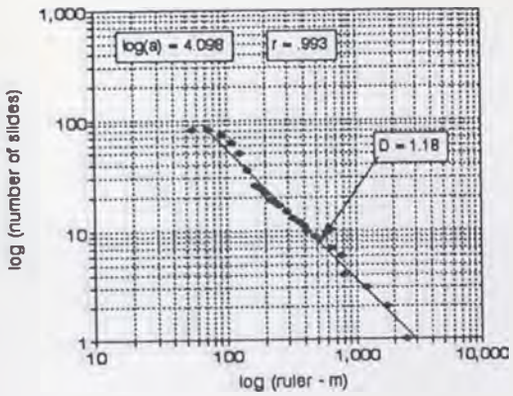

No.34 Ohbora Landslide
Whole Blocks Ruler-Length

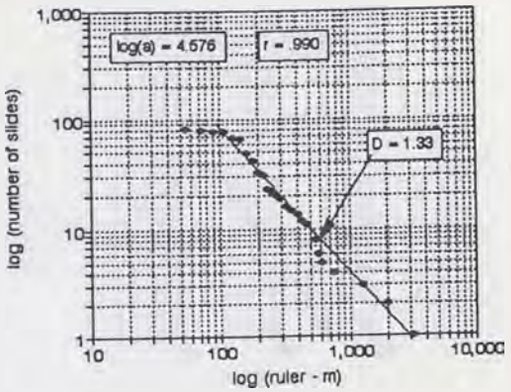

No.34 Ohbora Landslide
2nd Level Blocks Ruler-Width

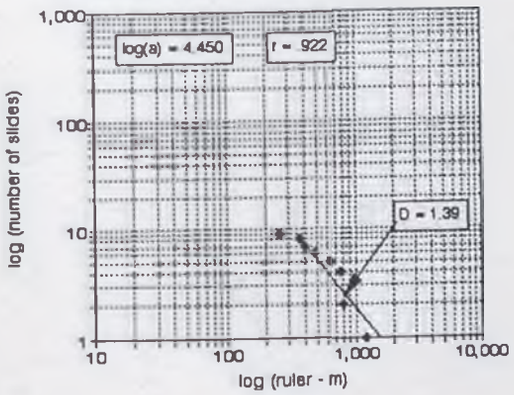

No.34 Ohbora Landslide
2nd Level Blocks Ruler-Length

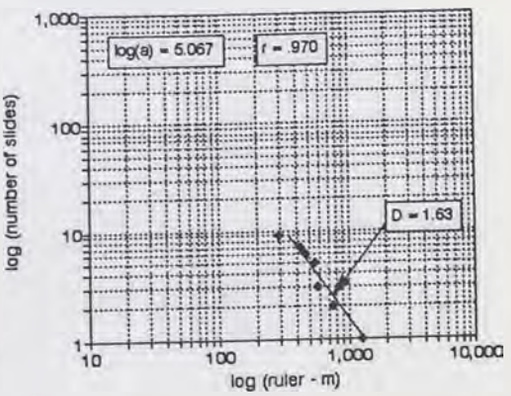

No.34 Ohbora Landslide
3rd Level Blocks Ruler-Width

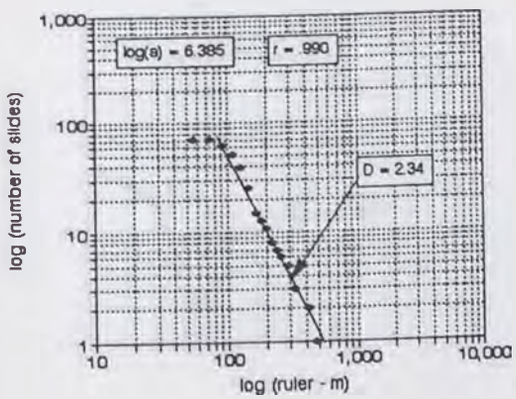

No.34 Ohbora Landslide
3rd Level Blocks Ruler-Length

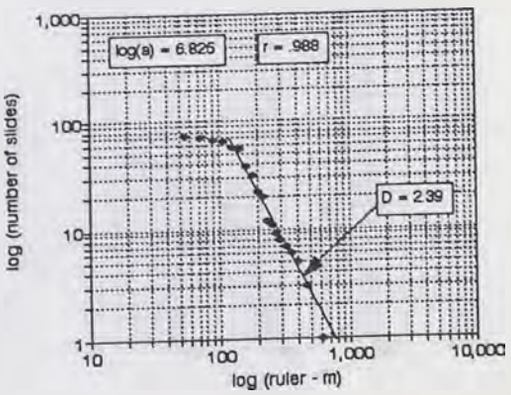

No.35 Urushinose Landslide
Whole Blocks Ruler - Width

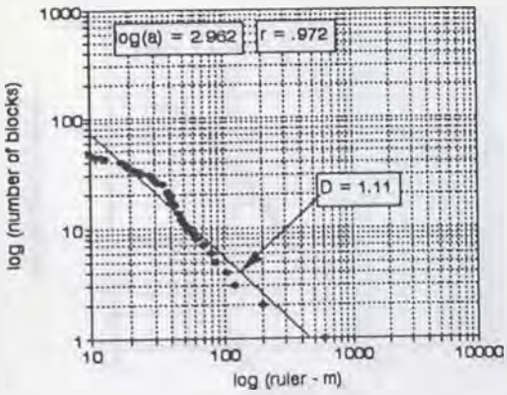

No.35 Urushinose Landslide
Whole Blocks Ruler - Length

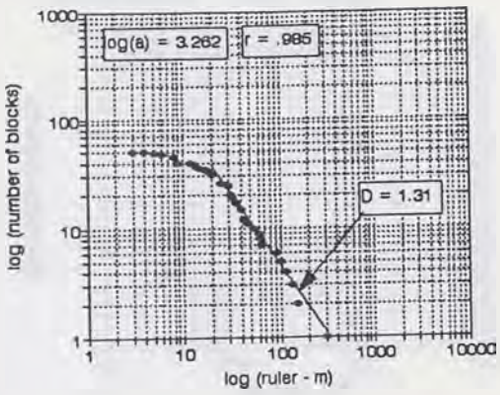

No.35 Urushinose Landslide
2nd Level Blocks Ruler - Width

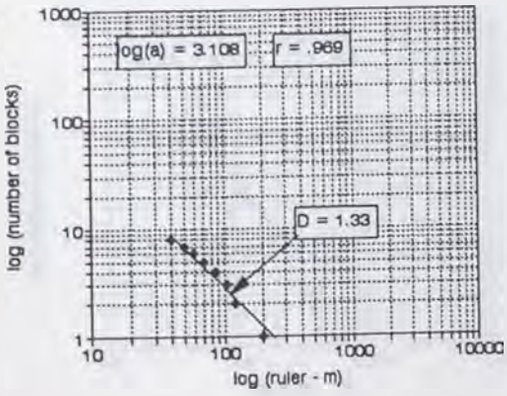

No.35 Urushinose Landslide
2nd Level Blocks Ruler - Length

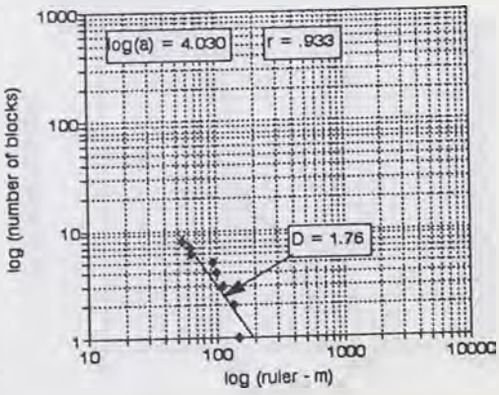

No.35 Urushinose Landslide
3rd Level Blocks Ruler - Width

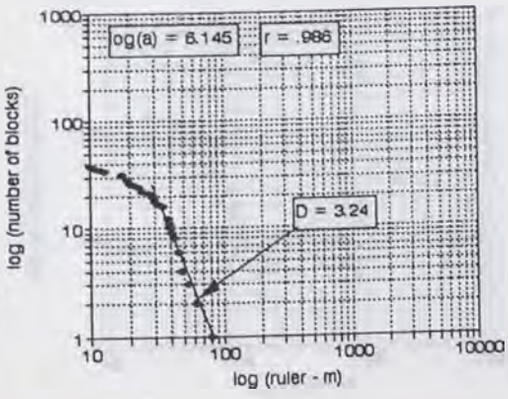

Urushinose Landslide
3rd Level Blocks Ruler - Length

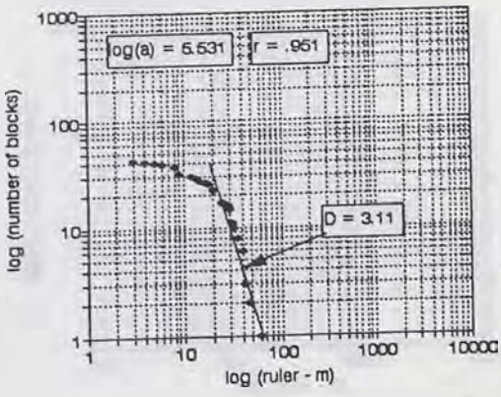

No.36 Nishinotani Landslide
Whole Blocks Ruler - Width

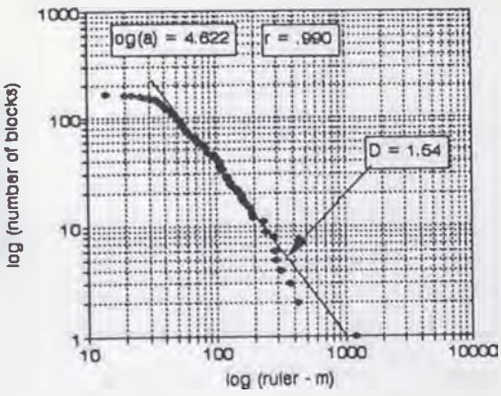

No.36 Nishinotani Landslide
Whole Blocks Ruler - Length

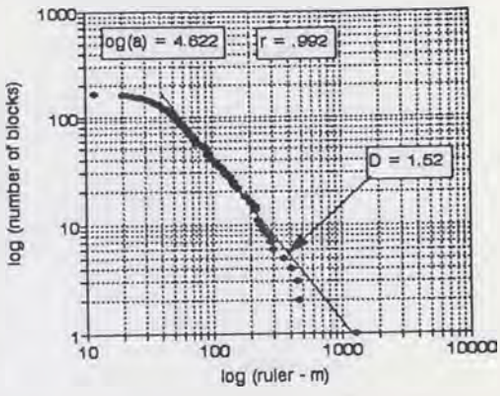

No.36 Nishinotani Landslide
2nd Level Blocks Ruler - Width

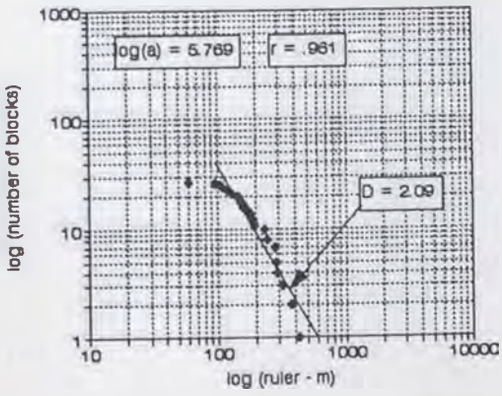

No.36 Nishinotani Landslide
2nd Level Blocks Ruler - Length

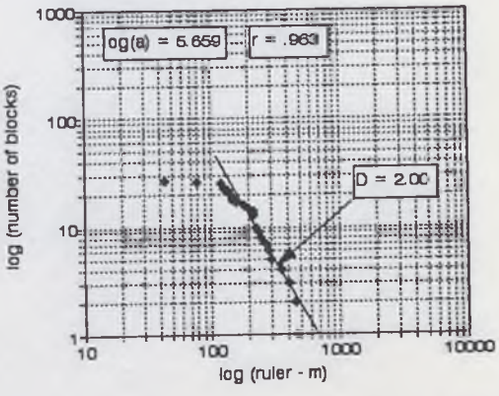

No.36 Nishinotani Landslide
3rd Level Blocks Ruler - Width

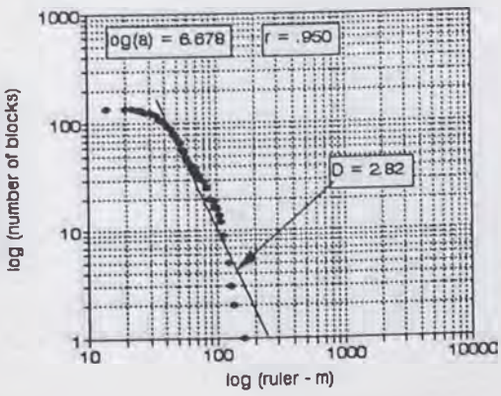

Nakatateyama Landslide
3rd Level Blocks Ruler - Length

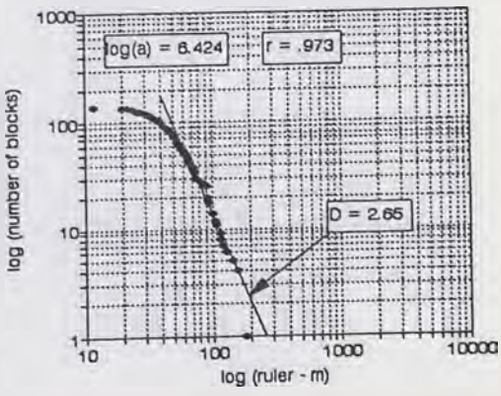

No.37 Youne Landslide
Whole Blocks Ruler - Width

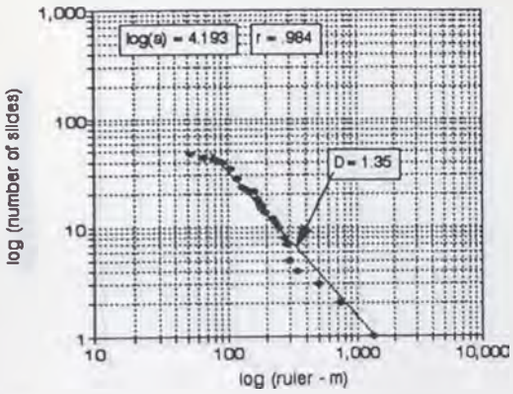

No.37 Youne Landslide
Whole Blocks Ruler - Length

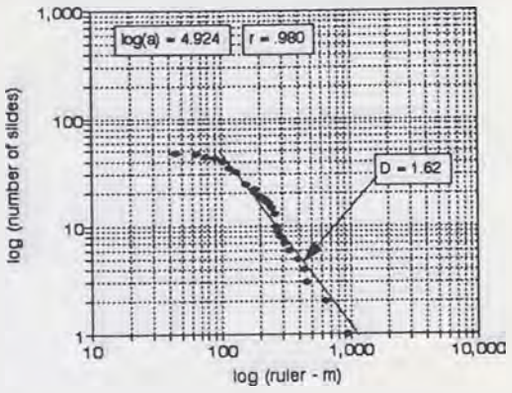

No.37 Youne Landslide
2nd Level Blocks Ruler - Width

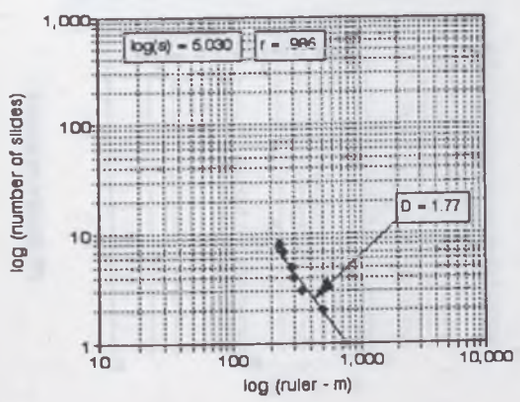

No.37 Youne Landslide
2nd Level Blocks Ruler - Length

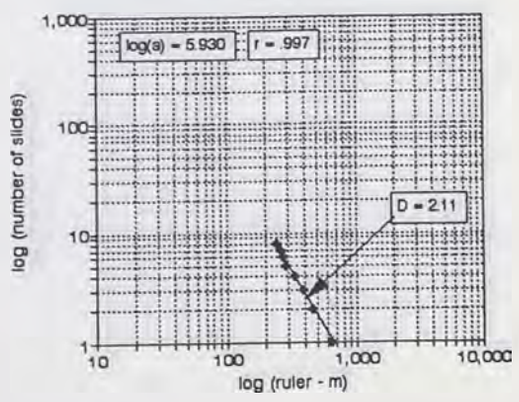

No.37 Youne Landslide
3rd Level Blocks Ruler - Width

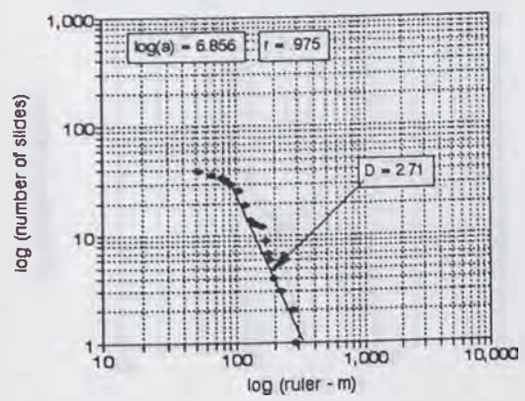

No.37 Youne Landslide
3rd Level Blocks Ruler - Length

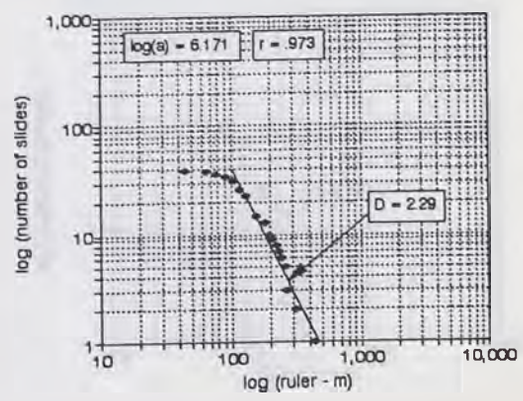

No.38 Nuta Landslide
Whole Blocks Ruler - Width

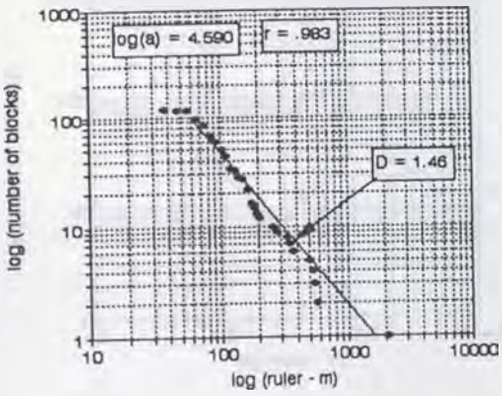

No.38 Nuta Landslide
Whole Blocks Ruler - Length

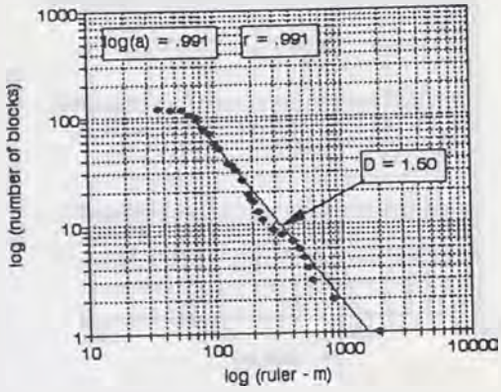

No.38 Nuta Landslide
2nd Level Blocks Ruler - Width

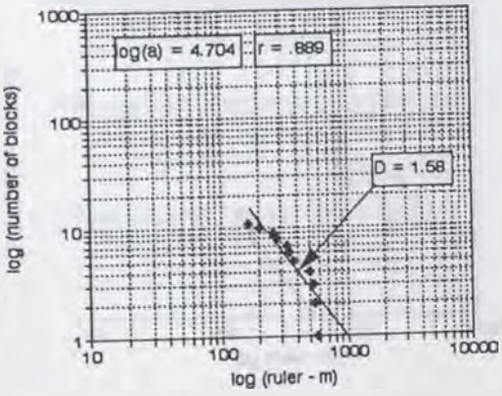

No.38 Nuta Landslide
2nd Level Blocks Ruler - Length

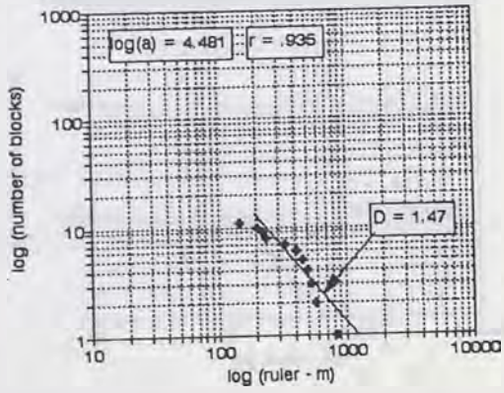

No.38 Nuta Landslide
3rd Level Blocks Ruler - Width

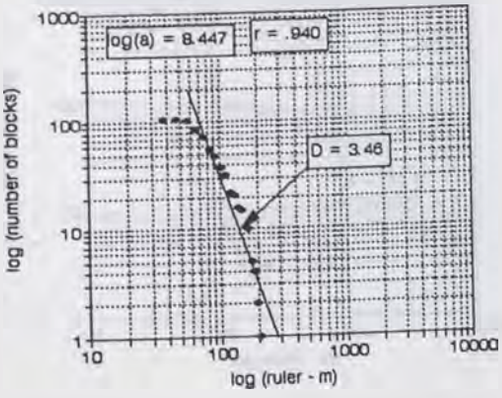

Nuta Landslide
3rd Level Blocks Ruler - Length

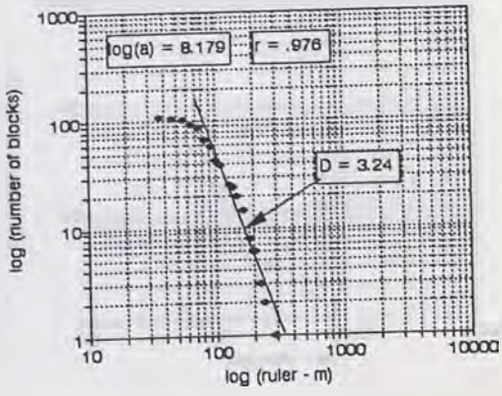

No.39 Nyuya Landslide
Whole Blocks Ruler-Width

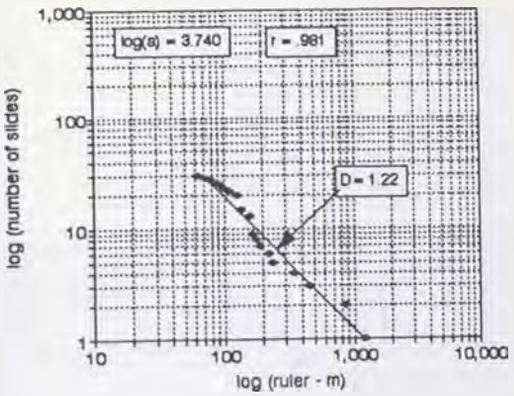

No.39 Nyuya Landslide
Whole Blocks Ruler-Length

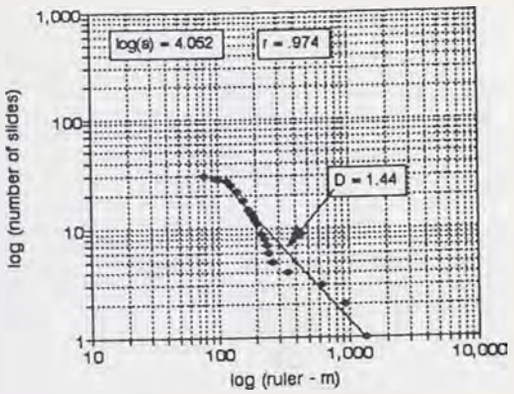

No.39 Nyuya Landslide
2nd Level Blocks Ruler-Width

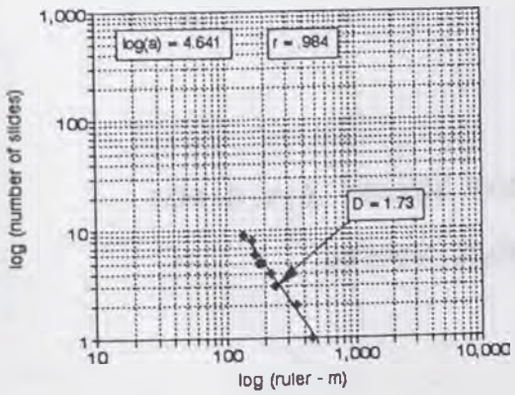

No.39 Nyuya Landslide
2nd Level Blocks Ruler-Length

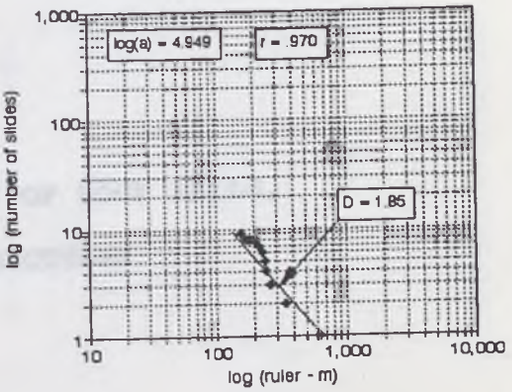

No.39 Nyuya Landslide
3rd Level Blocks Ruler-Width

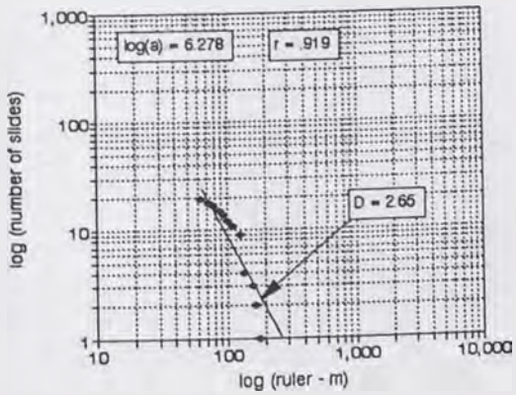

No.39 Nyuya Landslide
3rd Level Blocks Ruler-Length

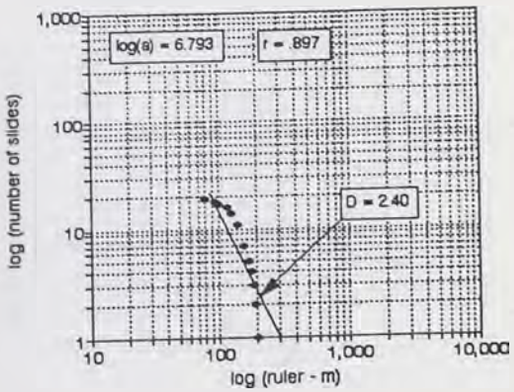

APPENDIX C:

LOG($N(r)$) VERSUS LOG(r) PLOTS OF ROCK FALLS, DEBRIS FLOWS, AND FRACTURES

Slide Mountain Rock Fragments
Rockfall Deposits R-1

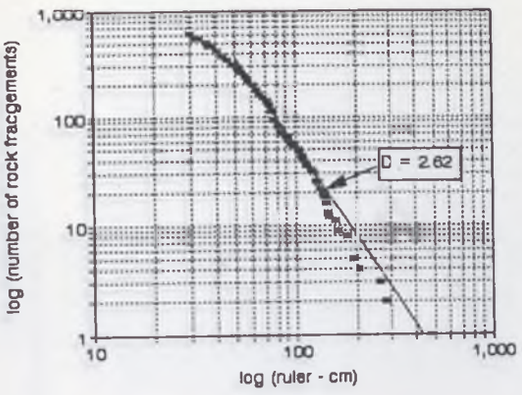

Slide Mountain Rock Fragments
Rockfall Deposits R-2

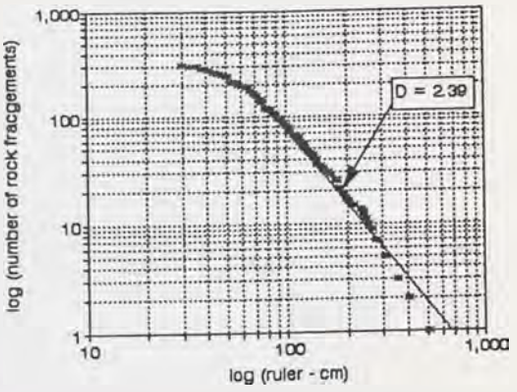

Slide Mountain Rock Fragments
Rockfall Deposits R-3

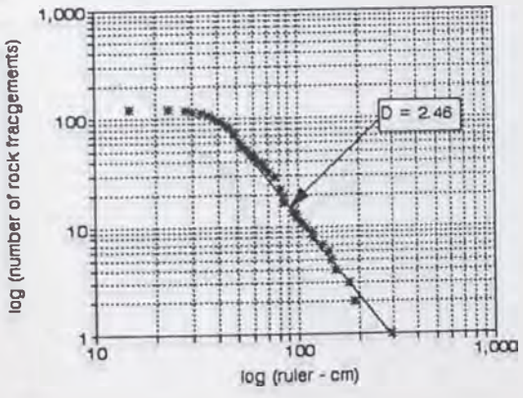

Slide Mountain Rock Fragments
Rockfall Deposits R-4

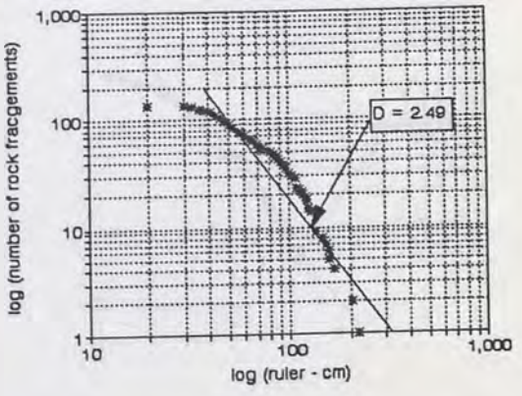

Slide Mountain Rock Fragments
Rockfall Deposits R-5

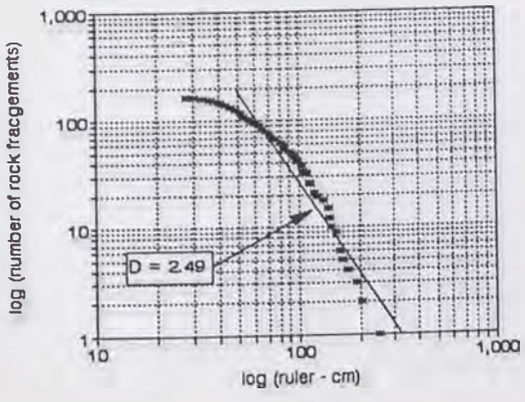

Slide Mountain Rock Fragments
Rockfall Deposits R-6

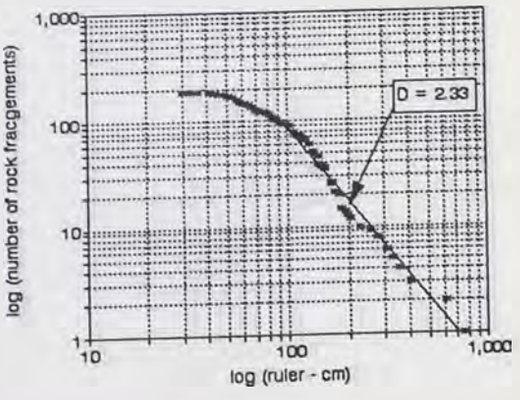

Slide Mountain Rock Fragments
Rockfall Deposits R-7

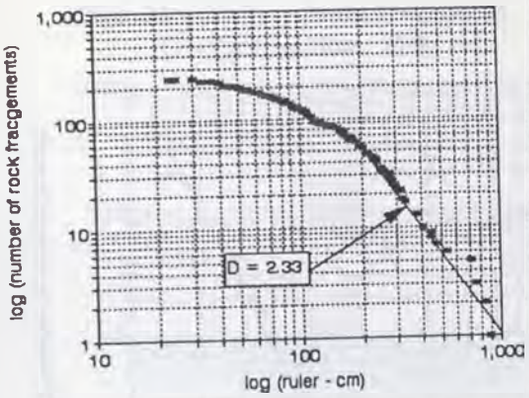

Slide Mountain Rock Fragments
Debris Flow Deposits D-1

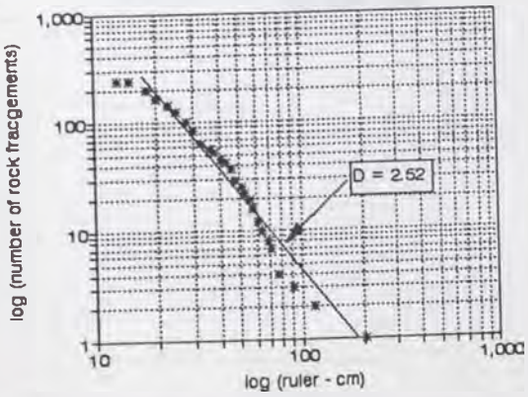

Slide Mountain Rock Fragments
Debris Flow Deposits D-2

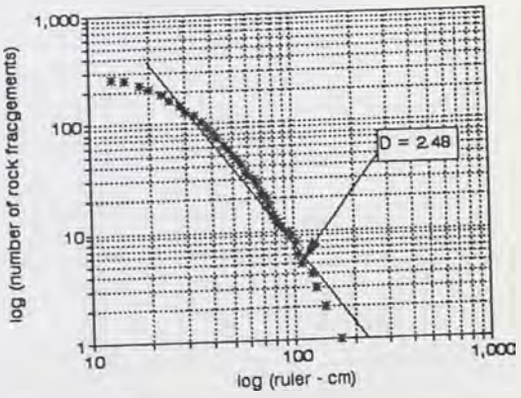

Slide Mountain Rock Fragments
Debris Flow Deposits D-3

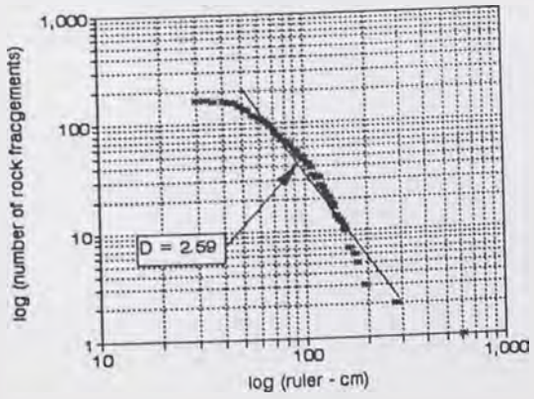

Slide Mountain Rock Fragments
Debris Flow Deposits D-4

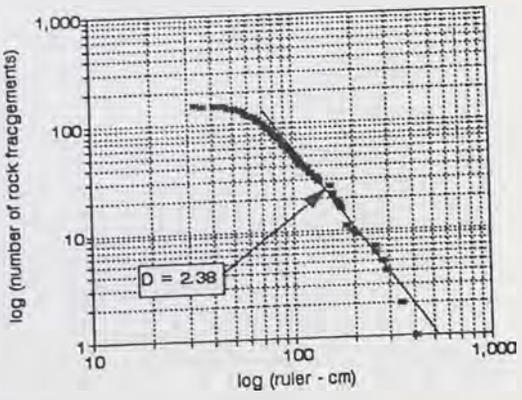

Slide Mountain Rock Fragments
Conglomerates C-1

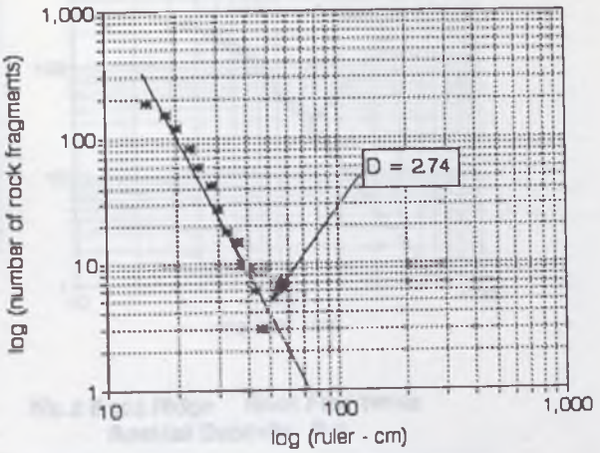

No.2 Boca Ridge Rock Fragments
Rockfall Deposits R-1

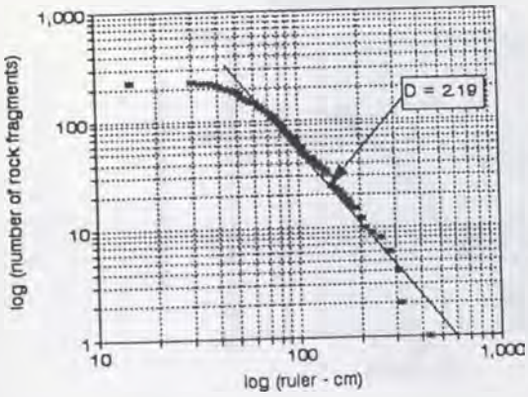

No.2 Boca Ridge Rock Fragments
Rockfall Deposits R-2

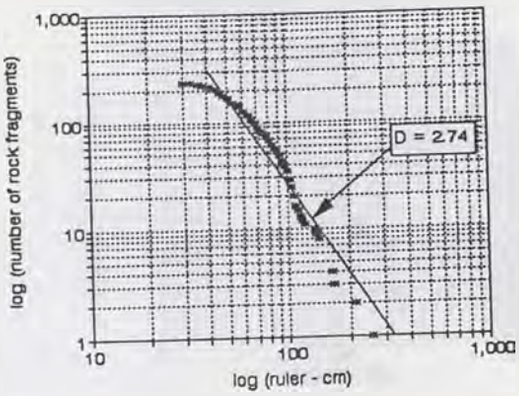

No.2 Boca Ridge Rock Fragments
Rockfall Deposits R-3

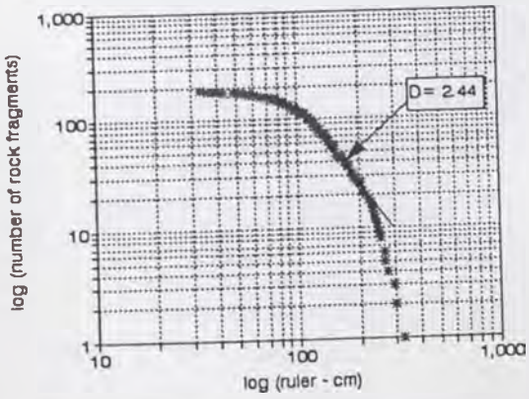

No.2 Boca Ridge Rock Fragments
Rockfall Deposits R-4

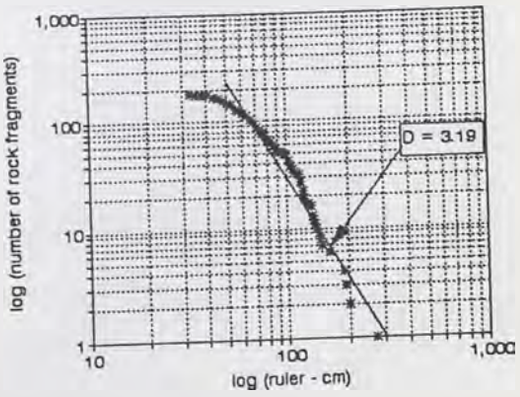

No.2 Boca Ridge Rock Fragments
Rockfall Deposits R-5

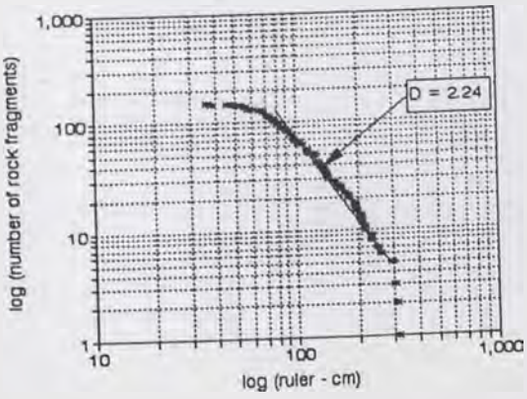

No.2 Boca Ridge Rock Fragments
Rockfall Deposits R-6

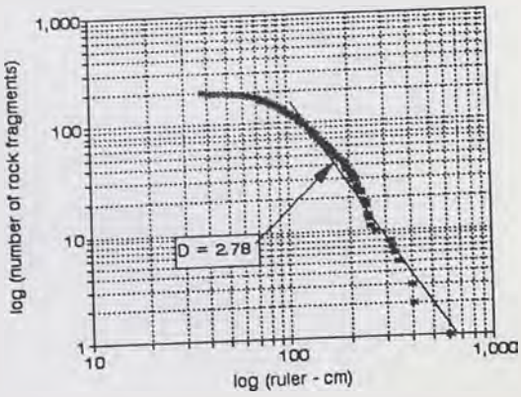

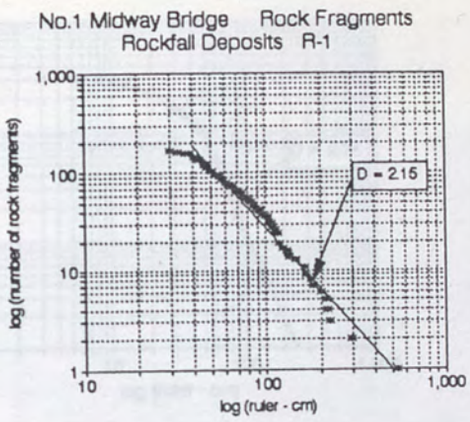
No.1 Midway Bridge Rock Fragments
Rockfall Deposits R-1
log (number of rock fragments)
1,000
100
10
1
10
100
1,000
log (ruler - cm)
D = 2.15

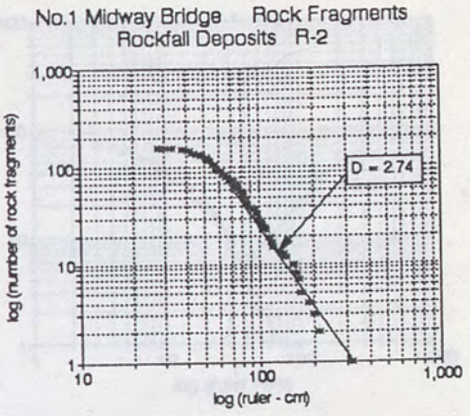
No.1 Midway Bridge Rock Fragments
Rockfall Deposits R-2
log (number of rock fragments)
1,000
100
10
1
10
100
1,000
log (ruler - cm)
D = 2.74

Slide Mountain Fracture Spaces
F-1

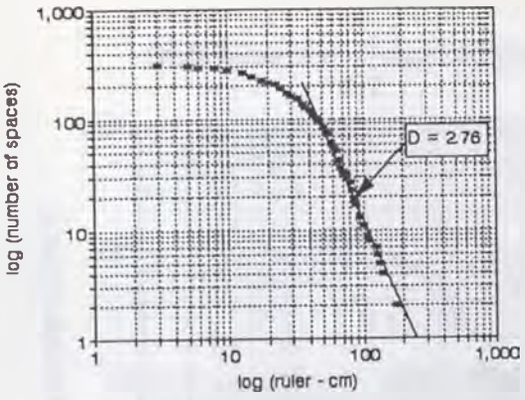

Slide Mountain Fracture Spaces
F-2

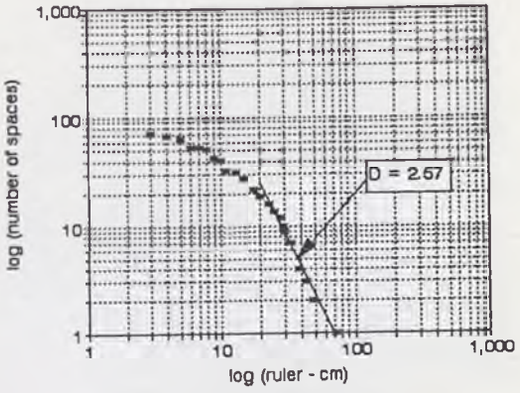

Slide Mountain Fracture Spaces
F-3

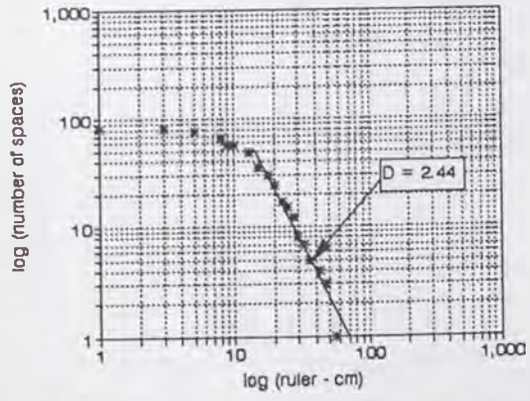

Slide Mountain Fracture Spaces
F-4

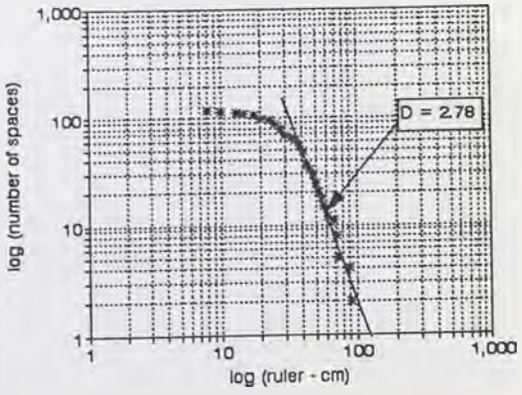

Slide Mountain Fracture Spaces
F-5

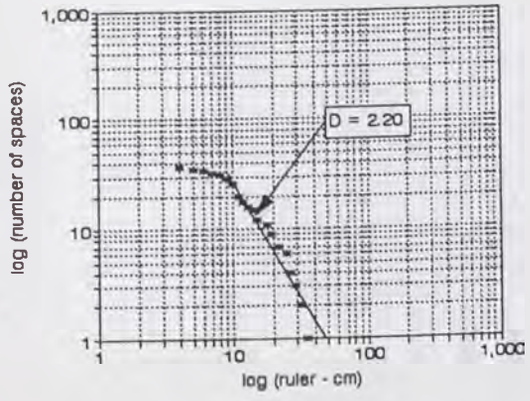

Slide Mountain Fracture Spaces
F-6

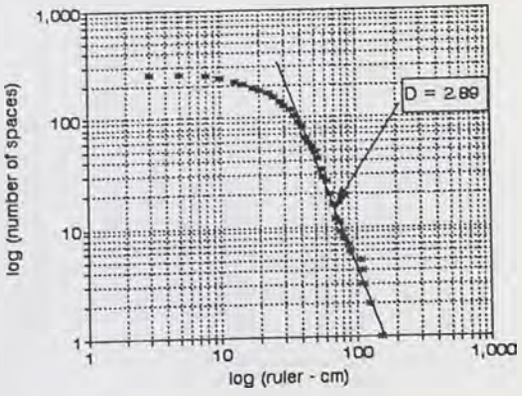

Slide Mountain Fracture Spaces
F-7

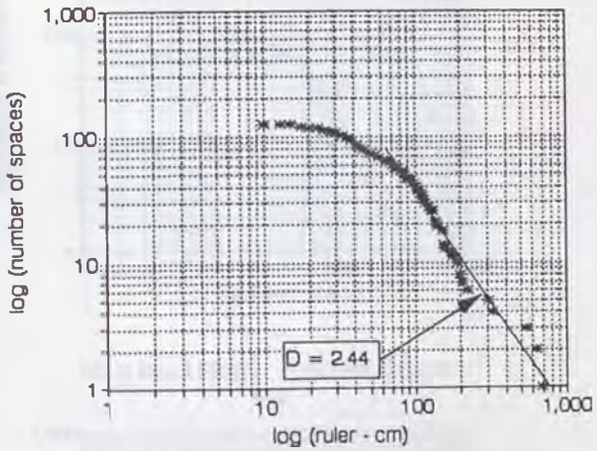

No.2 Boca Ridge Fracture Spaces
F-1

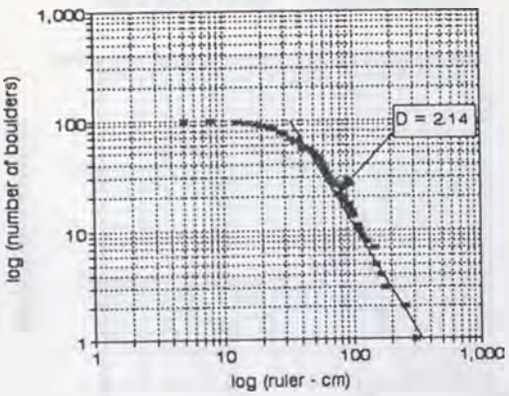

No.2 Boca Ridge Fracture Spaces
F-2

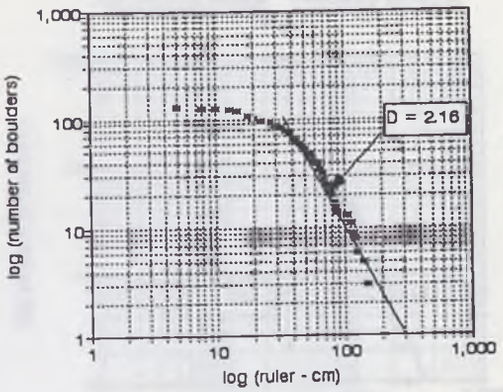

No.2 Boca Ridge Fracture Spaces
F-3

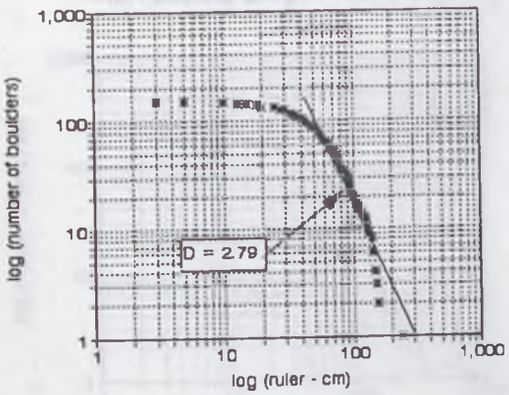

No.2 Boca Ridge Fracture Spaces
F-4

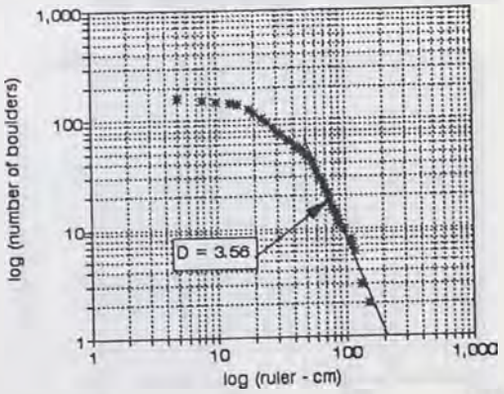

No.2 Boca Ridge Fracture Spaces
F-5

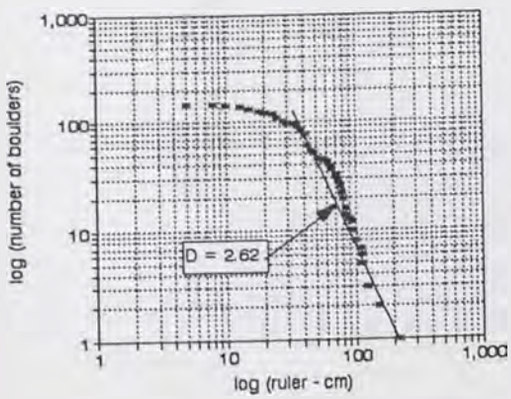

No.2 Boca Ridge Fracture Spaces
F-6

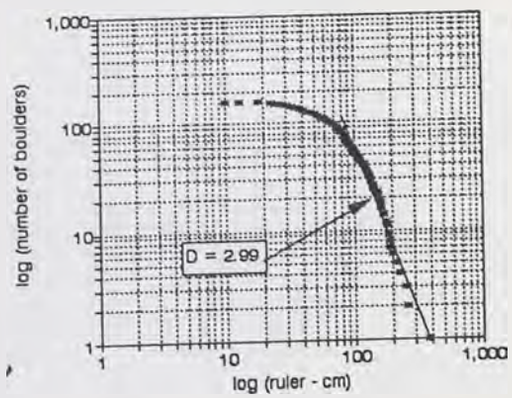

No.2 Boca Ridge Fracture Spaces
F-7

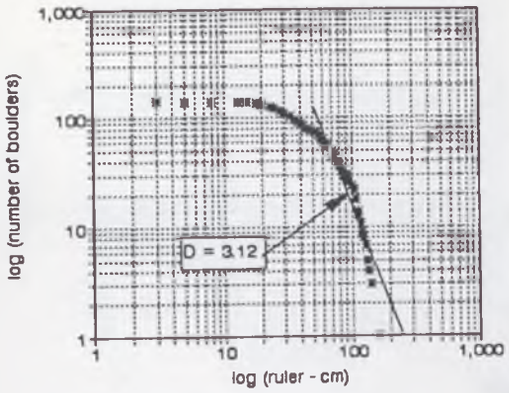

No.2 Boca Ridge Fracture Spaces
F-8

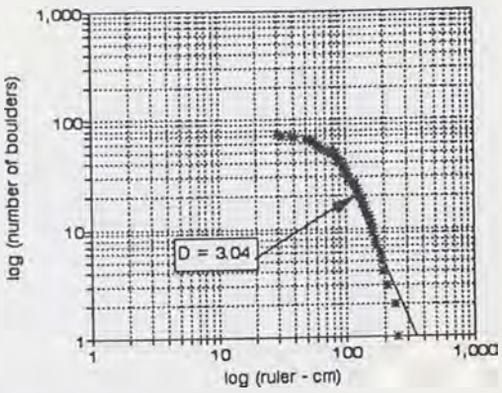

No.1 Midway Bridge Fracture Spaces
F-1

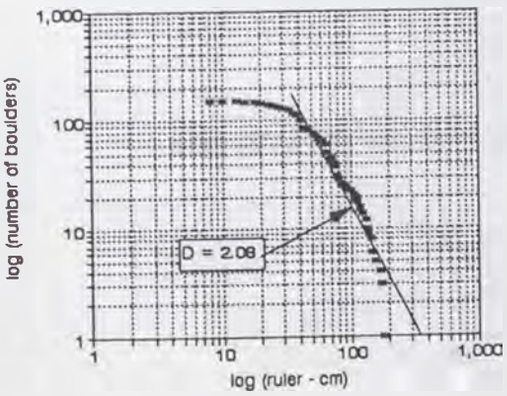

No.1 Midway Bridge Fracture Spaces
F-2

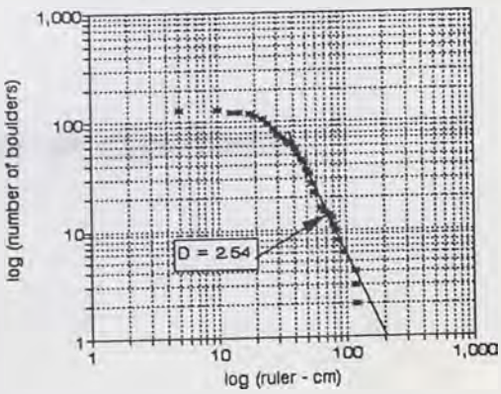

APPENDIX D:

LOG($N(r)$) VERSUS LOG(r) PLOTS OF LINEAMENTS

No.1 Midway Bridge Linearment D
Box Counting Method

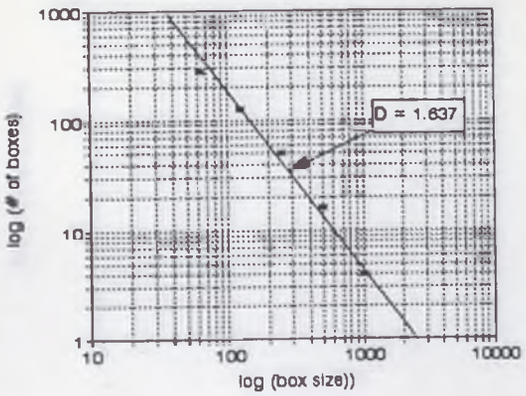

No.2 Boca Ridge Linearment D
Box Counting Method

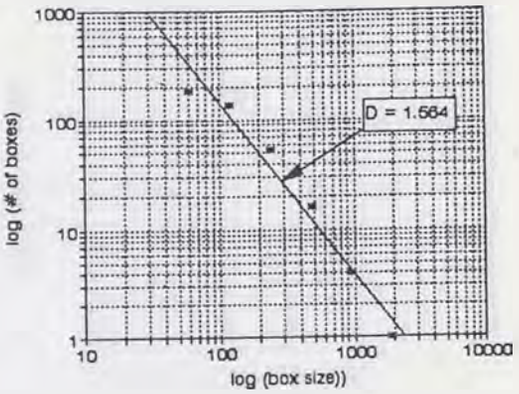

No. 3 Palos Verdes Linearment D
Box Counting Method

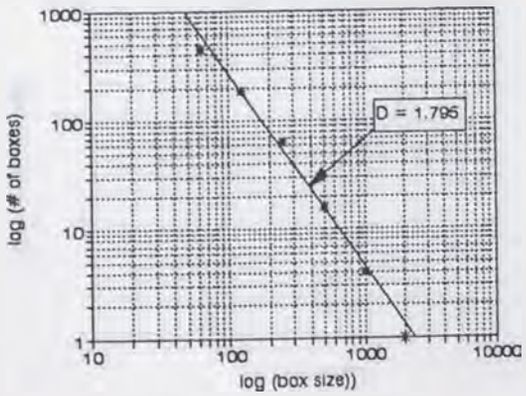

No. 4 Big Rock Mesa Linearment D
Box Counting Method

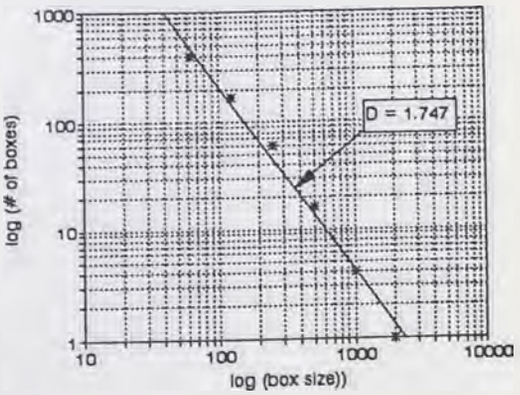

No. 5 Thistle Linearment D
Box Counting Method

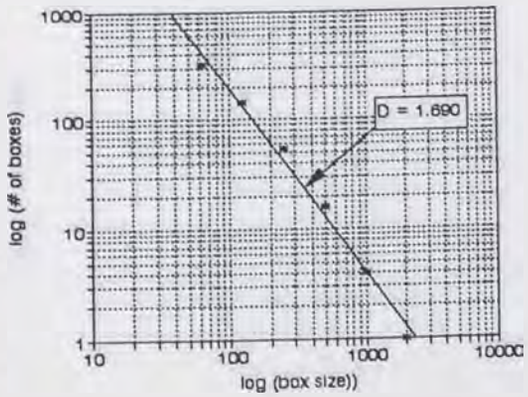

No. 7 Upper Gross Linearment D
Box Counting Method

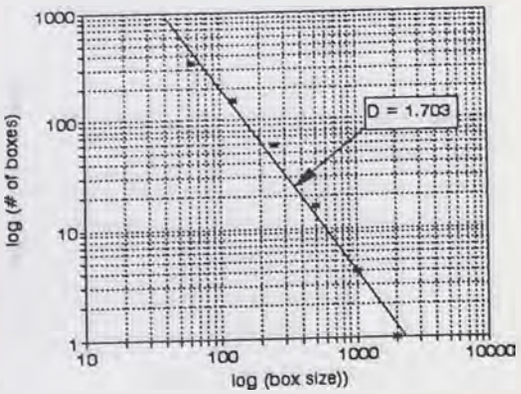

No. 12 Kiritani Landslide
Linerment Box counting

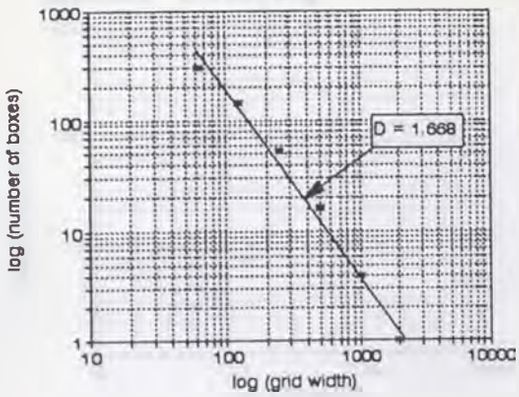

No. 13 Katsurabara Landslide
Linerment Box counting

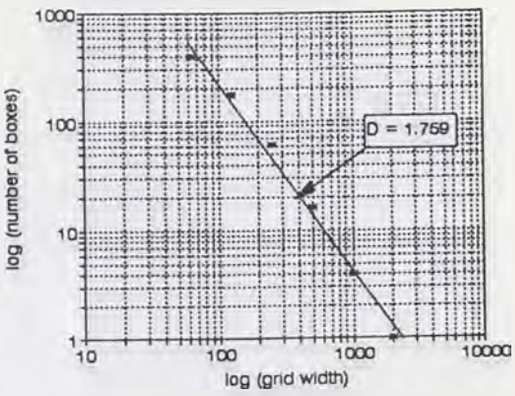

No. 15 Takisaka Landslide
Linerment Box counting

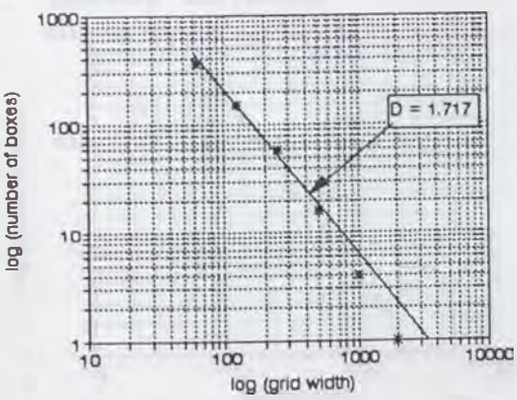

No. 17 Mushigame Landslide
Linerment Box counting

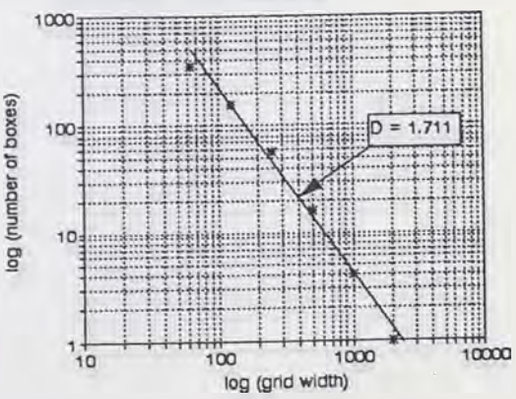

No. 19 Karuizawa Landslide
Linerment Box counting

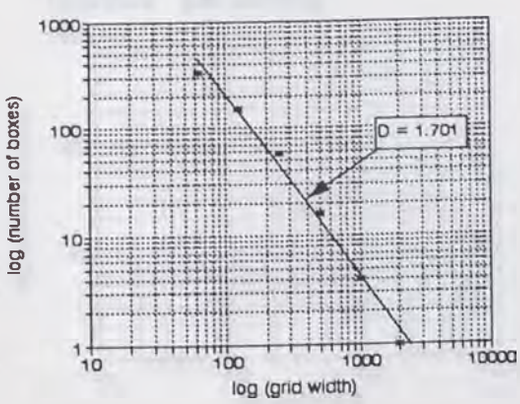

No. 20 Happoudai Landslide
Linerment Box counting

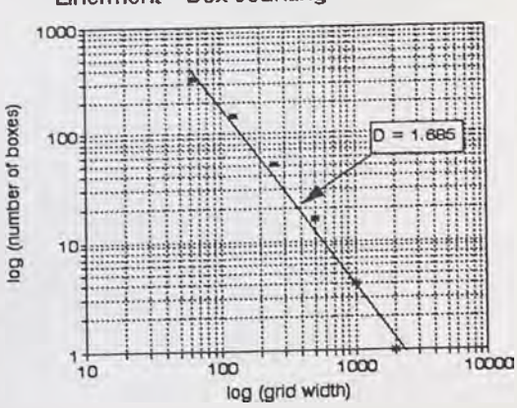

No. 21 Raiden Landslide
Linerment Box counting

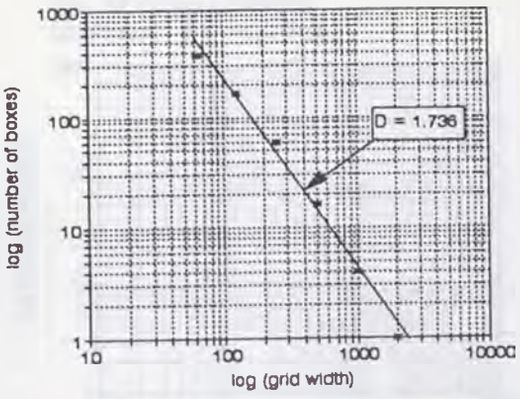

No. 22 Nishinakanoho Landslide
Linerment Box counting

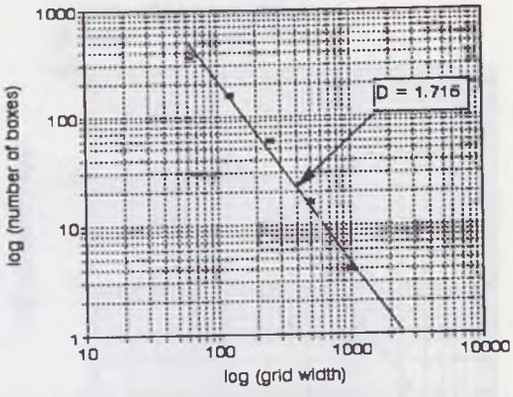

No. 24 Kitaurata Landslide
Linerment Box counting

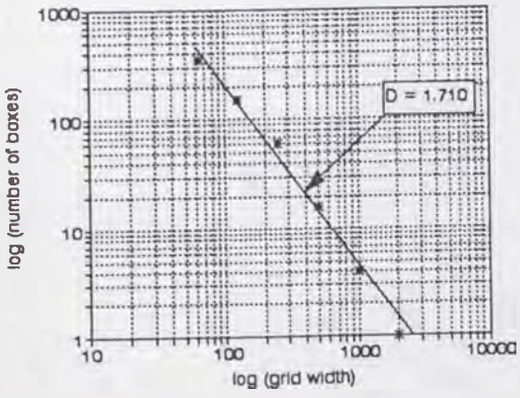

No. 31 Maseguchi Landslide
Linerment Box counting

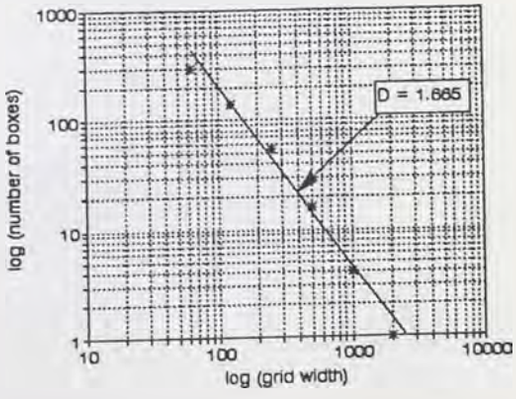

No. 32 Maruta Landslide
Linerment Box counting

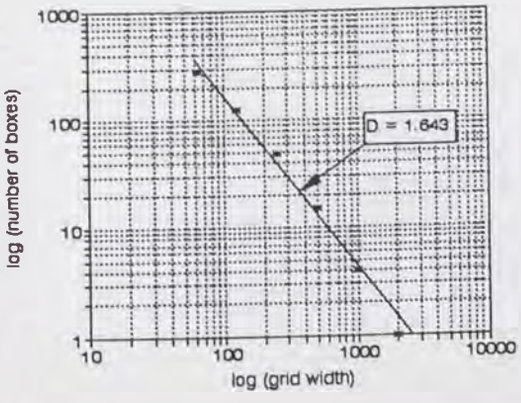

No. 37 Youne Landslide
Linerment Box counting

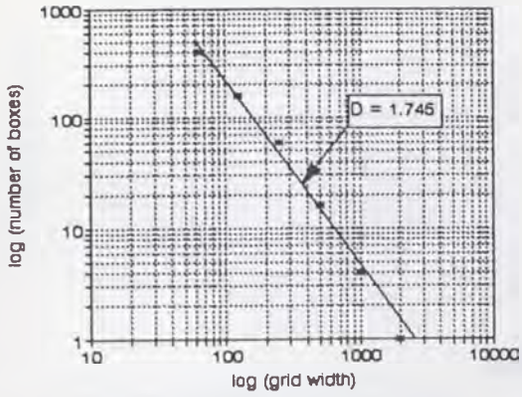

No. 39 Nyuya Landslide
Linerment Box counting

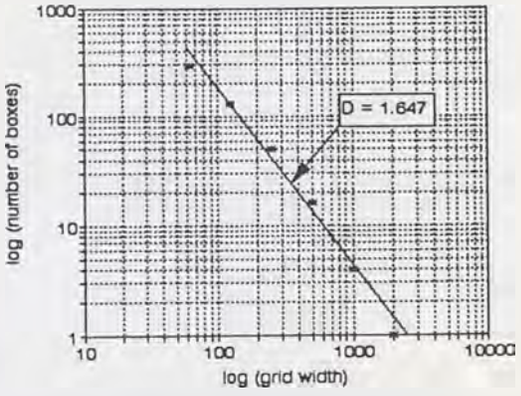

APPENDIX E:

LOG($N(r)$) VERSUS LOG(r) PLOTS OF MODEL B

No. 1 Midway Bridge Landslide (width)
Model B Fractal Dimension

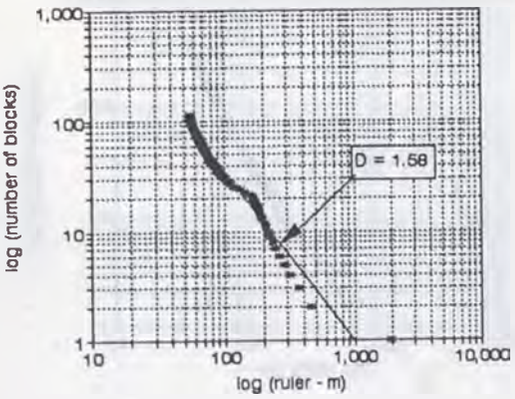

No. 1 Midway Bridge Landslide (Length)
Model B Fractal Dimension

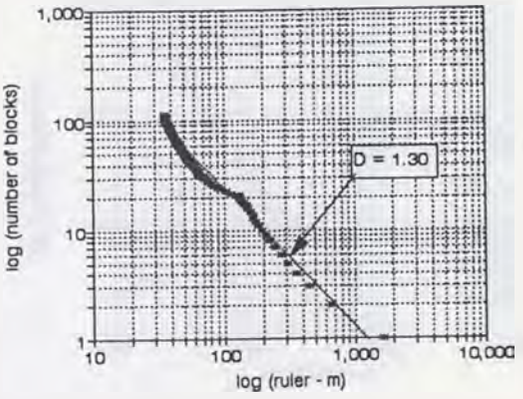

No. 2 Boca Ridge Landslide (Width)
Model B Fractal Dimension

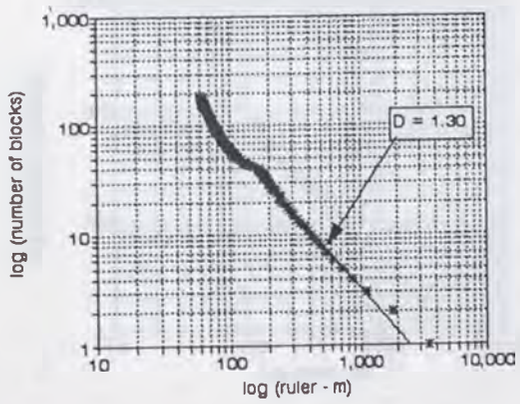

No. 2 Boca Ridge Landslide (Length)
Model B Fractal Dimension

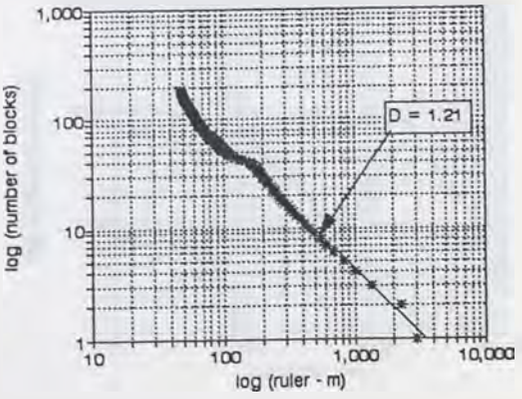

No. 3 Palos Verdes Landslide (Width)
Model B Fractal Dimension

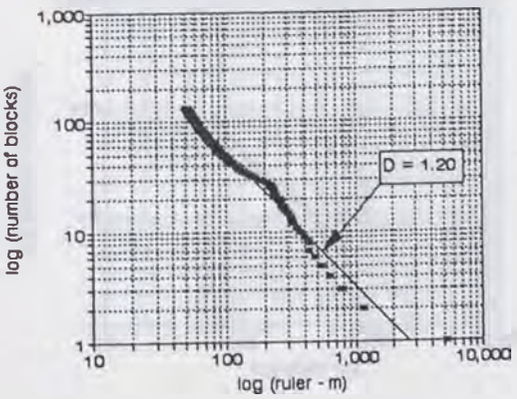

No. 3 Palos Verdes Landslide (Length)
Model B Fractal Dimension

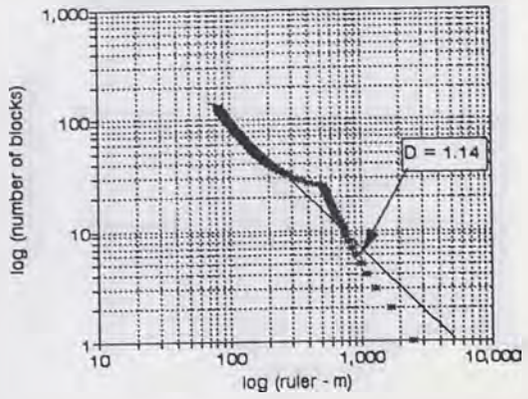

No. 4 Big Rock Mesa Landslide (Width)
Model B Fractal Dimension

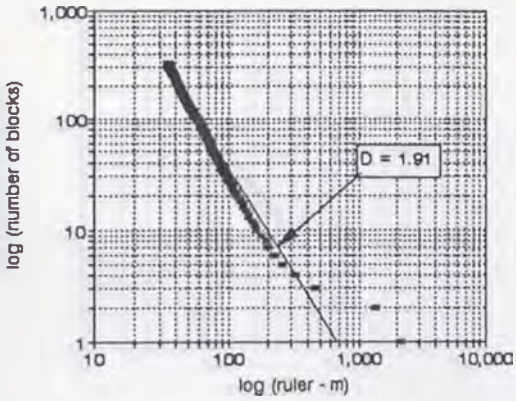

No. 4 Big Rock Mesa Landslide (Length)
Model B Fractal Dimension

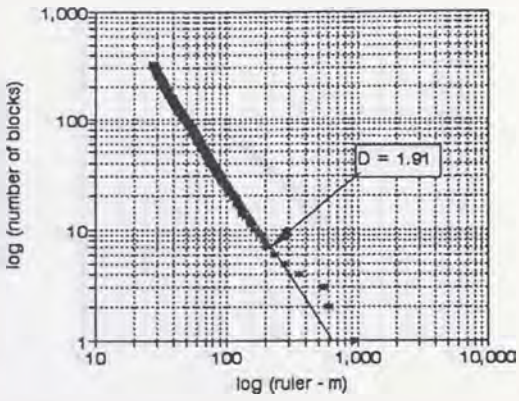

No. 5 Thristle Landslide (Width)
Model B Fractal Dimension

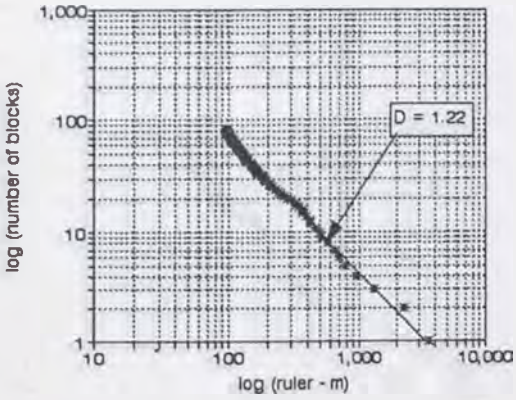

No. 5 Thristle Landslide (Length)
Model B Fractal Dimension

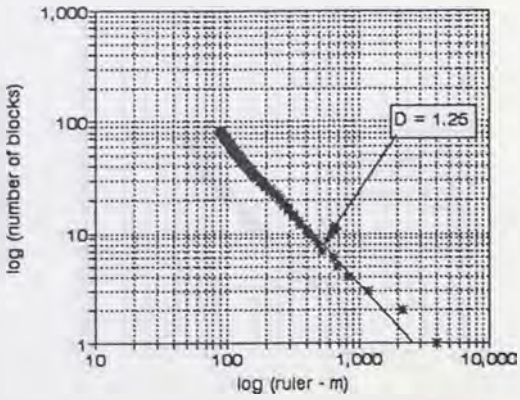

No. 6 Lower Gross Landslide (Width)
Model B Fractal Dimension

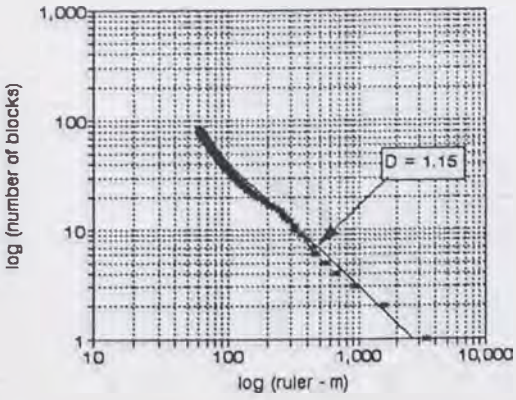

No. 6 Lower Gross Landslide (Length)
Model B Fractal Dimension

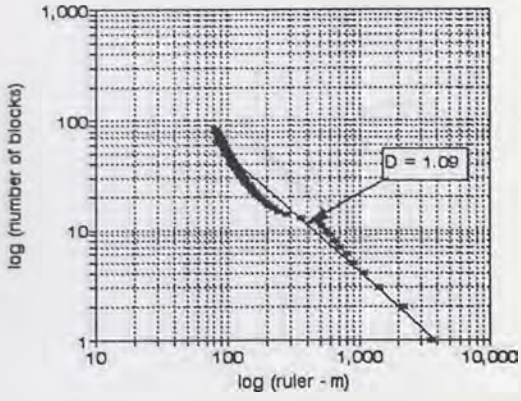

No. 7 Upper Gross Landslide (Width)
Model B Fractal Dimension

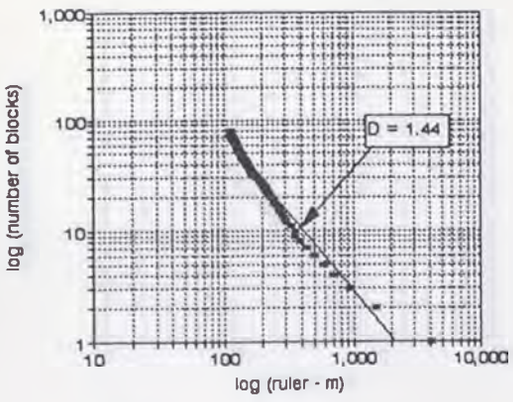

No. 7 Upper Gross Landslide (Length)
Model B Fractal Dimension

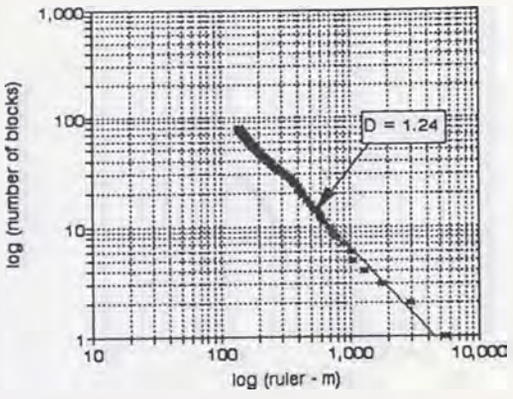

No. 8 Meadow Mt. Landslide (Width)
Model B Fractal Dimension

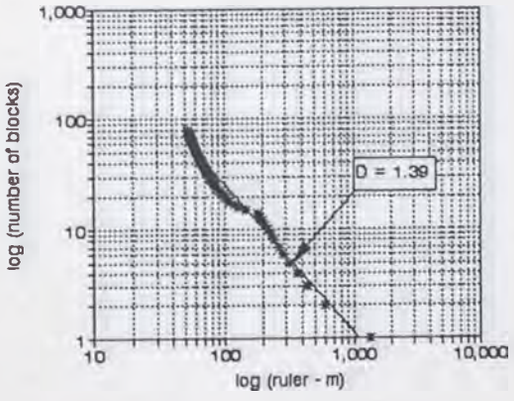

No. 8 Meadow Mt. Landslide (Length)
Model B Fractal Dimension

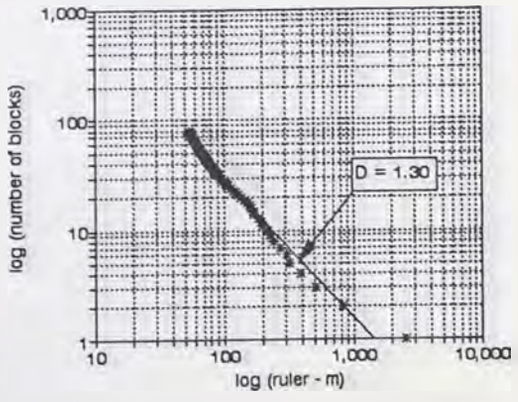

No. 9 Mayunmarca Landslide (Width)
Model B Fractal Dimension

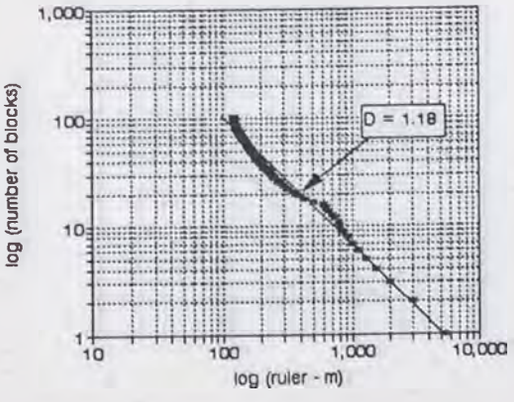

No. 9 Mayunmarca Landslide (Length)
Model B Fractal Dimension

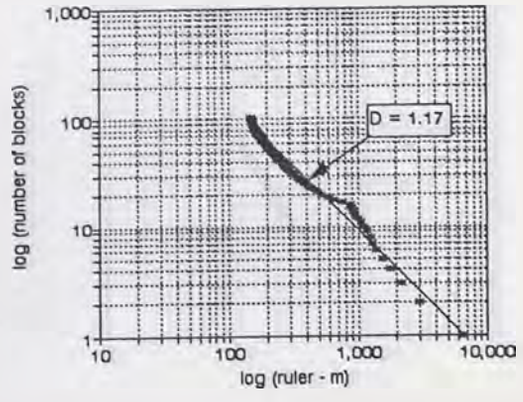

No. 10 La Frasse Landslide (Width)
Model B Fractal Dimension

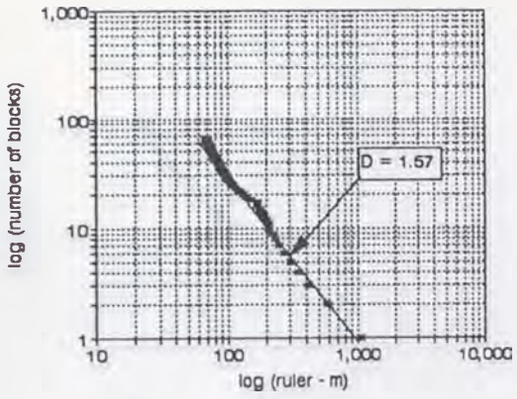

No. 10 La Frasse Landslide (Length)
Model B Fractal Dimension

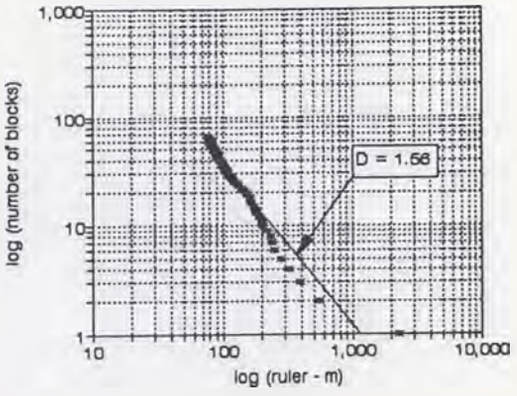

No. 11 Arvey Landslide (Width)
Model B Fractal Dimension

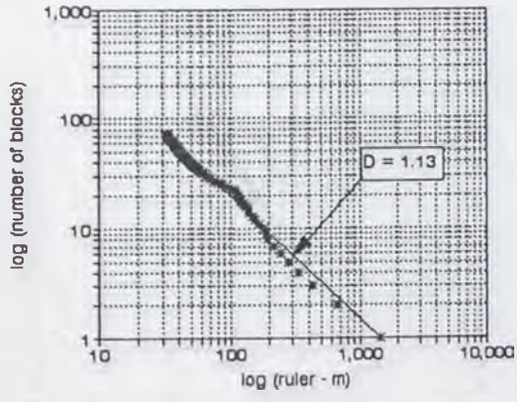

No. 11 Arvey Landslide (Length)
Model B Fractal Dimension

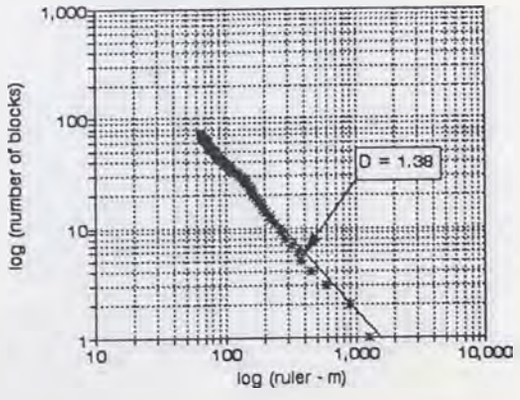

No. 12 Kiritani Landslide (Width)
Model B Fractal Dimension

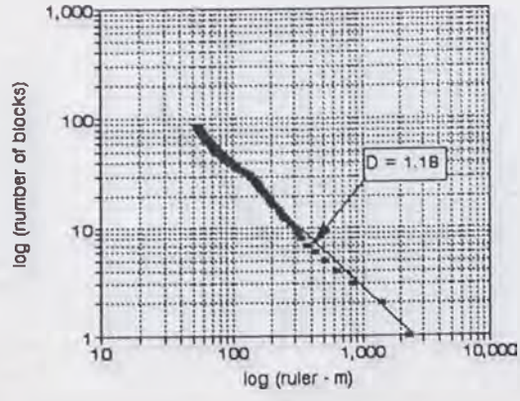

No. 12 Kiritani Landslide (Length)
Model B Fractal Dimension

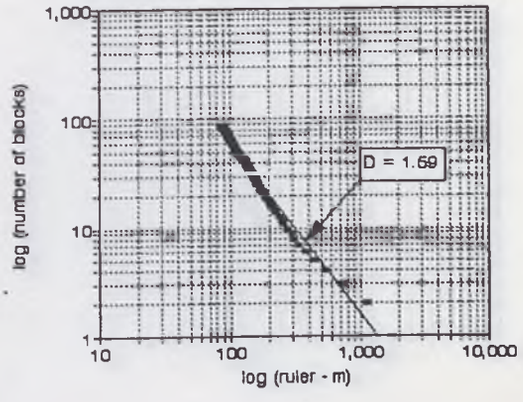

No. 13 Katsurabara Landslide (Width)
Model B Fractal Dimension

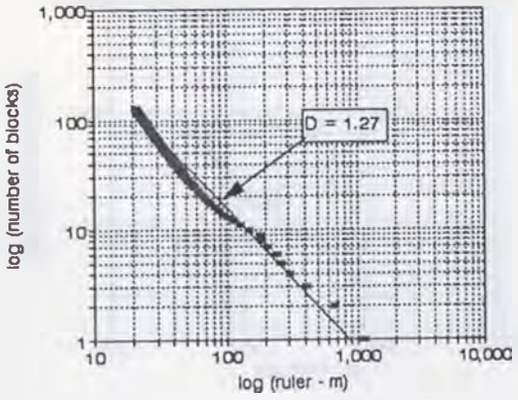

No. 13 Katsurabara Landslide (Length)
Model B Fractal Dimension

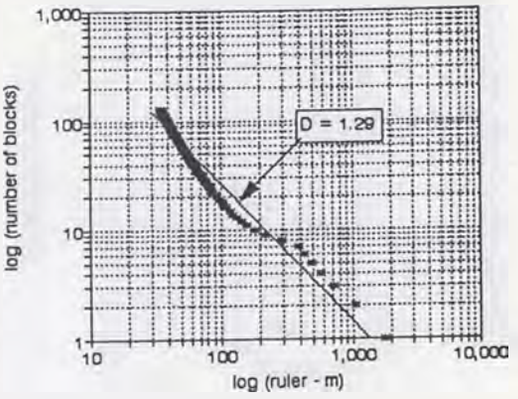

No. 14 Hitohane Landslide (Width)
Model B Fractal Dimension

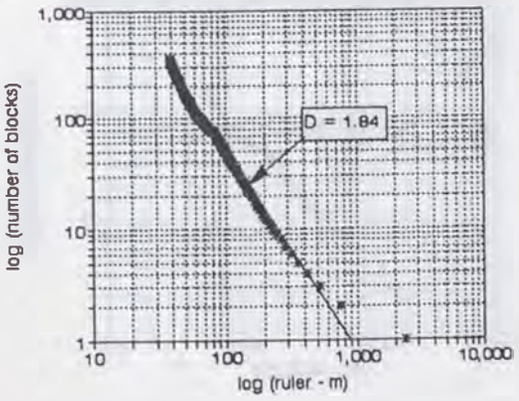

No. 14 Hitohane Landslide (Width)
Model B Fractal Dimension

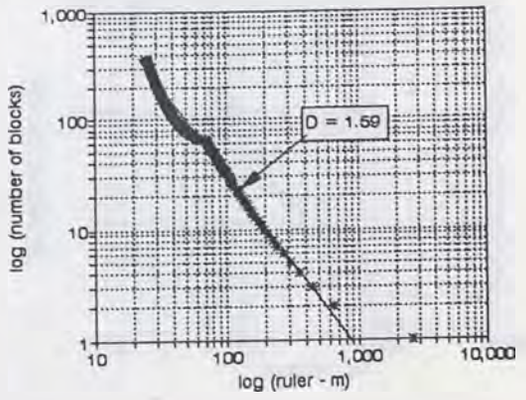

No. 15 Takisaka Landslide (Width)
Model B Fractal Dimension

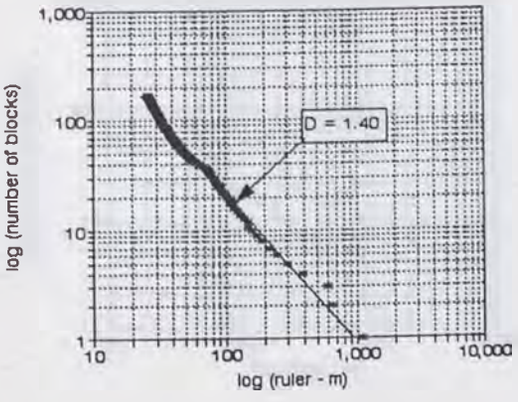

No. 15 Takisaka Landslide (Length)
Model B Fractal Dimension

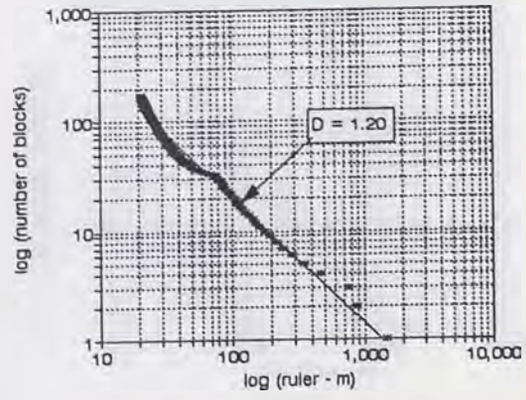

No. 16 Sakae Landslide (Width)
Model B Fractal Dimension

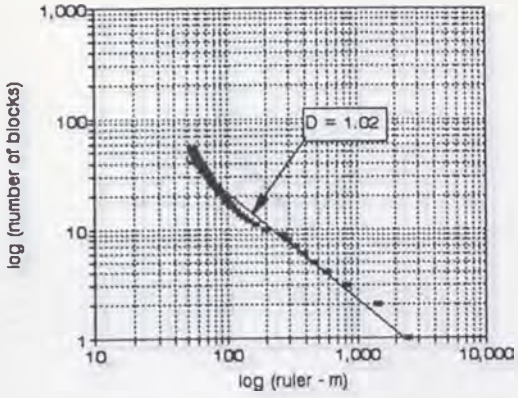

No. 16 Sakae Landslide (Length)
Model B Fractal Dimension

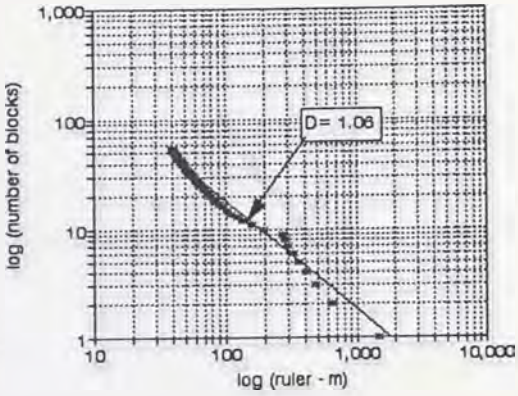

No. 17 Mushigame Landslide (Width)
Model B Fractal Dimension

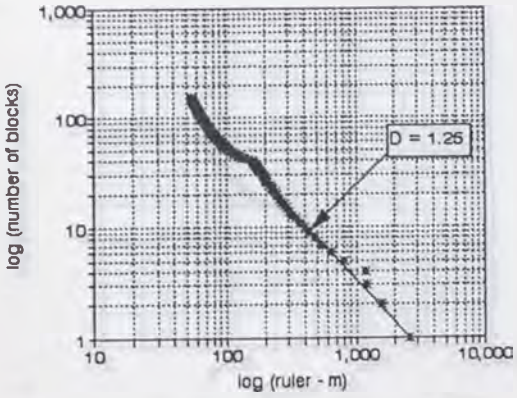

No. 17 Mushigame Landslide (Length)
Model B Fractal Dimension

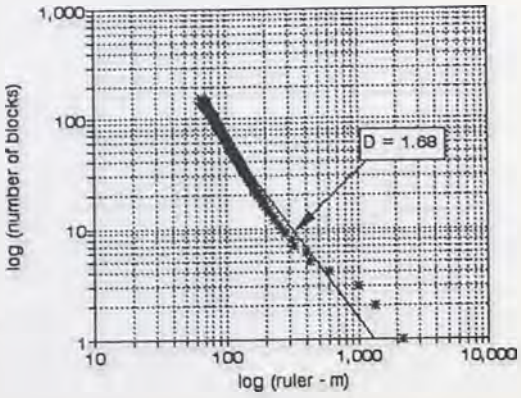

No. 18 Higashinomyo Landslide (Width)
Model B Fractal Dimension

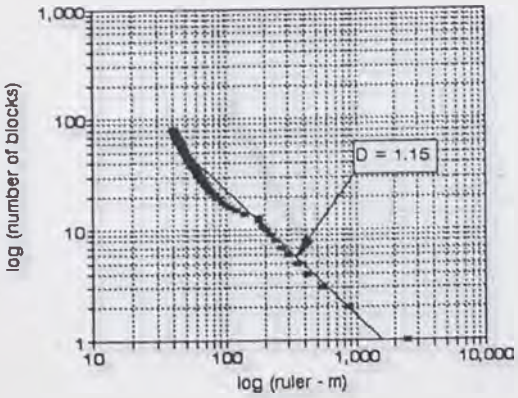

No. 18 Higashinomyo Landslide (Length)
Model B Fractal Dimension

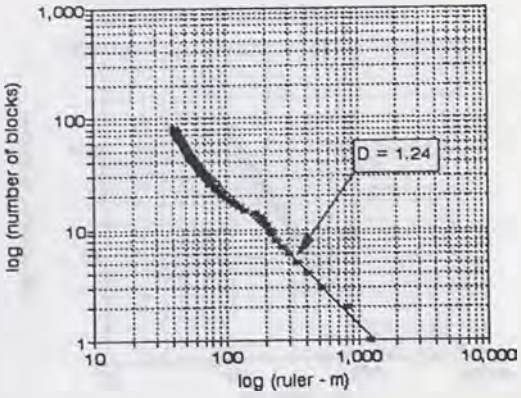

No. 19 Karuizawa Landslide (Width)
Model B Fractal Dimension

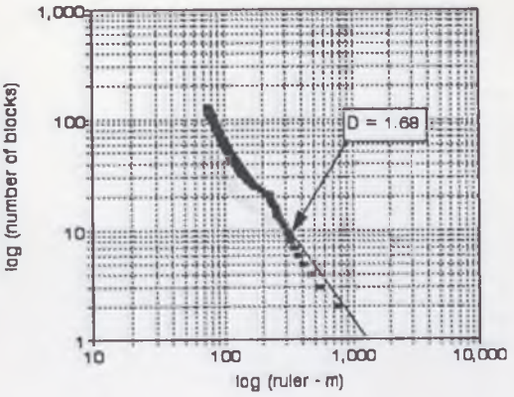

No. 19 Karuizawa Landslide (Length)
Model B Fractal Dimension

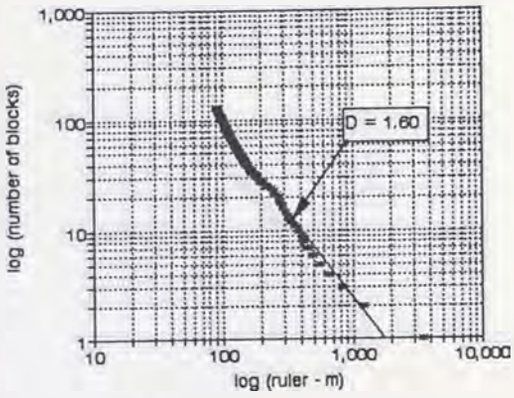

No. 20 Happoudal Landslide (Width)
Model B Fractal Dimension

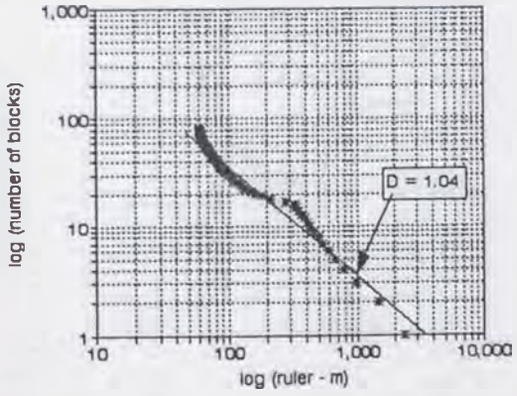

No. 20 Happoudal Landslide (Length)
Model B Fractal Dimension

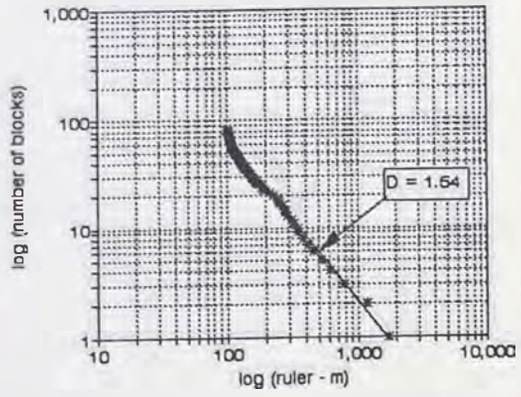

No. 21 Ralden Landslide (Width)
Model B Fractal Dimension

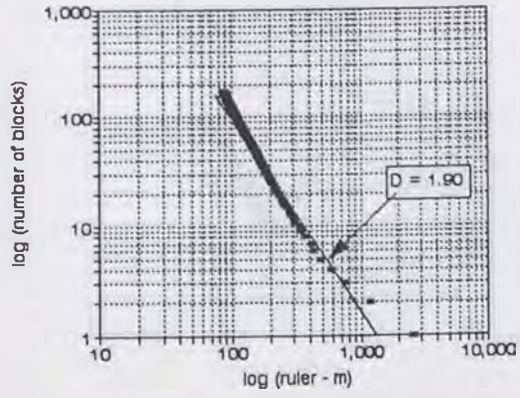

No. 21 Ralden Landslide (Length)
Model B Fractal Dimension

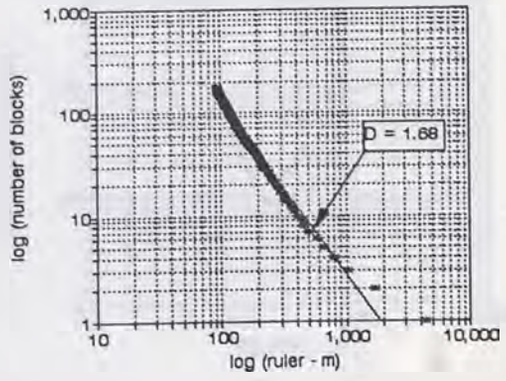

No. 22 Nishinakanoho Landslide (Width)
Model B Fractal Dimension

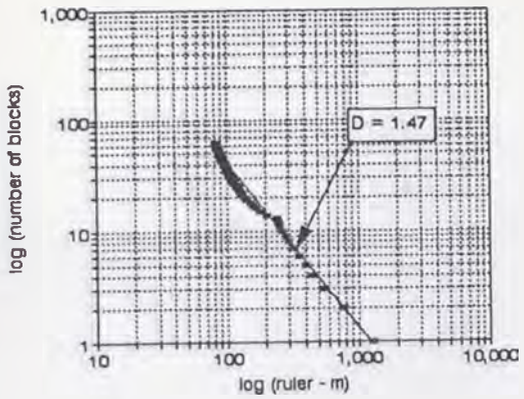

No. 22 Nishinakanoho Landslide (Length)
Model B Fractal Dimension

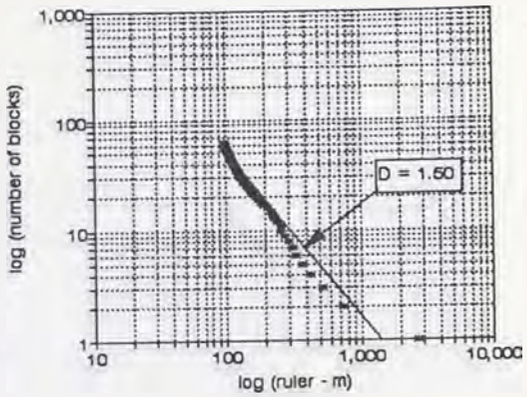

No. 23 Mizunashi Landslide (Width)
Model B Fractal Dimension

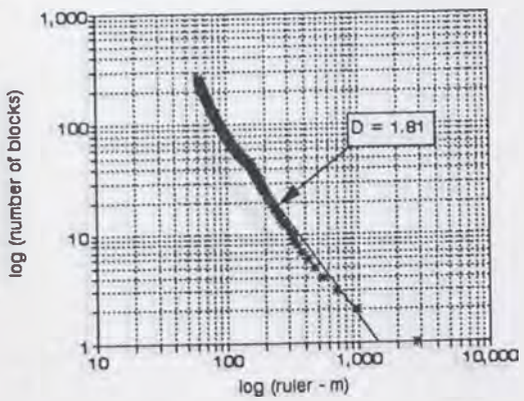

No. 23 Mizunashi Landslide (Length)
Model B Fractal Dimension

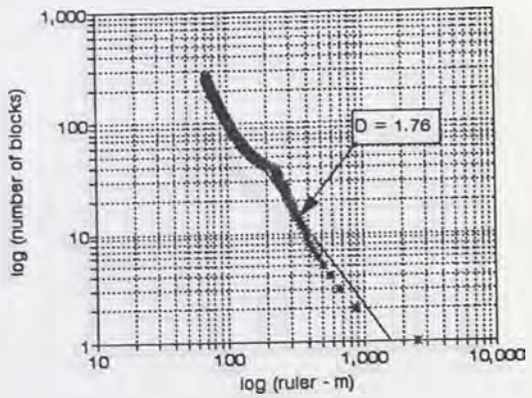

No. 24 Kitaurata Landslide (Width)
Model B Fractal Dimension

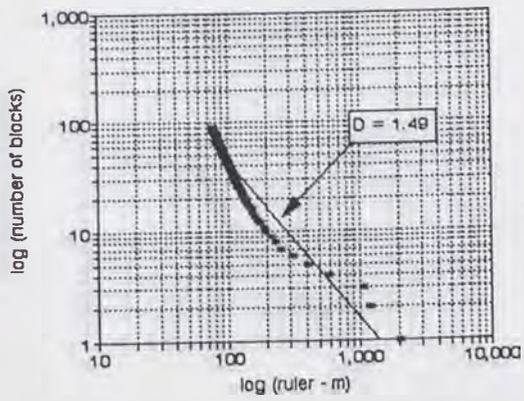

No. 24 Kitaurata Landslide (Length)
Model B Fractal Dimension

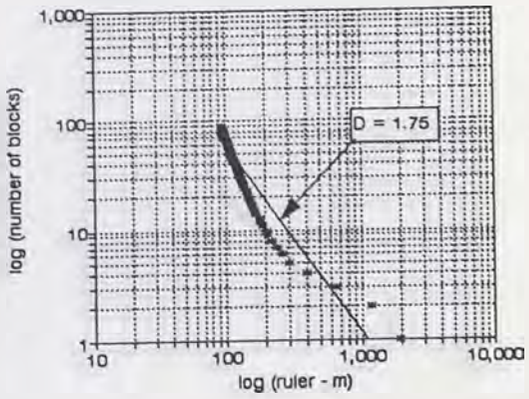

No. 25 Uenoyama Landslide (Width)
Model B Fractal Dimension

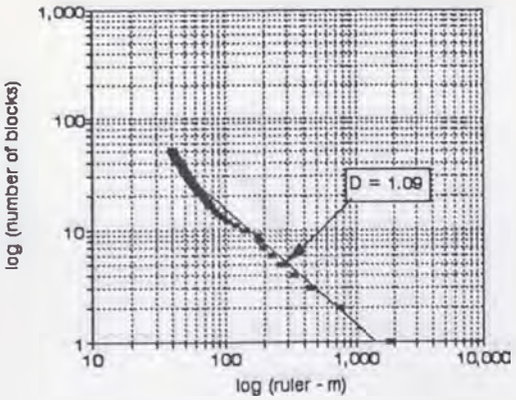

No. 25 Uenoyama Landslide (Length)
Model B Fractal Dimension

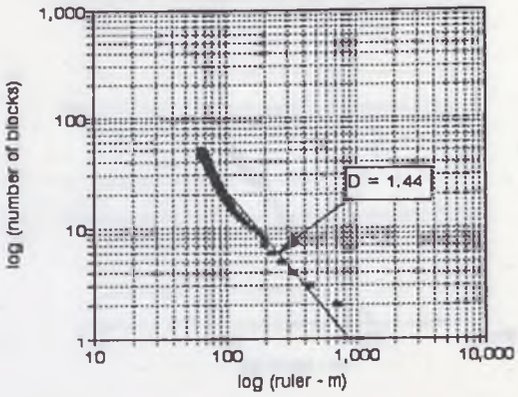

No. 26 Nakatateyama Landslide (Width)
Model B Fractal Dimension

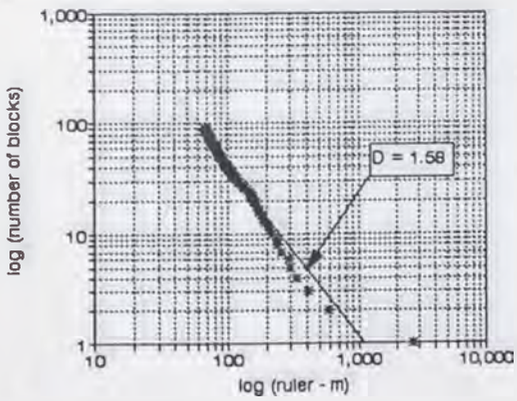

No. 26 Nakatateyama Landslide (Length)
Model B Fractal Dimension

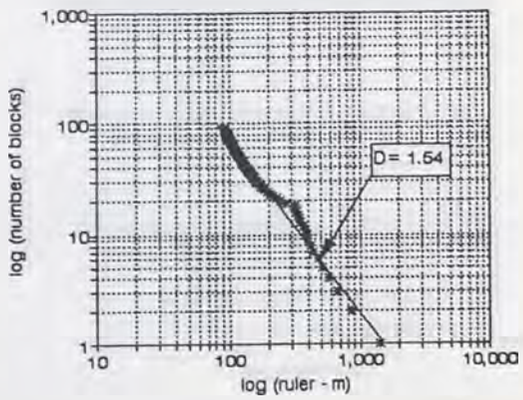

No. 27 Yumoto Landslide (Width)
Model B Fractal Dimension

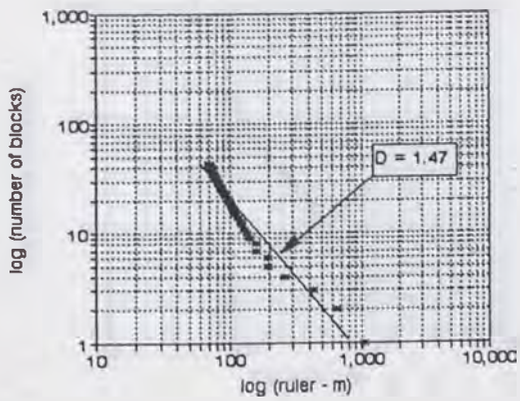

No. 27 Yumoto Landslide (Length)
Model B Fractal Dimension

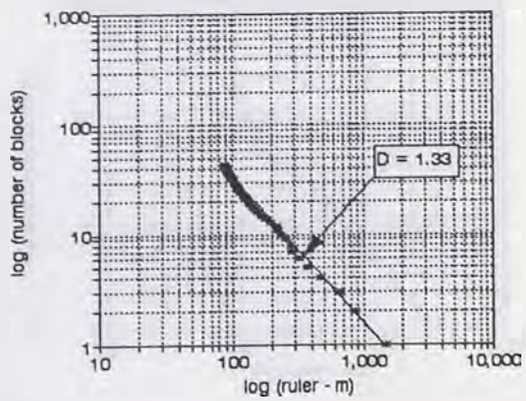

No. 28 Yuyama Landslide (Width)
Model B Fractal Dimension

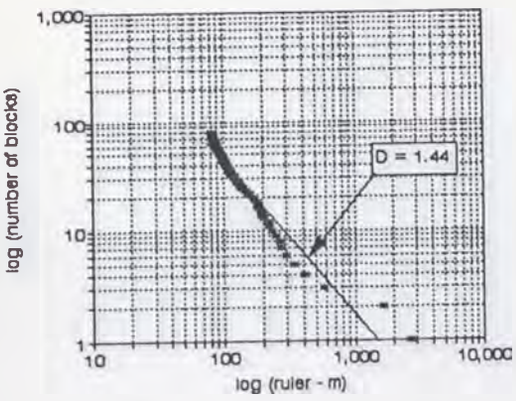

No. 28 Yuyama Landslide (Length)
Model B Fractal Dimension

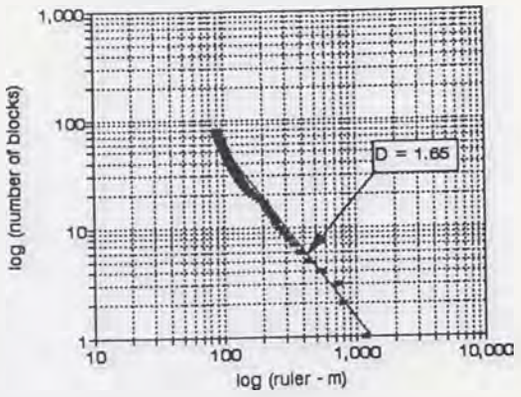

No. 29 Kamatsuka Landslide (Width)
Model B Fractal Dimension

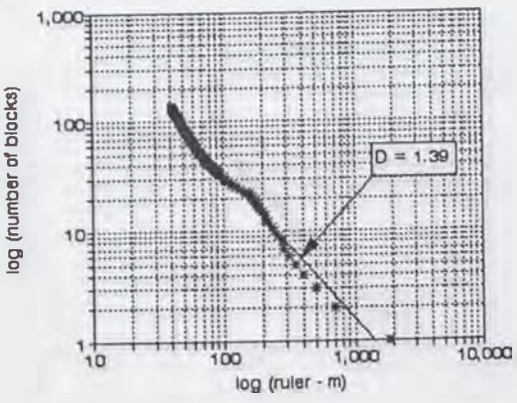

No. 29 Kamatsuka Landslide (Length)
Model B Fractal Dimension

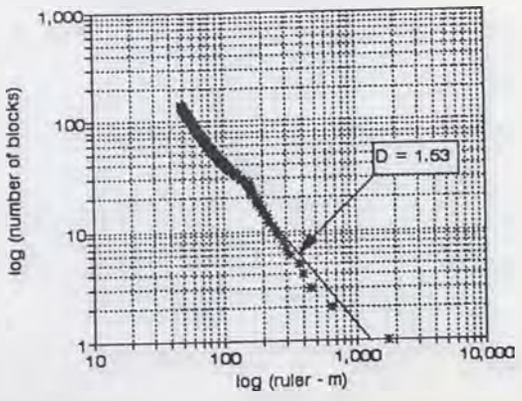

No. 30 Maruyama Landslide (Width)
Model B Fractal Dimension

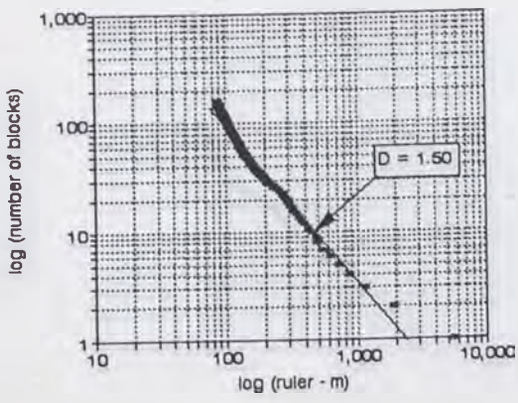

No. 30 Maruyama Landslide (Length)
Model B Fractal Dimension

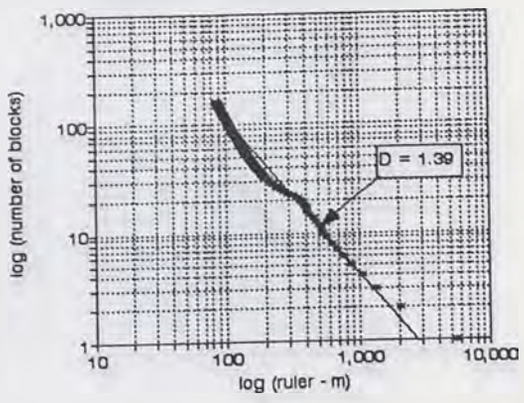

No. 31 Maseguchi Landslide (Width)
Model B Fractal Dimension

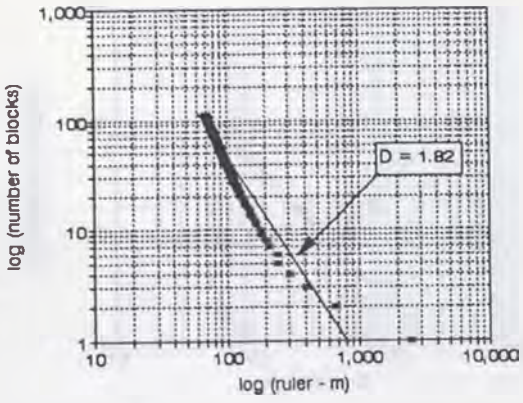

No. 31 Maseguchi Landslide (Length)
Model B Fractal Dimension

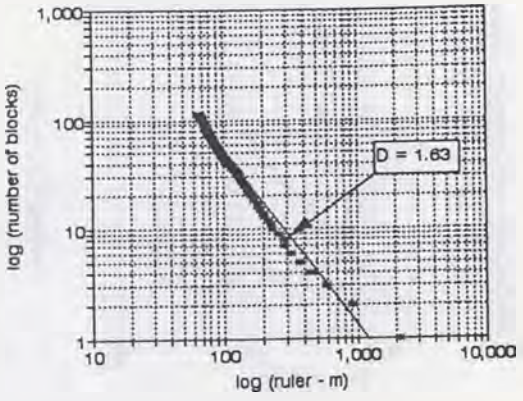

No. 32 Maruta Landslide (Width)
Model B Fractal Dimension

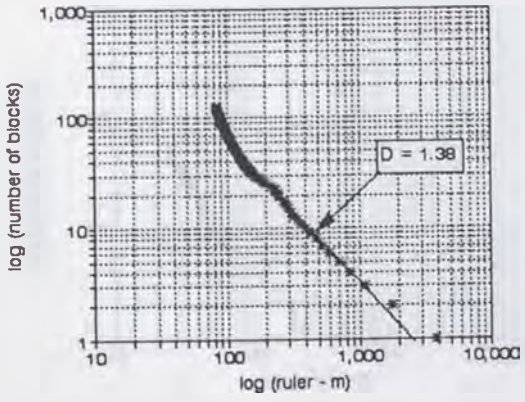

No. 32 Maruta Landslide (Length)
Model B Fractal Dimension

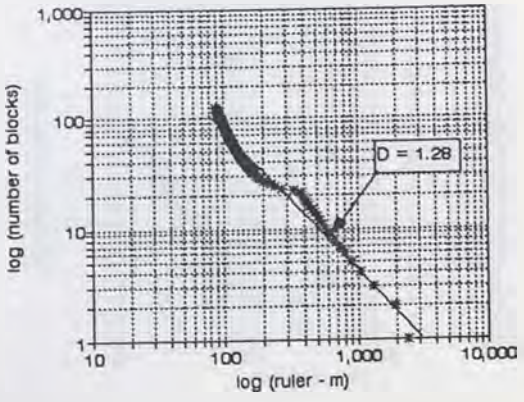

No. 33 Kodomari Landslide (Width)
Model B Fractal Dimension

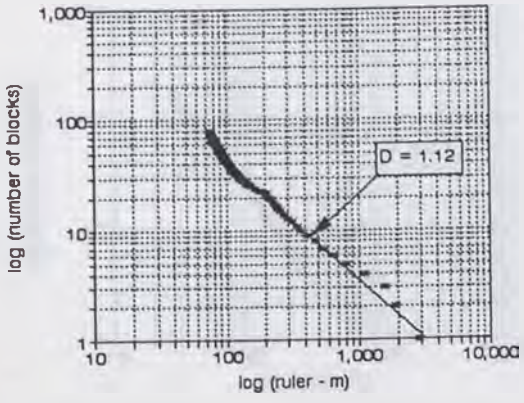

No. 33 Kodomari Landslide (Length)
Model B Fractal Dimension

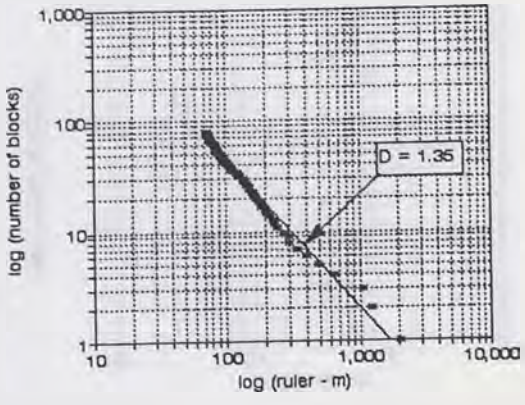

No. 34 Ohbora Landslide (Width)
Model B Fractal Dimension

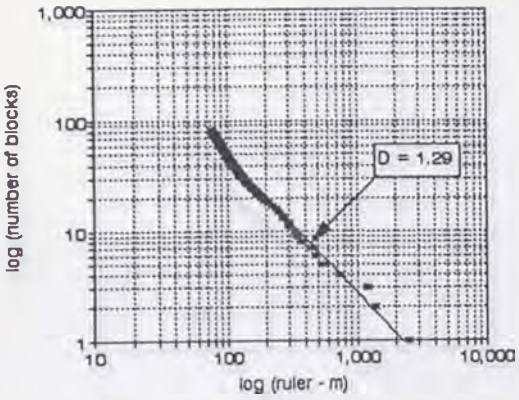

No. 34 Ohbora Landslide (Length)
Model B Fractal Dimension

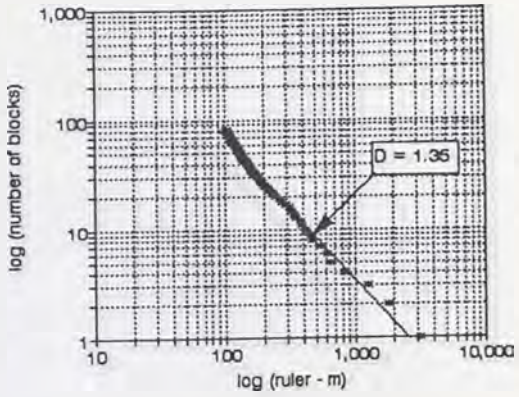

No. 35 Urushinose Landslide (Width)
Model B Fractal Dimension

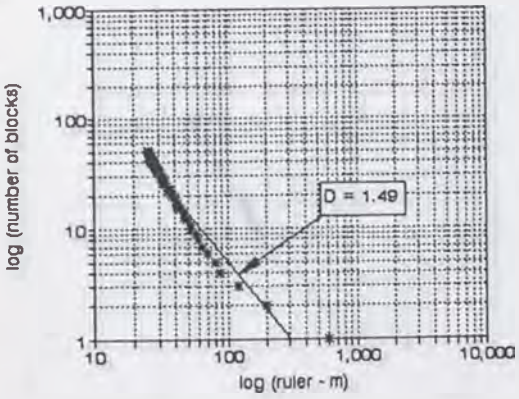

No. 35 Urushinose Landslide (Length)
Model B Fractal Dimension

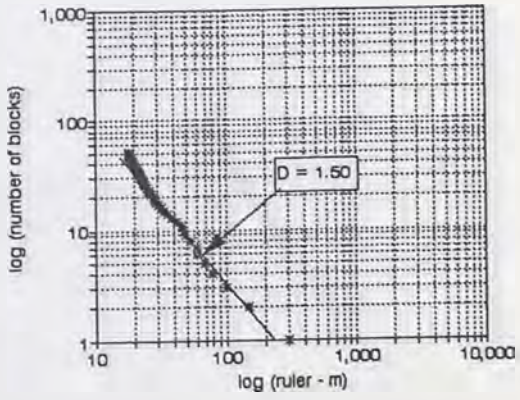

No. 36 Nishinotani Landslide (Width)
Model B Fractal Dimension

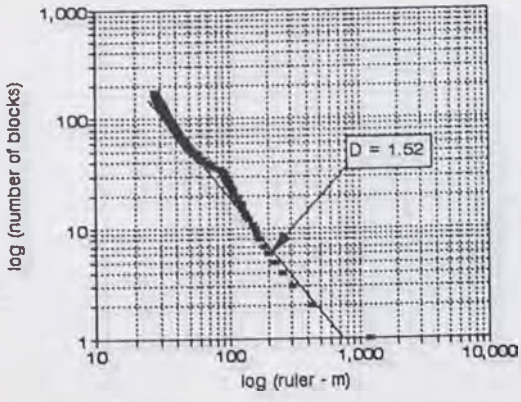

No. 36 Nishinotani Landslide (Length)
Model B Fractal Dimension

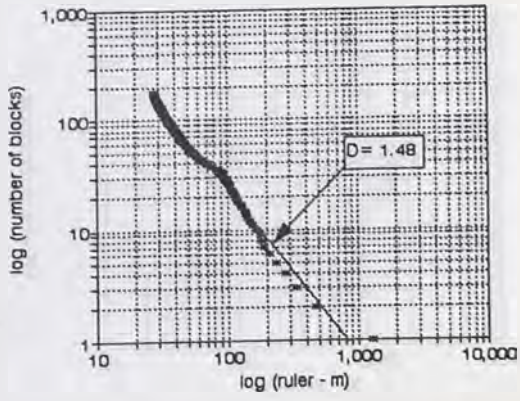

No. 37 Youne Landslide (Width)
Model B Fractal Dimension

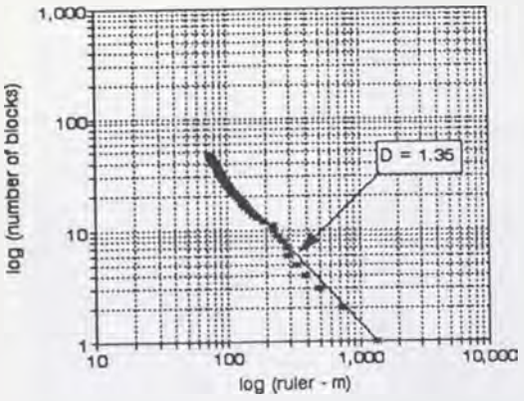

No. 37 Youne Landslide (Length)
Model B Fractal Dimension

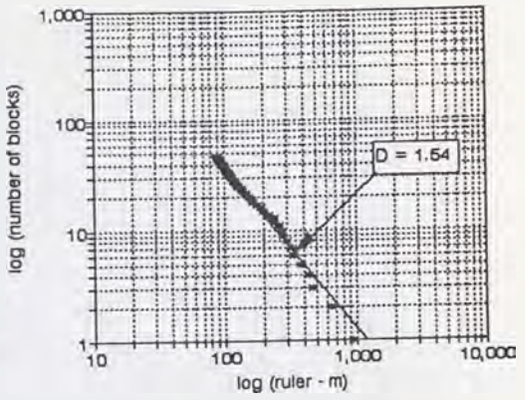

No. 38 Nuta Landslide (Width)
Model B Fractal Dimension

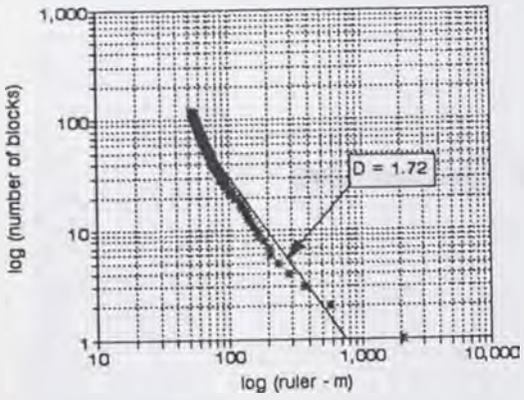

No. 38 Nuta Landslide (Length)
Model B Fractal Dimension

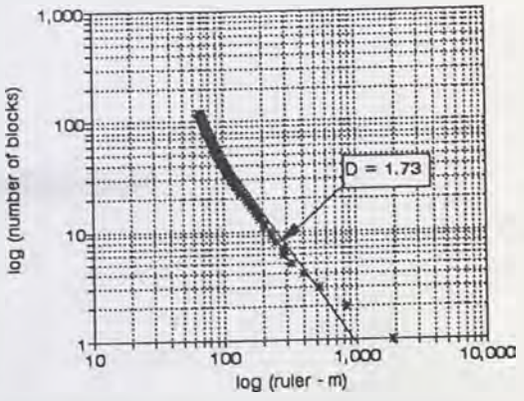

No. 39 Nyuya Landslide (Width)
Model B Fractal Dimension

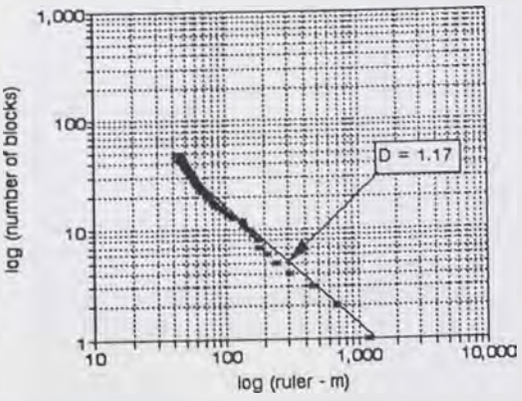

No. 39 Nyuya Landslide (Length)
Model B Fractal Dimension

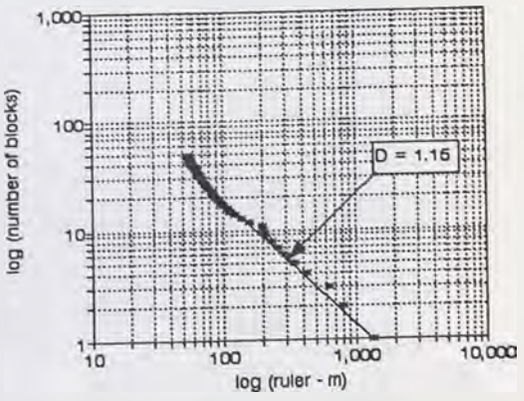

APPENDIX F:

STATISTICAL DATA OF LANDSLIDES

Statistical List of Landslide Blocks

		Whole Blocks						
		# of	width			length		
		blocks	max	average	std. dev	max	average	std. dev
1	Midway Bridge	103	1,930	122.9	191.7	1,690	117.5	181.0
2	Boca Ridge	188	3,500	186.0	235.7	3,000	164.5	245.8
3	Palos Verdes	131	5,240	285.4	476.1	2,500	331.9	333.7
4	Bick Rock Mesa	329	2,140	71.7	142.3	960	66.6	91.8
5	Thristle	84	3,600	330.9	465.8	4,030	378.6	531.8
6	Lower Gross	83	3,410	319.5	449.9	3,600	305.6	488.8
7	Upper Gross	80	4,030	339.0	493.2	5,500	460.7	730.5
8	Meadow Mt.	79	1,350	129.3	168.1	2,560	207.2	317.8
9	Mayunmarca	93	5,400	506.7	638.9	6,500	679.0	822.4
10	La Frasse	67	1,060	159.0	152.0	2,300	223.0	285.1
11	Arvey	73	1,460	121.7	186.1	1,270	169.9	193.5
12	Kiritani	87	2,330	202.7	302.9	1,730	277.4	309.3
13	Katsurabara	131	1,120	85.8	122.2	1,760	121.1	186.8
14	Hitohane	365	2,360	88.2	142.4	2,640	113.4	163.7
15	Takisaka	171	1,100	77.3	118.4	1,470	82.6	148.2
16	Sakae	55	2,500	260.5	397.2	1,500	218.8	218.8
17	Mushigame	156	2,630	169.1	285.0	2,240	182.1	225.4
18	Higashinomyo	81	2,490	139.6	285.4	1,230	142.6	182.4
19	Karuizawa	130	2,300	192.6	231.3	3,500	239.0	349.5
20	Happoudai	71	2,380	254.8	328.4	1,750	275.0	273.4
21	Raiden	176	2,630	212.6	260.8	4,380	218.2	362.5
22	Nishinakanoho	62	1,280	206.3	195.9	2,700	253.4	348.8
23	Mizunashi	263	2,800	118.5	193.4	2,550	131.0	183.7
24	Kitaurata	90	2,040	181.3	288.5	1,950	200.7	253.4
25	Uenoyama	52	1,810	162.4	256.5	1,060	149.0	175.2
26	Nakatateyama	91	2,700	172.0	283.9	1,420	193.4	194.8
27	Yumoto	44	1,060	181.9	189.7	1,470	227.3	253.8
28	Yuyama	80	2,700	191.9	310.0	1,190	178.0	207.6
29	Kamatsuka	138	1,850	124.1	179.5	1,750	168.4	192.8
30	Maruyama	163	5,650	285.6	546.1	5,500	324.9	533.2
31	Maseguchi	113	2,480	177.1	248.9	2,130	191.1	228.4
32	Maruta	124	3,830	224.9	384.6	2,480	253.4	333.7
33	Kodomari	80	2,830	251.1	425.3	2,040	234.7	294.2
34	Ohbora	83	2,510	240.5	317.9	3,090	285.9	361.7
35	Urushinose	51	600	48.8	84.8	300	39.0	49.3
36	Nishinotani	165	1,200	87.5	110.3	1,300	93.4	122.4
37	Youne	47	1,360	190.1	208.7	950	205.4	159.5
38	Nuta	119	2,054	135.6	202.2	1,924	146.5	199.9
39	Nyuuya	30	1,210	210.3	239.3	1,370	254.2	268.5
40	Hikinota							

Statistical List of Landslide Blocks

		Second Level Blocks								
		# of	width				length			
	Simbol	blocks	max	average	midian	std. dev.	max	average	midian	std. dev.
1	Midway Bridge	18	464	222.9	196	77.3	667	246.4	196	137.1
2	Boca Ridge	35	1,813	529.3	411	381.9	2,296	477.3	375	442.2
3	Palos Verdes	22	1,143	590.4	536	223.1	1,714	774.9	702	343.5
4	Bick Rock Mesa	43	463	176.4	133	99.8	511	180.5	143	116.3
5	Thristle	12	2,256	755.0	576	520.8	2,160	906.0	708	598.5
6	Lower Gross	11	1,584	904.4	960	401.8	2,160	925.1	864	522.5
7	Upper Gross	18	1,512	669.3	636	340.9	2,952	938.7	708	688.3
8	Meadow Mt.	12	602	297.2	277	123.8	818	496.5	500	198.9
9	Mayunmarca	13	3,000	1,100.0	900	625.7	3,000	1,684.6	1,750	681.5
10	La Frasse	14	582	303.0	285	121.5	545	385.3	364	116.7
11	Arvey	18	667	211.3	179	139.6	917	298.9	238	203.9
12	Kiritani	23	1,400	384.8	238	287.5	1,150	570.1	450	359.3
13	Katsurabara	6	676	360.4	338	160.0	1,054	563.1	473	224.7
14	Hitohane	57	755	205.9	168	129.0	655	265.1	202	150.2
15	Takisaka	27	598	182.6	127	120.4	760	195.5	137	154.9
16	Sakae	9	1,450	597.2	525	344.6	450	395.8	375	109.0
17	Mushigame	33	1,220	283.4	244	205.3	610	297.5	244	178.3
18	Higashinomyo	11	870	309.6	232	193.4	826	411.1	406	186.2
19	Karuizawa	17	750	470.6	475	165.2	1,200	635.3	575	261.1
20	Happoudai	15	1,475	511.7	450	301.4	1,175	568.3	450	256.5
21	Raiden	25	1,188	577.0	475	237.8	1,675	527.0	500	278.4
22	Nishinakanoho	11	762	448.1	443	148.4	745	501.3	479	144.7
23	Mizunashi	32	995	296.6	257	162.4	878	323.2	286	179.1
24	Kitaurata	14	1,064	441.4	279	347.7	656	401.5	426	148.9
25	Uenoyama	7	745	341.9	319	181.5	724	369.8	301	181.1
26	Nakatateyama	15	585	314.4	301	117.2	869	413.7	408	212.7
27	Yumoto	8	426	270.4	240	102.1	674	407.8	345	153.0
28	Yuyama	13	567	313.7	248	120.3	798	313.7	266	155.2
29	Kamatsuka	17	702	322.9	277	139.3	660	446.8	426	161.7
30	Maruyama	17	1,875	694.1	625	375.7	2,050	948.5	875	418.6
31	Maseguchi	20	674	339.1	248	185.2	922	385.6	310	198.9
32	Maruta	20	1,489	516.8	350	353.3	1,950	693.3	610	416.4
33	Kodomari	18	1,897	403.4	293	393.8	1,064	372.3	310	249.3
34	Ohbora	9	1,200	628.3	636	274.7	1,273	577.8	545	281.9
35	Urushinose	8	200	90.9	82	48.5	150	97.2	97	32.7
36	Nishinotani	27	430	198.7	180	87.5	470	218.5	216	106.5
37	Youne	8	727	358.8	293	159.7	649	362.0	312	127.5
38	Nuta	11	574	375.0	352	138.7	851	407.0	407	197.5
39	Nyuuya	9	460	231.0	190	101.2	635	286.6	246	132.3
40	Hikinota									

Statistical List of Landslide Blocks

		Third Level Blocks								
		# of	width				length			
	Simbol	blocks	max	average	midian	std. dev.	max	average	midian	std. dev.
1	Midway Bridge	84	214	80.0	71	31.5	167	71.2	63	31.4
2	Boca Ridge	153	242	108.0	103	41.8	254	93.3	85	44.8
3	Palos Verdes	108	429	177.5	155	84.1	786	221.6	190	123.9
4	Bick Rock Mesa	284	197	44.9	38	26.7	197	43.7	36	25.6
5	Thristle	71	696	213.2	168	126.6	696	238.0	192	138.9
6	Lower Gross	71	432	185.4	168	79.4	360	163.3	144	66.9
7	Upper Gross	61	360	181.0	168	62.5	1,032	237.0	192	164.1
8	Meadow Mt.	66	178	80.3	80	32.0	308	118.4	96	62.6
9	Mayunmarca	79	800	347.2	300	172.2	1,300	439.9	350	259.5
10	La Frasse	52	206	102.7	97	34.9	242	139.3	127	61.0
11	Arvey	54	190	66.9	57	35.8	357	106.4	95	67.8
12	Kiritani	63	313	102.5	80	53.9	308	147.6	138	60.2
13	Katsurabara	124	261	64.2	54	42.2	297	86.5	78	46.9
14	Hitohane	307	173	58.9	55	26.6	223	77.0	68	36.7
15	Takisaka	142	147	45.4	39	23.4	108	46.0	42	20.5
16	Sakae	39	263	128.8	113	47.0	275	146.9	125	62.6
17	Mushigame	119	244	94.3	73	42.6	427	120.6	98	65.9
18	Higashinomyo	69	174	78.3	72	32.0	217	84.0	72	37.5
19	Karuizawa	112	313	131.6	113	53.5	425	149.8	125	68.6
20	Happoudai	55	275	146.1	138	53.9	350	168.2	150	64.2
21	Raiden	150	425	104.5	125	59.8	450	88.5	125	62.6
22	Nishinakanoho	50	248	131.8	124	37.9	319	150.0	142	53.2
23	Mizunashi	230	321	82.1	71	44.4	388	93.7	82	46.1
24	Kitaurata	74	230	95.1	89	31.0	266	123.8	124	42.2
25	Uenoyama	44	186	96.5	80	38.0	195	93.1	89	31.9
26	Nakatateyama	75	301	109.9	106	47.8	390	133.0	124	60.2
27	Yumoto	34	195	115.0	106	32.5	284	128.8	106	46.6
28	Yuyama	65	266	118.1	89	42.3	248	116.2	89	36.7
29	Kamatsuka	120	277	81.6	64	45.3	404	115.9	106	67.7
30	Maruyama	144	475	151.3	156	77.9	525	145.1	175	88.8
31	Maseguchi	92	248	116.8	106	38.9	284	127.8	106	49.5
32	Maruta	103	301	133.2	124	51.9	337	146.3	133	56.2
33	Kodomari	60	248	130.8	124	44.5	301	143.0	124	60.4
34	Ohbora	72	473	139.6	127	74.6	618	186.6	164	99.0
35	Urushinose	42	80	27.7	26	16.3	60	21.7	20	13.5
36	Nishinotani	137	160	57.5	50	27.6	180	59.9	52	31.5
37	Youne	39	286	125.4	104	55.1	442	154.2	130	78.7
38	Nuta	107	204	93.1	83	37.7	287.0	103.1	93	45.4
39	Nyuuya	19	175	113.6	111	30.1	206	143.3	143	34.4
40	Hikinota									

APPENDIX G:

FRACTAL DIMENSION LISTS

Fractal Dimensions of Landslides in each Geology Area

No		Width			Length			Width/Length		
		Whole	2nd	3rd	Whole	2nd	3rd	Whole	2nd	3rd
	MUDSTONE									
14	Hitohane	1.64	1.84	3.80	1.66	1.83	3.96	0.99	1.01	0.96
16	Sakae	1.12	1.22	2.41	1.42	2.36	2.00	0.79	0.52	1.21
17	Mushigame	1.31	1.72	3.17	1.56	1.67	2.59	0.84	1.03	1.22
18	Higashinomyo	1.22	1.51	2.88	1.29	1.58	2.56	0.95	0.96	1.13
19	Karuizawa	1.61	2.30	3.29	1.43	1.82	3.08	1.13	1.26	1.07
20	Happoudai	1.35	1.78	2.63	1.46	1.73	3.25	0.92	1.03	0.81
21	Raiden	1.53	2.03	3.16	1.48	1.85	3.19	1.03	1.10	0.99
22	Nishinakanoho	1.51	2.09	3.53	1.35	2.00	3.32	1.12	1.05	1.06
24	Kitaurata	1.19	1.13	3.95	1.43	1.41	4.17	0.83	0.80	0.95
31	Masoguchi	1.49	1.39	3.56	1.54	1.53	3.15	0.97	0.91	1.13
32	Maruta	1.37	1.46	3.58	1.36	1.83	3.50	1.01	0.80	1.02
	average	1.39	1.68	3.27	1.45	1.78	3.16	0.96	0.95	1.05
	std. deviation	0.166	0.355	0.459	0.100	0.243	0.591	0.106	0.186	0.116
	SS, MS									
3	Palos Verdes	1.48	1.84	2.21	1.57	2.59	2.08	0.94	0.71	1.06
4	Big Rock Mesa	1.48	1.86	3.39	1.53	1.63	3.37	0.97	1.14	1.01
25	Uenoyama	1.25	1.34	2.45	1.32	1.38	3.50	0.95	0.97	0.70
29	Kamatsuka	1.46	1.96	2.49	1.55	1.94	2.28	0.94	1.01	1.09
30	Maruyama	1.34	1.45	2.92	1.33	1.65	2.77	1.01	0.88	1.05
33	Kodomari	1.21	1.29	3.42	1.38	1.43	2.88	0.88	0.90	1.19
34	Ohbora	1.18	1.39	2.34	1.33	1.63	2.39	0.89	0.85	0.98
	average	1.34	1.59	2.75	1.43	1.75	2.75	0.94	0.92	1.01
	std. deviation	0.122	0.263	0.464	0.106	0.382	0.502	0.042	0.125	0.141
	TUFF									
15	Takisaka	1.36	1.57	2.86	1.30	1.44	3.02	1.05	1.09	0.95
23	Mizunashi	1.60	1.84	3.27	1.64	2.60	3.18	0.98	0.71	1.03
26	Nakatateyama	1.44	1.96	2.89	1.58	2.68	2.99	0.91	0.73	0.97
27	Yumoto	1.40	1.41	3.41	1.30	1.86	3.00	1.08	0.76	1.14
28	Yuyama	1.40	2.15	3.50	1.47	1.89	4.14	0.95	1.14	0.85
	average	1.44	1.79	3.19	1.46	2.09	3.27	0.99	0.88	0.98
	std. devistion	0.084	0.266	0.264	0.140	0.474	0.442	0.061	0.188	0.096
	VOLCANIC									
1	Midway Bridge	1.53	2.77	3.27	1.42	1.79	2.90	1.08	1.55	1.13
2	Boca Ridge	1.33	1.49	3.62	1.29	1.35	3.01	1.03	1.10	1.20
12	Kiritani	1.24	1.36	2.34	1.34	1.46	3.34	0.93	0.93	0.70
13	Katsurabara	1.38	1.37	1.90	1.44	1.82	2.26	0.96	0.75	0.84
	average	1.37	1.75	2.78	1.37	1.61	2.88	1.00	1.08	0.97
	std. deviation	0.105	0.593	0.692	0.061	0.204	0.392	0.060	0.295	0.205
	MESOZOIC									
5	Thristle	1.32	1.31	2.13	1.29	1.15	2.08	1.02	1.14	1.02
6	Lower Gross	1.28	1.30	2.17	1.17	1.62	2.89	1.09	0.80	0.75
7	Upper Gros	1.30	1.44	3.51	1.20	1.36	2.05	1.08	1.06	1.71
8	Meadow	1.43	2.15	3.41	1.24	1.48	2.41	1.15	1.45	1.41
9	Mayunmarca	1.52	1.64	2.31	1.40	2.10	2.02	1.09	0.78	1.14
36	Nishinotani	1.54	2.09	2.82	1.52	2.00	2.65	1.01	1.05	1.06
	average	1.40	1.66	2.73	1.30	1.62	2.35	1.08	1.05	1.18
	std. deviation	0.105	0.348	0.567	0.122	0.337	0.331	0.047	0.225	0.306
	SCHIST									
10	La Frasse	1.59	2.13	3.57	1.36	2.11	3.49	1.17	1.01	1.02
11	Arvey	1.24	1.58	2.24	1.42	1.54	2.33	0.87	1.03	0.96
35	Urushinose	1.11	1.33	3.24	1.31	1.76	3.11	0.85	0.76	1.04
37	Youne	1.35	1.77	2.71	1.62	2.11	2.29	0.83	0.84	1.18
38	Nuta	1.46	1.58	3.46	1.50	1.47	3.24	0.97	1.07	1.07
39	Nyuya	1.22	1.73	2.65	1.30	1.79	2.77	0.94	0.97	0.96
40	Hikinota	1.19								
	average	1.31	1.69	2.98	1.42	1.80	2.87	0.94	0.95	1.04
	std. deviation	0.156	0.243	0.479	0.113	0.248	0.450	0.114	0.112	0.076

Fractal Dimension of Each Dipping Type

			Fractal Dimension	
No	Landslide	Dip	width	length
1	Midway Bridge	90	1.53	1.42
5	Thristle	60	1.32	1.29
38	Nuta	45	1.46	1.50
17	Mushigame	35	1.31	1.56
30	Maruyama	35	1.34	1.33
20	Happoudai	30	1.35	1.46
23	Mizunashi	30	1.60	1.64
27	Yumoto	30	1.40	1.30
28	Yuyama	30	1.40	1.47
31	Maseguchi	30	1.49	1.54
39	Nyuuya	30	1.22	1.30
19	Karuizawa	25	1.61	1.43
6	Lower Gross	20	1.28	1.17
7	Upper Gross	20	1.30	1.20
16	Sakae	20	1.12	1.42
25	Uenoyama	20	1.25	1.32
26	Nakatateyama	20	1.44	1.58
3	Palos Verdes	15	1.48	1.57
8	Meadow Mt.	15	1.43	1.24
9	Mayunmarca	15	1.52	1.40
10	La Frasse	15	1.59	1.36
32	Maruta	15	1.37	1.36
33	Kodomari	15	1.21	1.38
37	Youne	15	1.35	1.62
14	Hitohane	13	1.64	1.66
2	Boca Ridge	10	1.33	1.29
13	Katsurabara	10	1.38	1.44
15	Takisaka	5	1.36	1.30
	average	25.464	1.396	1.413
	std. deviation	16.917	0.127	0.132
12	Kiritani	0	1.24	1.34
21	Raiden	0	1.53	1.48
22	Nishinakanoho	0	1.51	1.35
36	Nishinotani	0	1.54	1.52
	average	0.000	1.455	1.423
	std. deviation	0.000	0.125	0.079
34	Ohbora	-15	1.18	1.33
29	Kamatsuka	-25	1.46	1.55
18	Higashinomyo	-30	1.22	1.29
24	Kitaurata	-30	1.19	1.43
4	Bick Rock Mes	-40	1.48	1.53
35	Urushinose	-60	1.11	1.31
	average	-33.333	1.273	1.407
	std. deviation	14.044	0.143	0.104
11	Arvey		1.24	1.42
40	Hikinota		1.19	

Fractal Dimension and Length/Width of Each Topography

No.	Landslide	Length/Width	Topography	Fractal Dimension	
				Width	Length
3	Palos Verdes	0.48	1	1.48	1.57
8	Meadow Mt.	1.90	1	1.43	1.24
9	Mayunmarca	1.20	1	1.52	1.40
16	Sakae	0.60	1	1.12	1.42
17	Mushigame	0.85	1	1.31	1.56
24	Kitaurata	0.96	1	1.19	1.43
34	Ohbora	1.23	1	1.18	1.33
36	Nishinotani	1.08	1	1.54	1.52
37	Youne	0.70	1	1.35	1.62
39	Nyuuya	1.13	2	1.22	1.30
	mean	1.013		1.334	1.439
	std, deviation	0.383		0.145	0.120
11	Arvey	0.87	2	1.24	1.42
27	Yumoto	1.39	2	1.40	1.30
28	Yuyama	0.44	2	1.40	1.47
33	Kodomari	0.72	2	1.21	1.38
	mean	0.855		1.313	1.393
	std, deviation	0.344		0.088	0.062
1	Midway Bridge	0.88	3	1.53	1.42
4	Bick Rock Mesa	0.45	3	1.48	1.53
5	Thristle	1.12	3	1.32	1.29
6	Lower Gross	1.06	3	1.28	1.17
10	La Frasse	2.17	3	1.59	1.36
12	Kiritani	0.74	3	1.24	1.34
13	Katsurabara	1.57	3	1.38	1.44
14	Hitohane	1.12	3	1.64	1.66
18	Higashinomyo	0.49	3	1.22	1.29
19	Karuizawa	1.52	3	1.61	1.43
20	Happoudai	0.74	3	1.35	1.46
23	Mizunashi	0.91	3	1.60	1.64
25	Uenoyama	0.59	3	1.25	1.32
26	Nakatateyama	0.53	3	1.44	1.58
29	Kamatsuka	0.95	3	1.46	1.55
30	Maruyama	0.97	3	1.34	1.33
31	Maseguchi	0.86	3	1.49	1.54
32	Maruta	0.65	3	1.37	1.36
35	Urushinose	0.50	3	1.11	1.31
38	Nuta	0.94	3	1.46	1.50
40	Hikinota	1.08	3	1.19	
	mean	0.944		1.398	1.426
	std, deviation	0.406		0.147	0.127
2	Boca Ridge	0.86	4	1.33	1.29
7	Upper Gross	1.36	4	1.30	1.20
15	Takisaka	1.34	4	1.36	1.30
21	Raiden	1.67	4	1.53	1.48
22	Nishinakanoho	2.11	4	1.51	1.35
	mean	1.467		1.406	1.324
	std, deviation	0.413		0.095	0.092

Fractal Dimension and Length/Width of Each Block Shape

No.	Landslide	Length/Width	Slide Shape	Fractal Dimension	
				Width	Length
9	Mayunmarca	1.20	bottle (4)	1.52	1.40
27	Yumoto	1.39	bottle (4)	1.40	1.30
39	Nyuuya	1.13	bottle (4)	1.22	1.30
	mean	1.241		1.380	1.333
	std, deviation	0.107		0.123	0.047
2	Boca Ridge	0.86	horse (2)	1.33	1.29
4	Bick Rock Mesa	0.45	horse (2)	1.48	1.53
5	Thristle	1.12	horse (2)	1.32	1.29
6	Lower Gros	1.06	horse (2)	1.28	1.17
8	Meadow Mt.	1.90	horse (2)	1.43	1.24
11	Arvey	0.87	horse (2)	1.24	1.42
12	Kiritani	0.74	horse (2)	1.24	1.34
14	Hitohane	1.12	horse (2)	1.64	1.66
16	Sakae	0.60	horse (2)	1.12	1.42
17	Mushigame	0.85	horse (2)	1.31	1.56
23	Mizunashi	0.91	horse (2)	1.60	1.64
24	Kitaurata	0.96	horse (2)	1.19	1.43
25	Uenoyama	0.59	horse (2)	1.25	1.32
32	Maruta	0.65	horse (2)	1.37	1.36
33	Kodomari	0.72	horse (2)	1.21	1.38
34	Ohbora	1.23	horse (2)	1.18	1.33
35	Urushinose	0.50	horse (2)	1.11	1.31
36	Nishinotani	1.08	horse (2)	1.54	1.52
37	Youne	0.70	horse (2)	1.35	1.62
40	Hikinota	1.08	horse (2)	1.19	
	mean	0.899		1.319	1.412
	std, deviation	0.317		0.148	0.137
1	Midway Bridge	0.88	rectangle (3)	1.53	1.42
3	Palos Verdes	0.48	rectangle (3)	1.48	1.57
7	Upper Gros	1.36	rectangle (3)	1.30	1.20
10	La Frasse	2.17	rectangle (3)	1.59	1.36
13	Katsurabara	1.57	rectangle (3)	1.38	1.44
15	Takisaka	1.34	rectangle (3)	1.36	1.30
18	Higashinomyo	0.49	rectangle (3)	1.22	1.29
20	Happoudai	0.74	rectangle (3)	1.35	1.46
21	Raiden	1.67	rectangle (3)	1.53	1.48
22	Nishinakanoho	2.11	rectangle (3)	1.51	1.35
26	Nakatateyama	0.53	rectangle (3)	1.44	1.58
28	Yuyama	0.44	rectangle (3)	1.40	1.47
29	Kamatsuka	0.95	rectangle (3)	1.46	1.55
31	Maseguchi	0.86	rectangle (3)	1.49	1.54
	mean	1.112		1.431	1.429
	std, deviation	0.574		0.098	0.112
19	Karuizawa	1.52	triangle (1)	1.61	1.43
30	Maruyama	0.97	triangle (1)	1.34	1.33
38	Nuta	0.94	triangle (1)	1.46	1.50
	mean	1.144		1.470	1.420
	std, deviation	0.268		0.110	0.070

Fractal Dimension and Length/Width of each Activity Level

No	Landslide	Activity	Length/Width	Fractal Dimension	
				Width	Length
2	Boca Ridge	Ancient	0.86	1.33	1.29
7	Upper Gross	Ancient	1.36	1.30	1.20
16	Sakae	Ancient	0.60	1.12	1.42
19	Karuizawa	Ancient	1.52	1.61	1.43
24	Kitaurata	Ancient	0.96	1.19	1.43
25	Uenoyama	Ancient	0.59	1.25	1.32
	mean		0.981	1.300	1.348
	std. deviation		0.355	0.155	0.086
1	Midway Bridge	Stable	0.88	1.53	1.42
12	Kiritani	Stable	0.74	1.24	1.34
13	Katsurabara	Stable	1.57	1.38	1.44
20	Happoudai	Stable	0.74	1.35	1.46
21	Raiden	Stable	1.67	1.53	1.48
22	Nishinakanoho	Stable	2.11	1.51	1.35
28	Yuyama	Stable	0.44	1.40	1.47
30	Maruyama	Stable	0.97	1.34	1.33
32	Maruta	Stable	0.65	1.37	1.36
33	Kodomari	Stable	0.72	1.21	1.38
35	Urushinose	Stable	0.50	1.11	1.31
	mean		0.998	1.361	1.395
	std. deviation		0.515	0.129	0.059
4	Bick Rock Mesa	Dormant	0.45	1.48	1.53
5	Thristle	Dormant	1.12	1.32	1.29
6	Lower Gross	Dormant	1.06	1.28	1.17
8	Meadow Mt.	Dormant	1.90	1.43	1.24
9	Mayunmarca	Dormant	1.20	1.52	1.40
14	Hitohane	Dormant	1.12	1.64	1.66
17	Mushigame	Dormant	0.85	1.31	1.56
26	Nakatateyama	Dormant	0.53	1.44	1.58
27	Yumoto	Dormant	1.39	1.40	1.30
29	Kamatsuka	Dormant	0.95	1.46	1.55
34	Ohbora	Dormant	1.23	1.18	1.33
40	Hikinota	Dormant	1.08	1.19	
	mean		1.072	1.388	1.419
	std. deviation		0.363	0.130	0.156
3	Palos Verdes	Active	0.48	1.48	1.57
10	La Frasse	Active	2.17	1.59	1.36
11	Arvey	Active	0.87	1.24	1.42
15	Takisaka	Active	1.34	1.36	1.30
18	Higashinomyo	Active	0.49	1.22	1.29
23	Mizunashi	Active	0.91	1.60	1.64
31	Maseguchi	Active	0.86	1.49	1.54
36	Nishinotani	Active	1.08	1.54	1.52
37	Youne	Active	0.70	1.35	1.62
38	Nuta	Active	0.94	1.46	1.50
39	Nyuuya	Active	1.13	1.22	1.30
	mean		0.997	1.414	1.460
	std. deviation		0.445	0.137	0.126

Coefficient of Correlation of log(N(r)) versus log(r) Plot of Landslide Blocks

No.		Width			Length		
		Whole	2nd	3rd	Whole	2nd	3rd
1	Midway Bridge	0.966	0.994	0.990	0.986	0.972	0.992
2	Boca Ridge	0.997	0.983	0.954	0.996	0.993	0.983
3	Palos Verdes	0.975	0.967	0.971	0.988	0.974	0.972
4	Big Rock Mesa	0.992	0.971	0.994	0.995	0.956	0.992
5	Thristle	0.992	0.990	0.970	0.990	0.977	0.965
6	Lower Gross	0.990	0.956	0.914	0.992	0.984	0.943
7	Upper Gros	0.993	0.980	0.956	0.997	0.989	0.991
8	Meadow	0.992	0.988	0.953	0.990	0.835	0.969
9	Mayunmarca	0.983	0.986	0.883	0.990	0.898	0.965
10	La Frasse	0.991	0.945	0.980	0.992	0.975	0.930
11	Arvey	0.986	0.988	0.952	0.991	0.990	0.956
12	Kiritani	0.995	0.995	0.945	0.998	0.973	0.945
13	Katsurabara	0.994	0.963	0.976	0.988	0.959	0.963
14	Hitohane	0.993	0.982	0.982	0.994	0.979	0.988
15	Takisaka	0.998	0.985	0.988	0.992	0.989	0.932
16	Sakae	0.993	0.983	0.928	0.976	0.967	0.975
17	Mushigame	0.989	0.987	0.951	0.995	0.936	0.982
18	Higashinomyo	0.981	0.988	0.941	0.995	0.949	0.953
19	Karuizawa	0.989	0.963	0.958	0.979	0.938	0.993
20	Happoudai	0.997	0.993	0.910	0.994	0.952	0.957
21	Raiden	0.989	0.961	0.987	0.980	0.945	0.991
22	Nishinakanoho	0.994	0.956	0.962	0.984	0.891	0.972
23	Mizunashi	0.984	0.963	0.990	0.992	0.991	0.995
24	Kitaurata	0.982	0.970	0.976	0.991	0.837	0.977
25	Uenoyama	0.981	0.981	0.922	0.988	0.991	0.981
26	Nakatateyama	0.973	0.948	0.990	0.995	0.983	0.987
27	Yumoto	0.984	0.998	0.984	0.997	0.964	0.962
28	Yuyama	0.978	0.972	0.980	0.981	0.978	0.984
29	Kamatsuka	0.990	0.975	0.973	0.983	0.918	0.994
30	Maruyama	0.987	0.934	0.963	0.997	0.937	0.947
31	Maseguchi	0.979	0.930	0.953	0.995	0.954	0.956
32	Maruta	0.988	0.979	0.965	0.993	0.994	0.973
33	Kodomari	0.967	0.971	0.945	0.987	0.979	0.910
34	Ohbora	0.993	0.922	0.990	0.990	0.970	0.988
35	Urushinose	0.972	0.969	0.986	0.993	0.933	0.951
36	Nishinotani	0.990	0.961	0.950	0.992	0.963	0.973
37	Youne	0.984	0.986	0.975	0.980	0.997	0.973
38	Nuta	0.983	0.889	0.940	0.991	0.935	0.976
39	Nyuya	0.981	0.984	0.919	0.974	0.970	0.897
40	Hikinota						
	Average	0.986	0.970	0.960	0.990	0.957	0.968
	Standard deviation	0.008	0.022	0.026	0.006	0.038	0.023

Fractal Limit and Map Scale

No.		limit (m)		1 / scale
		width	length	
1	Midway Bridge	50	40	24,000
2	Boca Ridge	60	50	24,000
3	Palos Verdes	100	110	24,000
4	Big Rock Mesa	30	30	2,300
5	Thristle	110	120	24,000
6	Lower Gross	120	95	24,000
7	Upper Gros	120		2,400
8	Meadow	60	70	4,800
9	Mayunmarca	200	230	50,000
10	La Frasse	80	90	12,500
11	Arvey	40	80	12,500
12	Kiritani	70	100	13,000
13	Katsurabara		50	13,000
14	Hitohane	40	45	1,300
15	Takisaka	30	30	5,000
16	Sakae	70	80	25,000
17	Mushigame	70	70	25,000
18	Higashinomyo	40		25,000
19	Karuizawa	100	100	25,000
20	Happoudai	100	110	25,000
21	Raiden	100	100	25,000
22	Nishinakanoho	90	100	25,000
23	Mizunashi	50	70	5,000
24	Kitaurata		80	25,000
25	Uenoyama		70	25,000
26	Nakatateyama	70	80	25,000
27	Yumoto		90	25,000
28	Yuyama	80	90	25,000
29	Kamatsuka	50	80	25,000
30	Maruyama	100	100	25,000
31	Maseguchi		90	25,000
32	Maruta	70	100	25,000
33	Kodomari	80	90	25,000
34	Ohbora	70	105	25,000
35	Urushinose	15	60	500
36	Nishinotani	40	40	5,000
37	Youne	80	90	18,450
38	Nuta	60	60	18,450
39	Nyuya	80	100	18,450
	Average	74.3	83.6	19,299
	Standard deviation	34.1	33.7	9,984

Table 6. Shape of log(N(r)) versus log(r) plot

No.		Whole Blocks		2nd Level Blocks		3rd Level Blocks		Bending Angle		Rate ofBending Site	
		Width	length	Width	Length	Width	Length	Width	length	Width	Length
1	Midway Bridge	5	5	1	2	1	1	0	0	1.00	1.00
2	Boca Ridge	1	1	2	1	8	8	30	33	0.83	0.83
3	Palos Verdes	5	7	2	8	8	8	21	31	0.59	0.59
4	Big Rock Mesa	5	3	8	8	1	1	0	0	1.00	1.00
5	Thristle	2	2	1	1	8	8	27	25	0.71	0.71
6	Lower Gross	2	2	8	1	8	8	21	18	0.74	0.68
7	Upper Gros	6	1	8	1	8	1	21	0	0.60	1.00
8	Meadow	2	6	1	8	8	8	37	21	0.79	0.54
9	Mayunmarca	1	1	1	1	8	8	36	27	0.74	0.71
10	La Frasse	2	2	1	1	8	8	22	24	0.41	0.72
11	Arvey	2	2	2	2	1	1	20	0	0.58	1.00
12	Kiritani	1	3	1	7	8	8	30	18	0.63	0.58
13	Katsurabara	2	2	1	1	7	8	13	9	0.38	0.39
14	Hitohane	5	5	8	7	8	8	13	17	0.39	0.45
15	Takisaka	1	1	7	1	7	7	14	20	0.28	0.42
16	Sakae	2	6	1	1	8	8	21	30	0.54	0.59
17	Mushigame	2	6	1	8	7	7	16	16	0.42	0.40
18	Higashinomyo	4	3	1	8	8	7	23	18	0.54	0.52
19	Karuizawa	4	5	1	8	7	1	12	0	0.43	1.00
20	Happoudai	1	1	1	8	8	7	20	16	0.52	0.39
21	Raiden	6	5	8	2	1	1	0	0	1.00	1.00
22	Nishinakanoho	1	5	8	8	8	8	12	14	0.55	0.59
23	Mizunashi	5	5	2	2	1	1	0	0	1.00	1.00
24	Kitaurata	2	2	7	8	1	1	0	0	1.00	1.00
25	Uenoyama	4	1	1	1	7	1	27	0	0.45	1.00
26	Nakatateyama	4	1	8	1	1	1	0	0	1.00	1.00
27	Yumoto	2	1	1	1	1	8	0	23	1.00	0.70
28	Yuyama	4	2	1	1	1	1	0	0	1.00	1.00
29	Kamatsuka	6	2	7	8	1	1	0	0	1.00	1.00
30	Maruyama	2	1	2	8	7	8	15	14	0.39	0.32
31	Maseguchi	5	4	7	8	8	7	20	16	0.63	0.39
32	Maruta	4	1	7	1	8	7	13	16	0.48	0.38
33	Kodomari	2	2	2	2	8	8	14	22	0.48	0.52
34	Ohbora	1	2	1	1	1	7	0	25	1.00	0.37
35	Urushinose	2	1	1	7	8	8	32	38	0.71	0.76
36	Nishinotani	5	6	8	7	7	7	19	0	0.50	1.00
37	Youne	2	2	1	1	8	1	21	0	0.63	1.00
38	Nuta	6	2	8	8	8	8	22	17	0.54	0.59
39	Nyuya	2	2	1	2	8	8	34	25	0.74	0.68
40	Hikinota										
	1 Total	7	11	19	16	11	13				
	2 Total	15	13	6	6	0	0				
	3 Total	0	3	0	0	0	0				
	4 Total	6	1	0	0	0	0				
	5 Total	7	6	0	0	0	0				
	6 Total	4	4	0	0	0	0				
	7 Total	0	1	5	4	7	8				
	8 Total	0	0	9	13	21	18				

Alpha and Alpha-0 (Alpha / Area) of Landslides

No	Landslide	Alpha (#of blocks)		Alpha-0 (#/Area)	
		Width	Length	Width (#/ha)	Length (#/ha)
1	Midway Bridge	40,272	21,979	83	45
2	Boca Ridge	50,933	33,343	37	24
3	Palos Verdes	142,233	335,738	132	313
4	Big Rock Mesa	42,855	51,523	366	440
5	Thristle	46,026	44,978	41	40
6	Lower Gross	32,434	15,740	37	18
7	Upper Gros	39,719	29,717	20	15
8	Meadow	21,281	14,158	142	94
9	Mayunmarca	314,051	228,560	125	91
10	La Frasse	59,156	28,840	340	166
11	Arvey	6,950	28,642	56	229
12	Kiritani	15,276	42,756	45	126
13	Katsurabara	14,622	31,623	100	217
14	Hitohane	146,893	238,781	417	678
15	Takisaka	14,588	11,482	110	86
16	Sakae	5,649	27,606	17	84
17	Mushigame	29,717	137,721	66	308
18	Higashinomyo	7,278	12,218	29	48
19	Karuizawa	167,109	82,224	291	143
20	Happoudai	33,651	69,823	84	173
21	Raiden	173,780	125,026	346	249
22	Nishinakanoho	56,624	28,054	199	98
23	Mizunashi	133,968	199,986	407	608
24	Kitaurata	9,750	45,186	29	133
25	Uenoyama	7,129	10,023	67	94
26	Nakatateyama	36,728	104,472	116	331
27	Yumoto	17,742	14,454	134	110
28	Yuyama	30,620	41,976	109	149
29	Kamatsuka	41,115	107,152	151	394
30	Maruyama	67,764	83,753	37	46
31	Maseguchi	62,517	95,499	159	243
32	Maruta	46,559	50,466	67	73
33	Kodomari	13,804	37,931	33	91
34	Ohbora	12,531	37,670	21	62
35	Urushinose	1,300	1,828	52	73
36	Nishinotani	41,879	41,879	411	411
37	Youne	15,596	83,946	156	839
38	Nuta	38,905	54,200	134	187
39	Nyuya	5,495	11,272	47	96
40	Hikinota	15,800		158	
	Average	51,507	68,262	134	196
	Standar deviation	61,319	71,666	119	186

1 ha = 10,000 square meters

Alpha-0 of Each Geology Area

No.		Alpha-0 (#/ha)	
		Width	Length
14	Hitohane	417	678
16	Sakae	17	84
17	Mushigame	66	308
18	Higashinomyo	29	48
19	Karuizawa	291	143
20	Happoudai	84	173
21	Raiden	346	249
22	Nishinakanoho	199	98
24	Kitaurata	29	133
31	Maseguchi	159	243
32	Maruta	67	73
	MUDSTONE	154.9	202.7
		133.9	169.5
3	Palos Verdes	132	313
4	Big Rock Mesa	366	440
25	Uenoyama	67	94
29	Kamatsuka	151	394
30	Maruyama	37	46
33	Kodomari	33	91
34	Ohbora	21	62
	SS, MS	115.3	205.7
		112.5	157.5
15	Takisaka	110	86
23	Mizunashi	407	608
26	Nakatateyama	116	331
27	Yumoto	134	110
28	Yuyama	109	149
	TUFF	175.2	256.8
		116.2	195.5
1	Midway Bridge	83	45
2	Boca Ridge	37	24
12	Kiritani	45	126
13	Katsurabara	100	217
	VOLCANIC	66.3	103.0
		26.1	76.0
5	Thristle	41	40
6	Lower Gross	37	18
7	Upper Gros	20	15
8	Meadow	142	94
9	Mayunmarca	125	91
36	Nishinotani	411	411
	MESOZOIC	129.3	111.5
		134.0	137.6
10	La Frasse	340	166
11	Arvey	56	229
35	Urushinose	52	73
37	Youne	156	839
38	Nuta	134	187
39	Nyuya	47	96
40	Hikinota	158	
	Schist	134.7	265.0
		95.5	262.1

APPENDIX H:

CORRESPONDENCE ANALYSIS RESULT

```
File name missing or blank - please enter file name
UNIT 5? LS-C3.DAT

          NUMBER OF INDIVIDUALS =          39
          NUMBER OF ATTRIBUTES  =          17
          NUMBER OF FACTORS     =           3

          CONTINGENCY TABLE, Y

IDEN

            Wd          Ln          Ar          Dp          Ht          Lw          Aa
  1    .19E+01     .17E+01     .48E+01     .11E+01     .30E+01     .88E+00     .10E+02
  2    .35E+01     .30E+01     .14E+02     .20E+01     .33E+01     .86E+00     .63E+01
  3    .52E+01     .25E+01     .11E+02     .10E+01     .35E+01     .48E+00     .80E+01
  4    .21E+01     .96E+01     .12E+01     .12E+01     .20E+01     .45E+00     .12E+02
  5    .36E+01     .40E+01     .11E+02     .80E+00     .57E+01     .11E+01     .81E+01
  6    .34E+01     .36E+01     .88E+01     .13E+01     .60E+01     .11E+01     .95E+01
  7    .40E+01     .55E+01     .20E+02    -.99E+02     .64E+01     .14E+01     .66E+01
  8    .14E+01     .26E+01     .15E+01     .55E+00     .40E+01     .19E+01     .89E+01
  9    .54E+01     .65E+01     .25E+02     .15E+01     .15E+02     .12E+01     .13E+02
  10   .11E+01     .23E+01     .17E+01     .10E+01     .30E+01     .22E+01     .74E+01
  11   .15E+01     .13E+01     .13E+01    -.99E+02     .25E+01     .87E+00     .11E+02
  12   .23E+01     .17E+01     .34E+01     .12E+01     .20E+01     .74E+00     .66E+01
  13   .11E+01     .18E+01     .15E+01     .80E+00     .22E+01     .16E+01     .71E+01
  14   .24E+01     .26E+01     .35E+01     .10E+01     .18E+01     .11E+01     .39E+01
  15   .11E+01     .15E+01     .13E+01     .13E+01     .23E+01     .13E+01     .89E+01
  16   .25E+01     .15E+01     .33E+01     .11E+01     .12E+01     .60E+00     .46E+01
  17   .26E+01     .22E+01     .45E+01     .15E+01     .15E+01     .85E+00     .38E+01
  18   .25E+01     .12E+01     .25E+01     .13E+01     .21E+01     .49E+00     .97E+01
  19   .23E+01     .35E+01     .57E+01     .85E+00     .26E+01     .15E+01     .42E+01
  20   .24E+01     .18E+01     .40E+01     .85E+00     .20E+01     .74E+00     .65E+01
  21   .26E+01     .44E+01     .50E+01     .70E+00     .15E+01     .17E+01     .20E+01
  22   .13E+01     .27E+01     .28E+01     .75E+00     .22E+01     .21E+01     .47E+01
  23   .28E+01     .25E+01     .33E+01     .10E+01     .18E+01     .91E+00     .40E+01
  24   .20E+01     .20E+01     .34E+01     .11E+01     .22E+01     .96E+00     .64E+01
  25   .18E+01     .11E+01     .11E+01     .80E+00     .85E+00     .59E+00     .46E+01
  26   .27E+01     .14E+01     .32E+01     .11E+01     .28E+01     .53E+00     .11E+02
  27   .11E+01     .15E+01     .13E+01     .90E+00     .26E+01     .14E+01     .10E+02
  28   .27E+01     .12E+01     .28E+01     .80E+00     .21E+01     .44E+00     .10E+02
  29   .19E+01     .18E+01     .27E+01     .85E+00     .24E+01     .95E+00     .78E+01
  30   .57E+01     .55E+01     .18E+02     .16E+01     .35E+01     .97E+00     .36E+01
  31   .25E+01     .21E+01     .39E+01     .80E+00     .32E+01     .86E+00     .85E+01
  32   .38E+01     .25E+01     .69E+01     .65E+00     .24E+01     .65E+00     .55E+01
  33   .28E+01     .20E+01     .42E+01     .13E+01     .13E+01     .72E+00     .36E+01
  34   .25E+01     .31E+01     .61E+01     .20E+01     .30E+01     .12E+01     .55E+01
  35   .60E+00     .30E+00     .25E+00     .25E+00     .15E+01     .50E+00     .27E+02
  36   .12E+01     .13E+01     .10E+01     .20E+00     .35E+01     .11E+01     .15E+02
  37   .14E+01     .95E+00     .10E+01     .35E+00     .25E+01     .70E-01     .15E+02
  38   .20E+01     .19E+01     .29E+01    -.99E+02     .50E+01     .94E+00     .15E+02
  39   .12E+01     .14E+01     .12E+01     .40E+00     .55E+01     .11E+01     .22E+02
PLEASE INSERT PAPER AND PRESS ENTER
```

PAGE TWO OF THREE

	Sa	To	Bs	Ac	Gp	Ge	Sk
1	.15E+02	.30E+01	.30E+01	.20E+01	.15E+00	.70E+01	.45E+01
2	.30E+01	.40E+01	.20E+01	.10E+01	.15E+00	.70E+01	.60E+01
3	.70E+01	.10E+01	.30E+01	.40E+01	.15E+00	.40E+01	.80E+01
4	.10E+02	.30E+01	.20E+01	.30E+01	.20E+00	.40E+01	.90E+01
5	.15E+02	.30E+01	.20E+01	.30E+01	.65E+00	.90E+01	.90E+01
6	.20E+02	.30E+01	.20E+01	.30E+01	.25E+01	.90E+01	.90E+01
7	-.99E+02	.40E+01	.30E+01	.10E+01	.25E+01	.90E+01	.80E+01
8	.13E+02	.10E+01	.20E+01	.30E+01	.30E+01	.90E+01	.90E+01
9	.23E+02	.10E+01	.40E+01	.30E+01	.25E+01	.90E+01	.90E+01
10	.15E+02	.30E+01	.30E+01	.40E+01	.15E+01	.80E+01	.90E+01
11	-.99E+02	.20E+01	.20E+01	.40E+01	.15E+01	.80E+01	-.99E+02
12	.40E+01	.30E+01	.20E+01	.20E+01	.20E+00	.60E+01	.00E+00
13	.85E+01	.30E+01	.30E+01	.20E+01	.20E+00	.60E+01	.70E+01
14	.25E+01	.30E+01	.20E+01	.30E+01	.15E+00	.30E+01	.80E+01
15	.50E+01	.40E+01	.30E+01	.40E+01	.15E+00	.20E+01	.25E+01
16	.10E+01	.10E+01	.20E+01	.10E+01	.30E-01	.30E+01	.45E+01
17	.42E+01	.10E+01	.20E+01	.30E+01	.15E+00	.30E+01	.60E+01
18	.72E+01	.30E+01	.30E+01	.40E+01	.15E+00	.30E+01	.75E+01
19	.20E+01	.30E+01	.10E+01	.10E+01	.15E+00	.30E+01	.50E+01
20	.30E+01	.30E+01	.30E+01	.20E+01	.15E+00	.30E+01	.80E+01
21	.20E+01	.40E+01	.30E+01	.20E+01	.50E-01	.30E+01	.00E+00
22	.25E+01	.40E+01	.30E+01	.20E+01	.50E-01	.30E+01	.00E+00
23	.50E+01	.30E+01	.20E+01	.40E+01	.15E+00	.20E+01	.75E+01
24	.85E+01	.10E+01	.20E+01	.10E+01	.50E-01	.30E+01	.80E+01
25	.30E+01	.30E+01	.20E+01	.10E+01	.15E+00	.40E+01	.80E+01
26	.80E+01	.30E+01	.30E+01	.30E+01	.15E+00	.10E+01	.50E+01
27	.95E+01	.20E+01	.40E+01	.30E+01	.15E+00	.20E+01	.90E+01
28	.50E+01	.20E+01	.30E+01	.20E+01	.15E+00	.20E+01	.45E+01
29	.30E+01	.30E+01	.30E+01	.30E+01	.15E+00	.50E+01	.80E+01
30	.25E+01	.30E+01	.10E+01	.20E+01	.10E-01	.50E+01	.80E+01
31	.85E+01	.30E+01	.30E+01	.40E+01	.80E-01	.30E+01	.90E+01
32	.35E+01	.30E+01	.20E+01	.20E+01	.30E-01	.30E+01	.70E+01
33	.35E+01	.20E+01	.20E+01	.20E+01	.80E-01	.40E+01	.90E+01
34	.35E+01	.10E+01	.20E+01	.30E+01	.30E-01	.40E+01	.30E+01
35	.25E+02	.30E+01	.20E+01	.20E+01	.15E+01	.80E+01	.80E+01
36	.20E+02	.10E+01	.20E+01	.40E+01	.15E+01	.90E+01	.00E+00
37	.17E+02	.10E+01	.20E+01	.40E+01	.15E+01	.80E+01	.90E+01
38	-.99E+02	.30E+01	.10E+01	.40E+01	.15E+01	.80E+01	.90E+01
39	.25E+02	.10E+01	.40E+01	.40E+01	.15E+01	.80E+01	.90E+01

PLEASE INSERT PAPER AND PRESS ENTER

PAGE THREE OF THREE

	Di	Dw	Dl
1	.00E+00	.15E+01	.14E+01
2	.10E+01	.13E+01	.13E+01
3	.10E+01	.15E+01	.16E+01
4	.11E+01	.15E+01	.15E+01
5	.15E+01	.13E+01	.13E+01
6	.11E+01	.13E+01	.12E+01
7	.11E+01	.13E+01	.12E+01
8	.10E+01	.14E+01	.12E+01
9	.10E+01	.15E+01	.14E+01
10	.10E+01	.16E+01	.14E+01
11	-.99E+02	.12E+01	.14E+01
12	.90E+00	.12E+01	.13E+01
13	.10E+01	.14E+01	.14E+01
14	.10E+01	.16E+01	.17E+01
15	.95E+00	.14E+01	.13E+01
16	.11E+01	.11E+01	.14E+01
17	.13E+01	.13E+01	.16E+01
18	.60E+00	.12E+01	.13E+01
19	.11E+01	.16E+01	.14E+01
20	.12E+01	.14E+01	.15E+01
21	.90E+00	.15E+01	.15E+01
22	.90E+00	.15E+01	.14E+01
23	.12E+01	.16E+01	.16E+01
24	.60E+00	.12E+01	.14E+01
25	.11E+01	.13E+01	.13E+01
26	.11E+01	.14E+01	.16E+01
27	.12E+01	.14E+01	.13E+01
28	.12E+01	.14E+01	.15E+01
29	.65E+00	.15E+01	.15E+01
30	.13E+01	.13E+01	.13E+01
31	.12E+01	.15E+01	.15E+01
32	.10E+01	.14E+01	.14E+01
33	.10E+01	.12E+01	.14E+01
34	.75E+00	.12E+01	.13E+01
35	.30E+00	.11E+01	.13E+01
36	.90E+00	.15E+01	.15E+01
37	.10E+01	.14E+01	.16E+01
38	.14E+01	.15E+01	.15E+01
39	.12E+01	.12E+01	.13E+01

PLEASE INSERT PAPER AND PRESS ENTER

EIGENVALUE SUMMARY

EIGENVALUE	PERCENT VARIATION
.1109028	44.909
.0537374	21.760
.0226365	9.166
.0158944	6.436
.0111856	4.529
.0088241	3.573
.0068714	2.783
.0047900	1.940
.0035847	1.452
.0025839	1.046
.0019116	.774
.0016000	.648
.0013760	.557
.0006734	.273
.0003460	.140
.0000331	.013

FACTORS FOR ATTRIBUTES

IDEN	FACTORS: 1 TO NUMFAC		
Wd	.4196	-.0793	-.0547
Ln	.3895	-.0645	.1317
Ar	.6993	.3756	-.0168
Dp	.3109	-.2141	.0384
Ht	.1081	.2482	.0415
Lw	.1295	-.2292	.2979
Aa	-.3400	-.0550	.0419
Sa	-.4023	.2357	.0030
To	.1949	-.3537	.2375
Bs	.0277	-.2664	.1161
Ac	-.0889	-.2477	.0461
Gp	-.4605	.6115	-.0420
Ge	-.0945	.1100	.0589
Sk	.0247	-.1862	-.3706
Di	.1529	-.2695	-.0097
Dw	.0986	-.2705	.0890
Dl	.0869	-.2928	.0513

FACTORS FOR INDIVIDUALS

IDEN	FACTORS: 1 TO NUMFAC		
1	-.1804	.1179	.1124
2	.5320	.1291	.0337
3	.2880	.0666	-.1291
4	-.0641	-.2100	.0093
5	.1148	.2140	-.0372
6	-.0747	.2755	-.0350
7	.3449	.3923	.0144
8	-.2986	.1199	-.0763
9	.2354	.4907	-.0045
10	-.2520	-.0168	-.0102
11	-.2920	-.0555	.0031
12	.0808	-.0721	.3838
13	-.1546	-.1713	.0200

15	-.1104	-.3462	.2990
16	.2813	-.2489	-.0736
17	.2296	-.1610	-.1051
18	-.1023	-.2312	-.0656
19	.4202	-.1234	.0683
20	.1647	-.2752	-.1210
21	.5211	-.2199	.5175
22	.2155	-.2926	.5620
23	.1633	-.2984	-.0942
24	-.0339	-.0413	-.1928
25	.0232	-.3965	-.2073
26	-.0977	-.1701	.0527
27	-.2244	-.2328	-.1080
28	-.0506	-.2036	.0299
29	.0371	-.2964	-.0621
30	.7712	.1903	-.0835
31	-.0162	-.1689	-.0981
32	.3482	-.1051	-.0910
33	.2406	-.2253	-.2546
34	.3018	-.0214	.1342
35	-.6856	.1111	.0045
36	-.5603	.2390	.2647
37	-.4766	.0676	-.1224
38	-.2224	-.0013	-.0421
39	-.5279	.1284	-.0158

PLEASE INSERT PAPER AND PRESS ENTER

CORRESPONDENCE ANALYSIS PLOT
FACTOR 1 VERSUS FACTOR 2

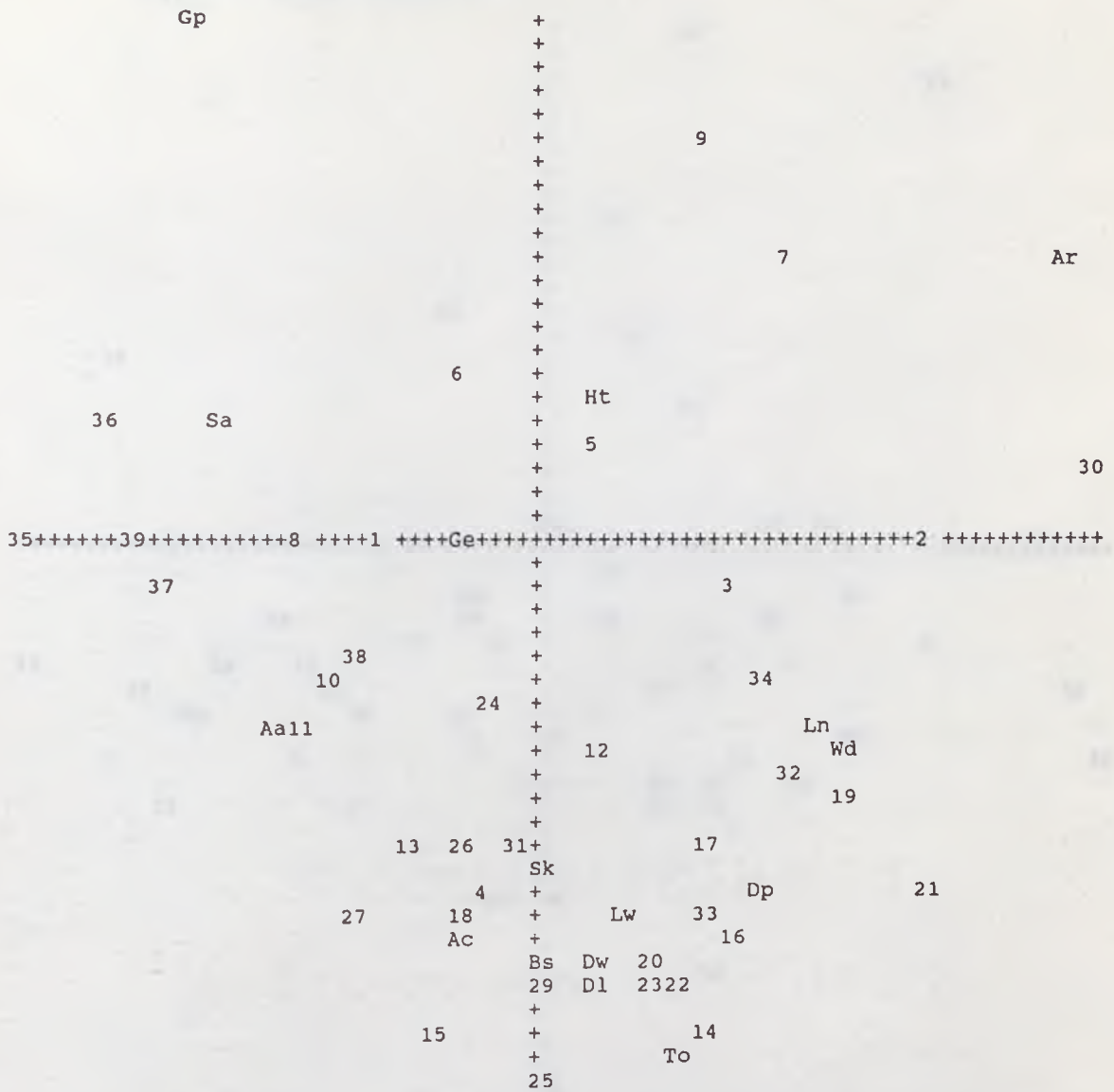

HORIZ AXIS IS LOCATED AT Y = .1075248E+00
VERT AXIS IS LOCATED AT X = .4280806E-01

X-AXIS RANGE (XMAX-XMIN) = .1456765E+01
Y-AXIS RANGE (YMAX-YMIN) = .1007954E+01

PLEASE INSERT PAPER AND PRESS ENTER

OVERPRINT SUMMARY
4 PRINTS OVER 28

CORRESPONDENCE ANALYSIS PLOT
FACTOR 1 VERSUS FACTOR 3

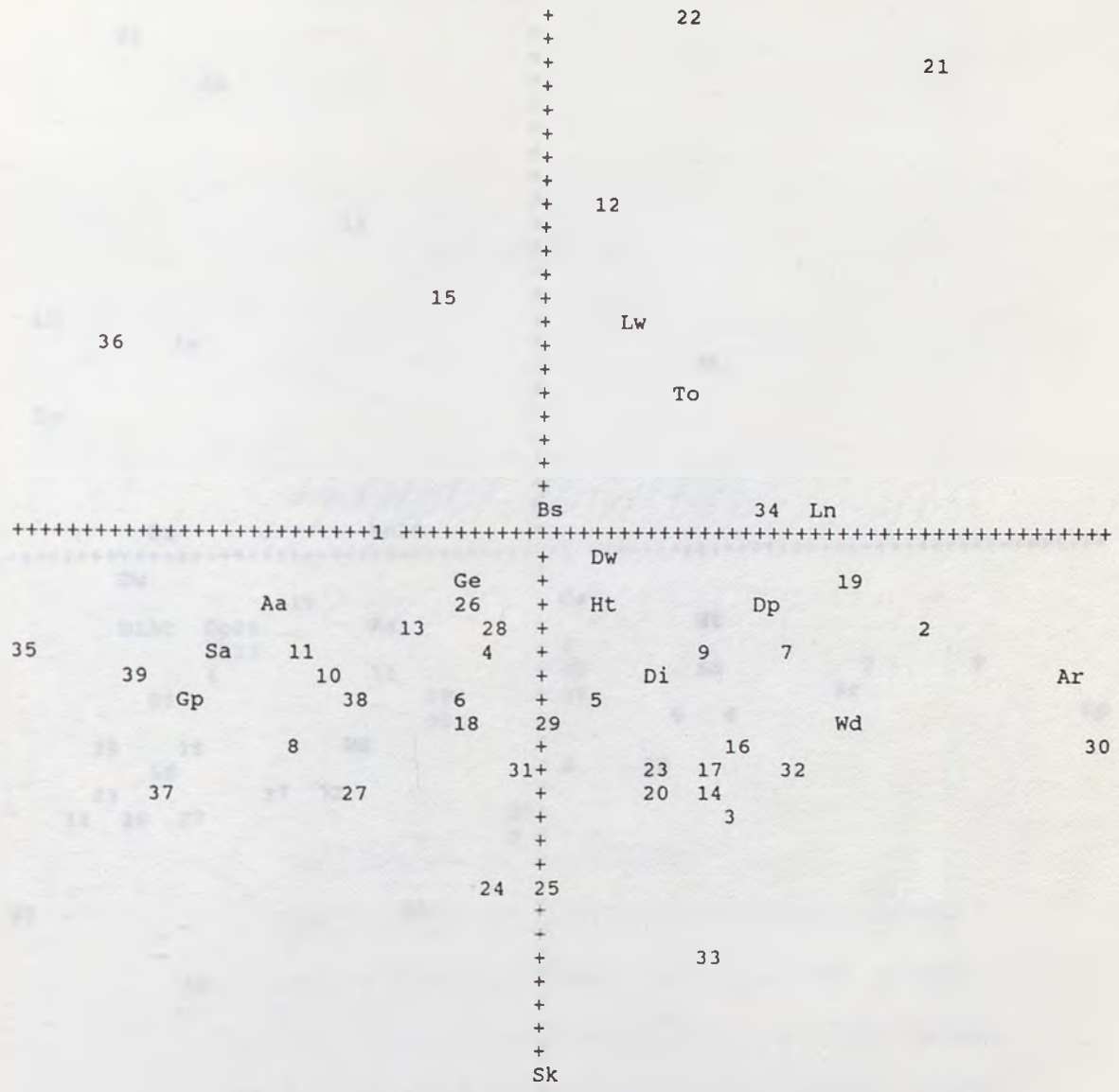

HORIZ AXIS IS LOCATED AT Y = .9568799E-01
VERT AXIS IS LOCATED AT X = .4280806E-01

X-AXIS RANGE (XMAX-XMIN) = .1456765E+01
Y-AXIS RANGE (YMAX-YMIN) = .9326684E+00

PLEASE INSERT PAPER AND PRESS ENTER

OVERPRINT SUMMARY
26 PRINTS OVER Ac

CORRESPONDENCE ANALYSIS PLOT
FACTOR 2 VERSUS FACTOR 3

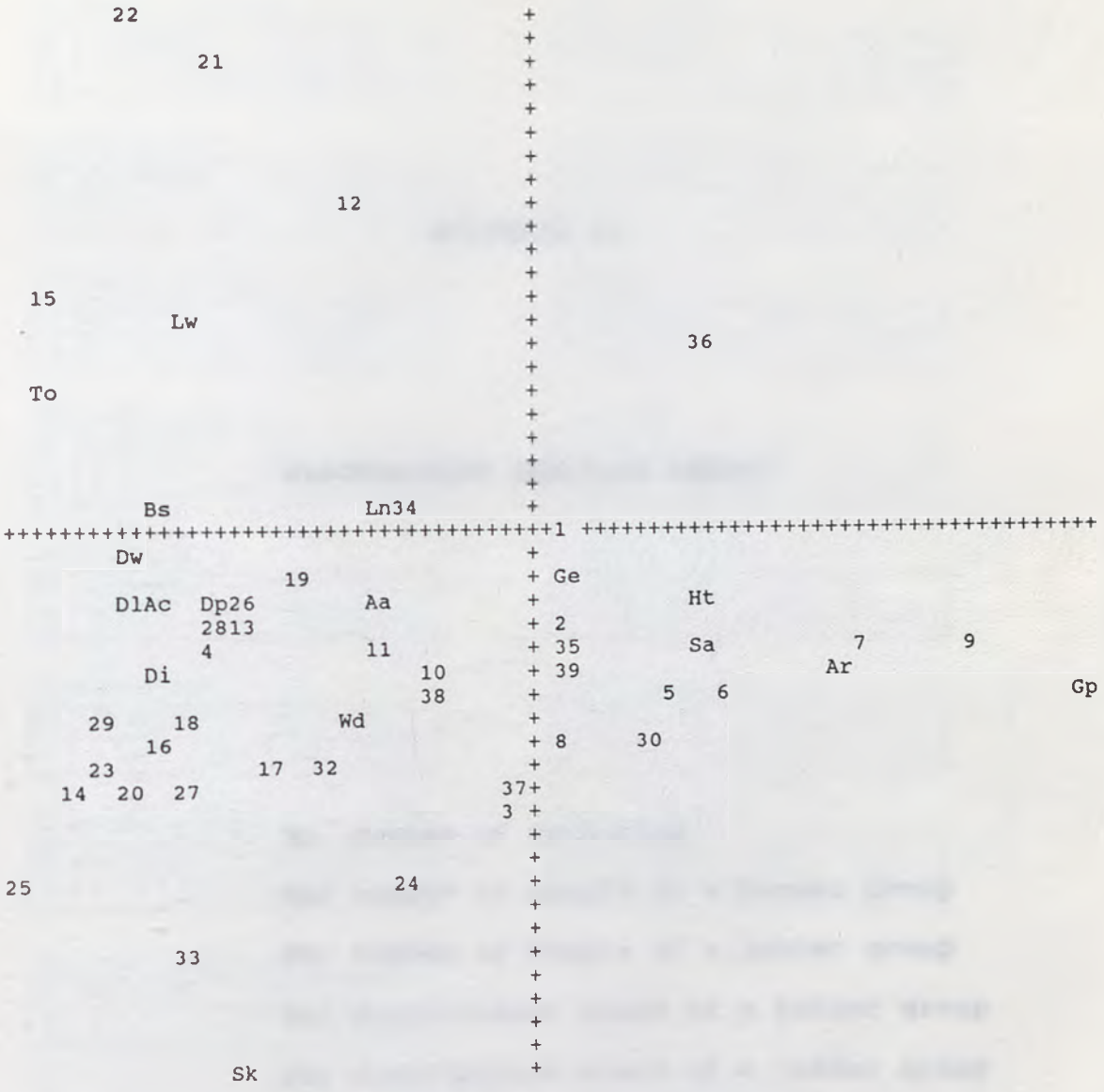

HORIZ AXIS IS LOCATED AT Y = .9568799E-01
VERT AXIS IS LOCATED AT X = .1075248E+00

X-AXIS RANGE (XMAX-XMIN) = .1007954E+01
Y-AXIS RANGE (YMAX-YMIN) = .9326684E+00

PLEASE INSERT PAPER AND PRESS ENTER

OVERPRINT SUMMARY
17 PRINTS OVER 31

APPENDIX I:

DISCRIMINANT ANALYSIS RESULT

M: number of variables

Na: number of sample of a former group

Nb: number of sample of a latter group

Ra: discriminant score of a former group

Rb: discriminant score of a latter group

F: F value

F Value Calculatin for Fractal Dimension

GEOLOGY

mudstone - sandstone

M	Na	Nb	Ra	Rb	F
2	11	7	3.0869	2.982	0.211

mudstone - tuff

M	Na	Nb	Ra	Rb	F
2	11	5	-1.644	-1.74	0.156

mudstone - volcanic

M	Na	Nb	Ra	Rb	F
2	11	4	11.611	10.88	0.994

Mesozoic - mudstone

M	Na	Nb	Ra	Rb	F
2	6	11	-11.8	-14.2	4.421

schist - mudstone

M	Na	Nb	Ra	Rb	F
2	6	11	-4.676	-4.85	0.313

sandstone - tuff

M	Na	Nb	Ra	Rb	F
2	7	5	-7.326	-8.64	1.722

sandstone - volcanic

M	Na	Nb	Ra	Rb	F
2	7	4	10.024	8.336	1.91

Mesozoic - sandstone

M	Na	Nb	Ra	Rb	F
2	6	7	0.759	-8.11	13.02

schist - sandstone

M	Na	Nb	Ra	Rb	F
2	6	7	-1.271	-1.28	0.017

tuff - volcanic

M	Na	Nb	Ra	Rb	F
2	5	4	9.9915	9.384	0.579

Mesozoic - tuff

M	Na	Nb	Ra	Rb	F
2	6	5	-0.17	-2.18	2.431

schist - tuff

M	Na	Nb	Ra	Rb	F
2	6	5	-6.537	-7.14	0.729

Mesozoic - volcanic

M	Na	Nb	Ra	Rb	F
2	6	4	-1.48	-3.16	1.762

Schist - volcanic

M	Na	Nb	Ra	Rb	F
2	6	4	4.028	3.625	0.423

Mesozoic - schist

M	Na	Nb	Ra	Rb	F
2	6	6	-3.703	-5.81	2.844

DIP

Dip - Horizontal

M	Na	Nb	Ra	Rb	F
2	28	4	-3.765	-4	0.389

Horizontal - Dipping Into

M	Na	Nb	Ra	Rb	F
2	4	6	-2.69	-6.23	3.719

Dip - Dipping Into

M	Na	Nb	Ra	Rb	F
2	28	6	6.259	5.157	2.638

Topography

1-2

M	Na	Nb	Ra	Rb	F
2	10	4	5.4365	5.27	0.218

2-3

M	Na	Nb	Ra	Rb	F
2	4	20	-4.648	-5.16	0.814

1-3

M	Na	Nb	Ra	Rb	F
2	10	20	-1.027	-1.49	1.488

2-4

M	Na	Nb	Ra	Rb	F
2	4	5	3.921	0.851	2.924

1-4

M	Na	Nb	Ra	Rb	F
2	10	5	6.5595	4.693	2.871

3-4

M	Na	Nb	Ra	Rb	F
2	20	5	7.0021	5.637	2.611

Block Shape

Horse - Triangle

M	Na	Nb	Ra	Rb	F
2	19	3	-4.512	-5.76	1.537

Horse - Rectangular

M	Na	Nb	Ra	Rb	F
2	19	14	-5.566	-6.31	2.885

Triangle - Rectangular

M	Na	Nb	Ra	Rb	F
2	3	14	2.9743	2.768	0.238

Bottle - Horse

M	Na	Nb	Ra	Rb	F
2	3	19	-2.322	-3.37	1.285

Bottle - Triangle

M	Na	Nb	Ra	Rb	F
2	3	3	-22.11	-23.5	0.808

Bottle - Rectangular

M	Na	Nb	Ra	Rb	F
2	3	14	-11.18	-11.9	0.885

Activity

Ancient - Stable

M	Na	Nb	Ra	Rb	F
2	6	11	-12.17	-12.6	0.806

Stable - Dormant

M	Na	Nb	Ra	Rb	F
2	11	11	-3.721	-3.84	0.304

Ancient - Dormant

M	Na	Nb	Ra	Rb	F
2	6	11	-8.059	-8.65	1.072

Stable - Active

M	Na	Nb	Ra	Rb	F
2	11	11	-8.77	-9.18	1.065

Ancient - Active

M	Na	Nb	Ra	Rb	F
2	6	11	-12.13	-13.2	1.852

Dormant - Active

M	Na	Nb	Ra	Rb	F
2	11	11	-1.938	-2.03	0.235

F Value Calculation for Alpha-0

GEOLOGY

mudstone - sandstoness

M	Na	Nb	Ra	Rb	F
2	11	7	0.1862	-0.03	0.428

sandstone - schist

M	Na	Nb	Ra	Rb	F
2	7	6	-0.242	-0.31	0.097

mudstone - tuff

M	Na	Nb	Ra	Rb	F
2	11	5	-0.256	-0.35	0.143

tuff - volcanic

M	Na	Nb	Ra	Rb	F
2	5	4	1.911	0.715	1.139

mudstone - volcanic

M	Na	Nb	Ra	Rb	F
2	11	4	0.9988	-0.45	1.965

tuff - Mesozoic

M	Na	Nb	Ra	Rb	F
2	5	6	1.1463	-0.4	1.876

mudstone - Mesozoic

M	Na	Nb	Ra	Rb	F
2	11	6	0.5512	0.122	0.778

tuff - schist

M	Na	Nb	Ra	Rb	F
2	5	6	0.4514	0.267	0.224

mudstone - schist

M	Na	Nb	Ra	Rb	F
2	11	6	0.0355	-0.16	0.362

volcanic - Mesozoic

M	Na	Nb	Ra	Rb	F
2	4	6	0.5539	-1.15	1.787

sandstone - tuff

M	Na	Nb	Ra	Rb	F
2	7	5	-0.264	-0.6	0.437

volcanic - schist

M	Na	Nb	Ra	Rb	F
2	4	6	-0.702	-1.54	0.881

sandstone volcanic

M	Na	Nb	Ra	Rb	F
2	7	4	0.9753	0.46	0.583

Mesozoic - schist

M	Na	Nb	Ra	Rb	F
2	5	6	-0.045	-0.6	0.672

sandstone - Mesozoic

M	Na	Nb	Ra	Rb	F
2	7	6	1.9751	-0.95	4.299

APPENDIX J:

ABBREVIATION LIST

Abbreviations used in this thesis are as follows:

D: fractal dimension

D_S: similarity dimension

D_D: divider dimension

D_B: box-counting dimension

D_W, $D_{W\text{-}whole}$: fractal dimension of width of whole blocks

D_L, $D_{L\text{-}whole}$: fractal dimension of length of whole blocks

$D_{W\text{-}2nd}$: fractal dimension of width of second-level blocks

$D_{L\text{-}2nd}$: fractal dimension of length of second-level blocks

$D_{W\text{-}3rd}$: fractal dimension of width of third-level blocks

$D_{L\text{-}3rd}$: fractal dimension of length of third-level blocks

D_{whole}: D_W, D_L

D_{2nd}: $D_{W\text{-}2nd}$, $D_{L\text{-}2nd}$

D_{3rd}: $D_{W\text{-}3rd}$, $D_{L\text{-}3rd}$

D_{Lin}: fractal dimension of lineaments

D_{Rock}: fractal dimension of rock fragments

D_{Fr}: fractal dimension of fractures

$D_{W\text{-}mean}$: mean fractal dimension of width of a certain group

$D_{L\text{-}mean}$: mean fractal dimension of length of a certain group

$D_{Avg\text{-}mean}$: $(D_{W\text{-}mean} + D_{L\text{-}mean})/2$

D_{MA}: fractal dimension of Model A

D_{MB}: fractal dimension of Model B

r: ruler of divider method; grid size of box counting method; coefficient of correlation

$N(r)$: number of something whose size is greater than the ruler, r

b: number of subsequent blocks in a preceding block

s: reduction factor (ratio of size of subsequent image to size of preceding image)

s_W: reduction factor of block width

s_L: reduction factor of block length